Navigating Cells and Cytoskeletal Networks with a Novel Family of AAA-ATPases

Jeffrey A.J. van Haren

ISBN: 978-90-8570-291-7

This thesis was printed by CPI-Wörhman Print Service, Zutphen

The research presented in this thesis was performed at the Department of Cell Biology of the Erasmus MC in Rotterdam, the Netherlands. This research was supported by the Nederlandse Organisatie voor Wetenschappelijk Onderzoek (NWO)

Printing of this thesis was financially supported by the Erasmus MC and the J.E. Jurriaanse Stichting

The sundial on the cover was designed and constructed by C.H. van Haren
The compass on the back was designed by Ipurush (http://openclipart.org/media/files/ipurush/8304)

Navigating Cells and Cytoskeletal Networks with a Novel Family of AAA-ATPases

Navigatie van cellen en het celskelet met behulp van een nieuwe familie van AAA-ATPases

Proefschrift

ter verkrijging van de graad van doctor aan de
Erasmus Universiteit Rotterdam
op gezag van de
rector magnificus

Prof.dr. S.W.J. Lamberts

en volgens besluit van het College voor Promoties

De openbare verdediging zal plaatsvinden op
woensdag 10 juni 2009 om 11:45 uur

door

Antonius Johannes van Haren

geboren te Tiel

Promotiecommissie

Promotor:	Prof.dr. F.G. Grosveld
Overige leden:	Dr. G. Jansen Dr. A. Akhmanova Dr.ir. D.N. Meijer
Copromotor:	Dr.ir. N.J. Galjart

Voor mijn moeder en mijn broer, en ter nagedachtenis aan mijn vader

To my mother and my brother, and to the memory of my father

Contents

Scope of the thesis

The cytoskeleton is of great importance for cell division, cell shape, cell migration and intracellular transport. This thesis describes how one of the three main cytoskeletal networks, namely the microtubule (MT) network, is regulated by MT plus-end tracking proteins (+TIPs) named “Navigators”. Furthermore, it describes the mechanisms by which two other +TIPs, named CLIP170 and EB1, associate with microtubule plus-ends.

Chapter 1 gives an introduction to the cytoskeleton, and describes the main cytoskeletal components, namely the actin, IF and microtubule networks. It also describes how the cytoskeleton is regulated during cell migration, outgrowth and division and how the MT network is organized in different cell types. Finally it gives an overview of how Microtubule Associated Proteins regulate the dynamics of the MT network.
Chapter 2 describes the mechanism by which a MT plus-end tracking protein named CLIP-170 associates with the ends of microtubules, and shows that this mechanism is much more dynamic than was previously thought.
Chapter 3 describes a novel family of +TIPs named Neuron Navigators, which use an AAA-ATPase domain to remodel the cytoskeleton.
Chapter 4 shows that Navigator proteins interact with EB proteins and that Navigators require these proteins to track growing microtubule ends. We also show that Navigators can associate with the actin cytoskeleton.
Chapter 5 describes the identification of interaction partners of Navigator proteins, using mass spectrometry. In addition we show that NAV1 has a potential role in nucleolar structure and in mitosis. Furthermore we show that Navigators have functional nuclear localization and nuclear export signals.
Chapter 6 discusses the results in this thesis and describes what is known about the pathways in which the *C.elegans* Navigator functions, and how mammalian Navigators might function in similar pathways.
Chapter 7 contains a summary of the work described in this thesis.

Chapter 1

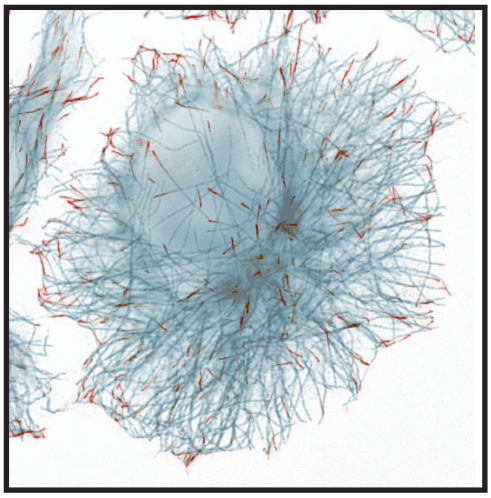

Introduction

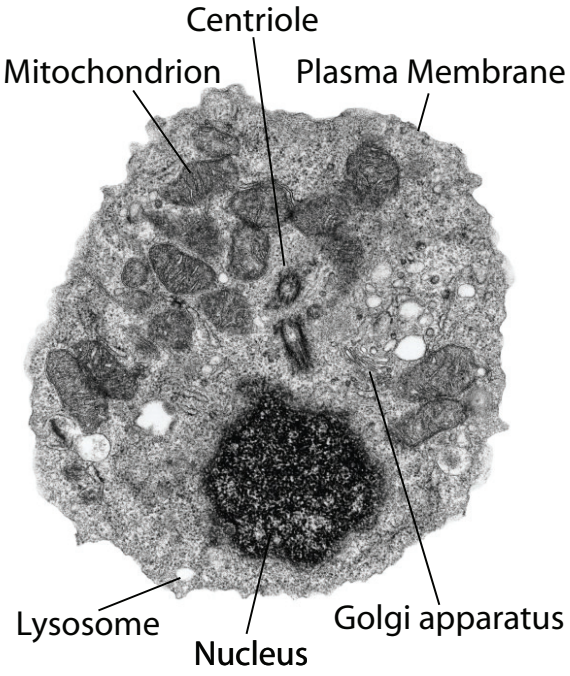

Figure1: A eukaryotic cell
An electron micrograph of a human lymphocyte, with major structures visible, including: plasma- membrane, nucleus, Golgi apparatus, mitochondria, endoplasmic reticulum, and lysosome.
(http://www.sinauer.com/cooper/4e/micro/01/01-02_AnimalCell(L-Large).jpg)

1 Introduction

1.1 Cells and their organization

Eukaryotic cells come in an amazing variety of functions and shapes. Organisms such as yeast are composed of just a single cell. Mammals, on the other hand, contain trillions of cells, which differ greatly from one another, both in morphology and function. The human body contains more than 200 different cell types, organized into highly specialized structures and tissues. Although cells can have completely differing morphology and function, the organization at the intracellular level is similar, even in divergent taxonomic kingdoms like Animalia and Fungi, and in the smallest single cell eukaryotes, such as yeast, when compared to the largest multicellular organisms, such as the African elephant (*Loxodonta africana*). All eukaryotic cells contain specific structures and functional units called organelles, which carry out the basic functions of the cell (see figure 1). These include for example the nucleus, which contains most of the genetic information in the form of DNA; mitochondria, the main function of which is to produce ATP; the ER, which folds and sorts proteins and routes to the Golgi, and so on. Another intracellular structure that is highly conserved is called “the cytoskeleton”. It is the main focus of this thesis, as the proteins that I have studied (microtubule plus-end tracking proteins and Navigators) act upon this structure and some of the processes that are controlled by it. In the following sections I therefore first outline the properties and functions of the three types of cytoskeletal networks. This is followed by a more in-depth description of some of the processes that involve the cytoskeleton, in particular the microtubule network. The last part of the introduction describes the various protein families controlling the behaviour and organization of the latter cytoskeleton.

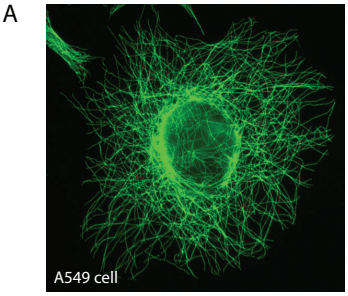

The microtubule network

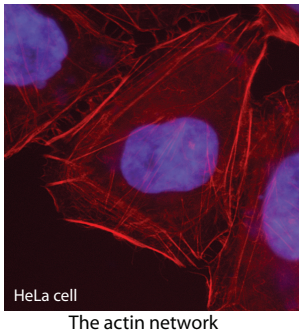

The actin network

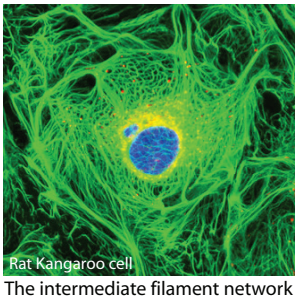

The intermediate filament network

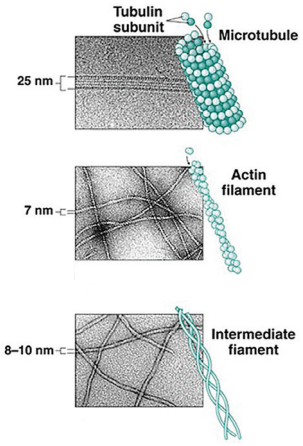

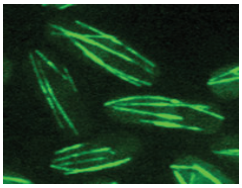

Fission Yeast MT network

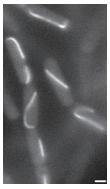

TubZ polymers,
Bacillus thuringiensis

Figure 2: The cytoskeleton
A) The microtubule network in an A549 cell as visualized by immunofluorescent labeling. (B) The actin network in a HeLa cell. (C) The intermediate filament network in a rat kangaroo kidney epithelial cell *(http://www.olympusfluoview.com/applications/protocols/cellscytokeratin.html)*. (D) Electron micrographs showing the separate cytoskeletal networks and a schematic drawing of the filaments. *(Adapted from Asking about life, A.J. Tobin & J.Dusheck, 2nd edition; http://campus.queens.edu/faculty/jannr/cells/cell%20pics/ cytoskeleton.jpg)*. (E) The MT network in fission yeast *(Damian Brunner lab website) (http://www-db.embl.de/jss/Embl GroupsHD/g_147.html)*. (F) Treadmillling TubZ polymers in Bacillus thuringiensis *(Larsen et al., 2007)*

1.2 General properties of the cytoskeleton

All eukaryotic cells contain filamentous networks of proteins that are responsible for cell shape. These networks are collectively called the cytoskeleton, a translation of the word cytosquelette which was coined by the French embryologist Paul Wintrebert in 1931 (Frixione, 2000). The cytoskeleton provides the structural support for cells, it is important for the organization of membranes and organelles inside the cell and it forms the “railways” on which intracellular transport takes place. The cytoskeleton also provides resistance against mechanical forces, it enables cells to migrate, and it is of critical importance for proper cell division.

The cytoskeleton is intimately linked to cell function, and as such, the cytoskeletal organization of different cell types varies greatly. For example, the cytoskeleton enables neurons to grow long processes, called axons and dendrites, via which they signal. On the other hand, contraction of muscle cells, which are large multinucleated cells (syncytia), is mediated by cytoskeletal elements named actomyosin filaments that form the contractile machinery and that almost completely fill up the muscle syncytium. A different type of sliding cytoskeletal elements is found in the flagellum of sperm, which enables these cells to swim. Macrophages, cells of our immune system that seek and destroy pathogens in our body, are able to migrate and even engulf invaders via quick cytoskeletal rearrangements that are different yet again. Finally, epithelial cells contain distinct apical and basolateral domains which are segregated by tight junctions acting as diffusion barriers. The cytoskeletal organization in these cells maintains this polarity and allows for polarized transport of cargoes to the correct domains (Musch, 2004).

The cytoskeleton is a very ancient structure, which has arisen early in the evolution of life and many of its different components are highly conserved (Erickson, 2007). Even prokaryotes contain cytoskeleton-like structures that play important roles in cell division and plasmid maintenance. The mammalian cytoskeleton is composed of several types of filamentous protein networks, including the actin cytoskeleton, the intermediate filament network and the microtubule network. Another cytoskeletal network is formed by the septin family. The actin and microtubule networks have been found in all eukaryotic organisms including yeast and plants cells (see figure 2).

1.3 Cytoskeletal networks

1.3.1 Actin filaments

The actin network is multifunctional: it is an important determinant of cell shape, helps in migration, mediates short range transport of cargo inside the cell, plays important roles in endocytosis, phagocytosis, cell adhesion and cell junction assembly, and is of critical importance during cell division, in particular during the final steps in the formation of two new daughter cells. An actin filament (F-actin) is composed of monomeric globular actin (G-actin), a protein of around 42 kDa. F-actin consists of 2 protofilaments that twist around each other to form a helical fiber with a diameter of around 7 nm. Actin filaments have two distinct ends, a slow growing (pointed) and a fast growing (barbed) end, because actin monomers always incorporate into the filament in the same orientation (Huxley, 1963; Wegner, 1976). Actin filaments therefore have polarity. Only ATP bound actin can incorporate into a filament. Once incorporated into a filament ATP will be hydrolysed. ADP-actin has a lower affinity for actin filaments and at the pointed end this results in loss of monomers from the filament. The mammalian genome encodes at least 6 isoforms of actin, some of which are specific for muscle, whereas other actin isoforms, (e.g. β-actin) are mainly expressed in non-muscle cells (Vandekerckhove and Weber, 1978). Actin is extremely conserved, and even in prokaryotes actin homologs have been found. An example of a prokaryotic actin homolog is ParM, which plays a role in the segregation of the bacterial genome during cell division (Garner et al., 2004; Garner et al., 2007).

Inside the cell, actin filaments are organized into different types of bundles, or fine meshworks, such as stress fibers, filopodia and lamellipodia, which have specific functions. Stress fibers are the main contractile units in non-muscle cells, and are used for migration, and for the remodeling of the extracellular matrix. Stress fibers are composed of contractile bundles of approximately 10-30 actin filaments. These bundles are held together by the actin-crosslinking proteins such as α-actinin (Pellegrin and Mellor, 2007). Filopodia are highly dynamic protrusions made of tight parallel bundles of actin with their barbed ends pushing against the plasma membrane. Filopodia are thought to be involved in the sensing of environmental cues (Passey et al., 2004). Lamellipodia are cellular protrusions that contain a fine branched meshwork of actin filaments and these are the structures that power cell migration (see paragraph 1.5.1).

The organization of actin into specific structures is mediated by actin binding proteins, among which are crosslinking, bundling, severing, and nucleating proteins. A main nucleator of actin filaments is the ARP2/3 complex (Winder and Ayscough,

2005). This complex nucleates actin filaments on the sides of existing filaments with a fixed angle of 70˚. The ARP2/3 complex is composed of 7 subunits and is active mainly at the leading edge of migrating cells. ARP2/3 can be activated by different proteins, like the WASP family members (Pollard, 2007; Pollard et al., 2000). Other actin nucleators include the formins and the protein spire (Kerkhoff, 2006; Pollard, 2007).

1.3.2 Intermediate filaments

Intermediate filaments (IFs) are long stable filaments composed of IF proteins. IFs are sturdy filaments that mainly serve to maintain the structural integrity of cells. IF proteins have variable globular domains at their N- and C- termini that play a role in assembly and stability of IFs. In addition they share a core domain consisting of four long α-helices. This core domain enables assembly into parallel coiled-coil dimers, which in turn dimerize into anti-parallel tetramers. Symmetrical tetramers are packed into a ropelike fiber with a diameter of 10 nm. IFs lack polarity because of the anti-parallel orientation of the tetramers. Unlike actin and microtubules, IF proteins do not bind nucleotides.

In humans, 65 intermediate filament proteins have been described, which can be divided into five classes, of which the keratins form the two largest. In humans 54 keratin genes have been described (Moll et al., 2008) (Oshima, 2007), which encode the “acidic” type I or the “basic” type II keratins. Keratins are abundantly expressed in epithelial cells and about ten keratins are specifically found in hair and nails. Keratins form heteropolymers by pairing type I and type II molecules (Moll et al., 2008). The other classes of IF proteins include vimentin, desmin and glial fibrillary acidic protein (GFAP) but also the neurofilaments NF-L, NF-M and NF-H, which are highly abundant in the axons of neurons, and the nuclear lamins, which form the nuclear lamina. These IFs assemble either into heteropolymers or homopolymers.

A number of genetic diseases is linked to the IF network. The symptoms are often linked to tissues that need to withstand a lot of mechanical strain such as muscles and skin. An example is Emery Dreifuss Muscular Dystrophy, which has been linked to mutations in lamin A/C or emerin. This disease is characterized by a slow degeneration of cardiac and skeletal muscles (Wilson, 2000). Another IF-related disease, Epidermolysis Bullosa Simplex, is caused by mutations in the genes encoding keratin 5 and 14, or the IF binding protein plectin 1. In this disorder the skin is extremely fragile and blisters even after the slightest mechanical stress (Pfendner et al., 2005a; Pfendner et al., 2005b).

1.3.3 Microtubules

Microtubules (MTs) are hollow cylinder-like structures with a diameter of ~25 nm. The length of MTs varies from several microns in fibroblasts to millimeters in some neurons. MTs are assembled from α/β-tubulin heterodimers that assemble in a head-to-tail fashion to form protofilaments. These protofilaments align in parallel to form a tube. Tubulin dimers in one protofilament interact laterally with the dimers in neighbouring protofilaments. Like F-actin, MTs are intrinsically polar, because tubulin dimers assemble into the MT in a head-to-tail fashion, with the beta-tubulin subunit exposed at the fast growing end (or plus-end) and the alpha-tubulin exposed at the minus-end. Because of the lateral and longitudinal bonds and the diameter of the tube, MTs are the most rigid component of the cytoskeleton (Gittes et al., 1993). Besides a structural role, MTs have other functions. For example, during mitosis MTs form the mitotic spindle that segregates the sister chromatids. MTs also form the tracks for long-range transport inside cells. Motor proteins of the kinesin and dynein family recognize the polarity of MTs and mediate transport towards plus or minus end.

In vivo, most MTs are composed of 13 protofilaments. *In vitro* grown MTs however, do not show this preference, and many contain 14 or even more protofilaments. Recently, it was shown that the addition of the *S.pombe* protein mal3 (which is homologous to the mammalian EB proteins, see paragraph 1.6.4) to the MT polymerization mixture, induces the growth of exclusively 13-protofilament MTs (des Georges et al., 2008), suggesting that specific proteins can restrict (or induce) the choice of protofilament number.

Prokaryotic tubulin homologs have been identified in different bacterial species. One of these, Ftsz, has been shown to assemble the cytokinetic ring essential for bacterial cell division (Addinall and Lutkenhaus, 1996; van den Ent et al., 2001). Another protein identified in *Bacillus thuringiensis* is named TubZ. This protein appears to be important for plasmid maintenance (Larsen et al., 2007).

1.3.4 Dynamic behaviour of MTs

MTs are very dynamic structures that can rapidly alter between growth and shrinkage states. A switch from growth to shrinkage is called “catastrophe”, while the converse process (i.e. a switch from shrinkage to growth) is called “rescue”. MTs have also been found to pause, that is, they are neither growing nor shrinking. This dynamic behavior of MTs, called dynamic instability, was first described *in vitro* (Mitchison and Kirschner, 1984). Some years later, it was shown that dynamic instability also occurs in cells (Cassimeris et al., 1988; Sammak and Borisy, 1988; Schulze and Kirschner, 1988). A dynamic MT network allows the cell to quickly adapt to a changing environment. A tubulin dimer can bind two GTP molecules. One of these molecules is trapped inside the dimer at a non-exchangable site in the α-tubulin molecule and cannot be hydrolysed. The other GTP molecule is bound at an exchangeable site, on the β-tubulin subunit, and is hydrolysed after incorporation into the MT lattice. The result of this coupled hydrolysis is that most of the β-tubulin subunits along the length of a MT contain GDP (although it was recently shown that a monoclonal antibody against GTP-tubulin recognized some patches of GTP-tubulin in the lattice (Dimitrov et al., 2008)). The conformation of GDP-bound tubulin is slightly more curved than that of GTP-tubulin. The presence of GDP-tubulin inside the lattice is therefore thought to induce mechanical strain and to favour MT depolymerisation. However, because the plus-end of a growing MT is capped by a layer of GTP-bound β-tubulin (Carlier, 1982), this so-called “GTP-cap” might protect the MT from undergoing catastrophe. Dynamic instability is linked to the hydrolysis of GTP inside the MT lattice (Hyman et al., 1992). With protected MT minus ends, dynamic instability takes place at the plus end. However, when minus ends are free, a phenomenon called “treadmilling” can occur, where MT depolymerization at the minus end is counterbalanced by growth at the plus-end, resulting in a displacement of the MT and flux (treadmilling) of subunits through the MT (Margolis and Wilson, 1981).

1.4 Organization of the MT network

The ability of the cytoskeleton to carry out its diverse and highly dynamic tasks requires an astoundingly complex network of regulatory proteins. These not only control the dynamics of the separate cytoskeletal elements but they also make sure that the different systems act in concert. In the following paragraphs I will first discuss some general mechanisms of regulation and then highlight specific aspects of the organization of the MT network.

1.4.1 General mechanisms for organizing the cytoskeleton

Many of the proteins that regulate cytoskeletal networks do this by interacting with the cytoskeleton. This can induce changes in the appearance of the network (e.g bundling), in its turnover, in its polymerization dynamics, including the nucleation of new filaments, or in the association of other proteins. Cytoskeletal elements have also been shown to exert force on each other, and this has an important function in the organization of the cytoskeleton and the regulation of cell shape. For example, the cortical actin meshwork forms a physical barrier for growing MTs. On the other hand, the actin-meshwork surrounding a MT may enhance its resistance against compressive forces (Brangwynne et al., 2006). A single growing MT can generate sufficient force to displace organelles and push out membranes. The force generated by polymerizing actin filaments in lamellipodia is what drives cell migration (see also paragraph 1.5.1). Interestingly, this force can be harnessed by intracellular bacteria, like *Listeria monocytogenes*, which can propel themselves through the cytoplasm by generating a comet of actin filaments. Most of these filaments have their barbed ends (fast growing ends) directed towards the bacterium, and actin polymerization takes place only at the front of the comet tail, pushing the bacterium forward at high speed. The force generated by the actin comet is large enough to push bacteria straight through the plasma membrane into the neighboring cells, which enables these pathogens to spread (Theriot et al., 1992).

Another way of regulating the cytoskeleton is by post-translational modification. For example, acetylation of MTs at lysine-40 of α-tubulin influences binding and motility of the MT motor protein kinesin-1 (Reed et al., 2006). Another important post-translational modification is the removal of the C-terminal tyrosine of α-tubulin by a tubulin tyrosine carboxypeptidase. This tyrosine can be added back by tubulin tyrosine ligase (TTL). The so called tubulin-tyrosination cycle (Idriss, 2000), was shown to be of vital importance for neuronal MT organization (Erck et al., 2005). Detyrosinated tubulin is a marker for stable MTs. The C-terminal tyrosine of α-tubulin has been shown to be important for the binding of a subset of MT binding proteins *in vivo* (Peris et al., 2006), including the CAP-Gly MTB containing +TIPs (see paragraph 1.6.4).

1.4.2 Centrosomal nucleation of MTs

One important way to orchestrate the organization of the cytoskeleton is to tightly regulate filament nucleation. Specialized structures are responsible for the formation of new filaments. In the case of MTs, an asymmetric distribution is often observed, in which MTs are nucleated near the cell center, at the “MT organizing center” (MTOC) and, as recently demonstrated, near the Golgi apparatus (Efimov et al., 2007). In interphase cells the MTOC, or centrosome, is usually localized near the nuclear envelope. Interestingly, in fibroblasts expressing mutant emerin, an integral nuclear membrane protein, centrosomes no longer localise near the nucleus (emerin is frequently mutated in patients suffering from Emery Dreifuss Muscular Dystrophy) (Salpingidou et al., 2007). The centrosome can both nucleate MTs and anchor them at their minus-end. The centrosome generates a radial MT array, whereas the Golgi complex nucleates a more asymmetric MT network.

The ability of centrosomes and the *trans*-Golgi network (TGN) to nucleate MTs relies on a specific isoform of tubulin named γ-tubulin. This protein is an important component of so-called γ-tubulin ring complexes (γ-TuRCs), structures with a diameter of 25-28nm that are thought to be responsible for nucleating MTs (Schnackenberg et al., 1998; Vogel et al., 1997; Zheng et al., 1995). The amount of γ-tubulin at the centrosome varies during the cell cycle (Khodjakov and Rieder, 1999), increasing at prophase, and decreasing to interphase levels when cells exit mitosis.

The rate of MT nucleation varies during the cell cycle, which does not correlate with the amount of γ-tubulin at the centrosomes (Piehl et al., 2004). Interestingly, injection of an antibody against γ-tubulin strongly decreased MT nucleation in metaphase, but much less efficiently in anaphase cells. RNAi experiments in the nematode *C. elegans* have shown that even in γ-tubulin depleted cells some MT nucleation still occurs. No centrosomal MT asters were formed in these cells during interphase, but they did appear during mitosis, although MT nucleation was much less efficient. This suggests that although γ-tubulin is the kinetically dominant centrosomal MT nucleator, alternative MT nucleation pathways exist in cells (Hannak et al., 2002).

1.4.2.1 Composition of the centrosome

The centrosome is a spherical structure that contains a pair of centrioles surrounded by a matrix, called pericentriolar material (PCM), which contains hundreds of

γ-TuRcs (Bornens, 2002). The γ-TuRcs are anchored to the centrosomal matrix by CG-NAP and kendrin (Takahashi et al., 2002). The structural stability of centrosomes and the ability to replicate depends on the centriole pair (Basto et al., 2006; Bobinnec et al., 1998). Centrioles, in turn, are composed of a cylindrical array of triplet MTs with 9-fold radial symmetry (figure 3). The centriole pair is linked to each other via a fibrous linker that associates with the proximal ends of the triplet MTs via the protein C-NAP1.

Of the two centrioles, one is more mature than the other. The mature centriole is called “mother centriole”, whereas the immature one, which is slightly shorter, is termed the “daughter centriole”. Mother and daughter centrioles have different properties. The mother centriole, for example, can develop into a basal body, from which a cilium grows. Another difference is that the mother centriole can anchor MTs, while the daughter centriole cannot (Piel et al., 2000). The mother centriole also differs structurally from the daughter in that it has nine distal and subdistal appendages. These subdistal appendages are required for MT anchorage via the protein ninein. The centrosomal matrix itself can also anchor MTs. This involves the proteins CAP350, FOP, EB1 and p150glued (Askham et al., 2002; Yan et al., 2006). In addition, it has been shown that pericentrosomal satellites, which contain PCM1, play an important role in MT anchorage (Bornens and Azimzadeh, 2007).

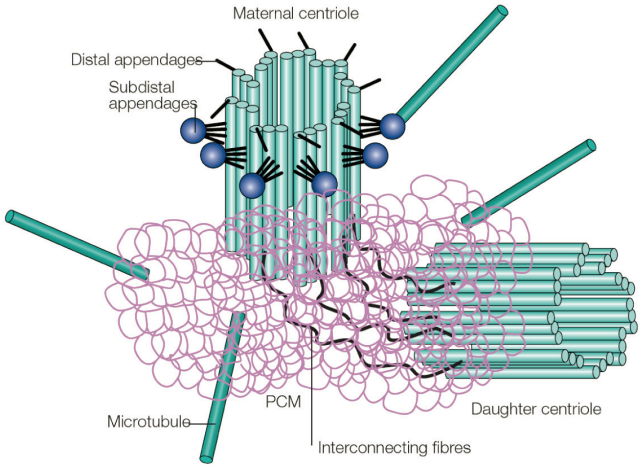

Figure 3: The centrosome
Schematic overview of the centrosome. *(Doxsey, S. 2001. Re-evaluating centrosome function. Nat Rev Mol Cell Biol. 2:688-98.)*

1.4.2.2 Centrosome replication cycle

In order to maintain the correct centrosome number in a cell, centrosomes need to be replicated. The centrosome replication cycle starts at the onset of S-phase. Replication is semiconservative (Kuriyama and Borisy, 1981), i.e. mother and daughter centrioles each serves as a “template” for a new centrosome. New daughter centrioles bud on the sides of the mother and daughter centriole. The formation of these buds requires the intracentriolar protein centrin. During G2 the mother and daughter centrioles (with their newly formed centrioles) separate. During mitosis the two separated centriole pairs localize to opposing poles of the mitotic spindle. As the cell exits from mitosis, each daughter cell inherits one centriole pair. This centriole pair disengages right after mitosis, which requires the disassembly of the fibrous linker. The separated centrioles are then ready for a next round of duplication during the following S phase (Bettencourt-Dias and Glover, 2009). It has been shown that centrosomes are inherited asymmetrically in differentiating self-renewing stem cells in *Drosophila* (Fuentealba et al., 2008; Yamashita et al., 2007).

When centrosome replication control fails or its structural integrity is disrupted, this can have dramatic effects during mitosis, because it can lead to the formation of mono- or multi-polar spindles. This may lead to abnormal chromosome segregation and can result in aneuploidy. Aneuploidy, in turn, has been linked to an increased tumor incidence (Weaver and Cleveland, 2005; Weaver and Cleveland, 2008; Weaver et al., 2007). Many proteins have been identified that play a role in centrosome replication control, including B23/nucleophosmin, BRCA1, p53, CDK1 and geminin (Bettencourt-Dias and Glover, 2009).

Remarkably enough, in *Drosophila*, the centrosome is not critical for survival. It was shown that *Drosophila* SAS-4 mutants (DSAS-4 is related to the human microcephaly protein CenpJ), that fail to form centrosomes, are viable. These flies, however, lack cilia and flagella (Basto et al., 2006). Mutant flies that lack centrosomin, which is an important PCM component essential for centrosome function, are also viable (Megraw et al., 2001). Finally, it has been shown that many *Drosophila* cell types do not contain centrosomes in interphase. Only when these cells go into mitosis do they assemble centrosomes, which are disassembled again when cells exit mitosis (Rogers et al., 2008).

1.4.3 Cell types containing non-centrosomal MTs

Although in fibroblasts the MT network is organized in a radial fashion, in many differentiated cell types the MT cytoskeleton has a completely different organization, and minus ends of MTs are not embedded in the MTOC. Such a non-centromal MT array can be generated in different ways. For example, MTs are nucleated at the centrosome and are subsequently released and transported to their final destination, where they are anchored. Alternatively, MTs are nucleated at other sites, such as the Golgi. Below, I list examples of cell types known to have a prominent non-centrosomal MT network.

Myoblasts are muscle precursor cells. During the development of the embryo, these cells fuse to form myotubes which later develop into multinucleated muscle fibers. During the transition from a mononucleated myoblast to a multinucleated myotube, the MT network rearranges dramatically. In myoblasts the MT network is similar to fibroblasts, with mostly centrosomal MTs. In myotubes however, the MT network runs parallel along the long axis of the myotube. Myotubes do not contain centrosomes, and MTs appear to be nucleated in the cytoplasm, where they often colocalize with γ-tubulin. The protein pericentrin, which normally localizes to centrosomes, localizes to the nuclear envelope in myotubes (Musa et al., 2003).

Epithelial cells also contain many non-centrosomal MTs, with most MT minus-ends oriented towards the apical side and most plus-ends pointing towards the basolateral membrane. This polar organization is thought to facilitate the directional transport of specific membrane components that define the highly divergent basolateral and apical surfaces (Musch, 2004).

Neurons are another cell type with a mainly non-centrosomal MT network. The neuronal centrosome is found in the cell body, yet MTs need to reach the outer ends of dendrites and axons. The length of these compartments greatly surpasses that of an average MT. Thus, MTs can not be embedded in the centrosome. In axons, virtually all MT plus-ends are oriented towards the growth cone, whereas in dendrites, MTs have a mixed orientation (Baas et al., 1988). It has been suggested that the polarity of the MT array in axons and dendrites plays a role in the sorting of specific cargo into these different neuronal compartments. There is still debate about the origin of most MTs inside the processes of neurons. In neurons only few MTs are linked to the centrosome. It has however been shown that MTs can be nucleated at the neuronal centrosome, and it was suggested that these MTs are subsequently released and actively transported away from the centrosome and into the neurites (Baas et al., 2005; Yu et al., 1993). MT release from the neuronal centrosome was

shown to involve katanin, a MT severing enzyme, as microinjection of a katanin antibody dramatically increased the number of MTs around the neuronal centrosome (Ahmad et al., 1999).

1.5 Specific cellular processes requiring actin and MTs

Many cellular processes are dependent on an intact and well functioning cytoskeletal network. I have, for example, touched upon MT-mediated transport. For a comprehension of the function of the navigator proteins, I will focus in the following sections on cell migration, axon outgrowth, and mitosis, and the involvement of actin and MTs.

1.5.1 Cell migration

Cell migration is important at various stages of differentiation and development, as well as in adult life. The coordinated migration of cells is often controlled by gradients of specific extracellular cues, called chemo-attractants or -repellents. Chemotaxis drives wound closure, enables leukocytes to migrate through the endothelium of the blood vessel wall and move to sites of inflammation, and plays an important role during the development of an embryo. In cell culture systems migration has been extensively studied in fibroblasts. In these cells migration involves the formation of a protrusion in the direction of migration, which is subsequently stabilized by attachment of the protrusion to the extracellular matrix (ECM). Such attachments, called focal adhesions, need to be dismantled as the cell body moves forward, to allow retraction of the trailing part of the cell (Vicente-Manzanares et al., 2005; Webb et al., 2002).

The actin network provides a lot of the force required for migration, while MTs are thought to be more important for the directionality of migration and the control of cell adhesion. For example, the contractile forces on focal adhesions require actin inside acto-myosin stress fibers. Actin also forms the protrusions (lamellipodia) that push the cell front forward. The lamellipodium at the leading edge forms the “motor” of cell migration. It contains a fine meshwork of actin filaments that have their barbed (growing) ends oriented towards the cell front. Polymerization of this network takes place strictly at the cell edge and this provides the protrusive force that pushes the cell forward. At the rear of the lamellipodium the actin network is disassembled. Actin polymerization in the lamellipodium is thought to be mainly mediated by the Arp2/3 complex which nucleates actin filaments on the sides of existing filaments

(see paragraph 1.3.1) (Borisy and Svitkina, 2000; Small et al., 1998; Wang, 1985). However, RNAi mediated knockdown of its subunits Arp3 did not impair migration of fibroblasts, and lamellipodia still formed normally in these cells (Di Nardo et al., 2005).

Cell migration requires a tight local control over the actin polymerization machinery. This is mediated by a highly complex network of signaling molecules. At the top of the signaling cascade one can find the Rho-GTPase family members, which are molecular switches that link membrane receptors to the cytoskeleton. Around 20 mammalian Rho-GTPases have been described, of which Rho, Cdc42 and Rac are the best characterized.

1.5.2 Rho-GTPases and cell migration

Rho-GTPases cycle between an active GTP bound and an inactive GDP bound state. This is regulated by the “guanine nucleotide exchange factors” (GEFs), which enhance the exchange of GDP for GTP, and “GTPase-activating proteins” (GAPs), which enhance hydrolysis of GTP bound by active Rho-GTPases, thereby causing inactivation. The human genome encodes more than 60 GEFs and 70 GAPs, which makes the control of Rho GTPases complex.

The first identified Rho-GTPase was RhoA. RhoA can be activated by Lysophosphatidic acid (LPA) via the G-protein coupled receptors LPA1, -2 and -3, which require PDZ domain-containing Rho-GEFs to activate RhoA. Active RhoA induces formation of stress fibers and focal adhesions (via the activation of Rho kinase (Rock)). Activation of other Rho-GTPases gives rise to different types of actin remodeling. For example, Rac and Cdc42 have completely different effects on the actin network compared to RhoA and to each other. Rac induces the formation of lamellipodia and membrane ruffles, while Cdc42 induces the formation of filopodia. Rho-GTPases also regulate each other, for example, Cdc42 can activate Rac, and Rac can activate Rho (Etienne-Manneville and Hall, 2002; Hall, 1998; Hall, 2005; Yamada et al., 2005). Rho-GTPases exert their effects on the actin network by activating different protein complexes. One of the targets of these proteins is the Arp2/3 complex. Well characterized activators of Arp2/3 include WASP, N-WASP and the WAVE/Scar complex. Rac has been shown to activate WAVE/Scar, which in turn activates Arp2/3. Cdc42 can activate WASP and N-WASP.

During migration, adhesion is started at the front of the lamellipodium by the formation of small adhesion clusters called focal complexes. These contain both integrins and adapter proteins. Integrins are a family of transmembrane receptors

that bind to ECM proteins and link the ECM to the cytoskeleton via adaptor proteins such as talin, vinculin, filamin and actinin (Critchley, 2004; Critchley et al., 1999). The formation of small integrin containing adhesion clusters is stimulated by Rac. Fluorescence-based microscopy studies have revealed that active Rac is mainly localized at the leading edge of the lamellipodium (Kraynov et al., 2000).

Focal complexes can mature into focal adhesions (FAs), which are not only adhesion sites, but also important signaling platforms. FAs contain more than 50 proteins, including paxillin, an adapter protein that recruits structural and signaling molecules to FAs (Zamir and Geiger, 2001) (Brown and Turner, 2004). FA disassembly at the rear of cells is critical for migration of many adherent cells (Webb et al., 2002). Disassembly involves dynamin-mediated endocytosis, myosin–mediated contractility, and proteolysis of adhesion molecules such as talin, which was shown to be cleaved by calpain (Franco et al., 2004).

The disassembly of FAs also involves MTs. Treatment of cells with nocodazole, a potent MT depolymerizing agent, results in an increased number of stress fibers and an increased size and number of focal adhesions. This is because MT depolymerization induces Rho. When nocodazole is washed out, FAs are disassembled in a Rho-independent manner (Bershadsky et al., 1996; Ezratty et al., 2005; Liu et al., 1998). FAs are targeted by MTs, and this causes their disassembly (Kaverina et al., 1999; Krylyshkina et al., 2003). Kinesin-1 is required for this process, and it was speculated that this protein transports components to the adhesion site that promote disassembly (Krylyshkina et al., 2002). Recently, it was shown that efficient targeting of MTs to FAs requires the MT plus-end tracking protein ACF7, which was shown to be important for MT guidance along F-actin (see paragraph 1.6.4).

The MT network appears to contribute in various ways to proper cell migration. For example, in fibroblasts and astrocytes perturbation of the MT network inhibits the formation of lamellipodia (Etienne-Manneville, 2004; Liao et al., 1995), suggesting crosstalk between actin and MTs. Furthermore it is thought that a polarized MT network contributes to polarized trafficking of cargoes. The MT network is selectively stabilized at the leading edge of migrating cells by several protein complexes, including proteins that localize to MT plus-ends, such as CLASPs and APC (see the +TIPs section in paragraph 1.6.4). Rho-GTPases take part in the regulation of the MT network in migrating cells. Cdc42, for example, stimulates the reorientation of the MTOC towards the leading edge of migrating cells. Rho-GTPases can however also regulate the dynamics of individual MTs. It has, for example, been shown that

the Cdc42/Rac effector IQGAP can capture MT ends via the MT end binding protein CLIP170 (Fukata et al., 2002; Gundersen, 2002). Interestingly it was also shown that IQGAP can form a ternary complex with activated Rac1/Cdc42 and APC to modulate actin and MT dynamics (Watanabe et al., 2005; Watanabe et al., 2004).

1.5.3 Axon guidance

Neurons project axons to targets that can be hundreds of microns away from the cell body. These axons extend along tightly constrained pathways created by specific attraction and repulsion signals in concert with alternating protein expression by the neuron itself. A well studied example of this is the *Xenopus* retinal ganglion cell, which projects its axon to the optic nerve by following a complex pathway involving multiple guidance cues (Campbell et al., 2001; de la Torre et al., 1997). The growth cone, a structure at the tip of a neurite, seems to be largely responsible for the outgrowth and guidance of axons. The growth cone is the place where signals are interpreted and translated into the cytoskeletal rearrangements required for rapidly changing directions. This was nicely documented by Harris et al. in 1987, who showed that when a growth cone is severed from the cell body it will continue to migrate in the correct direction (Harris et al., 1987). Some years later, it was shown that severed growth cones in culture can autonomously respond to the guidance molecules netrin and Sema3A. Interestingly, it was also shown that the response downstream of these guidance cues involves the translational machinery and a functional proteasome, suggesting that inside the growth cone specific translation and protein degradation takes place, which are both required for growth cone guidance (Campbell and Holt, 2001; Dickson and Senti, 2002; Harris et al., 1987).

Different guidance molecules have been identified so far, including members of the netrin family (Bradford et al., 2009; Serafini et al., 1994), slit, semaphorin, ephrin, as well as factors like FGF and the morphogen sonic hedgehog (Dickson, 2002; Stoeckli, 2006). These guidance molecules bind to specific receptors on the surface of the growth cone. It is thought that the receptors for Netrin-1, Sema3A, BDNF and other guidance molecules are associated with, and depend on, lipid rafts for proper functioning. When lipid rafts are disrupted, growth cones fail to respond to specific chemotactants (Guirland et al., 2004).

Chemotactants can be both “attractive” and “repulsive” for a particular growth cone. In part this depends on the expression of different receptors for the same guidance molecule. For example, it has been shown that the receptor Deleted in Colorectal Carcinoma (DCC) mediates netrin attraction and that the Unc-5 receptor

mediates axon repulsion by netrin, depending on a netrin-induced interaction between Unc-5 and DCC (Chisholm and Tessier-Lavigne, 1999; Hong et al., 1999). Interestingly, cells have been shown to switch their response to netrin. Netrin initially attracts and later repels the axons of *Xenopus* retinal ganglion cells (RGC), as they exit the eye and project to the brain. In cultured RGCs the netrin response correlates with the age of the cells. Young RGC are attracted by netrin, and older cells are repelled by it. The older cells express lower levels of the DCC receptor and had lower levels of cAMP, another netrin response factor (Cohen-Cory, 2002; Shewan et al., 2002). During development a hierarchy of guidance cues determines axonal pathfinding at the CNS midline. The midline itself is a source of netrin, which attracts crossing axons towards and into the midline. Interestingly, netrin responsiveness is lost following midline crossing, and another protein, named slit, takes over. Slit, a chemorepellent also produced at the midline, binds to Roundabout (Robo) receptors, which mediate repulsion of axons away from the midline (Giger and Kolodkin, 2001).

1.5.4 Coupling external signals to internal organization in axon guidance

Downstream of activated guidance receptors specific signaling pathways exist that mediate cytoskeletal rearrangements required for axon guidance. Chemoattractants are thought to activate Cdc42 and Rac, which are both positive regulators of growth cone progression. An example of this is the netrin attraction pathway. Netrin-1 binds the DCC receptor, which activates the Rho GEF Trio. Trio in turn activates Rac, which stimulates growth cone protrusion (Briancon-Marjollet et al., 2008). In contrast, Rho activation has been shown to induce growth cone collapse and neurite retraction (Hall, 1998). Repulsion cues are therefore thought to activate Rho (see Figure 4B). An example of this is RGMa, a repulsive guidance molecule that binds to the Unc-5 receptor, which in turn signals to LARG, a PDZ domain containing Rho GEF. The activation of LARG is followed by RhoA activation and growth cone collapse (Hata et al., 2009). MTs play an important role in the guidance of growth cones. Taxol, a MT stabilizing agent, and nocodazole, a MT depolymerizing agent, can induce growth cone turning when applied locally (Buck and Zheng, 2002). MTs are capable of inducing asymmetry in the shape of the growth cone, and stabilize a growth cone in a specific direction, downstream of guidance cues. Inside the axon shaft MTs form a parallel array, but in the growth cone these parallel bundles splay apart. Dynamic MTs extend into the peripheral domain (see Figure 4a) and into filopodia where they

interact with F-actin bundles (Dent and Gertler, 2003; Zhou et al., 2002). Proteins that associate with the growing plus-ends of MTs, play important roles in growth cone guidance (see paragraph 1.6.4 for more info on +TIPs). Recently the actin binding protein drebrin was shown to interact with the MT plus-end binding protein EB3 inside filopodia, and this interaction is important during neuritogenesis (Geraldo et al., 2008).(see paragraph 1.6.4)

Besides EB3, other MT plus-end binding proteins have been coupled to growth cone steering behavior, including APC, CLASP and Neuron Navigator 1 (Martinez-Lopez et al., 2005; Zhou et al., 2004). In Xenopus growth cones, CLASP associates with a specific subset of MTs that extend into the peripheral domain of the growth cone. Interestingly, high level expression of CLASP led to reduced MT growth and leading edge advance of growth cones. In addition, its *Drosophila* orthologue Orbit/MAST was shown to function downstream of Abl tyrosine kinase in the Slit repulsion pathway, which repels axons from the midline (Lee et al., 2004).

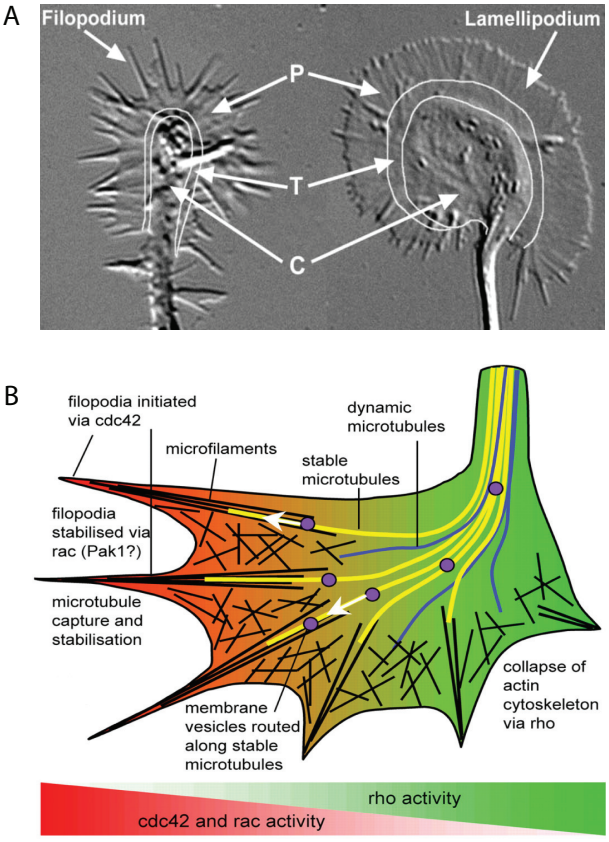

Figure 4: Growth cone morphology and steering
A) Pictures of growth cones, showing the central (C), transitional(T) and peripheral domains (P). *(Dent and Gertler, 2003)*
B) Schematic overview of growth cone turning. Cdc42 and Rac are positive regulators of growth cone progression, whereas Rho activation induces growthcone collapse *(adapted from Rajnicek, A.M., L.E. Foubister, and C.D. McCaig. 2006. Growth cone steering by a physiological electric field requires dynamic microtubules, microfilaments and Rac-mediated filopodial asymmetry. J Cell Sci. 119:1736-45)*

1.5.5 The MT network during cell division

Cell division requires drastic rearrangements of the interior of the cell. Genetic material and organelles must be divided over the daughter cells. Mitosis proceeds in multiple steps (McIntosh and Koonce, 1989)(see Figure 5). The cytoskeleton plays an important role in this process. MTs, for example, form the mitotic spindle, which segregates the sister chromatids, whereas actin forms the contractile system that pinches apart the two daughter cells during the last stages of cell division.

During mitosis, the MT network is organized into a bipolar spindle with centrosomes located at both poles (see Figure 5). Most MT minus ends are oriented towards the poles of the spindle. Astral MTs are important for positioning the spindle (Gadde and Heald, 2004; Wittmann et al., 2001). To physically separate the sister chromatids, MT bundles (or K-fibres) attach to the chromatids via kinetochores, which are large multiprotein complexes that assemble onto centromeric DNA (Maiato et al., 2004; McIntosh et al., 2002; Rieder and Salmon, 1998). Two sister kinetochores assemble on one chromosome (which at this point consists of two sister chromatids), and these connect to K-fibers of different poles. More than 80 proteins have been identified that play a role in the attachment of MTs to the kinetochores (Cheeseman and Desai, 2008; Kotwaliwale and Biggins, 2006). These proteins include MT-end binding proteins such as CLASP1 and CLASP2 (Maiato et al., 2003; Mimori-Kiyosue et al., 2006; Pereira et al., 2006).

Tubulin subunits inside K-fibers move towards the poles by a mechanism called poleward flux. This is caused by depolymerization of MTs at MT minus ends and polymerization at plus ends. In Drosophila it has been shown that this flux is generated by the motor protein KLP10a, which is localized at the spindle poles. When chromosomes segregate, the plus-ends of kinetochore attached MTs also start to depolymerize, while the chromosomes stay attached to the K-fibers. Recently it was shown that the Ndc80 kinetochore complex can form load bearing attachments to depolymerizing MTs via biased diffusion (Powers et al., 2009). It has been shown that depolymerization of K-fibers is stimulated by the action of MT severing enzymes including the protein katanin. The combined action of poleward flux and plus-end depolymerization is called the pacman and flux mechanism. This is what generates the movement of the chromosomes towards the spindle poles (McIntosh et al., 2002; Rogers et al., 2005; Zhang et al., 2007).

Interpolar MTs emanate from the spindle poles and connect to MTs of the opposite pole. These antiparallel MTs are linked together via Eg5, a plus-end directed tetrameric kinesin (Sharp et al., 1999). *In vitro*, Eg5 was shown to crosslink

and slide antiparallel MTs (Kapitein et al., 2005). Eg5 action elongates the spindle, as this motor protein walks towards the plus-end thereby “pushing” MT minus-ends away from each other (Valentine et al., 2006). Recently it was shown that this activity of Eg5 is counteracted by dynein, Lis1 and CLIP170 (Tanenbaum et al., 2008).

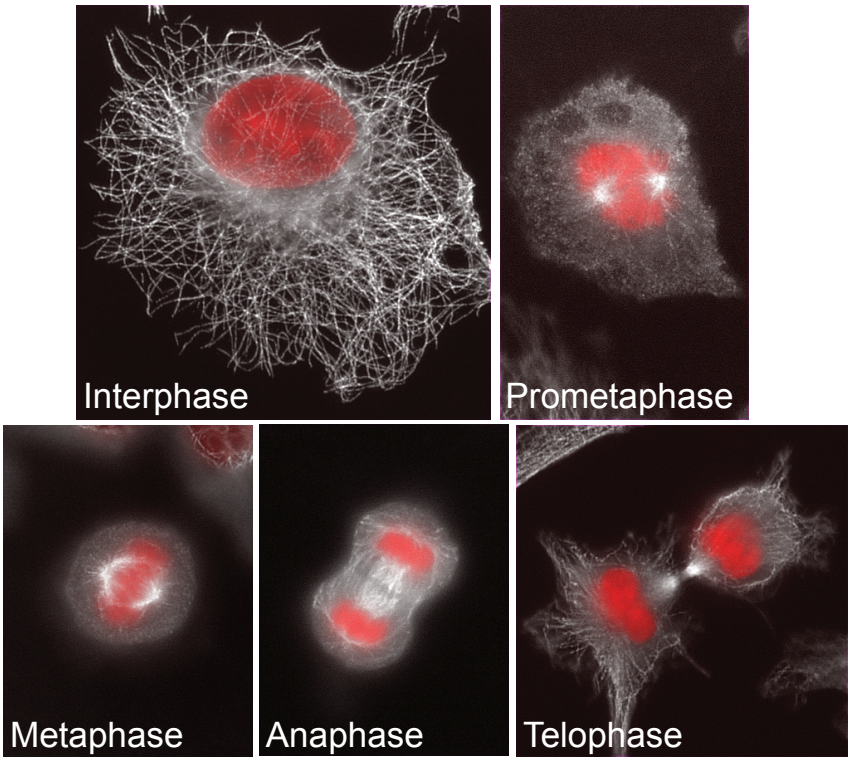

Figure 5: The Microtubule network during mitosis
The MT network (white) and DNA (red) during interphase and mitosis in A549 cells. During Prophase, the centrosomes move to opposite poles of the cell and the chromatin in the nucleus starts to condense (not shown). Prometaphase: The nuclear envelope breaks down and kinetochores start to form around the centromeres. MT bundles associate with the kinetochores and start with the alignment of the chromosomes at the equatorial plane. Metaphase: chromosomes are aligned at the equatorial plane. The spindle is held in position by astral MTs that interact with the cell cortex. Anaphase: during anaphase, the chromatids are pulled towards the poles of the spindle. Telophase: the nuclear envelope reassembles around the separated sister chromosomes. Cleavage furrow progresses and this requires a contractile cortical actomyosin network. Myosins are activated (by phosphorylation) specifically in a ring in the middle of the spindle. During the final step of mitosis the two daughter cells physically separate in a process called cytokinesis.

1.6 MT associated proteins

Thus far I have focused on the organization of the cytoskeleton, and the processes it regulates, with a particular emphasis on MTs. In the following sections I will describe proteins that are known to regulate the behaviour of the MT network. I have divided these sections according to the main localization of the respective proteins.

1.6.1 General MAPs

Proteins that can associate with MTs are collectively called MT-associated proteins, or MAPs. The first MAPs were found because they co-purified with brain MTs, in a protocol that employed multiple rounds of MT polymerization and depolymerization (Shelanski et al., 1973). The first MAPs identified were called MAP1 and 2 (Murphy and Borisy, 1975). These structural MAPs bind along the MTs and were found to stimulate MT assembly. Other MAPs have been found to stabilize MTs, crosslink MTs into bundles, enhance the polymerization of MTs or suppress catastrophe. The MAP family includes high molecular weight MAPs like MAP1A, MAP1B, MAP2 and MAP4 and smaller MAPs like Tau. Some MAPs can crosslink MTs to other cytoskeletal elements (Maccioni and Cambiazo, 1995).

MAPs tend to have repeating MT binding (MTB) domains, which enable them to bind to more than one tubulin dimer (Amos and Schlieper, 2005; Maccioni and Cambiazo, 1995). MAPs are usually extended molecules whose binding to MTs is regulated by phosphorylation (Cassimeris and Spittle, 2001). MAP2 and Tau are prototypic MAPs predominantly expressed in neurons. Both proteins stimulate MT polymerization and suppress catastrophe. Interestingly, it has been shown that MAP2c can also bind to F-actin via its MTB domain (Roger et al., 2004). Many MAPs play an important role in the brain where they often have a function in neuronal migration. Defects in axonal outgrowth and neuronal migration have been described in mice with disrupted MAP1b and Tau genes (Takei et al., 2000). In humans, increased phosphorylation of Tau has been linked to Alzheimer's disease, a progressive degenerative disease of the brain that results in dementia (Gendron and Petrucelli, 2009).

An important MAP is ch-TOG/XMAP215. This protein was shown to play a role in mitotic spindle organization in human somatic cells (Gergely et al., 2003). Ch-TOG/XMAP215 increases MT polymerization speed 8 fold in *Xenopus* egg extracts (Gard and Kirschner, 1987), but at high concentrations it can also induce depolymerization. Kerssemakers et al. used a clever *in vitro* system to investigate

the mechanism by which XMAP215 affects MT polymerization. They coupled an axoneme to a bead that was held in place by an optical trap. Next they grew MTs from the axoneme against a barrier. The growing MTs caused displacement of the bead. When they added XMAP215 to the system they observed bead-displacements of 40-60 nm, which is far greater than a single tubulin dimer (8nm). This suggested a model whereby XMAP215 incorporates preformed short protofilaments into the MT lattice (Kerssemakers et al., 2006). This fits with a previous finding that XMAP215 can induce the formation of partial oligomeric rings of tubulin (Cassimeris et al., 2001). In contrast, others have shown that XMAP215 is a processive MT polymerase that binds one tubulin-dimer in solution (Asbury, 2008; Brouhard et al., 2008).

1.6.2 MT severing enzymes

A special subfamily of the MAPs are the MT severing enzymes of which three have been identified so far, i.e. Katanin, Spastin and Fidgetin. These enzymes belong to the AAA+ ATPase family of ATP hydrolyzing enzymes (see paragraph 1.7.3). All three enzymes have been shown to play a role in the pacman and flux mechanism that moves chromosomes during mitosis (Zhang et al., 2007). Katanin was the first MT severing enzyme identified (McNally and Vale, 1993). It functions not only in mitosis but also in the outgrowth of neurons; katanin and spastin both play a role in axonal branching (Ahmad et al., 1999; Karabay et al., 2004; Yu et al., 2008).

Spastin and katanin use a similar AAA domain for severing MTs, but their MT binding domain differs (Roll-Mecak and Vale, 2005) (for more information about how these AAA-ATPases work, see paragraph 1.7.3). Spastin is frequently mutated in patients with Hereditary Spastic Paraplegia, a neurodegenerative disorder characterized by progressive spasticity of the lower limbs (Burger et al., 2000). Some mutations in patients were found to affect MT severing activity. Mutations in the MT severing enzyme fidgetin have been shown to lead to reduced or absent semicircular canals, microphthalmia and skeletal abnormalities (Yang et al., 2005).

1.6.3 Motor proteins

MTs form the intracellular “railroads” for transport of cargo throughout the cell. The transporters are molecular motors. These can be divided into two subclasses: motors that walk towards the plus-end and motors that are minus-end directed (Schroer, 2000). Most motor proteins of the kinesin family are plus-end directed motors. Kinesins have a globular motor domain located in their heavy chain, which hydrolyses ATP and which mediates MT binding. One of the best studied kinesins, kinesin-1 forms homodimers via its central coiled coil regions, and has two motor domains which it uses to “walk” along the MT. The C-terminal tail of kinesins is important for their binding to cargo (Hirokawa et al., 1989). Kinesins not only have a role in the actual transport of specific components and organelles in interphase, they also participate in mitosis, for example reeling in the kinetochore MTs and their attached chromosomes towards the spindle poles.

A remarkable kinesin is MCAK. This kinesin localizes to the ends of growing MTs and uses its enzymatic activity to induce depolymerization of MTs from their plus-ends. It is thought that MT destabilizing kinesins have affinity for a more curved conformation of MT ends (Desai et al., 1999).

Dyneins are minus-end directed motor proteins. Two types of dyneins exist, axonemal and cytoplasmic dynein. Axonemal dynein is found in cilia and flagella and is crucial for their mechanical action, i.e. beating (Milisav, 1998; Woolley, 2000). This leaves cytoplasmic dynein as the major MT minus-end directed motor inside the cyoplasm of cells. In addition, cytoplasmic dynein also mediates transport inside cilia. The heavy chain of cytoplasmic dynein contains the motor domain, which has 6 tandem AAA+ type ATPase regions, that fold in to a ring structure (Neuwald et al., 1999) (King, 2000). Dynein consist of a dimer of the heavy chains and intermediate and light chains. Because dyneins and kinesins differ in their motor domain, the mechanisms they use to move along MTs is also different.

Cytoplasmic dynein interacts with the dynactin complex, and this is thought to be important for linking cargo to dynein. This multisubunit complex contains the MT end binding protein p150glued, which may help to stabilize the interaction of dynein with the MT lattice, and is required for most types of cytoplasmic dynein activity (Schroer, 2004). Interestingly it has also been shown that p150glued interacts with kinesin (Deacon et al., 2003).

1.6.4 MT plus-end tracking proteins

A subclass of MAPs was discovered ~10 years ago that specifically recognizes the growing ends of MTs and was therefore name “plus-end-tracking protein”, or +TIP in its abbreviated form (Schuyler and Pellman, 2001) (see Figure 6). The first plus-end-tracking protein described was CLIP-170. A GFP-fusion protein of CLIP-170 showed comet-like fluorescent dashes in living cells, moving mostly from the cell center to the periphery (Diamantopoulos et al., 1999; Perez et al., 1999; Rickard and Kreis, 1990). Since its initial description the +TIP family has expanded, and over 15 +TIPs have already been described (Akhmanova and Steinmetz, 2008). The biochemical function of +TIPs varies greatly. Many influence MT dynamic instability, and some are able to link MTs to cellular structures like vesicles, the cell membrane, and other cytoskeletal elements (Akhmanova and Hoogenraad, 2005; Galjart and Perez, 2003).

The intracellular function of +TIPs also varies. For example, +TIPs are essential in mitosis, regulating MT-kinetochore attachments and spindle length. A special +TIP is Drosophila RhoGEF2, which is involved in signal transduction (Rogers et al., 2004). Several +TIPs play a role during cell migration, neuronal outgrowth and axon guidance (Dent and Gertler, 2003; Watanabe et al., 2005). These +TIPs include CLASPs, APC and Navigators (Lee et al., 2004; Martinez-Lopez et al., 2005; Zhou et al., 2004). Recently it was shown that a novel +TIP named STIM1 can remodel the ER network, by linking it to growing MTs (Grigoriev et al., 2008). The mechanisms by which +TIPs accumulate at MT ends will be discussed in the next paragraph (1.6.5).

Members of the mammalian +TIP family are conserved throughout evolution and orthologs can be found in different species. However, different species may have a different number of orthologous proteins. For example, three mammalian end binding (EB) proteins have been identified, whereas only one protein exists in fission and budding yeast (mal3p and bim1p, respectively), and 5 proteins in *Drosophila*. EB family members associate with both MT plus-ends and centrosomes (Berrueta et al., 1998; Bu and Su, 2001; Juwana et al., 1999). These proteins have a similar domain architecture, with an N-terminal calponin homology (CH) domain, a central coiled-coil domain which is responsible for dimerization and protein-protein interactions, and an acidic C-terminal tail. The C-terminal domain of EB1 and EB3 (including the EBH domain and the acidic tail) is important for their interaction with CLASPs, APC, p150(glued) and ACF7, which are also +TIPs (Bu and Su, 2003; Mimori-Kiyosue et al., 2005; Slep et al., 2005). EB2 is slightly different with an additional 43 amino acids at the N-terminus and a slightly differing C-terminal tail. It is likely that

there is partial redundancy between EB proteins, but specific functions have also been demonstrated. For example, EB1 and EB3 have been shown to control the association of CLIPs with MT ends, while EB2 does not (Komarova et al., 2005). EB3 has a specific function in myoblast fusion that can not be replaced by EB1 (Straube and Merdes, 2007).

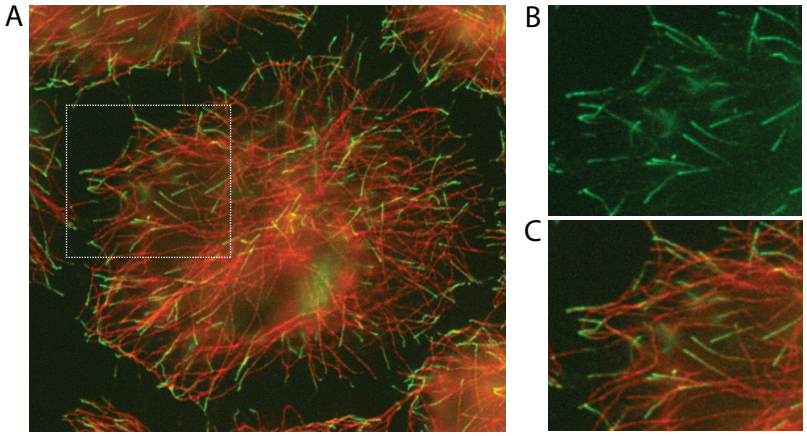

Figure 6: The microtubule plus-end tracking protein EB1
HeLa cells, microtubules are labeled in red, EB1 is labeled in green.
(A) Picture showing the MT network and EB1 staining in HeLa cells. (B) Enlargement of A showing EB1. (C) Enlargement of A showing EB1 and the MT network.

In the last years it has become clear that EB proteins (especially EB1 and EB3) form the “master +TIPs” that interact with every other +TIP described to date (Lansbergen and Akhmanova, 2006; Morrison, 2007). EB1 was first described as an interaction partner of the adenomatous polyposis gene product, APC (Su et al., 1995), and its original name stems from the fact that it interacts with the C-terminus (the end) of APC. Most +TIPs directly interact with EB proteins. In addition, the plus-end localization of many +TIPs requires EBs. This has been shown *in vivo* by knocking down EBs (Grigoriev et al., 2008; Jaworski et al., 2009; Komarova et al., 2005), but it has also been demonstrated *in vitro* (Bieling et al., 2008; Bieling et al., 2007; Dixit et al., 2009). EB1 itself uses a calponin homology (CH) domain to associate with MT ends. Recently it was shown that a single EB1 CH domain alone is sufficient to track MT ends (Komarova et al., 2009).

Several motifs have been identified in other +TIPs that mediate their interaction with MT plus-ends. CLIP-170, and its homologues CLIP-115, as well as p150glued, contain CAP-Gly (Cytoskeleton-associated protein glycine-rich) MTB

domains. It has been shown that these domains in CLIP170 can bind to the EEY/F motif at the C-terminus of both tyrosinated α-tubulin and EB1/3 molecules. Besides binding to the EEY/F motif some CAP-Gly motifs have been shown to bind to the EB homology (EBH domain), a domain of around 50 aminoacids near the C-terminus of EBs, which consists of an antiparallel four-helix bundle. The EBH domain has a deep hydrophobic cavity on its surface, which mediates interactions with other +TIPs (Hayashi et al., 2007; Honnappa et al., 2006; Mishima et al., 2007; Steinmetz and Akhmanova, 2008; Su and Qi, 2001; Weisbrich et al., 2007). Many +TIPs have been found to contain an IP-diresidue in their EB interaction domain, which has been shown to be essential for the interaction of EB1 and APC (Honnappa et al., 2005; Mimori-Kiyosue et al., 2005).

Cytoplasmic Linker Proteins (CLIPs) are MT rescue factors (Komarova et al., 2002). Interestingly, CLIP170 was initially actually shown to link endocytic vesicles to MTs (Pierre et al., 1992). Later on it was shown that CLIP170 can associate with kinetochores via its C-terminus (Dujardin et al., 1998). After these studies the role of CLIP-170 at MT ends was highlighted. *In vivo*, CLIP170 was shown to be important for the formation of the spermatid manchette, and consistently CLIP170 knockout mice have reduced fertility (Akhmanova et al., 2005).

CLIP170 forms a long rod shaped dimer of around 135 nm with two kinks in the central rod domain, which make it a flexible molecule (Scheel et al., 1999). At the N-terminus each monomer has two CAP-Gly motifs responsible for MT binding. In the central region of the protein coiled coils are found which mediate dimerization and at the C-terminus, each CLIP170 monomer has 2 zinc-knuckle domains, which mediate interactions with other proteins and itself. Besides association with EBs, CLIP170 interacts with several proteins including p150glued, LIS1 and CLASPs (Coquelle et al., 2002). CLIP170 has been shown to fold back on itself via an intramolecular interaction of the CAP-Gly domains and the C-terminal zinc-knuckles, which is thought to inactivate it from binding to MTs, and its binding partners, p150glued and LIS1 (Lansbergen et al., 2004).

CLIP115 resembles CLIP170 but lacks C-terminal zinc-knuckles (De Zeeuw et al., 1997). Like CLIP170, it forms a dimer and contains 2 CAP-Gly domains per monomer. Together with an adjacent basic, serine-rich regions, these are necessary for its ability to bind MTs (Hoogenraad et al., 2000). CLIP displacement from MT ends by a dominant negative approach resulted in a sevenfold reduction in the catastrophe frequency of MTs in cultured cells. The normal phenotype could be restored by expression of the CAP-Gly-motif containing head domain of CLIP-170 (Komarova et

al., 2002). These results show that CLIPs are MT rescue factors. Consistently, it was shown that the purified dimeric head domain of CLIP-170 can promote MT rescue *in vitro*, and that this fragment induces the formation of oligomeric tubulin rings (Arnal et al., 2004; Galjart, 2005).

The CLIP-Associating Proteins (CLASPs) were first found as interaction partners of CLIP-115 and CLIP-170. It was reported that these proteins colocalized with CLIPs at MT plus-ends and had a MT stabilizing effect (Akhmanova et al., 2001). CLASPs localize to MT plus-ends, the Golgi apparatus, kinetochores and the cell cortex. Even though CLASP and CLIPs interact directly, CLIPs appear to be less important for CLASP plus-end localization, because when CLIP-170 was removed from the MT end by expression of a dominant negative construct, this did not affect CLASP localization to MT ends (Komarova et al., 2002). Furthermore it was shown that in TTL knockout fibroblasts, CLASPs still localize to plus-ends while CLIPs cannot (Peris et al., 2006).

CLASPs are interesting proteins because they can stabilize MTs in a highly selective manner. CLASP1 and 2 have been shown to bind to EB1 and stabilize MTs at the cell cortex (Akhmanova et al., 2001; Mimori-Kiyosue et al., 2005). CLASP localization to the cortex requires a complex of the proteins ELKS and LL5β. It was also shown that CLASPs attach MT ends to the cortex via a complex with these proteins (Lansbergen et al., 2006). Furthermore, CLASP2 is important for the persistent motility of mouse embryonic fibroblasts. CLASP knockout fibroblasts migrate with a similar speed as wild type cells but show a more random migration pattern. CLASP2 was shown to stabilize MTs at the leading edge of migrating fibroblasts. In addition it was shown that CLASP2 requires the protein ACF7 for its cortical localization. It is unclear if ACF7 and LL5β/ELKS reside in the same complex (Drabek et al., 2006). Phosphorylation can regulate CLASP localization as it was shown that inactivation of GSK3β resulted in increased accumulation of CLASP2 at MT ends (Akhmanova et al., 2001). It was also shown that CLASP binds along the MT lattice in the lamellipodia of migrating Ptk1 cells, and that this is regulated downstream of Rac1 and GSK3β (Wittmann and Waterman-Storer, 2005).

Another +TIP, ACF7, is a 600kDa ATPase that belongs to the spectraplakin family, which also includes the mammalian BPAG1 and the Drosophila short stop protein. Spektraplakins crosslink different cytoskeletal elements, and link the cytoskeleton to the plasma membrane (Roper et al., 2002). ACF7 can associate with both actin and MT networks (Karakesisoglou et al., 2000). This giant protein localizes to MT-ends and focal adhesions and has been shown to guide MTs along

actin fibers towards FAs (Kodama et al., 2003; Wu et al., 2008). ACF7 is of great importance for proper cell migration of keratinocytes. In an assay to study polarized migration of cells, called a wound healing assay, ACF7-deficient keratinocytes moved only 20 percent of the distance into the wound whereas normal keratinocytes were able to close the wound within 36 hrs. ACF7 was recently shown to possess an ATPase activity, that is stimulated by actin polymers, and this activity is necessary for its function. Interestingly, ACF7 interacts with CLASP2 (Wu et al., 2008). This fits well with data from Drabek et al. who found that CLASP2 requires ACF7 for its localization to the cell edge (Drabek et al., 2006).

1.6.5 Recognizing MT plus-ends.

Several models have been proposed to explain how +TIPs recognize the ends of MTs. In the first model +TIPs were supposed to be “treadmilling”, recognizing a distinct structural feature on the MT end, binding for a few seconds, and then dissociating. In the treadmilling model release can be an active process, caused for example by phosphorylation of the +TIP. After dissociation the same +TIP molecule is available for another round of binding to the very distal end of the MT that has moved away because of MT growth. This causes a kind of treadmilling of the +TIP at the MT end. The “co-polymerization” model is a variant of the “treadmilling” model. In this view the +TIP associates with a tubulin dimer and incorporates together with the tubulin dimer at the plus-end. Dissociation of the +TIP occurs again after a few seconds. A third model involves motor mediated-transport, where a plus-end directed motor protein takes along the +TIP to the MT end. Finally, +TIPs may “hitchhike” on other +TIPs in order to bind.

Although “treadmilling” and “co-polymerization” models have prevailed for a number of years, they are no longer considered valid for the +TIPs studied so far. In the last 2 years, important discoveries have been made regarding plus end-binding mechanisms. In living cells, CLIP-170 and EB3 were shown to exchange very rapidly on MT plus-ends and to bind sites on the MT end repeatedly and with low affinity (see Chapter 2). These data are consistent with results using a novel *in vitro* plus-end tracking system, where it was shown that purified Mal3p (the fission yeast homolog of EB1) can autonomously track growing MT-ends (Bieling et al., 2007). Individual Mal3p molecules exchange very rapidly on MT ends. Mal3p is essential for the plus end tracking of the yeast +TIPs Tea1 and Tip1, and delivery of Tip1 (yeast CLIP170) depends on the kinesin Tea1. More recently two groups published that mammalian EB proteins, purified from bacteria, are also capable

of tracking plus-ends autonomously, without the requirement for other proteins or post translational modifications (Bieling et al., 2008; Dixit et al., 2009). In contrast to the situation in yeast, mammalian CLIP170 only requires EB1, and not kinesin, to track MT-ends. These data suggest that the comet-like structures observed in live cell imaging experiments reflect turn over of MT end binding sites rather than the association-dissociation profile of a +TIP. The disappearance of these binding sites can be described by exponential decay.

The necessity of the C-terminal tyrosine of α-tubulin for plus-end tracking of CAP-Gly-domain-containing +TIPs was demonstrated *in vivo*, in fibroblasts lacking the tubulin-tyrosine ligase (TTL) (Peris et al., 2006). Recent *in vitro* data indicate that not only the C-terminal tyrosine of α-tubulin is required, but that also the C-terminus of EB1 is of critical importance for CLIP170 binding to MT-ends (Bieling et al., 2008). It should be noted that *in vivo* data suggest that in EB-depleted cells an EB-protein lacking the C-terminal residue, can partially rescue CLIP-170 association with MT ends (Komarova et al., 2005). Thus, there is not a complete correlation yet between *in vivo* and *in vitro* data. In conclusion, fast exchange seems to be the way by which mammalian CLIPs and EBs associate with MT ends (see also Chapter 2). Thus, while the localization of CLIP170 and its orthologue TIP1p has been conserved throughout evolution, the mechanisms by which these proteins associate has changed.

It is still not clear what structure at the MT-end is recognized by EB molecules themselves. *In vitro* data suggest that the ends of growing MTs are structurally distinct from the rest of the lattice (Mandelkow et al., 1991). This was also found *in vivo* in interphase fibroblasts (Zovko et al., 2008). However, the length of MT-end structures observed with cryo-EM is much shorter than the length of an average EB1 or CLIP170 comet, which can be more than a micron long. This suggests that there is yet another structural feature, which is not easily discernible using EM. One interesting candidate that might be the “structural difference” recognized by EB proteins, is the GTP-cap. However, it still needs to be convincingly demonstrated that the GTP-cap turns over using an exponential decay mechanism.

1.7 Neuron Navigators

1.7.1 The *C. elegans unc-53* gene

In 1974 Brenner published "The Genetics of *C. elegans*" (Brenner, 1974). In this landmark paper 300 mutants of *C. elegans* are described, and 100 genes are defined. Of these mutants, 77 affected movement of the nematode. These genes were called "*unc*", which stands for "UNCoordinated". The *unc* phenotype encompasses a whole range of locomotory defects, ranging from small aberrations in movement to paralysis. One of the genes identified was *unc-53*. Important clues about the function of *unc-53* have been provided by different groups (Chen et al., 1997; Hedgecock et al., 1987; Hekimi and Kershaw, 1993; Siddiqui, 1990; Stringham et al., 2002; Trent et al., 1983). Combined, the results have shown that *unc-53* is involved in axon guidance of different neurons, including mechanosensory neurons (ALM, PLM, AVM and PVM). *Unc-53* is also important for the elongation of body wall muscle cells, sex myoblast migration, excretory canal outgrowth and development of the male copulatory organs. In addition, mutations in *unc-53* cause egg laying defects.

1.7.2 Mammalian Neuron Navigators

Maes et al. were the first to report on the identification of the "neuron navigator" family, which are mammalian homologs of *unc-53* (Maes et al., 2002). The name "neuron navigator" implies a role for these proteins in the navigation of neurons; however mammalian navigators are not exclusively expressed in neurons. Navigator homologs are found in many species, e.g. *Xenopus tropicalis*, *Danio rerio, Mus Musculus,* and also *Drosophila melanogaster* seems to have a navigator homolog. This protein, named Sickie, has been shown to play a role in the innate immune response, being required for the activation of Relish, which is an NFκB family member (Foley and O'Farrell, 2004). It is unclear if Sickie plays a role in neurite outgrowth and/or cell migration. Navigator homologs have not been identified in yeast or plants.

Humans have three Navigator genes, namely *NAV1*, *NAV2* and *NAV3*, which are located on chromosomes 1q32.1, 11p15.1, and 12q21.1 respectively (Maes et al., 2002). The navigator genes are differentially regulated, both during development and in the adult and each give rise to several protein isoforms (Coy et al., 2002; Maes et al., 2002; Peeters et al., 2004). Navigators are large proteins of over 200 kDa. Different domains and motifs have been recognized in these proteins. One of these domains is an AAA+ ATPase domain, which is conserved in all navigator proteins and is located at the C-terminus. This enzymatic domain is thought to be

important for Navigator function, because the *unc-53* mutant alleles n152 and n166, which show defects in cellular outgrowth, express truncated forms of the protein that lack the ATPase domain. The domain structure of navigators is discussed more extensively in Chapters 3-5.

Different groups have published data that connect mammalian navigators to cellular outgrowth and neuronal development, in line with the function of UNC-53. For example, *NAV2* is an all-trans retinoic acid (atRA)-responsive gene in human neuroblastoma cells (SH-SY5Y) that extend neurites after exposure to atRA. AtRA is a vitamine A metabolite that plays an important role in neuronal development, including neurite outgrowth and the development of dorsal root ganglia (DRG). The expression of NAV2 was shown to be decreased in the DRGs of vitamin A-deficient rat embryos (Merrill et al., 2002). The ability of atRA to induce neurite outgrowth in SH-SY5Y cells depends on NAV2, since NAV2-depletion by RNAi abolished atRA-induced neurite outgrowth (Muley et al., 2008). In fact mammalian NAV2 can rescue specific defects in *unc-53* mutant worms, indicating that NAV2 is orthologous to UNC-53 (Muley et al., 2008). Mice carrying a hypomorphic mutation in the *Nav2* gene showed impaired functioning of several sensory systems (Peeters et al., 2004). Hypoplasia of the optic nerve was also observed. RNAi mediated knockdown of mNav1 causes loss of directionality in the leading processes of pontine-migrating cells, providing evidence for a role of mNav1 in Netrin-1-induced directional migration (Martinez-Lopez et al., 2005).

Navigators have been reported to be upregulated or misregulated in a variety of cancers, including colon cancer, neuroblastomas and cutaneous T cell lymphomas (Coy et al., 2002; Ishiguro et al., 2002; Karenko et al., 2005). Ishiguro et al. found that NAV2 was abundantly expressed in 16 of 20 colon cancers examined but hardly detectable in corresponding non-cancerous mucosa (Ishiguro et al., 2002). They identified NAV2 as a gene that is downregulated by the expression of AdAPC (a 20 amino acid repeat domain in APC), and that RNAi mediated knockdown of NAV2 in SW480 cells resulted in increased apoptosis. Interestingly, this paper also shows that a recombinant polypeptide containing the AAA+ domain of NAV2 fused to GST, has 3' to 5' helicase activity and exonuclease activity in vitro.

Navigators have been reported to localize to both the cytoplasm and nucleus and NAV3 has been suggested to be part of the nuclear pore complex (NPC) (Coy et al., 2002; Ishiguro et al., 2002). In 2005 it was described that Neuron navigator 1 (NAV1) is a +TIP (Martinez-Lopez et al., 2005). Recently UNC-53 was shown to associate with Abi1 (Schmidt et al., 2009), implying a role for UNC-53 in the

regulation of the actin network. Combined the results suggest that Navigators can localize to various intracellular compartments and might be involved in a number of cellular processes.

1.7.3 Navigators belong to the AAA+ ATPase superfamily

The name AAA+ ATPases stands for "ATPases Associated with diverse cellular Activities". This type of ATPases belongs to a large family of P-loop NTPases. As the name AAA suggests, these ATP hydrolyzing enzymes have been found to participate in an astonishing range of cellular activities. The AAA+ superfamily includes proteasome components (CDC48), proteins involved in vesicular fusion (NSF), assembly of mitochondrial membrane complexes (bcs1p), and peroxisome biogenesis (pex1p). It includes chaperones, helicases, minus-end directed motor proteins (dyneins) and the MT severing enzymes, katanin and spastin.

ATP hydrolysis is thought to provide the energy for AAA+ ATPases to carry out their mechanical duty. The ATPase domain of AAA+ ATPases is around 250 amino acids long and it contains a number of conserved domains necessary for binding and hydrolyzing ATP. This includes a Walker A motif (or P-loop) that mediates ATP binding, a Walker B motif, and sensor-1 and sensor-2 motifs. The latter mediate ATP hydrolysis (Iyer et al., 2004; White and Lauring, 2007). Many AAA+ ATPases function as oligomeric ring structures, with a central pore, which has been shown to be of critical importance. For example, the protein unfolding chaperone ClpA translocates protein substrates through its pore to unfold them (Hinnerwisch et al., 2005).

The number of AAA+ domains varies between AAA+ ATPases. NSF, for example, has two domains whereas dynein has six. Spastin, katanin and the navigators each only have one ATPase domain. Depending on the number of domains, these enzymes are thought to form single hexameric rings or double-rings (White and Lauring, 2007). Katanin oligomerizes into single hexameric rings with a diameter of 14-16 nm (McNally and Vale, 1993). It requires both ATP and MTs to assemble into oligomers (Hartman and Vale, 1999). Katanin is composed of two subunits, p60 and p80. The p60 subunit of katanin contains the ATPase domain and the p80 subunit contains a WD40 domain which targets katanin to the centrosome (Hartman et al., 1998). Spastin also forms hexameric rings with a central pore that interacts with the C-terminus of tubulin (White et al., 2007). Mutations in the pore abolish MT severing activity (Ogura et al., 2008). These results indicate that Navigators might also form ring structures.

The AAA+ superclade has been categorized into separate clades, which each are composed of several subfamilies, based on sequence and structural signatures. These include the katanin p60/fidgetin family, the NSF-1 family and the CDC48 family, which belong to the classical AAA clade (Iyer et al., 2004). The ATPase domain of Navigator proteins is part of the helix-2 insert clade, which consists of 7 families, including Dynein/Midasin and the McrB family. Navigators are most homologous to ATPases from the McrB subfamily. The McrB family has an NTPase subunit that resembles that of the Mcr restriction-modification system and seems to differ from most of the AAA+ proteins in that it utilizes GTP rather than ATP (Iyer et al., 2004; Neuwald et al., 1999). In the case of Navigators is not clear what nucleotide is used. The exact function of the NTPase domain of Navigators remains a riddle. The only report addressing this important aspect of Navigator function attributed 3' to 5' DNA helicase activity to the NAV2 AAA+ domain (Ishiguro et al., 2002).

References

Addinall, S.G., and J. Lutkenhaus. 1996. FtsZ-spirals and -arcs determine the shape of the invaginating septa in some mutants of Escherichia coli. *Mol Microbiol*. 22:231-7.

Ahmad, F.J., W. Yu, F.J. McNally, and P.W. Baas. 1999. An essential role for katanin in severing microtubules in the neuron. *J Cell Biol*. 145:305-15.

Akhmanova, A., and C.C. Hoogenraad. 2005. Microtubule plus-end-tracking proteins: mechanisms and functions. *Curr Opin Cell Biol*. 17:47-54.

Akhmanova, A., C.C. Hoogenraad, K. Drabek, T. Stepanova, B. Dortland, T. Verkerk, W. Vermeulen, B.M. Burgering, C.I. De Zeeuw, F. Grosveld, and N. Galjart. 2001. Clasps are CLIP-115 and -170 associating proteins involved in the regional regulation of microtubule dynamics in motile fibroblasts. *Cell*. 104:923-35.

Akhmanova, A., A.-L. Mausset-Bonnefont, W. Van Cappellen, N. Keijzer, C.C. Hoogenraad, T. Stepanova, K. Drabek, J. van der Wees, M. Mommaas, J. Onderwater, H. van der Meulen, J. Hoogerbrugge, J. Vreeburg, E.-J. Uringa, A. Grootegoed, F. Grosveld, and N. Galjart. 2005. The microtuble plus end tracking protein CLIP-170 associates with the spermatid manchette and is essential for spermatogenesis. *Genes Dev*. 19:2501-2515.

Akhmanova, A., and M.O. Steinmetz. 2008. Tracking the ends: a dynamic protein network controls the fate of microtubule tips. *Nat Rev Mol Cell Biol*. 9:309-22.

Amos, L.A., and D. Schlieper. 2005. Microtubules and maps. *Adv Protein Chem*. 71:257-98.

Arnal, I., C. Heichette, G.S. Diamantopoulos, and D. Chretien. 2004. CLIP-170/Tubulin-Curved Oligomers Coassemble at Microtubule Ends and Promote Rescues. *Curr Biol*. 14:2086-95.

Asbury, C.L. 2008. XMAP215: a tip tracker that really moves. *Cell*. 132:19-20.

Askham, J.M., K.T. Vaughan, H.V. Goodson, and E.E. Morrison. 2002. Evidence that an interaction between EB1 and p150(Glued) is required for the formation and maintenance of a radial microtubule array anchored at the centrosome. *Mol Biol Cell*. 13:3627-45.

Baas, P.W., J.S. Deitch, M.M. Black, and G.A. Banker. 1988. Polarity orientation of microtubules in hippocampal neurons: uniformity in the axon and nonuniformity in the dendrite. *Proc Natl Acad Sci U S A*. 85:8335-9.

Baas, P.W., A. Karabay, and L. Qiang. 2005. Microtubules cut and run. *Trends Cell Biol*. 15:518-24.

Basto, R., J. Lau, T. Vinogradova, A. Gardiol, C.G. Woods, A. Khodjakov, and J.W. Raff. 2006. Flies without centrioles. *Cell*. 125:1375-86.

Berrueta, L., S.K. Kraeft, J.S. Tirnauer, S.C. Schuyler, L.B. Chen, D.E. Hill, D. Pellman, and B.E. Bierer. 1998. The adenomatous polyposis coli-binding protein EB1 is associated with cytoplasmic and spindle microtubules. *Proc Natl Acad Sci U S A*. 95:10596-601.

Bershadsky, A., A. Chausovsky, E. Becker, A. Lyubimova, and B. Geiger. 1996. Involvement of microtubules in the control of adhesion-dependent signal transduction. *Curr Biol*. 6:1279-89.

Bettencourt-Dias, M., and D.M. Glover. 2009. SnapShot: centriole biogenesis. *Cell*. 136:188-188 e1.

Bieling, P., S. Kandels-Lewis, I.A. Telley, J. van Dijk, C. Janke, and T. Surrey. 2008. CLIP-170 tracks growing microtubule ends by dynamically recognizing composite EB1/tubulin-binding sites. *J Cell Biol*. 183:1223-33.

Bieling, P., L. Laan, H. Schek, E.L. Munteanu, L. Sandblad, M. Dogterom, D. Brunner, and T. Surrey. 2007. Reconstitution of a microtubule plus-end tracking system in vitro. *Nature*. 450:1100-5.

Bobinnec, Y., A. Khodjakov, L.M. Mir, C.L. Rieder, B. Edde, and M. Bornens. 1998. Centriole disassembly in vivo and its effect on centrosome structure and function in vertebrate cells. *J Cell Biol*. 143:1575-89.

Borisy, G.G., and T.M. Svitkina. 2000. Actin machinery: pushing the envelope. *Curr Opin Cell Biol*. 12:104-12.

Bornens, M. 2002. Centrosome composition and microtubule anchoring mechanisms. *Curr Opin Cell Biol*. 14:25-34.

Bornens, M., and J. Azimzadeh. 2007. Origin and evolution of the centrosome. *Adv Exp Med Biol*. 607:119-29.

Bradford, D., S.J. Cole, and H.M. Cooper. 2009. Netrin-1: diversity in development. *Int J Biochem Cell Biol*. 41:487-93.

Brangwynne, C.P., F.C. MacKintosh, S. Kumar, N.A. Geisse, J. Talbot, L. Mahadevan, K.K. Parker, D.E.

Ingber, and D.A. Weitz. 2006. Microtubules can bear enhanced compressive loads in living cells because of lateral reinforcement. *J Cell Biol*. 173:733-41.
Brenner, S. 1974. The genetics of Caenorhabditis elegans. *Genetics*. 77:71-94.
Briancon-Marjollet, A., A. Ghogha, H. Nawabi, I. Triki, C. Auziol, S. Fromont, C. Piche, H. Enslen, K. Chebli, J.F. Cloutier, V. Castellani, A. Debant, and N. Lamarche-Vane. 2008. Trio mediates netrin-1-induced Rac1 activation in axon outgrowth and guidance. *Mol Cell Biol*. 28:2314-23.
Brouhard, G.J., J.H. Stear, T.L. Noetzel, J. Al-Bassam, K. Kinoshita, S.C. Harrison, J. Howard, and A.A. Hyman. 2008. XMAP215 is a processive microtubule polymerase. *Cell*. 132:79-88.
Brown, M.C., and C.E. Turner. 2004. Paxillin: adapting to change. *Physiol Rev*. 84:1315-39.
Bu, W., and L.K. Su. 2001. Regulation of microtubule assembly by human EB1 family proteins. *Oncogene*. 20:3185-92.
Bu, W., and L.K. Su. 2003. Characterization of functional domains of human EB1 family proteins. *J Biol Chem*. 278:49721-31.
Buck, K.B., and J.Q. Zheng. 2002. Growth cone turning induced by direct local modification of microtubule dynamics. *J Neurosci*. 22:9358-67.
Burger, J., N. Fonknechten, M. Hoeltzenbein, L. Neumann, E. Bratanoff, J. Hazan, and A. Reis. 2000. Hereditary spastic paraplegia caused by mutations in the SPG4 gene. *Eur J Hum Genet*. 8:771-6.
Campbell, D.S., and C.E. Holt. 2001. Chemotropic responses of retinal growth cones mediated by rapid local protein synthesis and degradation. *Neuron*. 32:1013-26.
Campbell, D.S., A.G. Regan, J.S. Lopez, D. Tannahill, W.A. Harris, and C.E. Holt. 2001. Semaphorin 3A elicits stage-dependent collapse, turning, and branching in Xenopus retinal growth cones. *J Neurosci*. 21:8538-47.
Carlier, M.F. 1982. Guanosine-5'-triphosphate hydrolysis and tubulin polymerization. Review article. *Mol Cell Biochem*. 47:97-113.
Cassimeris, L., D. Gard, P.T. Tran, and H.P. Erickson. 2001. XMAP215 is a long thin molecule that does not increase microtubule stiffness. *J Cell Sci*. 114:3025-33.
Cassimeris, L., N.K. Pryer, and E.D. Salmon. 1988. Real-time observations of microtubule dynamic instability in living cells. *J Cell Biol*. 107:2223-31.
Cassimeris, L., and C. Spittle. 2001. Regulation of microtubule-associated proteins. *Int Rev Cytol*. 210:163-226.
Cheeseman, I.M., and A. Desai. 2008. Molecular architecture of the kinetochore-microtubule interface. *Nat Rev Mol Cell Biol*. 9:33-46.
Chen, E.B., C.S. Branda, and M.J. Stern. 1997. Genetic enhancers of sem-5 define components of the gonad-independent guidance mechanism controlling sex myoblast migration in Caenorhabditis elegans hermaphrodites. *Dev Biol*. 182:88-100.
Chisholm, A., and M. Tessier-Lavigne. 1999. Conservation and divergence of axon guidance mechanisms. *Curr Opin Neurobiol*. 9:603-15.
Cohen-Cory, S. 2002. The double life of netrin. *Nat Neurosci*. 5:926-8.
Coquelle, F.M., M. Caspi, F.P. Cordelieres, J.P. Dompierre, D.L. Dujardin, C. Koifman, P. Martin, C.C. Hoogenraad, A. Akhmanova, N. Galjart, J.R. De Mey, and O. Reiner. 2002. LIS1, CLIP-170's key to the dynein/dynactin pathway. *Mol Cell Biol*. 22:3089-102.
Coy, J.F., S. Wiemann, I. Bechmann, D. Bachner, R. Nitsch, O. Kretz, H. Christiansen, and A. Poustka. 2002. Pore membrane and/or filament interacting like protein 1 (POMFIL1) is predominantly expressed in the nervous system and encodes different protein isoforms. *Gene*. 290:73-94.
Critchley, D.R. 2004. Cytoskeletal proteins talin and vinculin in integrin-mediated adhesion. *Biochem Soc Trans*. 32:831-6.
Critchley, D.R., M.R. Holt, S.T. Barry, H. Priddle, L. Hemmings, and J. Norman. 1999. Integrin-mediated cell adhesion: the cytoskeletal connection. *Biochem Soc Symp*. 65:79-99.
de la Torre, J.R., V.H. Hopker, G.L. Ming, M.M. Poo, M. Tessier-Lavigne, A. Hemmati-Brivanlou, and C.E. Holt. 1997. Turning of retinal growth cones in a netrin-1 gradient mediated by the netrin receptor DCC. *Neuron*. 19:1211-24.
De Zeeuw, C.I., C.C. Hoogenraad, E. Goedknegt, E. Hertzberg, A. Neubauer, F. Grosveld, and N. Galjart. 1997. CLIP-115, a novel brain-specific cytoplasmic linker protein, mediates the localization of dendritic lamellar bodies. *Neuron*. 19:1187-99.
Deacon, S.W., A.S. Serpinskaya, P.S. Vaughan, M. Lopez Fanarraga, I. Vernos, K.T. Vaughan, and V.I.

Gelfand. 2003. Dynactin is required for bidirectional organelle transport. *J Cell Biol*. 160:297-301.

Dent, E.W., and F.B. Gertler. 2003. Cytoskeletal dynamics and transport in growth cone motility and axon guidance. *Neuron*. 40:209-27.

des Georges, A., M. Katsuki, D.R. Drummond, M. Osei, R.A. Cross, and L.A. Amos. 2008. Mal3, the Schizosaccharomyces pombe homolog of EB1, changes the microtubule lattice. *Nat Struct Mol Biol*. 15:1102-8.

Desai, A., S. Verma, T.J. Mitchison, and C.E. Walczak. 1999. Kin I kinesins are microtubule-destabilizing enzymes. *Cell*. 96:69-78.

Di Nardo, A., G. Cicchetti, H. Falet, J.H. Hartwig, T.P. Stossel, and D.J. Kwiatkowski. 2005. Arp2/3 complex-deficient mouse fibroblasts are viable and have normal leading-edge actin structure and function. *Proc Natl Acad Sci U S A*. 102:16263-8.

Diamantopoulos, G.S., F. Perez, H.V. Goodson, G. Batelier, R. Melki, T.E. Kreis, and J.E. Rickard. 1999. Dynamic localization of CLIP-170 to microtubule plus ends is coupled to microtubule assembly. *J Cell Biol*. 144:99-112.

Dickson, B.J. 2002. Molecular mechanisms of axon guidance. *Science*. 298:1959-64.

Dickson, B.J., and K.A. Senti. 2002. Axon guidance: growth cones make an unexpected turn. *Curr Biol*. 12:R218-20.

Dimitrov, A., M. Quesnoit, S. Moutel, I. Cantaloube, C. Pous, and F. Perez. 2008. Detection of GTP-tubulin conformation in vivo reveals a role for GTP remnants in microtubule rescues. *Science*. 322:1353-6.

Dixit, R., B. Barnett, J.E. Lazarus, M. Tokito, Y.E. Goldman, and E.L. Holzbaur. 2009. Microtubule plus-end tracking by CLIP-170 requires EB1. *Proc Natl Acad Sci U S A*. 106:492-7.

Drabek, K., M. van Ham, T. Stepanova, K. Draegestein, R. van Horssen, C.L. Sayas, A. Akhmanova, T. Ten Hagen, R. Smits, R. Fodde, F. Grosveld, and N. Galjart. 2006. Role of CLASP2 in microtubule stabilization and the regulation of persistent motility. *Curr Biol*. 16:2259-64.

Dujardin, D., U.I. Wacker, A. Moreau, T.A. Schroer, J.E. Rickard, and J.R. De Mey. 1998. Evidence for a role of CLIP-170 in the establishment of metaphase chromosome alignment. *J Cell Biol*. 141:849-62.

Efimov, A., A. Kharitonov, N. Efimova, J. Loncarek, P.M. Miller, N. Andreyeva, P. Gleeson, N. Galjart, A.R. Maia, I.X. McLeod, J.R. Yates, 3rd, H. Maiato, A. Khodjakov, A. Akhmanova, and I. Kaverina. 2007. Asymmetric CLASP-dependent nucleation of noncentrosomal microtubules at the trans-Golgi network. *Dev Cell*. 12:917-30.

Erck, C., L. Peris, A. Andrieux, C. Meissirel, A.D. Gruber, M. Vernet, A. Schweitzer, Y. Saoudi, H. Pointu, C. Bosc, P.A. Salin, D. Job, and J. Wehland. 2005. A vital role of tubulin-tyrosine-ligase for neuronal organization. *Proc Natl Acad Sci U S A*. 102:7853-8.

Erickson, H.P. 2007. Evolution of the cytoskeleton. *Bioessays*. 29:668-77.

Etienne-Manneville, S. 2004. Actin and microtubules in cell motility: which one is in control? *Traffic*. 5:470-7.

Etienne-Manneville, S., and A. Hall. 2002. Rho GTPases in cell biology. *Nature*. 420:629-35.

Ezratty, E.J., M.A. Partridge, and G.G. Gundersen. 2005. Microtubule-induced focal adhesion disassembly is mediated by dynamin and focal adhesion kinase. *Nat Cell Biol*. 7:581-90.

Foley, E., and P.H. O'Farrell. 2004. Functional dissection of an innate immune response by a genome-wide RNAi screen. *PLoS Biol*. 2:E203.

Franco, S.J., M.A. Rodgers, B.J. Perrin, J. Han, D.A. Bennin, D.R. Critchley, and A. Huttenlocher. 2004. Calpain-mediated proteolysis of talin regulates adhesion dynamics. *Nat Cell Biol*. 6:977-83.

Frixione, E. 2000. Recurring views on the structure and function of the cytoskeleton: a 300-year epic. *Cell Motil Cytoskeleton*. 46:73-94.

Fuentealba, L.C., E. Eivers, D. Geissert, V. Taelman, and E.M. De Robertis. 2008. Asymmetric mitosis: Unequal segregation of proteins destined for degradation. *Proc Natl Acad Sci U S A*. 105:7732-7.

Fukata, M., T. Watanabe, J. Noritake, M. Nakagawa, M. Yamaga, S. Kuroda, Y. Matsuura, A. Iwamatsu, F. Perez, and K. Kaibuchi. 2002. Rac1 and Cdc42 capture microtubules through IQGAP1 and CLIP-170. *Cell*. 109:873-85.

Gadde, S., and R. Heald. 2004. Mechanisms and molecules of the mitotic spindle. *Curr Biol*. 14:R797-805.

Galjart, N. 2005. CLIPs and CLASPs and cellular dynamics. *Nat Rev Mol Cell Biol*. 6:487-98.
Galjart, N., and F. Perez. 2003. A plus-end raft to control microtubule dynamics and function. *Curr Opin Cell Biol*. 15:48-53.
Gard, D.L., and M.W. Kirschner. 1987. A microtubule-associated protein from Xenopus eggs that specifically promotes assembly at the plus-end. *J Cell Biol*. 105:2203-15.
Garner, E.C., C.S. Campbell, and R.D. Mullins. 2004. Dynamic instability in a DNA-segregating prokaryotic actin homolog. *Science*. 306:1021-5.
Garner, E.C., C.S. Campbell, D.B. Weibel, and R.D. Mullins. 2007. Reconstitution of DNA segregation driven by assembly of a prokaryotic actin homolog. *Science*. 315:1270-4.
Gendron, T.F., and L. Petrucelli. 2009. The role of tau in neurodegeneration. *Mol Neurodegener*. 4:13.
Geraldo, S., U.K. Khanzada, M. Parsons, J.K. Chilton, and P.R. Gordon-Weeks. 2008. Targeting of the F-actin-binding protein drebrin by the microtubule plus-tip protein EB3 is required for neuritogenesis. *Nat Cell Biol*. 10:1181-9.
Gergely, F., V.M. Draviam, and J.W. Raff. 2003. The ch-TOG/XMAP215 protein is essential for spindle pole organization in human somatic cells. *Genes Dev*. 17:336-41.
Giger, R.J., and A.L. Kolodkin. 2001. Silencing the siren: guidance cue hierarchies at the CNS midline. *Cell*. 105:1-4.
Gittes, F., B. Mickey, J. Nettleton, and J. Howard. 1993. Flexural rigidity of microtubules and actin filaments measured from thermal fluctuations in shape. *J Cell Biol*. 120:923-34.
Grigoriev, I., S.M. Gouveia, B. van der Vaart, J. Demmers, J.T. Smyth, S. Honnappa, D. Splinter, M.O. Steinmetz, J.W. Putney, Jr., C.C. Hoogenraad, and A. Akhmanova. 2008. STIM1 is a MT-plus-end-tracking protein involved in remodeling of the ER. *Curr Biol*. 18:177-82.
Guirland, C., S. Suzuki, M. Kojima, B. Lu, and J.Q. Zheng. 2004. Lipid rafts mediate chemotropic guidance of nerve growth cones. *Neuron*. 42:51-62.
Gundersen, G.G. 2002. Microtubule capture: IQGAP and CLIP-170 expand the repertoire. *Curr Biol*. 12:R645-7.
Hall, A. 1998. Rho GTPases and the actin cytoskeleton. *Science*. 279:509-14.
Hall, A. 2005. Rho GTPases and the control of cell behaviour. *Biochem Soc Trans*. 33:891-5.
Hannak, E., K. Oegema, M. Kirkham, P. Gonczy, B. Habermann, and A.A. Hyman. 2002. The kinetically dominant assembly pathway for centrosomal asters in Caenorhabditis elegans is gamma-tubulin dependent. *J Cell Biol*. 157:591-602.
Harris, W.A., C.E. Holt, and F. Bonhoeffer. 1987. Retinal axons with and without their somata, growing to and arborizing in the tectum of Xenopus embryos: a time-lapse video study of single fibres in vivo. *Development*. 101:123-33.
Hartman, J.J., J. Mahr, K. McNally, K. Okawa, A. Iwamatsu, S. Thomas, S. Cheesman, J. Heuser, R.D. Vale, and F.J. McNally. 1998. Katanin, a microtubule-severing protein, is a novel AAA ATPase that targets to the centrosome using a WD40-containing subunit. *Cell*. 93:277-87.
Hartman, J.J., and R.D. Vale. 1999. Microtubule disassembly by ATP-dependent oligomerization of the AAA enzyme katanin. *Science*. 286:782-5.
Hata, K., K. Kaibuchi, S. Inagaki, and T. Yamashita. 2009. Unc5B associates with LARG to mediate the action of repulsive guidance molecule. *J Cell Biol*. 184:737-50.
Hayashi, I., M.J. Plevin, and M. Ikura. 2007. CLIP170 autoinhibition mimics intermolecular interactions with p150Glued or EB1. *Nat Struct Mol Biol*. 14:980-1.
Hedgecock, E.M., J.G. Culotti, D.H. Hall, and B.D. Stern. 1987. Genetics of cell and axon migrations in Caenorhabditis elegans. *Development*. 100:365-82.
Hekimi, S., and D. Kershaw. 1993. Axonal guidance defects in a Caenorhabditis elegans mutant reveal cell-extrinsic determinants of neuronal morphology. *J Neurosci*. 13:4254-71.
Hinnerwisch, J., W.A. Fenton, K.J. Furtak, G.W. Farr, and A.L. Horwich. 2005. Loops in the central channel of ClpA chaperone mediate protein binding, unfolding, and translocation. *Cell*. 121:1029-41.
Hirokawa, N., K.K. Pfister, H. Yorifuji, M.C. Wagner, S.T. Brady, and G.S. Bloom. 1989. Submolecular domains of bovine brain kinesin identified by electron microscopy and monoclonal antibody decoration. *Cell*. 56:867-78.
Hong, K., L. Hinck, M. Nishiyama, M.M. Poo, M. Tessier-Lavigne, and E. Stein. 1999. A ligand-gated association between cytoplasmic domains of UNC5 and DCC family receptors converts netrin-induced growth cone attraction to repulsion. *Cell*. 97:927-41.
Honnappa, S., C.M. John, D. Kostrewa, F.K. Winkler, and M.O. Steinmetz. 2005. Structural insights into

the EB1-APC interaction. *Embo J*. 24:261-9.
Honnappa, S., O. Okhrimenko, R. Jaussi, H. Jawhari, I. Jelesarov, F.K. Winkler, and M.O. Steinmetz. 2006. Key interaction modes of dynamic +TIP networks. *Mol Cell*. 23:663-71.
Hoogenraad, C.C., A. Akhmanova, F. Grosveld, C.I. De Zeeuw, and N. Galjart. 2000. Functional analysis of CLIP-115 and its binding to microtubules. *J Cell Sci*. 113:2285-97.
Huxley, H.E. 1963. Electron Microscope Studies on the Structure of Natural and Synthetic Protein Filaments from Striated Muscle. *J Mol Biol*. 7:281-308.
Hyman, A.A., S. Salser, D.N. Drechsel, N. Unwin, and T.J. Mitchison. 1992. Role of GTP hydrolysis in microtubule dynamics: information from a slowly hydrolyzable analogue, GMPCPP. *Mol Biol Cell*. 3:1155-67.
Idriss, H.T. 2000. Man to trypanosome: the tubulin tyrosination/detyrosination cycle revisited. *Cell Motil Cytoskeleton*. 45:173-84.
Ishiguro, H., T. Shimokawa, T. Tsunoda, T. Tanaka, Y. Fujii, Y. Nakamura, and Y. Furukawa. 2002. Isolation of HELAD1, a novel human helicase gene up-regulated in colorectal carcinomas. *Oncogene*. 21:6387-94.
Iyer, L.M., D.D. Leipe, E.V. Koonin, and L. Aravind. 2004. Evolutionary history and higher order classification of AAA+ ATPases. *J Struct Biol*. 146:11-31.
Jaworski, J., L.C. Kapitein, S.M. Gouveia, B.R. Dortland, P.S. Wulf, I. Grigoriev, P. Camera, S.A. Spangler, P. Di Stefano, J. Demmers, H. Krugers, P. Defilippi, A. Akhmanova, and C.C. Hoogenraad. 2009. Dynamic microtubules regulate dendritic spine morphology and synaptic plasticity. *Neuron*. 61:85-100.
Juwana, J.P., P. Henderikx, A. Mischo, A. Wadle, N. Fadle, K. Gerlach, J.W. Arends, H. Hoogenboom, M. Pfreundschuh, and C. Renner. 1999. EB/RP gene family encodes tubulin binding proteins. *Int J Cancer*. 81:275-84.
Kapitein, L.C., E.J. Peterman, B.H. Kwok, J.H. Kim, T.M. Kapoor, and C.F. Schmidt. 2005. The bipolar mitotic kinesin Eg5 moves on both microtubules that it crosslinks. *Nature*. 435:114-8.
Karabay, A., W. Yu, J.M. Solowska, D.H. Baird, and P.W. Baas. 2004. Axonal growth is sensitive to the levels of katanin, a protein that severs microtubules. *J Neurosci*. 24:5778-88.
Karakesisoglou, I., Y. Yang, and E. Fuchs. 2000. An epidermal plakin that integrates actin and microtubule networks at cellular junctions. *J Cell Biol*. 149:195-208.
Karenko, L., S. Hahtola, S. Paivinen, R. Karhu, S. Syrja, M. Kahkonen, B. Nedoszytko, S. Kytola, Y. Zhou, V. Blazevic, M. Pesonen, H. Nevala, N. Nupponen, H. Sihto, I. Krebs, A. Poustka, J. Roszkiewicz, K. Saksela, P. Peterson, T. Visakorpi, and A. Ranki. 2005. Primary cutaneous T-cell lymphomas show a deletion or translocation affecting NAV3, the human UNC-53 homologue. *Cancer Res*. 65:8101-10.
Kaverina, I., O. Krylyshkina, and J.V. Small. 1999. Microtubule targeting of substrate contacts promotes their relaxation and dissociation. *J Cell Biol*. 146:1033-44.
Kerkhoff, E. 2006. Cellular functions of the Spir actin-nucleation factors. *Trends Cell Biol*. 16:477-83.
Kerssemakers, J.W., E.L. Munteanu, L. Laan, T.L. Noetzel, M.E. Janson, and M. Dogterom. 2006. Assembly dynamics of microtubules at molecular resolution. *Nature*. 442:709-12.
Khodjakov, A., and C.L. Rieder. 1999. The sudden recruitment of gamma-tubulin to the centrosome at the onset of mitosis and its dynamic exchange throughout the cell cycle, do not require microtubules. *J Cell Biol*. 146:585-96.
King, S.M. 2000. AAA domains and organization of the dynein motor unit. *J Cell Sci*. 113 (Pt 14):2521-6.
Kodama, A., I. Karakesisoglou, E. Wong, A. Vaezi, and E. Fuchs. 2003. ACF7: an essential integrator of microtubule dynamics. *Cell*. 115:343-54.
Komarova, Y., C.O. De Groot, I. Grigoriev, S.M. Gouveia, E.L. Munteanu, J.M. Schober, S. Honnappa, R.M. Buey, C.C. Hoogenraad, M. Dogterom, G.G. Borisy, M.O. Steinmetz, and A. Akhmanova. 2009. Mammalian end binding proteins control persistent microtubule growth. *J Cell Biol*. 184:691-706.
Komarova, Y., G. Lansbergen, N. Galjart, F. Grosveld, G.G. Borisy, and A. Akhmanova. 2005. EB1 and EB3 Control CLIP Dissociation from the Ends of Growing Microtubules. *Mol Biol Cell*. 16:5334-45.
Komarova, Y.A., A.S. Akhmanova, S. Kojima, N. Galjart, and G.G. Borisy. 2002. Cytoplasmic linker proteins promote microtubule rescue in vivo. *J Cell Biol*. 159:589-99.
Kotwaliwale, C., and S. Biggins. 2006. Microtubule capture: a concerted effort. *Cell*. 127:1105-8.

Kraynov, V.S., C. Chamberlain, G.M. Bokoch, M.A. Schwartz, S. Slabaugh, and K.M. Hahn. 2000. Localized Rac activation dynamics visualized in living cells. *Science*. 290:333-7.

Krylyshkina, O., K.I. Anderson, I. Kaverina, I. Upmann, D.J. Manstein, J.V. Small, and D.K. Toomre. 2003. Nanometer targeting of microtubules to focal adhesions. *J Cell Biol*. 161:853-9.

Krylyshkina, O., I. Kaverina, W. Kranewitter, W. Steffen, M.C. Alonso, R.A. Cross, and J.V. Small. 2002. Modulation of substrate adhesion dynamics via microtubule targeting requires kinesin-1. *J Cell Biol*. 156:349-59.

Kuriyama, R., and G.G. Borisy. 1981. Centriole cycle in Chinese hamster ovary cells as determined by whole-mount electron microscopy. *J Cell Biol*. 91:814-21.

Lansbergen, G., and A. Akhmanova. 2006. Microtubule plus end: a hub of cellular activities. *Traffic*. 7:499-507.

Lansbergen, G., I. Grigoriev, Y. Mimori-Kiyosue, T. Ohtsuka, S. Higa, I. Kitajima, J. Demmers, N. Galjart, A.B. Houtsmuller, F. Grosveld, and A. Akhmanova. 2006. CLASPs attach microtubule plus ends to the cell cortex through a complex with LL5beta. *Dev Cell*. 11:21-32.

Lansbergen, G., Y. Komarova, M. Modesti, C. Wyman, C.C. Hoogenraad, H.V. Goodson, R.P. Lemaitre, D.N. Drechsel, E. van Munster, T.W. Gadella, Jr., F. Grosveld, N. Galjart, G.G. Borisy, and A. Akhmanova. 2004. Conformational changes in CLIP-170 regulate its binding to microtubules and dynactin localization. *J Cell Biol*. 166:1003-14.

Larsen, R.A., C. Cusumano, A. Fujioka, G. Lim-Fong, P. Patterson, and J. Pogliano. 2007. Treadmilling of a prokaryotic tubulin-like protein, TubZ, required for plasmid stability in Bacillus thuringiensis. *Genes Dev*. 21:1340-52.

Lee, H., U. Engel, J. Rusch, S. Scherrer, K. Sheard, and D. Van Vactor. 2004. The Microtubule Plus End Tracking Protein Orbit/MAST/CLASP Acts Downstream of the Tyrosine Kinase Abl in Mediating Axon Guidance. *Neuron*. 42:913-26.

Liao, G., T. Nagasaki, and G.G. Gundersen. 1995. Low concentrations of nocodazole interfere with fibroblast locomotion without significantly affecting microtubule level: implications for the role of dynamic microtubules in cell locomotion. *J Cell Sci*. 108 (Pt 11):3473-83.

Liu, B.P., M. Chrzanowska-Wodnicka, and K. Burridge. 1998. Microtubule depolymerization induces stress fibers, focal adhesions, and DNA synthesis via the GTP-binding protein Rho. *Cell Adhes Commun*. 5:249-55.

Maccioni, R.B., and V. Cambiazo. 1995. Role of microtubule-associated proteins in the control of microtubule assembly. *Physiol Rev*. 75:835-64.

Maes, T., A. Barcelo, and C. Buesa. 2002. Neuron navigator: a human gene family with homology to unc-53, a cell guidance gene from Caenorhabditis elegans. *Genomics*. 80:21-30.

Maiato, H., J. DeLuca, E.D. Salmon, and W.C. Earnshaw. 2004. The dynamic kinetochore-microtubule interface. *J Cell Sci*. 117:5461-77.

Maiato, H., E.A. Fairley, C.L. Rieder, J.R. Swedlow, C.E. Sunkel, and W.C. Earnshaw. 2003. Human CLASP1 is an outer kinetochore component that regulates spindle microtubule dynamics. *Cell*. 113:891-904.

Mandelkow, E.M., E. Mandelkow, and R.A. Milligan. 1991. Microtubule dynamics and microtubule caps: a time-resolved cryo-electron microscopy study. *J Cell Biol*. 114:977-91.

Margolis, R.L., and L. Wilson. 1981. Microtubule treadmills--possible molecular machinery. *Nature*. 293:705-11.

Martinez-Lopez, M.J., S. Alcantara, C. Mascaro, F. Perez-Branguli, P. Ruiz-Lozano, T. Maes, E. Soriano, and C. Buesa. 2005. Mouse Neuron navigator 1, a novel microtubule-associated protein involved in neuronal migration. *Mol Cell Neurosci*. 28:599-612.

McIntosh, J.R., E.L. Grishchuk, and R.R. West. 2002. Chromosome-microtubule interactions during mitosis. *Annu Rev Cell Dev Biol*. 18:193-219.

McIntosh, J.R., and M.P. Koonce. 1989. Mitosis. *Science*. 246:622-8.

McNally, F.J., and R.D. Vale. 1993. Identification of katanin, an ATPase that severs and disassembles stable microtubules. *Cell*. 75:419-29.

Megraw, T.L., L.R. Kao, and T.C. Kaufman. 2001. Zygotic development without functional mitotic centrosomes. *Curr Biol*. 11:116-20.

Merrill, R.A., L.A. Plum, M.E. Kaiser, and M. Clagett-Dame. 2002. A mammalian homolog of unc-53 is regulated by all-trans retinoic acid in neuroblastoma cells and embryos. *Proc Natl Acad Sci U S A*. 99:3422-7.

Milisav, I. 1998. Dynein and dynein-related genes. *Cell Motil Cytoskeleton*. 39:261-72.
Mimori-Kiyosue, Y., I. Grigoriev, G. Lansbergen, H. Sasaki, C. Matsui, F. Severin, N. Galjart, F. Grosveld, I. Vorobjev, S. Tsukita, and A. Akhmanova. 2005. CLASP1 and CLASP2 bind to EB1 and regulate microtubule plus-end dynamics at the cell cortex. *J Cell Biol*. 168:141-53.
Mimori-Kiyosue, Y., I. Grigoriev, H. Sasaki, C. Matsui, A. Akhmanova, S. Tsukita, and I. Vorobjev. 2006. Mammalian CLASPs are required for mitotic spindle organization and kinetochore alignment. *Genes Cells*. 11:845-57.
Mishima, M., R. Maesaki, M. Kasa, T. Watanabe, M. Fukata, K. Kaibuchi, and T. Hakoshima. 2007. Structural basis for tubulin recognition by cytoplasmic linker protein 170 and its autoinhibition. *Proc Natl Acad Sci U S A*. 104:10346-51.
Mitchison, T., and M. Kirschner. 1984. Dynamic instability of microtubule growth. *Nature*. 312:237-42.
Moll, R., M. Divo, and L. Langbein. 2008. The human keratins: biology and pathology. *Histochem Cell Biol*. 129:705-33.
Morrison, E.E. 2007. Action and interactions at microtubule ends. *Cell Mol Life Sci*. 64:307-17.
Muley, P.D., E.M. McNeill, M.A. Marzinke, K.M. Knobel, M.M. Barr, and M. Clagett-Dame. 2008. The atRA-responsive gene neuron navigator 2 functions in neurite outgrowth and axonal elongation. *Dev Neurobiol*. 68:1441-53.
Murphy, D.B., and G.G. Borisy. 1975. Association of high-molecular-weight proteins with microtubules and their role in microtubule assembly in vitro. *Proc Natl Acad Sci U S A*. 72:2696-700.
Musa, H., C. Orton, E.E. Morrison, and M. Peckham. 2003. Microtubule assembly in cultured myoblasts and myotubes following nocodazole induced microtubule depolymerisation. *J Muscle Res Cell Motil*. 24:301-8.
Musch, A. 2004. Microtubule organization and function in epithelial cells. *Traffic*. 5:1-9.
Neuwald, A.F., L. Aravind, J.L. Spouge, and E.V. Koonin. 1999. AAA+: A class of chaperone-like ATPases associated with the assembly, operation, and disassembly of protein complexes. *Genome Res*. 9:27-43.
Ogura, T., Y. Matsushita-Ishiodori, A. Johjima, M. Nishizono, S. Nishikori, M. Esaki, and K. Yamanaka. 2008. From the common molecular basis of the AAA protein to various energy-dependent and -independent activities of AAA proteins. *Biochem Soc Trans*. 36:68-71.
Oshima, R.G. 2007. Intermediate filaments: a historical perspective. *Exp Cell Res*. 313:1981-94.
Passey, S., S. Pellegrin, and H. Mellor. 2004. What is in a filopodium? Starfish versus hedgehogs. *Biochem Soc Trans*. 32:1115-7.
Peeters, P.J., A. Baker, I. Goris, G. Daneels, P. Verhasselt, W.H. Luyten, J.J. Geysen, S.U. Kass, and D.W. Moechars. 2004. Sensory deficits in mice hypomorphic for a mammalian homologue of unc-53. *Brain Res Dev Brain Res*. 150:89-101.
Pellegrin, S., and H. Mellor. 2007. Actin stress fibres. *J Cell Sci*. 120:3491-9.
Pereira, A.L., A.J. Pereira, A.R. Maia, K. Drabek, C.L. Sayas, P.J. Hergert, M. Lince-Faria, I. Matos, C. Duque, T. Stepanova, C.L. Rieder, W.C. Earnshaw, N. Galjart, and H. Maiato. 2006. Mammalian CLASP1 and CLASP2 cooperate to ensure mitotic fidelity by regulating spindle and kinetochore function. *Mol Biol Cell*. 17:4526-42.
Perez, F., G.S. Diamantopoulos, R. Stalder, and T.E. Kreis. 1999. CLIP-170 highlights growing microtubule ends in vivo. *Cell*. 96:517-27.
Peris, L., M. Thery, J. Faure, Y. Saoudi, L. Lafanechere, J.K. Chilton, P. Gordon-Weeks, N. Galjart, M. Bornens, L. Wordeman, J. Wehland, A. Andrieux, and D. Job. 2006. Tubulin tyrosination is a major factor affecting the recruitment of CAP-Gly proteins at microtubule plus ends. *J Cell Biol*. 174:839-49.
Pfendner, E., F. Rouan, and J. Uitto. 2005a. Progress in epidermolysis bullosa: the phenotypic spectrum of plectin mutations. *Exp Dermatol*. 14:241-9.
Pfendner, E.G., S.G. Sadowski, and J. Uitto. 2005b. Epidermolysis bullosa simplex: recurrent and de novo mutations in the KRT5 and KRT14 genes, phenotype/genotype correlations, and implications for genetic counseling and prenatal diagnosis. *J Invest Dermatol*. 125:239-43.
Piehl, M., U.S. Tulu, P. Wadsworth, and L. Cassimeris. 2004. Centrosome maturation: measurement of microtubule nucleation throughout the cell cycle by using GFP-tagged EB1. *Proc Natl Acad Sci U S A*. 101:1584-8.
Piel, M., P. Meyer, A. Khodjakov, C.L. Rieder, and M. Bornens. 2000. The respective contributions of the mother and daughter centrioles to centrosome activity and behavior in vertebrate cells. *J Cell*

Biol. 149:317-30.
Pierre, P., J. Scheel, J.E. Rickard, and T.E. Kreis. 1992. CLIP-170 links endocytic vesicles to microtubules. *Cell*. 70:887-900.
Pollard, T.D. 2007. Regulation of actin filament assembly by Arp2/3 complex and formins. *Annu Rev Biophys Biomol Struct*. 36:451-77.
Pollard, T.D., L. Blanchoin, and R.D. Mullins. 2000. Molecular mechanisms controlling actin filament dynamics in nonmuscle cells. *Annu Rev Biophys Biomol Struct*. 29:545-76.
Powers, A.F., A.D. Franck, D.R. Gestaut, J. Cooper, B. Gracyzk, R.R. Wei, L. Wordeman, T.N. Davis, and C.L. Asbury. 2009. The Ndc80 kinetochore complex forms load-bearing attachments to dynamic microtubule tips via biased diffusion. *Cell*. 136:865-75.
Reed, N.A., D. Cai, T.L. Blasius, G.T. Jih, E. Meyhofer, J. Gaertig, and K.J. Verhey. 2006. Microtubule acetylation promotes kinesin-1 binding and transport. *Curr Biol*. 16:2166-72.
Rickard, J.E., and T.E. Kreis. 1990. Identification of a novel nucleotide-sensitive microtubule-binding protein in HeLa cells. *J Cell Biol*. 110:1623-33.
Rieder, C.L., and E.D. Salmon. 1998. The vertebrate cell kinetochore and its roles during mitosis. *Trends Cell Biol*. 8:310-8.
Roger, B., J. Al-Bassam, L. Dehmelt, R.A. Milligan, and S. Halpain. 2004. MAP2c, but not tau, binds and bundles F-actin via its microtubule binding domain. *Curr Biol*. 14:363-71.
Rogers, G.C., S.L. Rogers, and D.J. Sharp. 2005. Spindle microtubules in flux. *J Cell Sci*. 118:1105-16.
Rogers, G.C., N.M. Rusan, M. Peifer, and S.L. Rogers. 2008. A multicomponent assembly pathway contributes to the formation of acentrosomal microtubule arrays in interphase Drosophila cells. *Mol Biol Cell*. 19:3163-78.
Rogers, S.L., U. Wiedemann, U. Hacker, C. Turck, and R.D. Vale. 2004. Drosophila RhoGEF2 Associates with Microtubule Plus Ends in an EB1-Dependent Manner. *Curr Biol*. 14:1827-33.
Roll-Mecak, A., and R.D. Vale. 2005. The Drosophila homologue of the hereditary spastic paraplegia protein, spastin, severs and disassembles microtubules. *Curr Biol*. 15:650-5.
Roper, K., S.L. Gregory, and N.H. Brown. 2002. The 'spectraplakins': cytoskeletal giants with characteristics of both spectrin and plakin families. *J Cell Sci*. 115:4215-25.
Salpingidou, G., A. Smertenko, I. Hausmanowa-Petrucewicz, P.J. Hussey, and C.J. Hutchison. 2007. A novel role for the nuclear membrane protein emerin in association of the centrosome to the outer nuclear membrane. *J Cell Biol*. 178:897-904.
Sammak, P.J., and G.G. Borisy. 1988. Direct observation of microtubule dynamics in living cells. *Nature*. 332:724-6.
Scheel, J., P. Pierre, J.E. Rickard, G.S. Diamantopoulos, C. Valetti, F.G. van der Goot, M. Haner, U. Aebi, and T.E. Kreis. 1999. Purification and analysis of authentic CLIP-170 and recombinant fragments. *J Biol Chem*. 274:25883-91.
Schmidt, K.L., N. Marcus-Gueret, A. Adeleye, J. Webber, D. Baillie, and E.G. Stringham. 2009. The cell migration molecule UNC-53/NAV2 is linked to the ARP2/3 complex by ABI-1. *Development*. 136:563-74.
Schnackenberg, B.J., A. Khodjakov, C.L. Rieder, and R.E. Palazzo. 1998. The disassembly and reassembly of functional centrosomes in vitro. *Proc Natl Acad Sci U S A*. 95:9295-300.
Schroer, T.A. 2000. Motors, clutches and brakes for membrane traffic: a commemorative review in honor of Thomas Kreis. *Traffic*. 1:3-10.
Schroer, T.A. 2004. Dynactin. *Annu Rev Cell Dev Biol*. 20:759-79.
Schulze, E., and M. Kirschner. 1988. New features of microtubule behaviour observed in vivo. *Nature*. 334:356-9.
Schuyler, S.C., and D. Pellman. 2001. Microtubule "plus-end-tracking proteins": The end is just the beginning. *Cell*. 105:421-4.
Serafini, T., T.E. Kennedy, M.J. Galko, C. Mirzayan, T.M. Jessell, and M. Tessier-Lavigne. 1994. The netrins define a family of axon outgrowth-promoting proteins homologous to C. elegans UNC-6. *Cell*. 78:409-24.
Sharp, D.J., K.L. McDonald, H.M. Brown, H.J. Matthies, C. Walczak, R.D. Vale, T.J. Mitchison, and J.M. Scholey. 1999. The bipolar kinesin, KLP61F, cross-links microtubules within interpolar microtubule bundles of Drosophila embryonic mitotic spindles. *J Cell Biol*. 144:125-38.
Shelanski, M.L., F. Gaskin, and C.R. Cantor. 1973. Microtubule assembly in the absence of added nucleotides. *Proc Natl Acad Sci U S A*. 70:765-8.

Shewan, D., A. Dwivedy, R. Anderson, and C.E. Holt. 2002. Age-related changes underlie switch in netrin-1 responsiveness as growth cones advance along visual pathway. *Nat Neurosci*. 5:955-62.

Siddiqui, S.S. 1990. Mutations affecting axonal growth and guidance of motor neurons and mechanosensory neurons in the nematode Caenorhabditis elegans. *Neurosci Res Suppl*. 13:S171-90.

Slep, K.C., S.L. Rogers, S.L. Elliott, H. Ohkura, P.A. Kolodziej, and R.D. Vale. 2005. Structural determinants for EB1-mediated recruitment of APC and spectraplakins to the microtubule plus end. *J Cell Biol*.

Small, J.V., K. Rottner, I. Kaverina, and K.I. Anderson. 1998. Assembling an actin cytoskeleton for cell attachment and movement. *Biochim Biophys Acta*. 1404:271-81.

Steinmetz, M.O., and A. Akhmanova. 2008. Capturing protein tails by CAP-Gly domains. *Trends Biochem Sci*. 33:535-45.

Stoeckli, E.T. 2006. Longitudinal axon guidance. *Curr Opin Neurobiol*. 16:35-9.

Straube, A., and A. Merdes. 2007. EB3 regulates microtubule dynamics at the cell cortex and is required for myoblast elongation and fusion. *Curr Biol*. 17:1318-25.

Stringham, E., N. Pujol, J. Vandekerckhove, and T. Bogaert. 2002. unc-53 controls longitudinal migration in C. elegans. *Development*. 129:3367-79.

Su, L.K., M. Burrell, D.E. Hill, J. Gyuris, R. Brent, R. Wiltshire, J. Trent, B. Vogelstein, and K.W. Kinzler. 1995. APC binds to the novel protein EB1. *Cancer Res*. 55:2972-7.

Su, L.K., and Y. Qi. 2001. Characterization of human MAPRE genes and their proteins. *Genomics*. 71:142-9.

Takahashi, M., A. Yamagiwa, T. Nishimura, H. Mukai, and Y. Ono. 2002. Centrosomal proteins CG-NAP and kendrin provide microtubule nucleation sites by anchoring gamma-tubulin ring complex. *Mol Biol Cell*. 13:3235-45.

Takei, Y., J. Teng, A. Harada, and N. Hirokawa. 2000. Defects in axonal elongation and neuronal migration in mice with disrupted tau and map1b genes. *J Cell Biol*. 150:989-1000.

Tanenbaum, M.E., L. Macurek, N. Galjart, and R.H. Medema. 2008. Dynein, Lis1 and CLIP-170 counteract Eg5-dependent centrosome separation during bipolar spindle assembly. *Embo J*. 27:3235-45.

Theriot, J.A., T.J. Mitchison, L.G. Tilney, and D.A. Portnoy. 1992. The rate of actin-based motility of intracellular Listeria monocytogenes equals the rate of actin polymerization. *Nature*. 357:257-60.

Trent, C., N. Tsuing, and H.R. Horvitz. 1983. Egg-laying defective mutants of the nematode Caenorhabditis elegans. *Genetics*. 104:619-47.

Valentine, M.T., P.M. Fordyce, and S.M. Block. 2006. Eg5 steps it up! *Cell Div*. 1:31.

van den Ent, F., L. Amos, and J. Lowe. 2001. Bacterial ancestry of actin and tubulin. *Curr Opin Microbiol*. 4:634-8.

Vandekerckhove, J., and K. Weber. 1978. At least six different actins are expressed in a higher mammal: an analysis based on the amino acid sequence of the amino-terminal tryptic peptide. *J Mol Biol*. 126:783-802.

Vicente-Manzanares, M., D.J. Webb, and A.R. Horwitz. 2005. Cell migration at a glance. *J Cell Sci*. 118:4917-9.

Vogel, J.M., T. Stearns, C.L. Rieder, and R.E. Palazzo. 1997. Centrosomes isolated from Spisula solidissima oocytes contain rings and an unusual stoichiometric ratio of alpha/beta tubulin. *J Cell Biol*. 137:193-202.

Wang, Y.L. 1985. Exchange of actin subunits at the leading edge of living fibroblasts: possible role of treadmilling. *J Cell Biol*. 101:597-602.

Watanabe, T., J. Noritake, and K. Kaibuchi. 2005. Regulation of microtubules in cell migration. *Trends Cell Biol*. 15:76-83.

Watanabe, T., S. Wang, J. Noritake, K. Sato, M. Fukata, M. Takefuji, M. Nakagawa, N. Izumi, T. Akiyama, and K. Kaibuchi. 2004. Interaction with IQGAP1 Links APC to Rac1, Cdc42, and Actin Filaments during Cell Polarization and Migration. *Dev Cell*. 7:871-83.

Weaver, B.A., and D.W. Cleveland. 2005. Decoding the links between mitosis, cancer, and chemotherapy: The mitotic checkpoint, adaptation, and cell death. *Cancer Cell*. 8:7-12.

Weaver, B.A., and D.W. Cleveland. 2008. The aneuploidy paradox in cell growth and tumorigenesis. *Cancer Cell*. 14:431-3.

Weaver, B.A., A.D. Silk, C. Montagna, P. Verdier-Pinard, and D.W. Cleveland. 2007. Aneuploidy acts both

oncogenically and as a tumor suppressor. *Cancer Cell*. 11:25-36.
Webb, D.J., J.T. Parsons, and A.F. Horwitz. 2002. Adhesion assembly, disassembly and turnover in migrating cells -- over and over and over again. *Nat Cell Biol*. 4:E97-100.
Wegner, A. 1976. Head to tail polymerization of actin. *J Mol Biol*. 108:139-50.
Weisbrich, A., S. Honnappa, R. Jaussi, O. Okhrimenko, D. Frey, I. Jelesarov, A. Akhmanova, and M.O. Steinmetz. 2007. Structure-function relationship of CAP-Gly domains. *Nat Struct Mol Biol*. 14:959-67.
White, S.R., K.J. Evans, J. Lary, J.L. Cole, and B. Lauring. 2007. Recognition of C-terminal amino acids in tubulin by pore loops in Spastin is important for microtubule severing. *J Cell Biol*. 176:995-1005.
White, S.R., and B. Lauring. 2007. AAA+ ATPases: achieving diversity of function with conserved machinery. *Traffic*. 8:1657-67.
Wilson, K.L. 2000. The nuclear envelope, muscular dystrophy and gene expression. *Trends Cell Biol*. 10:125-9.
Winder, S.J., and K.R. Ayscough. 2005. Actin-binding proteins. *J Cell Sci*. 118:651-4.
Wittmann, T., A. Hyman, and A. Desai. 2001. The spindle: a dynamic assembly of microtubules and motors. *Nat Cell Biol*. 3:E28-34.
Wittmann, T., and C.M. Waterman-Storer. 2005. Spatial regulation of CLASP affinity for microtubules by Rac1 and GSK3{beta} in migrating epithelial cells. *J Cell Biol*. 169:929-39.
Woolley, D. 2000. The molecular motors of cilia and eukaryotic flagella. *Essays Biochem*. 35:103-15.
Wu, X., A. Kodama, and E. Fuchs. 2008. ACF7 regulates cytoskeletal-focal adhesion dynamics and migration and has ATPase activity. *Cell*. 135:137-48.
Yamada, T., Y. Ohoka, M. Kogo, and S. Inagaki. 2005. Physical and functional interactions of the lysophosphatidic acid receptors with PDZ domain-containing Rho guanine nucleotide exchange factors (RhoGEFs). *J Biol Chem*. 280:19358-63.
Yamashita, Y.M., A.P. Mahowald, J.R. Perlin, and M.T. Fuller. 2007. Asymmetric inheritance of mother versus daughter centrosome in stem cell division. *Science*. 315:518-21.
Yan, X., R. Habedanck, and E.A. Nigg. 2006. A complex of two centrosomal proteins, CAP350 and FOP, cooperates with EB1 in microtubule anchoring. *Mol Biol Cell*. 17:634-44.
Yang, Y., C.L. Mahaffey, N. Berube, A. Nystuen, and W.N. Frankel. 2005. Functional characterization of fidgetin, an AAA-family protein mutated in fidget mice. *Exp Cell Res*. 304:50-8.
Yu, W., V.E. Centonze, F.J. Ahmad, and P.W. Baas. 1993. Microtubule nucleation and release from the neuronal centrosome. *J Cell Biol*. 122:349-59.
Yu, W., L. Qiang, J.M. Solowska, A. Karabay, S. Korulu, and P.W. Baas. 2008. The microtubule-severing proteins spastin and katanin participate differently in the formation of axonal branches. *Mol Biol Cell*. 19:1485-98.
Zamir, E., and B. Geiger. 2001. Molecular complexity and dynamics of cell-matrix adhesions. *J Cell Sci*. 114:3583-90.
Zhang, D., G.C. Rogers, D.W. Buster, and D.J. Sharp. 2007. Three microtubule severing enzymes contribute to the “Pacman-flux” machinery that moves chromosomes. *J Cell Biol*. 177:231-42.
Zheng, Y., M.L. Wong, B. Alberts, and T. Mitchison. 1995. Nucleation of microtubule assembly by a gamma-tubulin-containing ring complex. *Nature*. 378:578-83.
Zhou, F.Q., C.M. Waterman-Storer, and C.S. Cohan. 2002. Focal loss of actin bundles causes microtubule redistribution and growth cone turning. *J Cell Biol*. 157:839-49.
Zhou, F.Q., J. Zhou, S. Dedhar, Y.H. Wu, and W.D. Snider. 2004. NGF-Induced Axon Growth Is Mediated by Localized Inactivation of GSK-3beta and Functions of the Microtubule Plus End Binding Protein APC. *Neuron*. 42:897-912.
Zovko, S., J.P. Abrahams, A.J. Koster, N. Galjart, and A.M. Mommaas. 2008. Microtubule plus-end conformations and dynamics in the periphery of interphase mouse fibroblasts. *Mol Biol Cell*. 19:3138-46.

Chapter 2

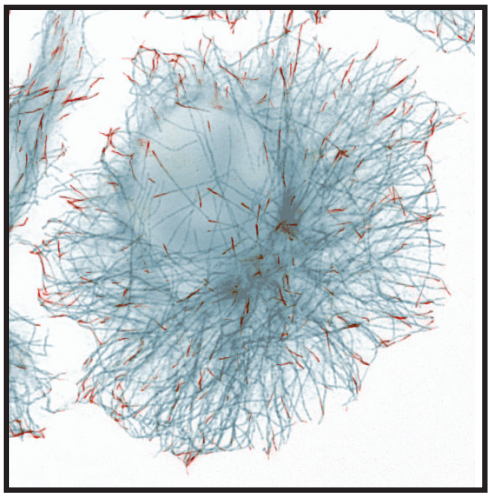

Dynamic behavior of GFP-CLIP-170 reveals fast protein turnover on microtubule plus-ends

Published February 18, 2008

JCB: REPORT

Dynamic behavior of GFP–CLIP-170 reveals fast protein turnover on microtubule plus ends

Katharina A. Dragestein,[1] Wiggert A. van Cappellen,[2] Jeffrey van Haren,[1] George D. Tsibidis,[3] Anna Akhmanova,[1] Tobias A. Knoch,[1] Frank Grosveld,[1] and Niels Galjart[1]

[1]Department of Cell Biology and Genetics and [2]Department of Reproduction and Development, Erasmus Medical Center, 3000 DR Rotterdam, Netherlands
[3]Institute of Electronic Structure and Laser, Foundation for Research and Technology - Hellas, 71110 Heraklion, Crete, Greece

Microtubule (MT) plus end–tracking proteins (+TIPs) specifically recognize the ends of growing MTs. +TIPs are involved in diverse cellular processes such as cell division, cell migration, and cell polarity. Although +TIP tracking is important for these processes, the mechanisms underlying plus end specificity of mammalian +TIPs are not completely understood. Cytoplasmic linker protein 170 (CLIP-170), the prototype +TIP, was proposed to bind to MT ends with high affinity, possibly by copolymerization with tubulin, and to dissociate seconds later. However, using fluorescence-based approaches, we show that two +TIPs, CLIP-170 and end-binding protein 3 (EB3), turn over rapidly on MT ends. Diffusion of CLIP-170 and EB3 appears to be rate limiting for their binding to MT plus ends. We also report that the ends of growing MTs contain a surplus of sites to which CLIP-170 binds with relatively low affinity. We propose that the observed loss of fluorescent +TIPs at plus ends does not reflect the behavior of single molecules but is a result of overall structural changes of the MT end.

Introduction

Microtubules (MTs) exhibit dynamic instability (Mitchison and Kirschner, 1984), repeatedly switching between growth and shrinkage phases, thereby constantly moving through the cytoplasm. This facilitates contacts between MT ends and relatively immobile cellular structures, such as chromosomes and focal adhesions, and allows the cell to react to external cues. Plus end–tracking proteins (+TIPs; Schuyler and Pellman, 2001) specifically bind to MT plus ends and are ideally positioned to influence MT dynamics and MT target interactions.

Fluorescently tagged +TIPs bound to the ends of growing MTs appear as cometlike dashes in time-lapse experiments. This unique behavior has been explained by different mechanisms (Akhmanova and Hoogenraad, 2005). For example, cytoplasmic linker protein 170 (CLIP-170), the prototype +TIP (Perez et al., 1999), was suggested to bind MT ends by treadmilling, binding with high affinity to newly synthesized MT ends and detaching with a half-life of 1–3 s (Perez et al., 1999; Folker et al., 2005; Komarova et al., 2005). +TIPs have also been proposed to copolymerize with tubulin (Arnal et al., 2004; Folker et al., 2005; Slep and Vale, 2007). In both models, the loss of fluorescence in the cometlike dash is correlated to the dissociation of +TIPs from MT ends.

The MT-binding domains of CLIP-170 were recently shown to interact with the C-terminal tails of α-tubulin as well as end-binding protein 1 (EB1; Honnappa et al., 2006). CLIP-170 but not EB1 fails to recognize the ends of detyrosinated MTs in cultured cells (Peris et al., 2006), showing that the C-terminal tyrosine of α-tubulin is essential for the accumulation of CLIP-170 on MT ends and that the presence of EB1 is not enough. On the other hand, evidence has been presented for a role of EB1 in the MT end localization of CLIP-170 (Komarova et al., 2005). To reconcile these results, we examined the dynamics of GFP–CLIP-170 on MT plus ends using FRAP and fluorescence correlation spectroscopy (FCS) approaches. We show that MT plus ends contain a surplus of binding sites for CLIP-170, to which CLIP-170 molecules bind with low affinity, resulting in a rapid exchange of CLIP-170 on MT plus ends. Our data imply that MT polymerization generates a large number of binding sites that decay exponentially. This turnover of binding sites explains the fluorescent comets of GFP–CLIP-170 and other +TIPs observed in cells. Our findings may lead to a reevaluation of other protein accumulations at MT plus ends.

Correspondence to Niels Galjart: n.galjart@erasmusmc.nl

Abbreviations used in this paper: CLIP-170, cytoplasmic linker protein 170; EB, end-binding protein; FCA, fluorescence cumulant analysis; FCS, fluorescence correlation spectroscopy; MEF, mouse embryonic fibroblast; MT, microtubule; PCH, photon-counting histogram; ROI, region of interest.

The online version of this article contains supplemental material.

The Journal of Cell Biology, Vol. 180, No. 4, February 25, 2008 729–737
http://www.jcb.org/cgi/doi/10.1083/jcb.200707203

Supplemental Material can be found at:
http://jcb.rupress.org/cgi/content/full/jcb.200707203/DC1

Published February 18, 2008

Results and discussion

Transient binding of GFP–CLIP-170 to MT ends

GFP–CLIP-170 behaves indistinguishably from endogenous CLIP-170 (Perez et al., 1999; Akhmanova et al., 2005), making it a useful tool to study the dynamic behavior of CLIP-170 in vivo. MT plus ends were visible as fluorescent comets in COS-7 cells transiently expressing GFP–CLIP-170. We studied these with high temporal resolution (Fig. 1 A and Video 1, available at http://www.jcb.org/cgi/content/full/jcb.200707203/DC1). When traversing regions of interest (ROIs) of 210 × 210 nm, MT plus ends appeared as fluorescent peaks in the corresponding fluorescence intensity track (Fig. 1, A and B). Mean peak decays could be fitted with an exponential curve, yielding a k_{decay} of 0.44 s^{-1} for COS-7 cells at 37°C (Fig. 1 C and Table I). This translates to a half-life of ∼1.6 s, which correlates well with reported half-lives of CLIP-170 on MT ends (Folker et al., 2005; Komarova et al., 2005).

This macroscopic loss of fluorescence of GFP–CLIP-170 on MT plus ends over time (i.e., the fluorescent decay) does not reveal the behavior of single CLIP-170 molecules. To gain more insight in the dynamics of GFP–CLIP-170 on MT plus ends, we performed FRAP experiments. Repeatedly bleaching a strip of 0.2 × 18.5 µm in an imaged area of 4.5 × 18.5 µm resulted mainly in bleaching of freely diffusing cytoplasmic GFP–CLIP-170 molecules but also in bleaching of MT-bound GFP–CLIP-170 (Fig. 1 D). We measured fluorescence intensity over time in areas of 210 × 210 nm on the bleached strip and observed recovery of fluorescence not only in the cytoplasm but also on MT plus ends (Fig. 1 E). These data, which were further supported by various control experiments (Fig. S1, available at http://www.jcb.org/cgi/content/full/jcb.200707203/DC1), indicate that bleached GFP–CLIP-170 molecules exchange with fluorescent ones on MT ends, which is not compatible with the original treadmilling model.

Exchange of CLIP-170 on MT plus ends under non–steady-state conditions

The recovery of GFP–CLIP-170 on MT plus ends takes place at the same time that total fluorescence decreases. Common FRAP models do not account for these non–steady-state conditions. Therefore, we applied a model in which fluorescence recovery is governed by k_{off} and a constant that describes overall remodeling of the MT plus end (Lele and Ingber, 2006). To calculate fluorescence recoveries on MT ends, we corrected the recovery on bleached GFP–CLIP-170–positive MT plus ends for the underlying overall loss of GFP–CLIP-170 fluorescence over time (Fig. 1 C). The resulting recoveries were subsequently described with a simple exponential curve. We calculated an apparent $k_{recovery}$ of 2.50 s^{-1} for the exchange of GFP–CLIP-170 on MT ends in COS-7 cells at 37°C (Fig. 1 F and Table I). This corresponds to a half-life of association of 0.28 s, which is about six times shorter than the half-life of GFP–CLIP-170–derived fluorescence on MT plus ends as described by k_{decay}.

Our data suggest that the disappearance of GFP–CLIP-170 from MT ends as described by k_{decay} (Fig. 1 C) reflects the loss of binding sites for CLIP-170 at MT ends rather than the dissociation of individual CLIP-170 molecules. As we observed the exchange of GFP–CLIP-170 molecules all along MT plus ends, even >1 µm distal from the tip (Fig. S1 G), the copolymerization of CLIP-170 with tubulin does not appear to be the dominant mechanism underlying the accumulation of CLIP-170 on MT plus ends.

EB3 also shows rapid turnover on MT plus ends

EB1 and EB3 are two highly related +TIPs that interact with many other +TIPs and are thought to play a central role in the association of +TIPs to MT ends (for review see Lansbergen and Akhmanova, 2006). In COS-7 cells transiently expressing EB3-GFP, we observed fluorescent peaks comparable with the peaks in cells expressing GFP–CLIP-170 (Fig. 1 G and Table I). A previous study in fixed cells showed overlapping fluorescence staining patterns for EB1 and CLIP-170 at MT ends (Komarova et al., 2005), supporting our results in live cells.

FRAP analysis revealed the recovery of EB3-GFP fluorescence in the cytoplasm and on MT plus ends in transiently transfected COS-7 cells (Fig. 1 H). After correction for cytoplasmic recovery and fluorescence decay, we found an apparent $k_{recovery}$ of 3.37 s^{-1} for the exchange of EB3-GFP on MT ends (Fig. 1 H and Table I). This corresponds to a half-life of association of 0.20 s, which is faster than the half-life of CLIP-170. Thus, there is a continuous exchange of GFP–CLIP-170 and EB3-GFP on MT plus ends.

Observed exchange of CLIP-170 and EB3 on MT ends appears limited by diffusion

The $k_{recovery}$ values of GFP–CLIP-170 in the cytoplasm and on MT ends of transiently transfected COS-7 cells are comparable; the same holds true for EB3-GFP (Table I). These results indicate that the time a CLIP-170 or EB3 molecule is actually bound to the MT end is short compared with the time it takes these molecules to diffuse through the bleached strip. The fact that the recovery of EB3-GFP is faster than the recovery of GFP–CLIP-170 is consistent with EB3-GFP being smaller and diffusing more rapidly.

Biochemical reaction rates are temperature dependent, with an approximate doubling of reaction constant every 10°C. We reasoned that the behavior of GFP–CLIP-170 at MT ends might be influenced by temperature changes. To evaluate CLIP-170 behavior in different cell types at different temperatures, we examined transiently transfected COS-7 cells as well as 3T3 cells that stably express GFP–CLIP-170 (Drabek et al., 2006). MT growth rates diminished from ∼0.4 µm/s at 37°C to 0.19 µm/s at 27°C in 3T3 cells (Fig. 2 A), emphasizing the temperature dependence of MT assembly.

Interestingly, reducing the temperature from 37 to 27°C increased the half-life of GFP–CLIP-170–derived fluorescence on MT plus ends from 1.4 to 2.7 s in 3T3 cells (Fig. 2 B) and from 1.6 to 2.8 s in transiently transfected COS-7 cells (Fig. 2 C and Table I). As longer fluorescent comets were more suitable for FRAP experiments and fluorescence decay at 27°C was identical in the cell types measured (Table I), we performed

Published February 18, 2008

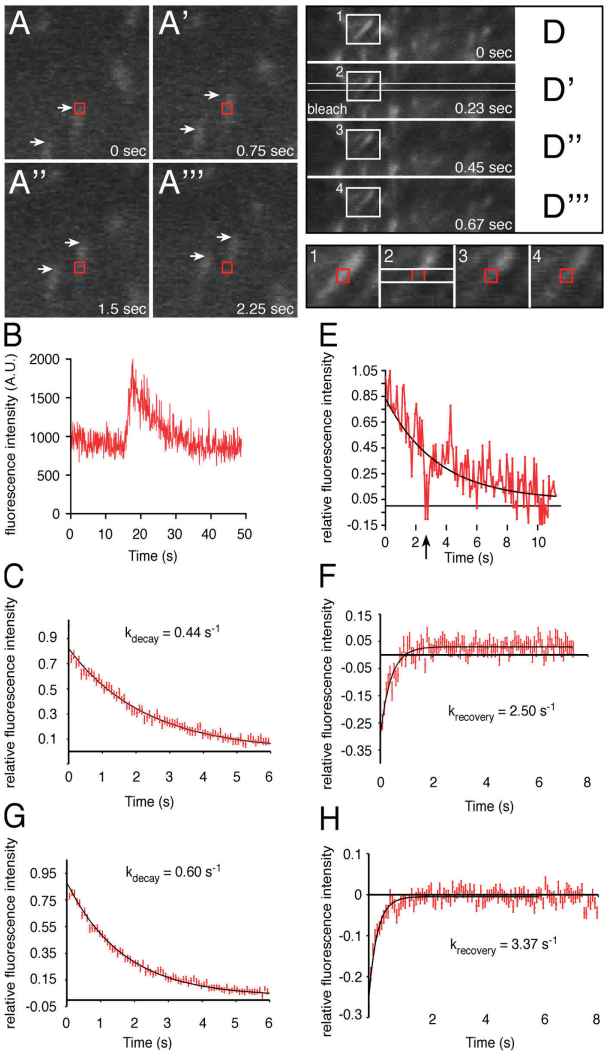

Figure 1. **Fast FRAP analysis.** (A–A''') Time-lapse imaging of COS-7 cells transiently expressing GFP–CLIP-170 (every 10th frame is shown). Two GFP–CLIP-170–labeled MT ends are indicated by arrows. In A, one of these is about to traverse a 210 × 210-nm ROI (red rectangles). After 2.25 s (A'''), this MT end has traversed the ROI. (B) Fluorescence intensity in an ROI of 210 × 210 nm as a GFP–CLIP-170–labeled MT end traverses. (C and G) Mean fluorescence decay of nonbleached, GFP–CLIP-170-labeled (C) or EB3-GFP–labeled (G) MT ends (k_{decay} is indicated). (D–D''') COS-7 cells transiently expressing GFP–CLIP-170 were imaged as in A. An area of 256 × 3 pixels (indicated in D') was bleached every 7.5 s, occasionally resulting in bleaching of MT end–bound GFP–CLIP-170. Rectangles 1–4 are shown enlarged underneath D–D'''. Fluorescence intensity was measured in ROIs of 210 × 210 nm (red rectangles). (E) Fluorescence intensity of a bleached GFP–CLIP-170–labeled MT end (black arrow indicates bleach; black line indicates mean fluorescence decay). (F and H) Mean fluorescence recovery of GFP–CLIP-170 (F) and of EB3-GFP (H) on MT ends ($k_{recovery}$ is indicated).

further FRAP experiments in transiently transfected mouse embryonic fibroblasts (MEFs) at 27°C. In wild-type MEFs, the recovery of cytoplasmic GFP–CLIP-170 ($k_{recovery}$ of 2.34 s^{-1}) did not differ significantly from the recovery of MT end–bound GFP–CLIP-170 ($k_{recovery}$ of 1.66 s^{-1}; Fig. 2 D and Table I). Thus, despite the fact that MT growth rates decreased and that binding sites for CLIP-170 disappeared more slowly at 27°C, the mean time a CLIP-170 molecule is bound to an MT plus end remains short. We propose that the diffusion of CLIP-170 and EB3 is rate limiting for the observed binding/unbinding reactions on MT plus ends.

Fast exchange of CLIP-170 on MT ends is independent of self-interaction

CLIP-170 is a rodlike molecule that can interact with itself in a head-to-tail fashion (Lansbergen et al., 2004). One could envision a first layer of CLIP-170 molecules bound to the MT surface and turning over by the treadmilling mechanism, to which

Published February 18, 2008

Table I. **Behavior of transiently transfected GFP-tagged +TIPs on MT plus ends**

+TIP	Cell type	Method	Temp	MT end k_{decay}	MT end $k_{recovery}$	Cytoplasm $k_{recovery}$
			°C	s^{-1}	s^{-1}	s^{-1}
EB3	COS-7	FRAP	37	0.60 (175) 0.58–0.62	3.37 (298) 2.89–3.85	3.43 (1,756) 2.75–4.12
Full-length CLIP-170	COS-7	FCS	37	0.48 (17) 0.39–0.59	ND	ND
Full-length CLIP-170	COS-7	FRAP	37	0.44 (77) 0.42–0.46	2.50 (94) 2.06–2.94	2.80 (534) 2.29–3.31
Full-length CLIP-170	COS-7	FRAP	27	0.25 (87) 0.23–0.27	ND	ND
Full-length CLIP-170	MEF (WT)	FRAP	27	0.25 (71) 0.23–0.26	1.66 (83) 1.36–1.97	2.34 (553) 1.90–2.78
Full-length CLIP-170	MEF (DKO)	FRAP	27	0.25 (171) 0.24–0.256	2.04 (214) 1.86–2.21	2.43 (1,550) 2.14–2.51
CLIP-170 XmnI	MEF (DKO)	FRAP	27	0.31 (86) 0.30–0.33	3.56 (93) 2.62–4.55	4.87 (666) 4.09–5.65

Mean k_{decay} and $k_{recovery}$ values are given with the 95% confidence interval (underneath) and the number (*n*) of fluorescent decays and recoveries, respectively, used to calculate mean values. WT, wild type; DKO, double knockout.

a second layer of CLIP-170 molecules bind through intermolecular head-to-tail interactions, enabling the second layer to turn over rapidly on the first layer. To investigate this, we tested GFP–CLIP-170XmnI, a fragment of GFP–CLIP-170 that contains only the MT-binding domain and that cannot self-interact (Komarova et al., 2002). FRAP analysis in transiently transfected COS-7 cells showed that GFP–CLIP-170XmnI exchanges on MT ends as well (unpublished data).

To eliminate the possibility of an interaction of fluorescent GFP–CLIP-170XmnI with endogenous nonfluorescent CLIP-170, we tested recovery of the truncated protein in MEFs derived from CLIP-115/CLIP-170 double knockout mice, which contain neither CLIP-115 nor CLIP-170 (unpublished data). FRAP analysis showed fast recovery of GFP–CLIP-170XmnI (Fig. 2 E and Table I) both in the cytoplasm ($k_{recovery}$ of 4.87 s^{-1}) and on MT ends ($k_{recovery}$ of 3.56 s^{-1}).

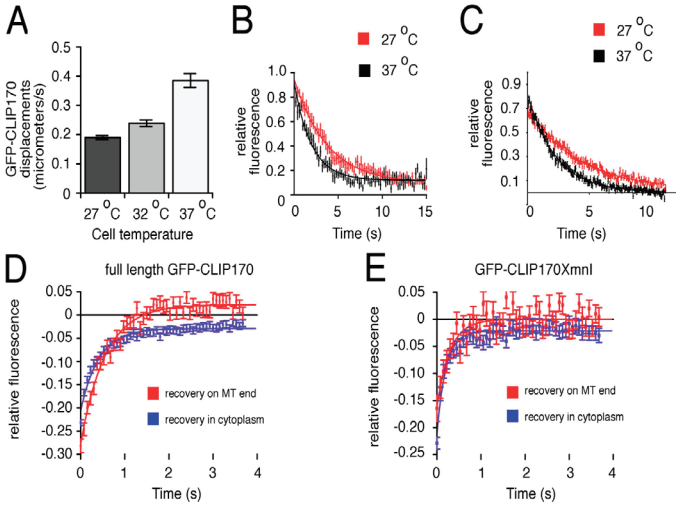

Figure 2. **Influence of temperature on GFP–CLIP-170 behavior.** (A) GFP–CLIP-170 comets analyzed in stably expressing 3T3 cells (13 MT ends analyzed at 37°C, 19 at 32°C, and 14 at 27°C). (B) Mean fluorescence decay of GFP–CLIP-170–labeled MT ends in stably expressing 3T3 cells measured at 37°C (black; 13 ends analyzed) and at 27°C (red; 12 ends analyzed). A fit (see Materials and methods) yields a half-life of GFP–CLIP-170 fluorescence of 1.35 s at 37°C and 2.67 s at 27°C. (C) Mean fluorescence decay of GFP–CLIP-170–labeled MT ends in transiently transfected COS-7 cells at 37°C (black) and 27°C (red). See Table I for values. (D and E) Fast FRAP analysis at 27°C in MEFs transiently transfected with GFP–CLIP-170 (D) or GFP–CLIP-170XmnI (E). Fluorescent recovery was measured in the cytoplasm (blue) and on MT ends (red). For $k_{recovery}$ values, see Table I. Error bars indicate SEM.

Published February 18, 2008

These results indicate that the binding of CLIP-170 molecules on MT ends does not occur via a layer of MT-bound CLIP-170. Furthermore, as $k_{recovery}$ values in the cytoplasm and on MT ends are not significantly different, the binding/unbinding of GFP–CLIP-170XmnI on MT plus ends also appears to be diffusion limited.

The fluorescence decay curves of GFP–CLIP-170 and GFP–CLIP-170XmnI are similar, yet the recovery of GFP–CLIP-170XmnI on MT plus ends is significantly faster than the recovery of GFP–CLIP-170 (Table I). These results are not well explained by the treadmilling model, which assumes that the fluorescence decay on MT plus ends is related to the dissociation rate of a +TIP.

CLIP-170 binds MT plus ends with low affinity

FCS is a sensitive single-molecule technique that allows the determination of concentration and diffusive behavior of proteins in vivo (Elson, 2004). Using FCS, we analyzed GFP–CLIP-170 in transiently transfected COS-7 cells (Fig. 3 A). Strikingly, peaks appeared in many fluorescence intensity measurements (Fig. 3 B) whose shape was indistinguishable from peaks observed in confocal imaging (compare respective decay constants in Table I). Combined with other experiments (Fig. S2, available at http://www.jcb.org/cgi/content/full/jcb.200707203/DC1), this suggests that peaks in FCS intensity tracks represent GFP–CLIP-170–labeled MT ends.

To correlate the cytoplasmic GFP–CLIP-170 concentration to the number of peak-bound GFP–CLIP-170 molecules, we calculated the number of particles present in the cytoplasm and on peaks of the fluorescence intensity tracks (Fig. 3 B) and found a positive correlation (Fig. 3 C). Peak fluorescence values still increased at the highest cytoplasmic concentrations of GFP–CLIP-170, indicating that the binding of GFP–CLIP-170 to MT ends was not yet saturated.

We recently generated GFP–CLIP-170 knock-in MEFs, in which GFP–CLIP-170 is expressed at an endogenous level (Akhmanova et al., 2005) and associates with the ends of growing MTs (Video 4, available at http://www.jcb.org/cgi/content/full/jcb.200707203/DC1). FCS revealed an intracellular GFP–CLIP-170 dimer concentration of 44 ± 11 nM (±SD; n = 26; 13 cells and four independent experiments), which corresponds to ~10 dimers in the measurement volume. This correlates with ~10 MT end–bound GFP–CLIP-170 molecules in knock-in MEFs (Fig. 3 C). Assuming that CLIP-170 does not bind other proteins and that there are ~100 binding sites for CLIP-170 per MT end (Fig. 3 C), the dissociation constant (K_d) for CLIP-170 binding to MT plus ends is 0.44 μM.

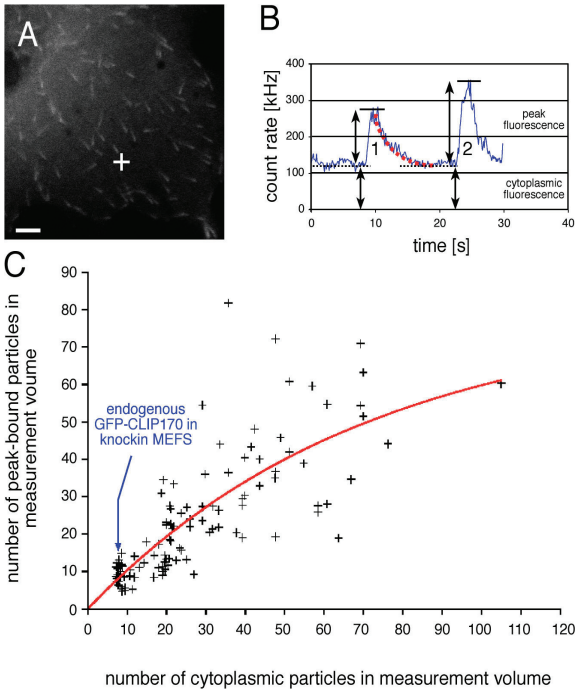

Figure 3. **Analyzing GFP–CLIP-170 on MT ends with FCS.** (A) Confocal image of a COS-7 cell transiently transfected with GFP–CLIP-170. The plus sign indicates the location of FCS measurement. Bar, 5 μm. (B) Intensity track of FCS measurement in a transfected COS-7 cell. Peaks of fluorescence are occasionally detected. The dotted red line indicates the exponential fluorescence decay; the bottom double-headed arrows indicate cytoplasmic fluorescence; the top double-headed arrows indicate peak fluorescence. (C) Comparison of the number of cytoplasmic and peak-bound GFP–CLIP-170 particles. Values as depicted in B were measured, and the number of particles was determined for 110 peaks. A scatter plot of these values is best approximated by the curve (indicated by the red line) $Y = Y_{max} \times (1 - e^{-kx})$.

Published February 18, 2008

Model for CLIP-170 interaction with MT plus ends

Taxol is an MT-stabilizing agent that changes MT conformation (Arnal and Wade, 1995) and causes the displacement of GFP–CLIP-170 from MT ends at micromolar concentrations (Perez et al., 1999). However, after application of a low dose (10 nM) of taxol to HeLa cells stably expressing GFP–CLIP-170, MT end binding was not abolished. The shape of MT end accumulations changed from a cometlike to a dotted pattern, and, unexpectedly, GFP–CLIP-170 remained bound to the ends of pausing and shrinking MTs (Fig. S3, available at http://www.jcb.org/cgi/content/full/jcb.200707203/DC1). These results suggest that CLIP-170 recognizes a structural, taxol-sensitive feature of MT ends.

We propose a fast exchange model for the binding of CLIP-170 to MT ends (Fig. 4). In our view, MT polymerization generates a vast number of binding sites that disappear exponentially (described by k_{decay}) and that can bind and release CLIP-170 molecules several times before disappearing. We assume that conformational changes govern binding site turnover. Future studies should reveal their nature (for example, whether they involve closure of a two-dimensional sheet of protofilaments into a hollow MT tube). Like CLIP-170, EB3 also turns over rapidly on MT plus ends. Diffusion plays a major role in the kinetics of CLIP-170 and EB3 exchange on MT ends. However, many interactions between +TIPs have been documented. These interactions differ between systems and are likely to influence binding behavior.

The fast exchange model implies that the fluorescence decay at MT ends, which is measured in kymographs, does not correlate with the dissociation of individual +TIP molecules but rather with the disappearance of binding sites for these proteins (hence the name k_{decay}). A combined knockdown of the +TIPs EB1 and EB3 resulted in a faster fluorescence decay of YFP–CLIP-170 (Komarova et al., 2005). We hypothesize that EB1-like proteins directly influence the turnover of binding sites at MT ends and that their depletion causes altered remodeling of MT ends and, thereby, a faster disappearance of CLIP-170.

GFP-CLASP2 is a +TIP in the cell body of migrating Ptk1 cells in which FRAP analysis indicated recovery along the MT end (Wittmann and Waterman-Storer, 2005). This result is well explained by the fast exchange model, whereas if treadmilling was the mechanism by which CLASP2 recognized MT ends, one would expect fluorescence to reappear only in MT segments of new plus end growth. Therefore, we propose that fast exchange is not limited to CLIP-170 and EB3 but is a more general mechanism for +TIP behavior at MT ends.

Materials and methods

Fluorescent fusion proteins

The GFP–CLIP-170 knock-in fusion protein is functional in vivo because GFP–CLIP-170 knock-in mice are completely normal, whereas CLIP-170 knockout mice have severe defects in spermatogenesis (Akhmanova et al., 2005). The GFP–CLIP-170 cDNA, which was used for transient transfections in COS-7 cells and for the generation of 3T3 and HeLa stable cell lines, has been described previously (Hoogenraad et al., 2000). It is based on a brain-specific CLIP-170 isoform (Akhmanova et al., 2005) and was cloned into the pEGFP vector (Clontech Laboratories, Inc.). This fusion protein is functional; when introduced into CLIP-115/-170–deficient MEFs, normal cellular morphology and protein localization are restored.

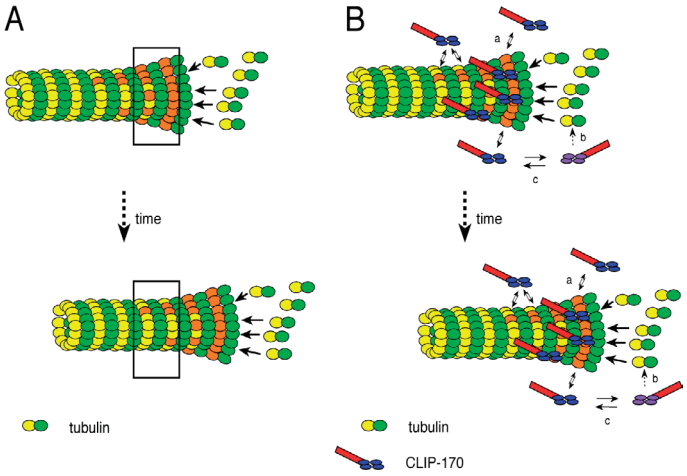

Figure 4. **Fast exchange model.** (A) MT polymerization generates a large number of binding sites (orange ellipses), which disappear with single-order reaction kinetics. Thus, as time progresses, less binding sites are present within the depicted rectangle. (B) Dimeric CLIP-170 exchanges rapidly on binding sites irrespective of the position on the MT end. Several interactions with CLIP-170 molecules can occur during the lifetime of a binding site. The equilibrium between cytoplasmic and MT end–bound CLIP-170 (reaction a) might be determined by posttranslational modifications (reaction c), conformational changes, and/or protein–protein interactions. As we find CLIP-170 exchange on MT ends distal of sites of MT polymerization, copolymerization of CLIP-170 with tubulin (reaction b) does not explain the cometlike distribution of +TIPs. However, it is not excluded (hence the stippled arrow), and modified forms of CLIP-170 (indicated by the purple ellipses) might bind tubulin with higher affinity.

Published February 18, 2008

Rat brain CLIP-170 cDNA was used to generate the truncated CLIP-170XmnI protein (amino acids 4–309), which is called CLIP-170 Head in the original study (Komarova et al., 2002). This Head domain of CLIP-170 is able to restore MT dynamics in cells in which CLIP-170 does not localize to MT ends (Komarova et al., 2002). EB3-GFP has been described previously (Stepanova et al., 2003). Positioning of GFP at the C terminus of EB3 prevents its interaction with CLIPs, whereas other protein–protein interactions are not perturbed (Komarova et al., 2005).

Cell lines and methods used for fluorescent protein expression

The GFP–CLIP-170 knock-in mice and MEFs have been described previously (Akhmanova et al., 2005). The CLIP-115/-170 double knockout MEFs were derived from double knockout mice, which were generated by crossing the Clip1 (CLIP-170 encoding gene) and Clip2 (CLIP-115 encoding gene) single knockout lines. The 3T3 cell system used to express GFP–CLIP-170 under control of the reverse tetracyclin transcriptional activator (Tet-on system) has been described previously (Drabek et al., 2006).

To examine the effect of taxol on GFP–CLIP-170 behavior, we generated a stable HeLa cell line expressing rat brain CLIP-170 N-terminally tagged with GFP and a short (22 amino acids) biotinylation sequence (Lansbergen et al., 2006). HeLa cells were transfected using Lipofectamine 2000 (Invitrogen) and selected with neomycin for cells expressing GFP–CLIP-170. One stable HeLa cell line was further characterized. These cells express ~2.5 times more GFP–CLIP-170 than endogenous CLIP-170 (Fig. S3 A, available at http://www.jcb.org/cgi/content/full/jcb.200707203/DC1). MT growth, as reflected by GFP–CLIP-170 comet displacements (Fig. S3 B), is comparable with that observed in other cell types. GFP–CLIP-170 behavior was studied in these cells before and 1 h after the application of 10 nM taxol. Consistent with previous results (Jordan et al., 1993), the nanomolar application of taxol interfered with interphase MT dynamics; the rate of GFP–CLIP-170 displacements was reduced, and movements were highly heterogeneous, as reflected by a high SEM (Fig. S3, C, G, and I). Videos of GFP–CLIP-170 in untreated and treated cells are shown as Videos 6 and 7 (available at http://www.jcb.org/cgi/content/full/jcb.200707203/DC1), respectively.

For transient transfections, we used Polyfect (QIAGEN), Fugene 6 (Roche), or diethylaminoethyl-dextran and analyzed cells 24 h after transfection. For protein extracts, cells were incubated in lysis buffer (20 mM Tris-HCl, pH 8, 100 mM NaCl, and 0.5% Triton X-100 supplemented with protease inhibitors [Roche]) for 10 min on ice. Cell lysates were centrifuged for 10 min at 13,000 rpm and 4°C. The supernatants were used for further experiments.

Live imaging

Cells were analyzed in normal culture medium (a 1:1 mixture of DME and F10 [Biowhittaker] supplemented with antibiotics and 5–10% (vol/vol) fetal calf serum). Fluorescence time-lapse analysis in transiently transfected COS-7 cells, 3T3 cells, and MEFs was performed on a confocal laser-scanning microscope (LSM510; Carl Zeiss, Inc.) as described previously (Stepanova et al., 2003; Akhmanova et al., 2005). We either used a 40× NA 1.2 water immersion lens or a 63× NA 1.4 oil immersion lens (Carl Zeiss, Inc.). In most of the experiments, cells were imaged at 37°C. For temperature-dependence experiments in 3T3 cells, the temperature was set to 27°C and subsequently increased to 32 and 37°C while cells were kept in the microscope set-up. In this way, the same cells could be examined at different temperatures. For temperature-dependence experiments in transiently transfected COS-7 cells, different cells were measured at 27 and 37°C.

Fluorescence time-lapse analysis in stably transfected HeLa cells was performed using an epifluorescent inverted microscope (200M; Carl Zeiss, Inc.) with a 100× NA 1.4 oil immersion lens (Carl Zeiss, Inc.), which was driven by Openlab software (PerkinElmer) and equipped with a camera (ORCA-ER; Hamamatsu). Time-lapse images were acquired before and 1 h after taxol application at one frame per second. The movement in time of GFP–CLIP-170 comets was measured as described previously (Stepanova et al., 2003). For Fig. S3, videos were imported into ImageJ (National Institutes of Health) and converted to 8 bit. Maximum intensity projections were generated on image stacks that were first processed with the walking average plug-in (set to 4) of ImageJ. Kymographs were generated using the kymograph plug-in (J. Rietdorf, European Molecular Biology Laboratory, Heidelberg, Germany). Images were inverted using ImageJ for better visualization in Fig. S3.

FRAP: experimental set-up

For FRAP analysis, images of 256 × 64 pixels (lateral pixel size of 70 nm) were acquired at 13.3 frames per second. Bleaching of an area of 256 × 3 pixels every 100th frame (i.e., every 7.5 s) resulted in occasional bleaching of GFP–CLIP-170–positive MT ends. Fluorescence recovery in a region of 3 × 3 pixels was measured. This area encompassed part of the fluorescent MT end. We measured bleached and nonbleached MT ends and cytoplasmic regions. For better visualization of MT ends, the walking average plug-in of ImageJ was used in Fig. 1 (five consecutive frames in A–A′′′ and three consecutive frames in D–D′′′).

Measurement of fluorescence decay and recovery

Data were analyzed with Prism (GraphPad) or with Aabel (Gigawiz Ltd.). To derive exponential decay curves for GFP–CLIP-170– and EB3-GFP–labeled MT ends from confocal images, we first subtracted the cytoplasmic background values, normalized curves to 1, and obtained an average curve. The average decay of fluorescent peaks was fitted as a first-order exponential decay with a nonlinear least square fitting routine: $I(t) = I(\infty) + (I[0] - I[\infty]) \times e^{-kdecay \times t}$, where t is time, I is normalized intensity, k_{decay} is the reaction constant, I(0) is the initial fluorescence value, and (I[0] − I[∞]) is the span of the reaction. The half-time of fluorescence decay was calculated as $\ln(2)/k_{decay}$.

To calculate the recovery of GFP–CLIP-170 and EB3-GFP fluorescence on MT ends after bleaching, we subtracted background values and normalized curves to 1. The resulting curves represent a combination of fluorescence decay and recovery after bleaching. We subsequently subtracted the fit of the averaged fluorescence decay to obtain a curve with only the mean fluorescence recovery. This curve could be fitted with the exponential equation $I(t) = I(\infty) - I(0) \times e^{-krecovery \times t}$, where t is time, I(t) indicates fluorescence intensity at time point t after the bleach, I(0) indicates fluorescence intensity before the bleach (as a result of subtraction with the fluorescent decay curve, this is a negative value), I(∞) indicates fluorescence intensity at an infinite time point after the bleach (as a result of subtraction with the fluorescent decay curve, this value is 0), and $k_{recovery}$ is a rate constant that is related to k_{off} (Lele and Ingber, 2006). The half-life of recovery was calculated as $\ln(2)/k_{recovery}$.

To calculate recovery in the cytoplasm, the FRAP curves were normalized to 1 by dividing each data point after the bleach by the mean prebleach value (obtained by averaging the last 10 points before the bleach). The same equation as described above was used to obtain cytoplasmic $k_{recovery}$ values. The half-life of recovery was calculated as $\ln(2)/k_{recovery}$. In the case of cytoplasmic recovery, I(∞) is 1 (if there is no immobile fraction). In Fig. 2 (D and E), we compared the recovery on MT ends with the recovery in the cytoplasm. To do this, we subtracted cytoplasmic values with 1 so that in both sets of recoveries, I(∞) is 0.

FRAP: control experiments

We considered several possible drawbacks to our fast FRAP experiments. First, as MTs have a diameter of only 25 nm, ROIs of 210 × 210 nm will contain cytoplasmic GFP–CLIP-170 molecules even in the presence of an MT plus end (Fig. S1 A). Thus, one limitation of our experiments could be that the fluorescence recovery observed after bleaching GFP–CLIP-170 on MT plus ends was caused by recovery in the cytoplasm. Therefore, we subtracted the mean fluorescence recovery in the cytoplasm from the fluorescence recovery on MT plus ends. Fluorescence still recovered on corrected bleached MT ends (Fig. S1, B and C), whereas no recovery remained when we took cytoplasmic bleaches and corrected them for cytoplasmic recoveries (Fig. S1 D; note that in this experiment, we did not normalize cytoplasmic bleaches). Thus, although an MT plus end traversing an ROI of 210 × 210 nm is small in terms of volume, bleaching of MT plus end–bound GFP–CLIP-170 can clearly be distinguished.

In a second control experiment, we took nonbleached peaks (outside of the bleached strip). We performed the same calculations on these peaks as on the truly bleached peaks. No recovery was observed on peaks away from the bleached strip, whereas peaks within the bleached strip did show a clear recovery (Fig. S1 E). Thus, even though the fast FRAP approach forces us to analyze images with relatively low signal to noise ratio, the recovery caused by bleaching can be clearly distinguished from random fluctuations.

As a third control experiment, we performed fast FRAP in transiently transfected COS-7 cells that abundantly overexpress GFP–CLIP-170 (Fig. S1 F). In such cells, GFP–CLIP-170 labels MTs along their length and appears immobile (the video belonging to this FRAP experiment is shown as Video 5, available at http://www.jcb.org/cgi/content/full/jcb.200707203/DC1). Under these conditions, we observed a four times faster recovery of GFP–CLIP-170 in the cytoplasm (blue data points; k = 1.9 s^{-1}; 95% confidence interval of 1.4–2.4 s^{-1}) than on MTs (green data points; k = 0.50 s^{-1}; 95% confidence interval of 0.43–0.57 s^{-1}). These data show that our FRAP set-up can distinguish between cytoplasmic and MT-bound CLIP-170 molecules when GFP–CLIP-170 dwells on MTs for longer periods of time.

Published February 18, 2008

Diffusion of GFP–CLIP-170 and GFP–CLIP-170XmnI measured with FRAP

In our FRAP set-up, diffusion of GFP–CLIP-170 cannot be neglected. Furthermore, the bleaching beam has a finite width, and although we outlined a bleach strip of 0.2 × 18.5 µm, the actual bleached area was larger and not precisely defined. Recently, a mathematical model was described that does not require a priori knowledge about the size and shape of the bleached area and that allows calculation of diffusion constants under the conditions we used (Seiffert and Oppermann, 2005). We adapted this method to estimate the diffusion coefficient (D) of GFP–CLIP-170 from the FRAP experiments. We divided the image of 256 × 64 pixels (with a lateral pixel size of 70 nm) in 20 strips of 3-pixel width. Thus, each strip was ∼0.2-µm wide and 18.5-µm long. For each strip, mean intensity was measured for the first 20 postbleach frames. Values were divided by the fluorescence value 75 ms before the bleach (prebleach value). At least six bleaches at the same position were performed to obtain a mean curve. The bleach profile in the imaged area is described by a Gaussian bleach profile (Fig. S1 H). The SD derived from the Gaussian is related to the full-width half-maximum (ω) by $\omega \approx 2.5$ SD. Furthermore, $\omega^2 = D/2 \times t$ (Seiffert and Oppermann, 2005), where D is the diffusion coefficient and t is time. Thus, by plotting ω^2 versus t (Fig. S1, I and J), we obtained a value for the diffusion constant D of 10.3 ± 6.1 $\mu m^2/s$ (n = 48; SD indicated) for GFP–CLIP-170 and D = 24.7 ± 15.2 $\mu m^2/s$ (n = 25; SD indicated) for GFP–CLIP-170XmnI. These values are comparable with the values measured by FCS (see the next section), strongly suggesting that diffusion coefficients can be determined with our FRAP set-up.

FCS

FCS measurements were conducted with an LSM510-Confocor II system (Carl Zeiss, Inc.) equipped with a continuous wave Ar laser, a C-Apochromat 40x NA 1.2 water immersion objective, and two avalanche photodiodes. The FCS measurement volume was 0.25 fl. EGFP was excited with the 488-nm line. Cell lysates were measured for 30 s at room temperature with 17.5-µW laser power. Experiments were repeated 10 times. Cultured cells were measured five times for 30 s at one position, with laser power ranging between 8.5 and 55 µW. Laser power was set to 17.5 µW for measuring GFP-VLP2/6 particles.

Experimentally obtained autocorrelation functions were analyzed with the Confocor II software package (Carl Zeiss, Inc.) and fitted with

$$G(t) = \frac{1 + \frac{T}{1-T} e^{-t/\tau_T}}{N} \left(\sum_{i=1}^{M} \frac{F_i}{(1 + t/\tau_i)\sqrt{1 + t/(S^2\tau_i)}} \right) + 1,$$

where t is time (in microseconds); τ_T is the triplet time, set to 9 µs for GFP; T is the fraction of triplet decay; S is the structural parameter, which was obtained from calibration measurements with rhodamine 6G (diffusion coefficient of 28×10^{-10} m^2/s at 20°C) and set to 6; N is the number of particles; M is the number of fluorescent species (one or two); F_i is the fraction of species i; and τ_i is the diffusion time of species i.

We verified our FCS set-up by analyzing the diffusion of GFP. The diffusion coefficient D of GFP was ∼50 $\mu m^2/s$ in the cytoplasm and 70 $\mu m^2/s$ in cell lysates (Fig. S2, A and B), which is comparable with published data (∼30 $\mu m^2/s$ in cells and 90 $\mu m^2/s$ in lysates; Kim and Schwille, 2003). We subsequently studied the dynamics of GFP–CLIP-170 in knock-in MEFs (Akhmanova et al., 2005). Fluorescence autocorrelation curves could be fitted with a two-component model, implying a fast-moving (i.e., freely diffusing) and a slow-moving fraction of GFP–CLIP-170 in MEFs. The fast-moving GFP–CLIP-170 species in MEFs has a diffusion coefficient that is three to four times lower than that of monomeric GFP and about two times lower than that of a GFP–GFP fusion protein (Fig. S2 A). Diffusion coefficients of EB3-GFP and GFP-EB1 are somewhat smaller than that of GFP–GFP. Similar results were obtained in cell lysates (Fig. S2 B). Data are consistent with the relative molecular mass of dimeric GFP–CLIP-170 (∼400 kD) being higher than that of the other proteins (GFP, 27 kD; GFP–GFP, 54 kD; dimeric EB3-GFP and GFP-EB1, ∼120 kD). Note that the diffusion coefficient is linear to the radius of a molecule. Thus, for a globular protein, a doubling of D correlates with a doubled radius or an eightfold increase in the relative molecular mass. Our results indicate that the fast GFP fraction of CLIP-170 is either part of a bigger complex or is not globular.

FCA and PCH analysis

Fluorescence cumulant analysis (FCA; Muller, 2004) was performed on raw data of FCS measurements, which we analyzed with the FCS data processor (Scientific Software Technologies Center). The first eight cumulants were determined; data were fitted with two components (background and GFP), and global analysis of 10 measurements of the same lysate was performed. Results were averaged over two to four different lysates. FCA revealed that GFP–CLIP-170, EB3-GFP, and GFP-EB1 have a molecular brightness that is two to three times that of GFP (Fig. S2 C), indicating that these proteins are dimeric. Values are higher than for a GFP–GFP fusion protein, which might be the result of fluorescence quenching in the latter.

The molecular brightness of the lysates was also examined using photon-counting histogram (PCH) analysis (Chen et al., 1999). Raw data of FCS measurements was converted into PCH curves using our own custom-written program and a binning time of 50 µs. Data thus obtained were analyzed using the Globals software package developed at the Laboratory for Fluorescence Dynamics (University of Illinois at Urbana-Champaign, Urbana, IL). The PCH analysis supported FCA results. Data are consistent with previous results (Pierre et al., 1992; Lansbergen et al., 2004) that indicate a dimeric, nonglobular conformation of CLIP-170.

Fluorescent peaks in FCS intensity tracks

When we performed FCS experiments in COS-7 cells transiently expressing GFP–CLIP-170, we observed peaks in the fluorescence intensity tracks of the FCS measurements. Most of these peaks had a relatively linear and steep upward slope and a curved downward slope (Fig. 3 B). Several experiments suggest that these peaks represent the ends of growing MTs labeled by GFP–CLIP-170. First, peaks were absent in cells expressing fluorescently tagged proteins that did not associate with MT ends. Also, they disappeared when cells expressing GFP–CLIP-170 were treated with nocodazole or high doses of taxol, reagents that perturb MT dynamics and have been shown to cause the dissociation of GFP–CLIP-170 from MT ends (Perez et al., 1999). Furthermore, peaks reached their maximum intensity after 1–2 s, corresponding to the time it takes an MT to traverse the FCS measurement volume (growth speed of an MT is ∼0.3 µm/s; measurement volume diameter is 0.4 µm).

To rule out that the peaks represent aggregates of GFP–CLIP-170, we analyzed a suspension of highly purified VLP2/6 rotavirus–like particles containing 120 GFP molecules each (Charpilienne et al., 2001). Particles (a gift of J. Cohen, Centre National de la Recherche Scientifique, National Institute of Agrarian Research, Gif-sur-Yvette, France) were stored in a concentration of ∼1 mg/ml at 4°C and were filtered through a Sephadex G25 column before FCS measurements. Intensity tracks of FCS measurements of these particles showed very sharp peaks (Fig. S2 E).

The downward slope of peaks could be well approximated with an exponential decay curve corresponding to first-order reaction kinetics (Fig. S2 D). The calculated k_{decay} of 0.48 s^{-1} for the disappearance of GFP–CLIP-170 (Table I) translates to a fluorescence half-life of ∼1.5 s, which correlates well with reported half-lives of CLIP-170 on MT ends (Folker et al., 2005; Komarova et al., 2005).

To calculate the number of particles on MT plus ends (Fig. 3 C), we assumed that fluorescence emitted from a cytoplasmic and an MT-bound GFP–CLIP-170 molecule is the same and that non-GFP–derived signal intensity is negligible. We first measured the number of particles in the cytoplasm (in measurements without a peak), calculated the brightness per cytoplasmic particle, and divided the height of a peak by the brightness. This yielded the number of particles on MT plus ends.

Comparison between FCS and time lapse

A given position in an imaged area is only intermittently illuminated by a laser in confocal time-lapse experiments but continuously in an FCS experiment. Consistently, we observed significant bleaching of the immobile nuclear protein GFP–histone H2B (Wachsmuth et al., 2003) in FCS experiments, whereas this was not the case in time-lapse imaging (Fig. S2 F). In fact, the curve showing the bleach-dependent decay of GFP–histone H2B was similar to the one showing fluorescence decay of GFP–CLIP-170 (Fig. S2 F). If CLIP-170 had been relatively immobile (as assumed in the treadmilling model), one would expect an FCS decay curve (reflecting a combination of dissociation and bleaching of CLIP-170) to be steeper than a time-lapse decay curve (only reflecting the dissociation of CLIP-170). The fact that time-lapse and FCS curves are so similar indicate short binding times of GFP–CLIP-170 on MT ends.

Online supplemental material

Fig. S1 shows results of FRAP-related experiments, and Fig. S2 shows FCS-related data. Fig. S3 shows results obtained with a newly generated GFP–CLIP-170–expressing HeLa cell line. Videos 1–7 are time-lapse analyses of GFP-tagged +TIPs. Video 1 shows GFP–CLIP-170 behavior in transiently transfected COS-7 cells analyzed at high temporal resolution, Videos 2 and 3 shows GFP–CLIP-170 behavior in stably transfected 3T3 cells at 37°C and 27°C (Video 2 and Video 3, respectively), and Video 4 shows

Published February 18, 2008

GFP–CLIP-170 expression in knock-in MEFs. Video 5 shows highly overexpressed GFP–CLIP-170 in transiently transfected COS-7 cells, where the protein accumulates along MTs. Videos 6 and 7 show GFP–CLIP-170 in stably transfected HeLa cells, which were either not treated (Video 6) or treated with 10 nM taxol (Video 7). Online supplemental material is available at http://www.jcb.org/cgi/content/full/jcb.200707203/DC1.

We thank Dr. S. Ibrahim for help with FCS, Dr. J. Cohen for GFP-VLP2/6 particles, M. van Royen for GFP–GFP cDNA, and W. van Beusekom for software development.

This work was supported by the Dutch Ministry of Economic Affairs (BSIK), the Netherlands Organization for Scientific Research (grants NWO-ALW and ZonMW), and the European Union (Molecular Imaging grant LSHG-CT-2003-503259 and Specific Targeted Research Project TRANS-REG grant LSHG-CT-2004-502950).

Submitted: 30 July 2007
Accepted: 28 January 2008

References

Akhmanova, A., and C.C. Hoogenraad. 2005. Microtubule plus-end-tracking proteins: mechanisms and functions. *Curr. Opin. Cell Biol.* 17:47–54.

Akhmanova, A., A.-L. Mausset-Bonnefont, W. Van Cappellen, N. Keijzer, C.C. Hoogenraad, T. Stepanova, K. Drabek, J. van der Wees, M. Mommaas, J. Onderwater, et al. 2005. The microtubule plus end tracking protein CLIP-170 associates with the spermatid manchette and is essential for spermatogenesis. *Genes Dev.* 19:2501–2515.

Arnal, I., and R.H. Wade. 1995. How does taxol stabilize microtubules? *Curr. Biol.* 5:900–908.

Arnal, I., C. Heichette, G.S. Diamantopoulos, and D. Chretien. 2004. CLIP-170/tubulin-curved oligomers coassemble at microtubule ends and promote rescues. *Curr. Biol.* 14:2086–2095.

Charpilienne, A., M. Nejmeddine, M. Berois, N. Parez, E. Neumann, E. Hewat, G. Trugnan, and J. Cohen. 2001. Individual rotavirus-like particles containing 120 molecules of fluorescent protein are visible in living cells. *J. Biol. Chem.* 276:29361–29367.

Chen, Y., J.D. Muller, P.T. So, and E. Gratton. 1999. The photon counting histogram in fluorescence fluctuation spectroscopy. *Biophys. J.* 77:553–567.

Drabek, K., M. van Ham, T. Stepanova, K. Draegestein, R. van Horssen, C.L. Sayas, A. Akhmanova, T. Ten Hagen, R. Smits, R. Fodde, et al. 2006. Role of CLASP2 in microtubule stabilization and the regulation of persistent motility. *Curr. Biol.* 16:2259–2264.

Elson, E.L. 2004. Quick tour of fluorescence correlation spectroscopy from its inception. *J. Biomed. Opt.* 9:857–864.

Folker, E.S., B.M. Baker, and H.V. Goodson. 2005. Interactions between CLIP-170, tubulin, and microtubules: implications for the mechanism of CLIP-170 plus-end tracking behavior. *Mol. Biol. Cell.* 16:5373–5384.

Honnappa, S., O. Okhrimenko, R. Jaussi, H. Jawhari, I. Jelesarov, F.K. Winkler, and M.O. Steinmetz. 2006. Key interaction modes of dynamic +TIP networks. *Mol. Cell.* 23:663–671.

Hoogenraad, C.C., A. Akhmanova, F. Grosveld, C.I. De Zeeuw, and N. Galjart. 2000. Functional analysis of CLIP-115 and its binding to microtubules. *J. Cell Sci.* 113:2285–2297.

Jordan, M.A., R.J. Toso, D. Thrower, and L. Wilson. 1993. Mechanism of mitotic block and inhibition of cell proliferation by taxol at low concentrations. *Proc. Natl. Acad. Sci. USA.* 90:9552–9556.

Kim, S.A., and P. Schwille. 2003. Intracellular applications of fluorescence correlation spectroscopy: prospects for neuroscience. *Curr. Opin. Neurobiol.* 13:583–590.

Komarova, Y.A., A.S. Akhmanova, S. Kojima, N. Galjart, and G.G. Borisy. 2002. Cytoplasmic linker proteins promote microtubule rescue in vivo. *J. Cell Biol.* 159:589–599.

Komarova, Y., G. Lansbergen, N. Galjart, F. Grosveld, G.G. Borisy, and A. Akhmanova. 2005. EB1 and EB3 control CLIP dissociation from the ends of growing microtubules. *Mol. Biol. Cell.* 16:5334–5345.

Lansbergen, G., and A. Akhmanova. 2006. Microtubule plus end: a hub of cellular activities. *Traffic.* 7:499–507.

Lansbergen, G., Y. Komarova, M. Modesti, C. Wyman, C.C. Hoogenraad, H.V. Goodson, R.P. Lemaitre, D.N. Drechsel, E. van Munster, T.W. Gadella Jr., et al. 2004. Conformational changes in CLIP-170 regulate its binding to microtubules and dynactin localization. *J. Cell Biol.* 166:1003–1014.

Lansbergen, G., I. Grigoriev, Y. Mimori-Kiyosue, T. Ohtsuka, S. Higa, I. Kitajima, J. Demmers, N. Galjart, A.B. Houtsmuller, F. Grosveld, and A. Akhmanova. 2006. CLASPs attach microtubule plus ends to the cell cortex through a complex with LL5beta. *Dev. Cell.* 11:21–32.

Lele, T.P., and D.E. Ingber. 2006. A mathematical model to determine molecular kinetic rate constants under non-steady state conditions using fluorescence recovery after photobleaching (FRAP). *Biophys. Chem.* 120:32–35.

Mitchison, T., and M. Kirschner. 1984. Dynamic instability of microtubule growth. *Nature.* 312:237–242.

Muller, J.D. 2004. Cumulant analysis in fluorescence fluctuation spectroscopy. *Biophys. J.* 86:3981–3992.

Perez, F., G.S. Diamantopoulos, R. Stalder, and T.E. Kreis. 1999. CLIP-170 highlights growing microtubule ends in vivo. *Cell.* 96:517–527.

Peris, L., M. Thery, J. Faure, Y. Saoudi, L. Lafanechere, J.K. Chilton, P. Gordon-Weeks, N. Galjart, M. Bornens, L. Wordeman, et al. 2006. Tubulin tyrosination is a major factor affecting the recruitment of CAP-Gly proteins at microtubule plus ends. *J. Cell Biol.* 174:839–849.

Pierre, P., J. Scheel, J.E. Rickard, and T.E. Kreis. 1992. CLIP-170 links endocytic vesicles to microtubules. *Cell.* 70:887–900.

Schuyler, S.C., and D. Pellman. 2001. Microtubule "plus-end-tracking proteins": the end is just the beginning. *Cell.* 105:421–424.

Seiffert, S., and W. Oppermann. 2005. Systematic evaluation of FRAP experiments performed in a confocal laser scanning microscope. *J. Microsc.* 220:20–30.

Slep, K.C., and R.D. Vale. 2007. Structural basis of microtubule plus end tracking by XMAP215, CLIP-170, and EB1. *Mol. Cell.* 27:976–991.

Stepanova, T., J. Slemmer, C.C. Hoogenraad, G. Lansbergen, B. Dortland, C.I. De Zeeuw, F. Grosveld, G. van Cappellen, A. Akhmanova, and N. Galjart. 2003. Visualization of microtubule growth in cultured neurons via the use of EB3-GFP (end-binding protein 3-green fluorescent protein). *J. Neurosci.* 23:2655–2664.

Wachsmuth, M., T. Weidemann, G. Muller, U.W. Hoffmann-Rohrer, T.A. Knoch, W. Waldeck, and J. Langowski. 2003. Analyzing intracellular binding and diffusion with continuous fluorescence photobleaching. *Biophys. J.* 84:3353–3363.

Wittmann, T., and C.M. Waterman-Storer. 2005. Spatial regulation of CLASP affinity for microtubules by Rac1 and GSK3β in migrating epithelial cells. *J. Cell Biol.* 169:929–939.

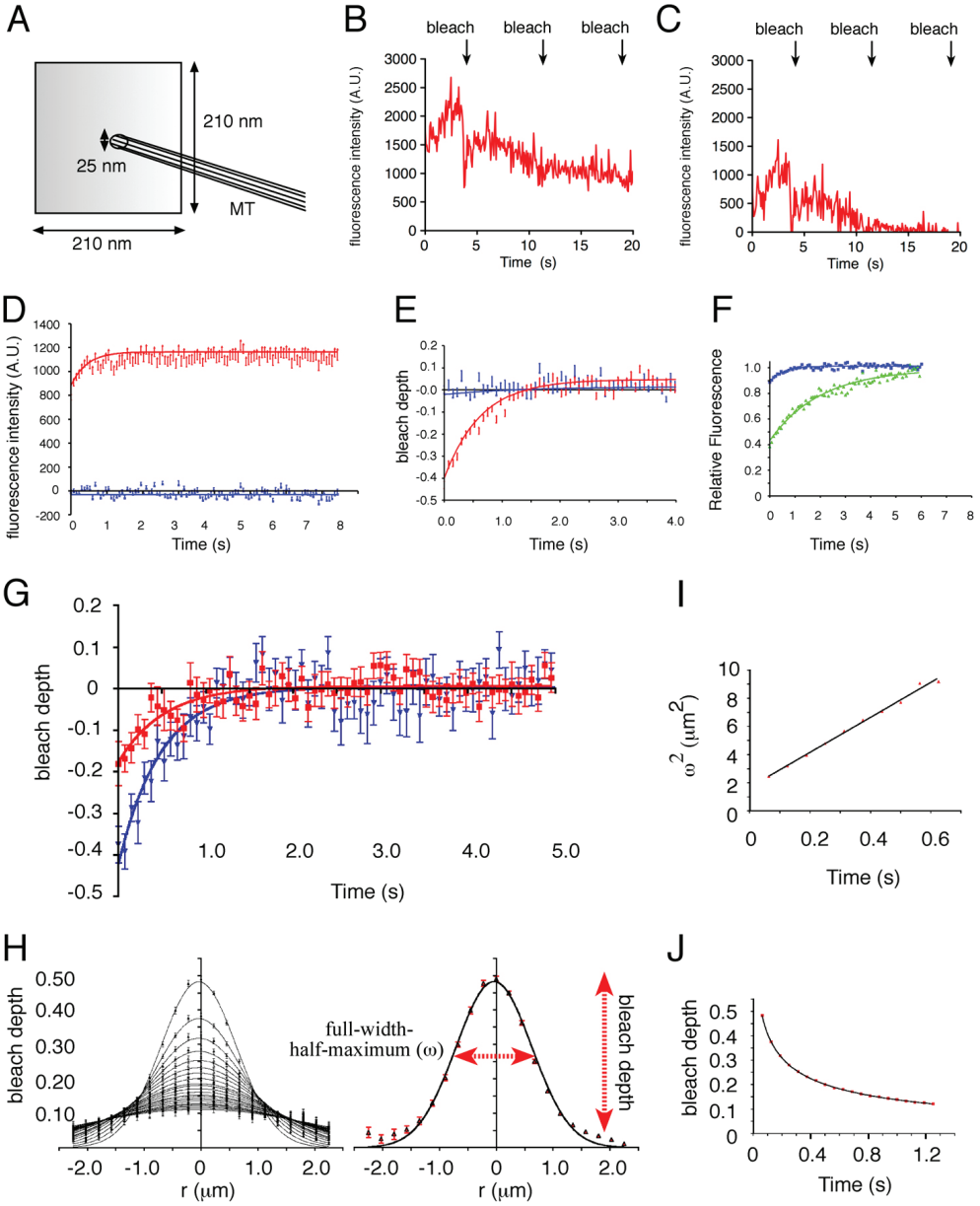
A
210 nm
25 nm
MT
210 nm
B
bleach
bleach
bleach
fluorescence intensity (A.U.)
Time (s)
C
bleach
bleach
bleach
fluorescence intensity (A.U.)
Time (s)
D
fluorescence intensity (A.U.)
Time (s)
E
bleach depth
Time (s)
F
Relative Fluorescence
Time (s)
G
bleach depth
Time (s)
I
ω2 (μm2)
Time (s)
H
bleach depth
r (μm)
full-width-
half-maximum (ω)
bleach depth
r (μm)
J
bleach depth
Time (s)

Figure S1. Dynamic behavior of GFP–CLIP-170 measured by FRAP.
A) Representation of the different dimensions in a fast FRAP analysis. An MT (diameter of 25 nm) traverses an ROI of 210 × 210 nm (3 × 3 pixels).
B and C) Fluorescence intensity of a repeatedly bleached GFP–CLIP-170–labeled MT end measured in an ROI of 210 × 210 nm. Raw data (B) was corrected for the average bleach occurring in the cytoplasm surrounding the MT end (C).
D) Comparison of corrected (blue) and noncorrected (red) cytoplasmic bleaches. This result is in stark contrast to the results in B and C, in which the correction of MT plus end bleaches with the cytoplasmic recovery still yields a recovery curve.
E) Comparison of nonbleached (blue) and bleached (red) peaks. Nonbleached peaks are outside the bleached strip. The same calculations were performed on these peaks as on truly bleached peaks. No bleach is observed on peaks that are distant from the bleached strip, whereas peaks within the bleached strip do show a clear bleach and recovery.
F) Fast FRAP analysis in transiently transfected COS-7 cells abundantly overexpressing GFP–CLIP-170, which labels MTs along their entire length (corresponds to Video 5). Recovery of GFP–CLIP-170 is shown in the cytoplasm (blue data points; $k = 1.9\ s^{-1}$) and on MTs (green data points; $k = 0.50\ s^{-1}$). Clearly, GFP–CLIP-170 recovers faster in the cytoplasm than on the MT (note: in the same experiment, we also performed fast FRAP analysis in cells expressing much lower amounts of CLIP-170; in these cells, we observed normal MT end recovery).
G) Position-dependent fluorescence recovery of GFP–CLIP-170 on MT ends. Our data suggest that individual CLIP-170 and EB3 molecules can exchange rapidly on MT plus ends. Thus, fluorescence decay at a given position on the MT end reflects the loss in time of binding sites for CLIP-170. This loss could be caused by a quantitative loss in number of binding sites and/or the weakening of interactions between CLIP-170 and binding sites on MT ends (i.e., a qualitative change). In the first case, no relationship between krecovery of GFP–CLIP-170 and the position on the MT plus end is expected. We tested this by comparing recovery curves over the length of MT plus ends. Recoveries were grouped according to the position of the bleach on the fluorescent peak. Fluorescent recoveries shown are shortly after the peak (blue; 0.5–0.9 s after the maximum; $k_{recovery} = 2.06 \pm 0.27\ s^{-1}$; $n = 25$) or somewhat later (red; 3.7–4.6 s after the maximum; $k_{recovery} = 1.96 \pm 0.45\ s^{-1}$; $n = 25$). Error bars represent SEM. krecovery did not differ significantly between these two datasets, although the bleach depth depended on the time interval between maximal fluorescence intensity and the bleach. Therefore, we propose that the disappearance of CLIP-170 fluorescence from MT plus ends is caused by a declining number of binding sites for CLIP-170. These results do no allow us to conclude whether the properties of these binding sites are similar over the length of the MT plus end because the binding and unbinding of CLIP-170 may be faster than diffusion.
H) Example of a bleach profile in FRAP experiments with GFP–CLIP-170. Maximum bleach depth decreases over time (fluorescence recovers), whereas the area containing bleached molecules increases.
I) Example of $\omega 2$ (micrometers squared) plotted versus t (seconds) for a FRAP experiment of GFP–CLIP-170.
J) Plot of maximum bleach depth versus time shows recovery of fluorescence in a representative FRAP experiment of GFP–CLIP-170.

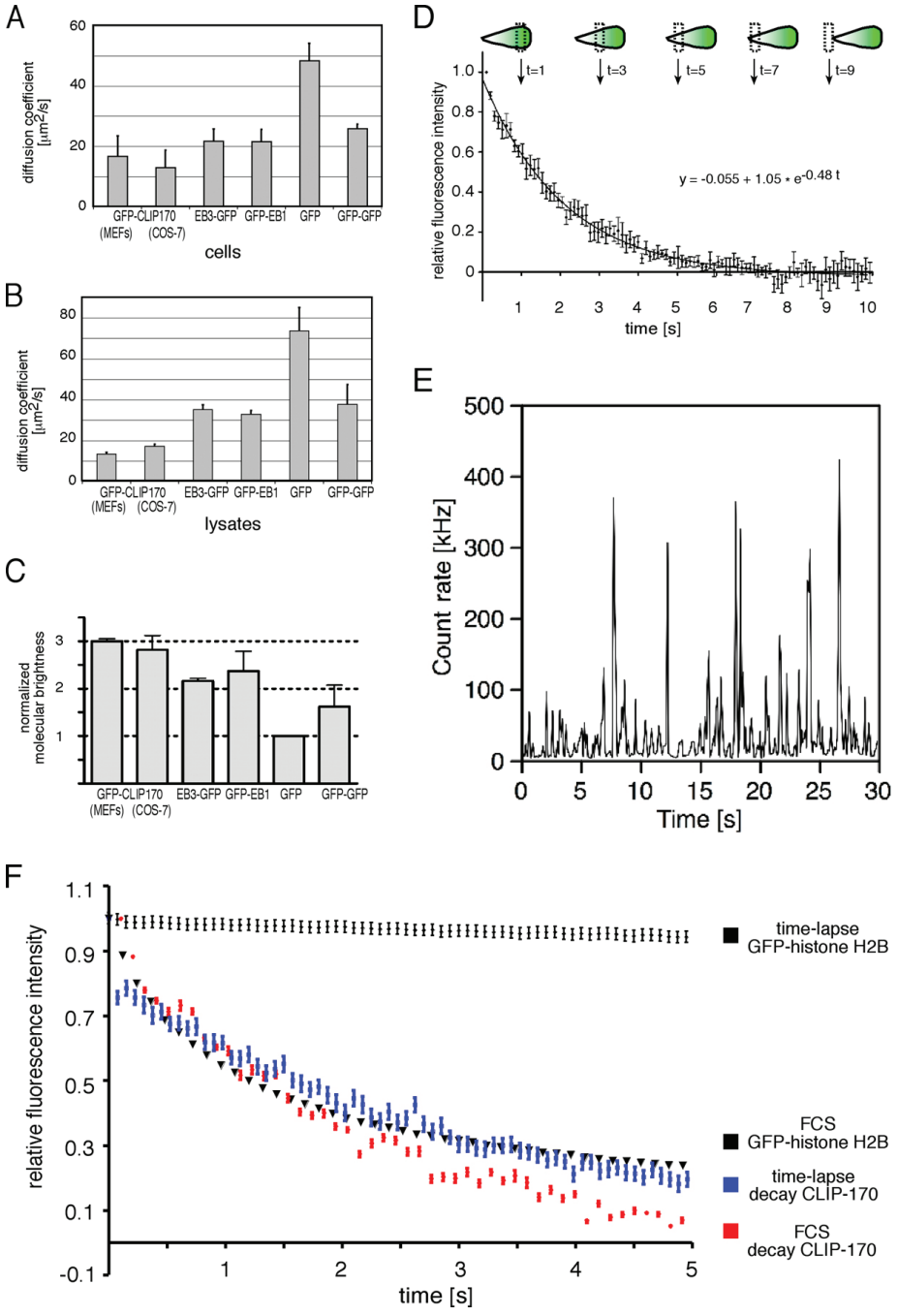

Figure S2. Dynamic behavior of GFP-tagged proteins measured by FCS, FCA, and FRAP.
See next page for the legend.

Figure S2. Dynamic behavior of GFP-tagged proteins measured by FCS, FCA, and FRAP.
A and B) Diffusion coefficients derived from FCS experiments in cells (A) expressing different fluorescently labeled proteins and in lysates (B) thereof. Both MEFs (expressing GFP–CLIP-170 at endogenous levels) and transfected COS-7 cells (expressing the indicated fluorescent proteins) were measured. Only fast components of the two-component analysis in cells are shown.
C) FCS data from cell lysates were used to calculate the molecular brightness of fluorescent proteins by FCA. Values were normalized to GFP. SD is indicated in all panels by error bars.
D) Fluorescence decay of GFP–CLIP-170 peaks in FCS measurements. Decay was measured at 17.5-μW laser power, normalized, averaged, and fitted (SEM indicated by error bars). A GFP–CLIP-170–positive MT end (visualized as a green comet) is drawn above the graph. As it enters and exits the FCS volume (dashed rectangle), fluorescence intensity is measured (examples indicate measurements at 1, 3, 5, 7, and 9 s). Fluorescence from consecutively older parts of the MT end shows an apparent decay.
E) Rotavirus-like particles containing 120 molecules of GFP-VLP2/6 each were analyzed with the FCS set-up. Sharp peaks characterize movement of particles through the measurement volume.
F) Comparison of the behavior of GFP–CLIP-170 and GFP–histone H2B in time in time-lapse and FCS experiments. Significant bleaching of the immobile nuclear protein GFP–histone H2B is observed with FCS (black triangles), whereas this is not the case in time-lapse experiments (black squares). The FCS curve showing the bleach-dependent decay of GFP–histone H2B is similar to the FCS and FRAP curves showing fluorescence decay of GFP–CLIP-170 (red and blue squares, respectively). Error bars indicate SEM.

Figure S3. Characterization of a HeLa cell line stably expressing GFP–CLIP-170.
A) Western blot analysis of a parent HeLa cell line (lane 1) and of the GFP–CLIP-170–expressing clone (lane 2). The expression of GFP–CLIP-170 was analyzed with antibodies against CLIP-170. Intensities of the signals were measured three times; the expression of CLIP-170 is ~2.5-fold lower (42 ± 3%) than that of GFP–CLIP-170. Control staining with antibodies against UBF (a nucleolar protein) show that equal amounts of protein lysates were loaded on gel. The positions of prestained protein standards and their apparent molecular weight (Mr) are indicated on the right.
B and C) Displacement of GFP–CLIP-170 in time (equivalent to MT growth rates) in untreated HeLa cells (B) and in cells treated with 10 nM taxol (C). Notice that not only MT growth rates are reduced in the treated cells but that also the variation in growth rates has significantly increased (n = number of dashes analyzed; SEM indicated).
D) Still image of a time-lapse analysis of GFP–CLIP-170 in stably expressing HeLa cells. Notice the fluorescent cometlike dashes, which are typical of GFP–CLIP-170 behavior (corresponds to Video 6).
E) Still image of a time-lapse analysis of GFP–CLIP-170 in stably expressing HeLa cells after treatment with 10 nM taxol. Notice the fluorescent dots that have appeared after taxol application (corresponds to Video 7).
F) Maximum intensity projections of the boxed area depicted in D. Tracks represent the movement of GFP–CLIP-170 in time in nontreated HeLa cells. Track length is not only determined by catastrophes (which cause GFP–CLIP-170 displacement from the MT end) but also by MT ends moving in and out of focus.
G) Maximum intensity projections of the boxed area depicted in E. Tracks represent the movement of GFP–CLIP-170 in cells treated with taxol.
H) Kymograph analysis of GFP–CLIP-170 in nontreated HeLa cells. Three representative kymographs are shown, with time plotted in the vertical axis and distance plotted horizontally. GFP–CLIP-170 moves with a relatively constant average speed and decorates MT plus ends in an even manner.
I) Kymograph analysis of GFP–CLIP-170 in HeLa cells treated with 10 nM taxol. Three kymographs are shown, with time plotted in the vertical axis and distance plotted horizontally. GFP–CLIP-170 moves erratically and even seems to remain bound on pausing and shrinking MTs. Moreover, it decorates MT plus ends in an uneven manner.

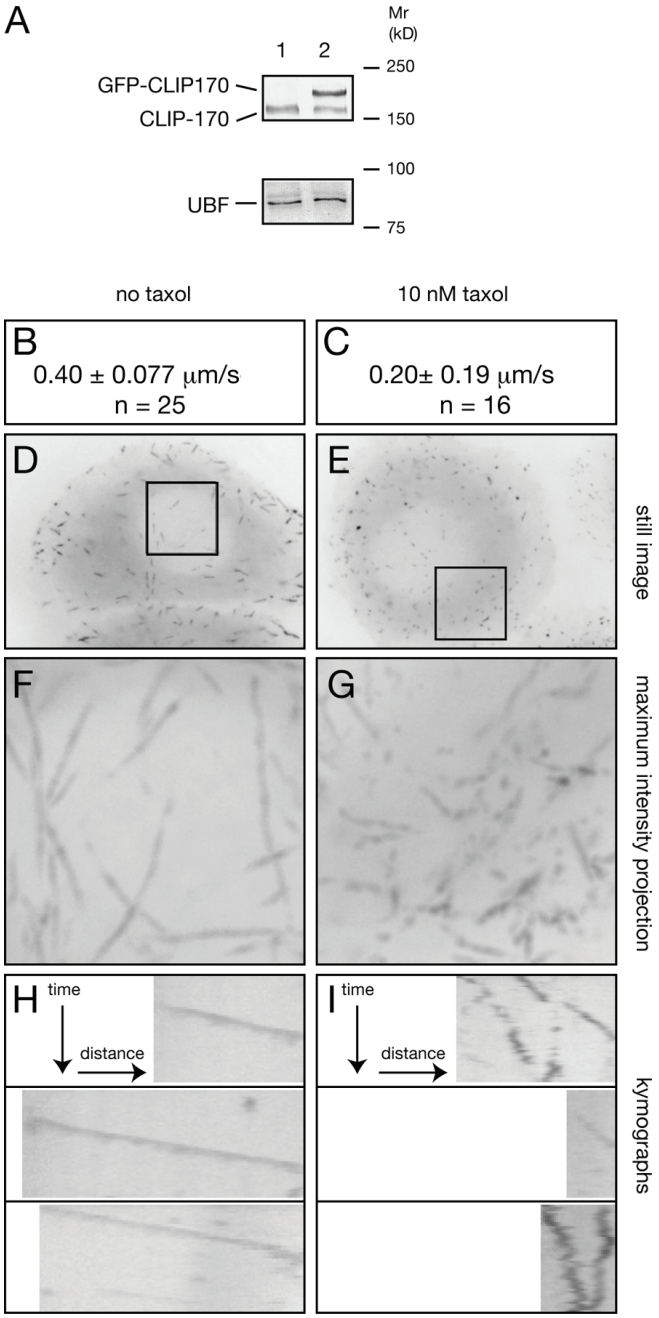

Figure S3. Characterization of a HeLa cell line stably expressing GFP–CLIP-170.
See previous page for the legend

Chapter 3

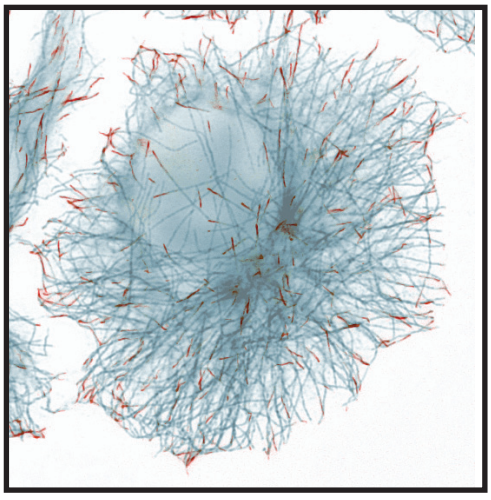

Mammalian Navigators are Microtubule Plus-End Tracking Proteins that can Reorganize the Cytoskeleton to induce Neurite-Like Extensions

Cell Motility and the Cytoskeleton (2009)

Mammalian Navigators are Microtubule Plus-End Tracking Proteins that can Reorganize the Cytoskeleton to Induce Neurite-Like Extensions

Jeffrey van Haren,[1] Katharina Draegestein,[1] Nanda Keijzer,[1] Jan Pieter Abrahams,[2] Frank Grosveld,[1] Pieter Johan Peeters,[3] Dieder Moechars,[3] and Niels Galjart[1]*

[1]*Department of Cell Biology and Genetics, Erasmus MC, Rotterdam, The Netherlands*
[2]*Department of Biophysical Structural Chemistry, Leiden Institute of Chemistry, Gorlaeus Laboratories, Leiden University, Leiden, The Netherlands*
[3]*Johnson & Johnson Pharmaceutical Research and Development, Beerse, Belgium*

Mammalian microtubule plus-end tracking proteins (+TIPs) specifically associate with the ends of growing microtubules. +TIPs are involved in many cellular processes, including mitosis, cell migration and neurite extension. Navigators are mammalian homologues of the *C. elegans* unc-53 protein, an ATPase that has been linked to the migration and outgrowth of muscles, axons and excretory canals. Here we show that all three mammalian Navigators are +TIPs, consistent with a previous study on Navigator 1 (NAV1) (Martinez-Lopez et al., Mol Cell Neurosci 2005;28:599–612). Overexpression of GFP-tagged Navigators causes displacement of CAP_GLY-motif containing +TIPs, such as CLIP-170, from microtubule ends, suggesting that the Navigator-binding sites on microtubule ends overlap with those of the CAP_GLY-motif proteins. In interphase cells, mammalian Navigators also prominently localize to centrosomes, a localization that does not depend on an intact microtubule network. Fluorescence recovery after photobleaching (FRAP) experiments indicate that NAV1 associates with intracellular structures other than microtubules or centrosomes. Expression of GFP-tagged Navigators induces the formation of neurite-like extensions in non-neuronal cells, showing that Navigators can dominantly alter cytoskeletal behavior. For NAV1 this function depends on its ATPase activity; it is not achieved by a classical type of MT bundling and stabilization. Combined our data suggest that Navigators are +TIPs that can reorganize the cytoskeleton to guide cell shape changes. Our data are consistent with a role for Navigators in neurite outgrowth. Cell Motil. Cytoskeleton 2009.

Key words: microtubules; unc-53; Navigators; ATPase

Additional Supporting Information may be found in the online version of this article.

Contract grant sponsors: Netherlands Organization for Scientific Research (NWO-ALW, NWO-MW), Netherlands Ministry of Economic Affairs (BSIK), Dutch Cancer Society (KWF), Cancer Genomics Centre of the Netherlands (CGC).

Nanda Keijzer's present address is Department of Neuroscience, Erasmus MC, P.O. Box 2040, 3000 CA Rotterdam, The Netherlands.

*Correspondence to: Niels Galjart, PhD, Department of Cell Biology and Genetics, Erasmus MC, P.O. Box 2040, 3000 CA Rotterdam, The Netherlands. E-mail: n.galjart@erasmusmc.nl

Received 10 January 2009; Accepted 23 March 2009

Published online 00 Month 2009 in Wiley InterScience (www.interscience.wiley.com).
DOI: 10.1002/cm.20370

INTRODUCTION

Microtubules (MTs) are polarized hollow tubes made up of α/β-tubulin dimers. These dimers assemble head-to-tail into linear protofilaments, which in turn associate laterally to form hollow MTs with a diameter of about 25 nm. The number of protofilaments per MT is tightly regulated and MTs grown in vivo mainly consist of 13 protofilaments. The two ends of a MT are structurally different. In many cell types, the minus-ends of MTs are embedded in the MT organizing center (MTOC), which is located near the nucleus. The plus-ends radiate into the cytoplasm and switch between episodes of growth and shrinkage, a process called dynamic instability. Dynamic instability was first described in vitro [Mitchison and Kirschner, 1984] and subsequently confirmed in living cells [Cassimeris et al., 1988; Sammak and Borisy, 1988; Schulze and Kirschner, 1988]. Dynamic instability results in a wider spread of MT length and a faster turnover of MTs than expected for passive polymerization. This allows the cell to constantly probe the cytoplasm and to quickly adapt to a changing environment.

The term "plus-end-tracking protein" (+TIP) was coined in 2001 to describe an emerging family of proteins that specifically localize to the ends of growing MTs [Schuyler and Pellman, 2001]. Thus, +TIPs probe the cytoplasm on growing MT ends. Dynamic plus-end-tracking was first described for CLIP-170, based on a GFP-fusion protein of CLIP-170 that was visible as "cellular fireworks" of comet-like fluorescent dashes moving mostly from the cell center to the periphery [Perez et al., 1999]. The family of +TIPs has been growing since its initial description, and new family members are described every year [for recent review, see Akhmanova and Steinmetz, 2008]. From these data it is clear that although +TIPs share the ability to track growing MT ends in vivo, they do not share a common microtubule binding (MTB) domain. CLIP-170, for example, as well as its homologues CLIP-115 and p150(glued), all contain a CAP_GLY (cytoskeleton-associated protein glycine-rich) [Riehemann and Sorg, 1993] MTB motif, which is not found in other +TIPs. The crystal structures of several CAP_GLY domains have been solved [Honnappa et al., 2006; Mishima et al., 2007; Weisbrich et al., 2007] and provide insight into their structure-function relationship. CAP_GLY domains contain a highly conserved groove that binds the C-terminus of α-tubulin and EB1-like family members. Furthermore, CAP_GLY domains were shown to bind to a conserved coiled-coil region of EB1, termed the "EB-domain".

Numerous functions have been linked to +TIPs. For example, +TIPs influence MT dynamic instability, they link MTs to other cellular structures like vesicles, the cell membrane, and components of the cytoskeleton, they are essential in mitosis, and they play a role in signal transduction. Axon outgrowth also relies on (a reorganization of) the MT cytoskeleton. Many of the critical decisions concerning axon outgrowth and guidance are made in the growth cone, where the MT network receives input from the cell exterior and collaborates with the actin cytoskeleton to guide axons [Dent and Gertler, 2003]. Different +TIPs, including APC and CLASP2, have been proposed to play a role in axon outgrowth [Lee et al., 2004; Zhou et al., 2004].

Mutations in the *unc-53* gene of *C. elegans* cause, among others, major axonal guidance defects [Hekimi and Kershaw, 1993] and affect sex myoblast migration [Chen et al., 1997]. Because of its function in axon outgrowth and cell migration the protein encoded by *unc-53* was called "Navigator". Genetic studies in nematodes indicate a pathway involving *unc-53* and several other genes, including *sem-5*, which is the *C. elegans* homologue of Grb2, a protein in the Ras pathway [Stringham et al., 2002]. Three mammalian homologs of *unc-53* exist, that were named Neuron Navigators (NAV1, NAV2, and NAV3). [Maes et al., 2002]. As Navigators have been characterized independently in different labs, a somewhat confusing nomenclature has evolved. For example, RAINB1 (which corresponds to NAV2), was isolated from human SH-SY5Y cells; RAINB1 is abundantly expressed in the rat nervous system and is sensitive to all-trans retinoic acid [Merrill et al., 2002]. The same protein was characterized as HELAD1 (helicase, APC-downregulated) and was implicated in the Wnt-APC signaling pathway, that is mutated in the majority of colorectal cancers [Ishiguro et al., 2002]. Finally, POMFIL-1 (pore membrane and/or filament interacting like protein 1), which is identical to NAV3, has been implicated in formation of nuclear pore complexes, and is frequently deleted or translocated in cutaneous T cell lymphomas [Coy et al., 2002; Karenko et al., 2005].

Navigator proteins belong to the AAA+ (*A*TPases *A*ssociated with diverse cellular *A*ctivities) group of ATPases [Frickey and Lupas, 2004]. Members of this superfamily of proteins were shown to be involved in a variety of cellular processes, including protein degradation, peroxisome biogenesis, signal transduction, the regulation of gene expression, membrane fusion, microtubule severing, and microtubule-mediated transport. Both NAV1 and NAV2 were shown to have MT binding ability and to have a potential role in neurite outgrowth. NAV1 has also been linked to netrin signaling [Martinez-Lopez et al., 2005; Muley et al., 2008]. Netrins are a family of proteins that direct cell and axon migration during development and that can both attract and repel axons [for review, see Moore et al., 2007]. Mouse GFP-tagged NAV1 was shown to colocalize with CLIPs at

MT ends, suggesting that NAV1 is a +TIP [Martinez-Lopez et al., 2005]. However, NAV2 could not be shown to accumulate at MT ends [Muley et al., 2008]. Nevertheless, Navigators do appear to couple ATPase activity to a MT binding potential.

Here we show that all three mammalian Navigators are +TIPs. Navigator binding sites on MT ends overlap with those of the CLIPs, suggesting that Navigators also rapidly turn over on MT ends. Interestingly, Navigators can localize in an asymmetric fashion and are capable of inducing the formation of neurite-like extensions in non-neuronal cells. Combined our data suggest that Navigators are +TIPs involved in the organization of the cytoskeleton.

MATERIALS AND METHODS

Constructs

We used human Navigator cDNAs to obtain constructs for expression in mammalian cells and bacteria [for NAV1, and -3, see Peeters et al., 2004], for NAV2 we obtained KIAA1419 from the Kazusa Research Institute [Ohara et al., 1997; Kikuno et al., 2004]. NAV1 cDNA was cloned in-frame with GFP using pEGFP-C1, whereas NAV2 and -3 cDNAs were cloned into pEGFP-C3 (pEGFP plasmids are from Invitrogen, Carlsbad, CA). For NAV2, the KIAA 1419 plasmid was digested with *Dra* I and *Nar* I and the NAV2 cDNA was inserted into the *Sma* I and *Acc* I sites of pEGFP-C3. This yields a fusion protein with a 42 amino acid linker sequence located between EGFP and NAV2.

The biotinylation recognition sequence [de Boer et al., 2003] was added in-frame to the N-terminus of GFP in the pEGFP-C1 vector, yielding pbio-GFP-C1 (a kind gift of Drs. C. Hoogenraad and A. Akhmanova, Erasmus MC). Both GFP-NAV1 and pbio-EGFP-C1 were cleaved with *Apa L*I and *Age* I and the fragment containing the biotinylation-tag was ligated into the NAV1-containing fragment of pEGFP-NAV1. The mutant form of NAV1 (pbio-GFP-NAV1-KA) was generated using a combination of site-directed mutagenesis and extension overlap PCR. Up- and downstream primers (containing *Mfe* I or *Sal* I restriction enzyme sites), as well as overlapping oligos containing the lysine (K) to alanine (A) mutation, were designed. The PCR fragment was cleaved with *Mfe* I and *Sal* I and ligated into *Mfe* I/*Sal* I-digested pbio-EGFP-NAV1. pBio-GFP-NAV2 was constructed by cleaving pEGFP-C3-NAV2 and pbio-EGFP-C1 with *Age* I and *Mlu* I, and the NAV2-containing fragment was cloned into the pbio-EGFP-C1 vector. The pbio-EGFP-NAV3 construct was generated by digesting GFP-NAV3 and pbio-EGFP-C1 with *Ase* I and *Bsr G*I. The fragment containing the biotinylation-tag was ligated into the NAV3-containing fragment of pEGFP-NAV3.

To generate new antisera against Navigators we amplified 5′ end (nt 1–777) and 3′ end (nt 4681–5622) of the NAV1 cDNA, and 5′ end (nt 1–900) and 3′ end (nt 6243–7155) of the NAV3 cDNA by PCR, digested the PCR products with *Sma* I/*Eco R*I (5′ end NAV1), *Bam HI*/*Eco R*I (5′ end and 3′ end NAV3), or *Bam HI*/*Sma* I (3′ end NAV1) and ligated these fragments into digested pGEX-3X (GE Healthcare, Den Bosch, NL). All primer sequences are available upon request. Constructs were confirmed by sequencing.

Antibodies

Bacterial proteins were produced in *E. coli* strain BL21. GST-NAV1-N and GST-NAV3-N fusion proteins contain the N-terminus of NAV1 and -3, respectively. These proteins were purified under native conditions using glutathione-sepharose 4B (GE Healthcare). GST-NAV1-C and GST-NAV3-C fusion proteins contain the C-terminus of NAV1 and -3, respectively. These proteins were purified using a Prep Cell (model 491, BioRad, Hercules, CA), under denaturing conditions. After purification, proteins were dialyzed with PBS, and concentrated using Centriprep YM-30 (Millipore, Billerica, MA). Polyclonal rabbit antibodies were made as described previously [Hoogenraad et al., 2000], using Ribi adjuvant (RIBI Immunochem Research, Hamilton, MT). For some immunofluorescence experiments, antisera were affinity-purified using the corresponding biotinylated Navigator proteins that were in turn purified to near homogeneity from HEK293T cell extracts, using superparamagnetic Dynabeads (M-280 streptavidin, Invitrogen Dynal). Antisera were incubated with beads, washed and eluted using 200 mM glycine (pH 2.8). The elute was quickly neutralized with 1 M Tris and then dialyzed with PBS.

The rabbit polyclonal anti-CLIP170 [Coquelle et al., 2002] and anti-GFP [Drabek et al., 2006] antisera have been described. The following commercial antibodies were used: mouse monoclonal anti-beta-tubulin and anti-acetylated tubulin antibodies (Sigma), mouse monoclonal anti-p150(glued) and anti-EB1 antisera (BD Biosciences, Breda, NL), and rabbit polyclonal anti-pericentrin antibodies (Covance).

Expression in Mammalian Cells

HeLa, G361, HEK293T, and COS-7 cells were grown as described [Drabek et al., 2006]. For immunofluorescence experiments cells were transfected using Fugene 6 (Roche), or Metafectene Pro (Biontex), at a confluency of ~30%. For pull down experiments, HEK293T cells were transfected using Lipofectamine 2000 (Invitrogen). In some experiments nocodazole (10 μM) was added for 30–60 min prior to analysis.

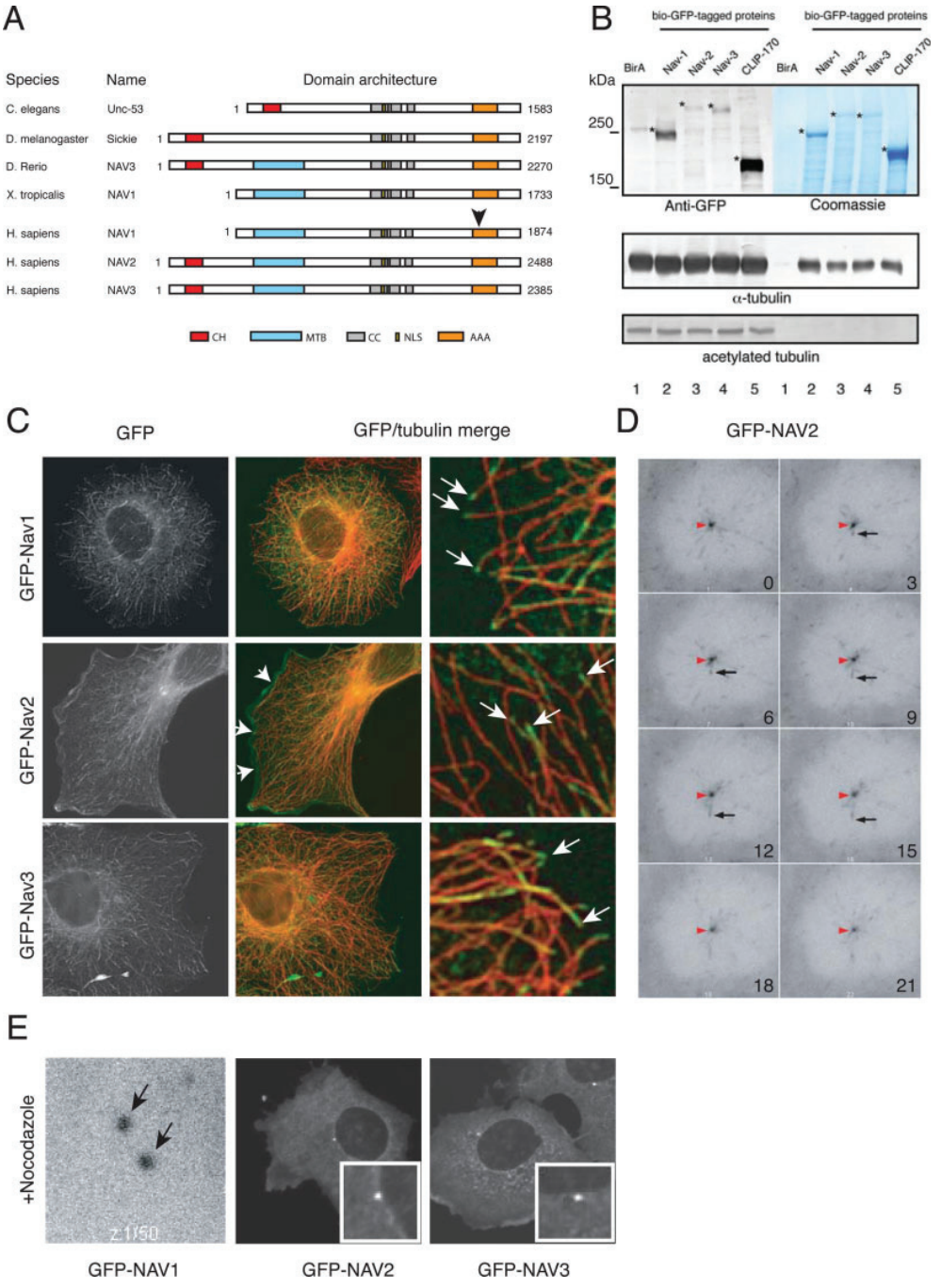
A
Species
Name
Domain architecture
C. elegans
Unc-53
1583
D. melanogaster
Sickie
2197
D. Rerio
NAV3
2270
X. tropicalis
NAV1
1733
H. sapiens
NAV1
1874
H. sapiens
NAV2
2488
H. sapiens
NAV3
2385
CH
MTB
CC
NLS
AAA
B
bio-GFP-tagged proteins
bio-GFP-tagged proteins
BirA
Nav-1
Nav-2
Nav-3
CLIP-170
kDa
250
150
Anti-GFP
Coomassie
α-tubulin
acetylated tubulin
1 2 3 4 5 1 2 3 4 5
C
GFP
GFP/tubulin merge
GFP-Nav1
GFP-Nav2
GFP-Nav3
D
GFP-NAV2
0
3
6
9
12
15
18
21
E
+Nocodazole
z-1/50
GFP-NAV1
GFP-NAV2
GFP-NAV3

Figure 1.

Protein Analysis

For pulldown assays with streptavidin-coated beads HEK293T cells were harvested 1 day after transfection, washed with PBS and lysed in lysis buffer [20 mM Tris-HCl pH 7.5, 150 mM NaCl, 1% Triton X-100 and protease inhibitors (Complete, Roche, Woerden, NL)]. Cell lysates were centrifuged for 10 min at 16,000 g. The supernatant was incubated with streptavidin-coated Dynabeads for 2 h at 4°C. Beads were washed four times (20 mM Tris pH 7.5, 150 mM NaCl, 0.1% Triton X-100). Finally the beads were resuspended in SDS sample buffer [Sambrook et al., 1989] and boiled for 10 min. Proteins were separated by SDS-PAGE and stained with Coomassie Brilliant Blue, or analyzed by Western blot [Sambrook et al., 1989]. Proteins were blotted for 1.5 h at 250 mA onto PVDF immobilon-P membrane (Millipore) using a semi-dry transfer cell (Bio-Rad). Blots were subsequently blocked with PBS, 2% BSA, 0.05% Tween for 30 min, and incubated with primary antibodies (1:2000 dilution) for 2 h at 4°C. Next, blots were washed three times in PBS with 0.2% Tween, and incubated with secondary antibodies [anti-mouse IgG (Fab specific), alkaline phosphatase conjugate, or anti-rabbit IgG (Fab specific), alkaline phosphatase conjugate (Sigma, Zwijndrecht, NL), 1:2500 dilution] for 1 h. After this the blots were washed three times and stained using SigmaFAST (Sigma).

Immunofluorescence Analysis

Cells were grown on coverslips, and either fixed in 4% paraformaldehyde (PFA) for 20 min at room temperature, or in methanol with EGTA (1 mM) for 10 min at −20°C. After fixation, cells were washed with PBS, permeabilized with 0.15% Triton X-100 for 10 min and blocked for 30 min (PBS, 1% BSA, 0.05% tween). Next, the coverslips were incubated with primary antibodies (1:100 dilution) for 2 h, washed three times with wash buffer (PBS, 0.05% tween) and incubated with secondary antibodies [Alexa Fluor-594-, -488- and -350-labelled goat-anti-mouse and goat-anti-rabbit antibodies (Invitrogen), or FITC-labeled goat anti-rabbit antibodies (Nordic Laboratories, Tilburg, NL)] for 1 h. After this, coverslips were washed three times in wash buffer, followed by 1 min in 70% ethanol and 1 min in 100% ethanol. Finally, the coverslips were air dried and mounted in Dapi/DABCO/Vectashield.

Images of fixed cells were collected as described [Drabek et al., 2006], using a Leica DMRBE microscope, equipped with a Hamamatsu CCD camera (C4880). Photoshop (Adobe), ImageJ (http://rsbweb.nih.gov/ij) and GraphicConverter (Lemke Software) were used to make overlays and colorize pictures.

Live Imaging

Live imaging experiments and fluorescence-based analyses were performed as described [Drabek et al., 2006; Dragestein et al., 2008]. We either used an epifluorescent microscope equipped with a Hamamatsu ORCA ER camera, or a Zeiss 510 LSM confocal laser scanning microscope. Bleaching experiments were performed as published previously [Drabek et al., 2006;

Fig. 1. Localization of GFP-tagged Navigators. **A**: Structure of Navigator proteins. The domain architecture of Navigator proteins from different species is schematically depicted. Amino acid numbers are indicated. MTB, MT-binding domain (blue); AAA, ATPase domain (orange); CH, calponin homology domain (red). Green rectangles represent potential coiled-coil (CC) domains. The arrowhead points to the approximate position of the Walker A motif inside the ATPase domain. We mutated a highly conserved lysine (K) to alanine (A) in order to generate a mutant NAV1 protein defective in ATPase activity. **B**: Characterization of bio-GFP-tagged Navigators. Biotinylated, GFP-tagged Navigators (lanes 2–4) and CLIP-170 (lane 5) were overexpressed in HEK293T cells and detected with anti-GFP antibody in crude lysates (upper left panel, asterisks indicate the different fusion proteins). The bio-GFP-fusion proteins were purified under mild conditions and stained with Coomassie brilliant blue (upper right panel). In each case a protein of the correct size is purified (the predicted weight of GFP-NAV1 is ∼230 kDa, of GFP-NAV2 ∼290 kDa, of GFP-NAV3 ∼280 kDa, and of GFP-CLIP170 ∼190 kDa). Molecular weight markers are indicated to the left (in kDa). Lane 1 shows an extract of cells expressing birA enzyme only. A further Western blot analysis shows that α-tubulin is purified along with biotinylated fusion proteins. Modified α-tubulin (acetylated), found in stable MTs, does not come down. **C**: Immunofluorescent analysis of bio-GFP-tagged Navigators in cultured cells. GFP-Navigators were transiently transfected. After 1 day cells were fixed and incubated with antibodies against α-tubulin (red). All three fusion proteins prominently localize to the ends of MTs. This is most obvious in the right hand panels which are enlargements of the middle figures (arrows indicate clear examples of bio-GFP-Navigators (green) at the ends of MTs (red)). The arrowheads in the middle panel point to GFP-Nav-2 distribution in actin-rich membrane ruffles at the cell periphery. **D**: Analysis of bio-GFP-NAV2 in live cells. COS-7 cells expressing GFP-NAV2 were analyzed using an epifluorescent microscope. Images were acquired at one frame per 3 s. Eight consecutive frames are shown here (see Supporting Information Movie S2 for time lapse). Signal was inverted for clarity. GFP-NAV2 localizes to a structure (indicated by the red arrowhead) near the nucleus (visible as a lighter halo) from which fluorescent comets and dots emanate in all directions into the cell. One such a comet is indicated by the arrow, it disappears after 15 s. We conclude that bio-GFP-NAV2 localizes to centrosomes and to the ends of growing MTs. **E**: Bio-GFP-Navigators localize to centrosomes independently of MTs. Bio-GFP-Navigator proteins were transiently expressed in COS-7 cells. After 1 day cells were incubated with nocodazole for 30 (GFP-NAV1) or 60 (GFP-NAV2 and -3) minutes. In the case of GFP-NAV1 we imaged live cells to show that GFP-NAV1 remains bound to centrosomes prior to and after nocodazole addition (see Supporting Information Movie S4 for a time lapse experiment). In the case of GFP-NAV2 and -3 we fixed cells after nocodazole addition and detected GFP signal (insets show centrosomal areas enlarged).

Dragestein et al., 2008] with minor modifications. In the single bleach experiment a rectangular region of interest (ROI) of 200 by 235 pixels (0.15 micron/pixel) was bleached after 14 images (frame rate set at one image per second). A total of 200 images was acquired in this experiment (total time of experiment 203.5 s). Both the fluorescence recovery after photobleaching (FRAP) inside the bleached zone, as well as the fluorescence loss in photobleaching (FLIP) in small ROIs outside of the bleach zone were calculated. Curves were first normalized, and subsequently values from 3 to 4 small nearby ROIs were averaged. In the iterated bleaching experiment nine images were acquired (frame rate set at one image per second) prior to bleaching. We subsequently repeatedly bleached a circular ROI with a diameter of 45 pixels (0.15 micron/pixel). Each bleach period lasted 2.7 s and was followed by a pauze of 1 s (for the acquisition of two images that are one second apart). A total of 400 images was acquired in this experiment (total time of experiment 726 s). For this bleach experiment only FLIP was measured in small ROIs outside of the bleach zone. First, the average background value was deducted from the fluorescence intensity in each ROI. Subsequently curves were normalized, and values from 4 small nearby ROIs were averaged to obtain FLIP measurements nearby and further away from the bleach zone.

RESULTS

Domain Structure of the Navigators

Navigator proteins have been detected in a variety of species and in each case a similar domain architecture is seen (Fig. 1A). One of the most important features of the Navigators is an AAA-type ATPase domain, which is located at the C-terminus of the proteins. This domain is 200–250 amino acids long and is characterized by a number of smaller motifs that are important for ATP binding and hydrolysis. These include the Walker A (P-loop) and the Walker B motif. To generate an ATPase-inactive mutant of NAV1 (called NAV1-KA) we mutated a highly conserved lysine (K) residue (at amino acid position 1523) of the Walker A motif (see Fig. 1A for its approximate position) to alanine (A). It has been shown for a number of AAA+ ATPases that mutating this conserved lysine to alanine abolishes nucleotide binding [see, e.g., Evans et al., 2005].

Other conspicuous motifs within Navigators are a calponin-homology (CH) domain at the N-terminus (which is lacking in NAV1), and stretches of amino acids with the potential to form coiled-coils (CC). The CH domain is known to have affinity for actin, although in EB1-like proteins a CH motif is involved in MT end binding. CC domains are often involved in protein-protein interactions. Finally, Buesa and co-workers identified a novel type of MTB domain in mouse NAV1 [Martinez-Lopez et al., 2005]. The corresponding region is indicated in the human Navigators (Fig. 1A).

Navigators are +TIPs

The biotin ligase from *E. coli* (birA) is widely used to specifically biotinylate proteins containing a short (15–22 amino acids) peptide sequence, the biotin-tag [de Boer et al., 2003]. Magnetic streptavidin-coated beads are used to isolate biotinylated fusion proteins. If purification is done under stringent conditions only the biotinylated protein will be isolated. Under mild purification conditions proteins interacting with the biotinylated bait will be co-purified. The streptavidin pull down is a single-step, high affinity procedure and has been used successfully to isolate cytoplasmic MT end binding proteins and interacting partners [Lansbergen et al., 2006]. We tagged Navigators at their N-terminus with a biotin recognition sequence followed by GFP (bio-GFP). As positive control we generated bio-GFP-tagged CLIP-170 [Dragestein et al., 2008]. We used cells expressing BirA only as negative control. Fusion proteins were overexpressed in HEK293T cells together with BirA. In purified samples bio-GFP-tagged proteins of the expected size were detected by coomassie brilliant blue staining (Fig. 1B, upper right hand panel, and data not shown). We positively identified each protein with anti-GFP antibodies (Fig. 1B, upper left hand panel). Both NAV1 and CLIP-170 have been shown to bind tubulin [Folker et al., 2005; Martinez-Lopez et al., 2005]. To demonstrate that the different bio-GFP fusion proteins are functional, we co-purified tubulin with bio-GFP-tagged Navigators and, as control, with CLIP-170. Western blot analysis shows that all three Navigators bind α-tubulin, as does CLIP-170 (Fig. 1B, middle panel). None of the bio-GFP fusion proteins binds acetylated tubulin, a posttranslationally modified form of α-tubulin found in MTs (Fig. 1C, lower panel). These results suggest that bio-GFP-tagged Navigators and CLIP-170 are properly folded, functional fusion proteins that are able to bind free tubulin dimers.

We next examined the localization of bio-GFP-tagged Navigators in transfected COS-7 cells. For all three proteins we detected signal at the ends of a subset of MTs (Fig. 1C). In time-lapse movies fluorescent comet- and dot-like structures were observed that often emanated at a centrosome and that moved through cells with the speed of growing MTs (Fig. 1D, Supporting Information Movies S1–S3, and data not shown). These data demonstrate that Navigators localize at the ends of growing MTs and are valid +TIPs. In interphase cells we noted that Navigators also localized at centrosomes (Supporting Information Movies S2, S4, S7, S8), even in the presence of the MT disrupting agent nocodazole

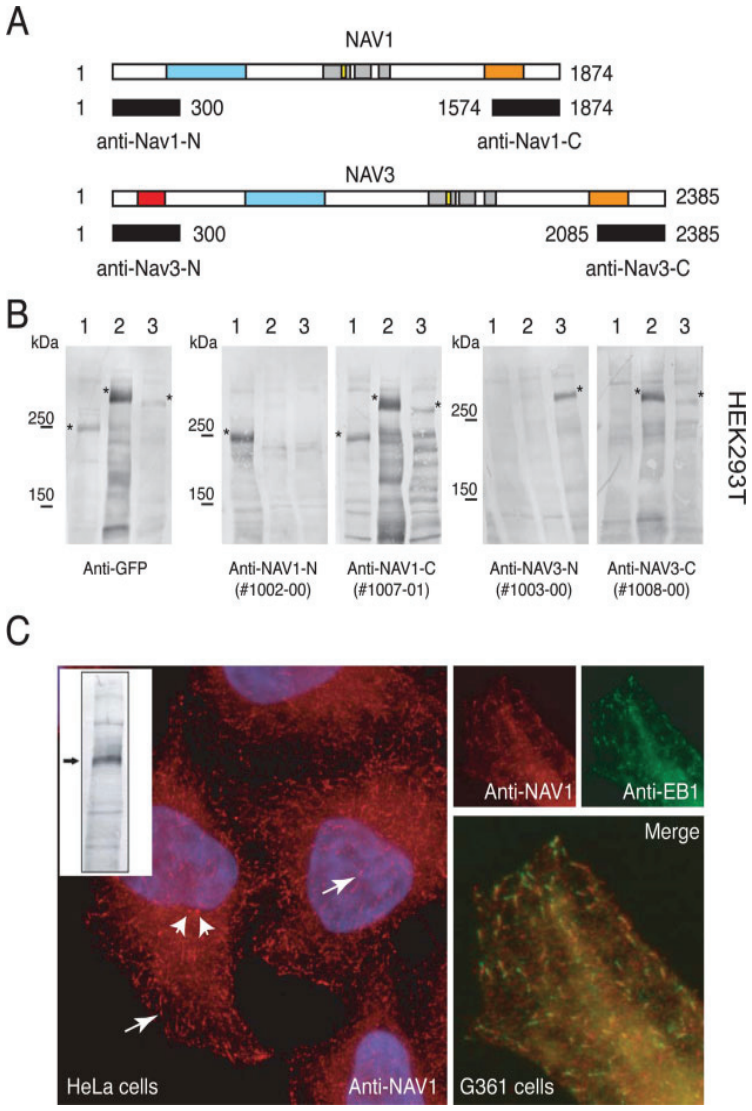

Fig. 2. Characterization of anti-Navigator antibodies. **A**: Position of the antigens. The domain architecture of NAV1 and -3 is shown. MTB (blue), ATPase (orange), CH (red), and potential coiled-coil (grey) domains are indicated. Black boxes represent the regions used for antibody generation. Amino acid numbers are indicated. **B**: Western blot analysis of anti-Navigator antisera. GFP-tagged NAV1-3 were expressed in HEK293T cells and protein extracts of transiently transfected cells were incubated on Western blot using four different anti-Navigator antibodies. Anti-GFP was used as positive control. The positions of GFP-NAV1-3 are indicated by asterisks. Molecular weight markers are indicated to the left (in kDa). **C**: Localization of Navigators in cultured cells. Western blot analysis shows NAV1 expression in HeLa cells (arrow marks NAV1 position on the blot, antibody #1002-00 was used). An immunofluorescent analysis in fixed HeLa and G361 cells (with antibody #1007-01) reveals localization of endogenous Navigators on MT ends. Two clear examples of MT end staining in HeLa cells are indicated by the large arrows (left panel), co-localization with EB1 is shown on the right. Navigators also localize on centrosomes (small arrows in left hand panel).

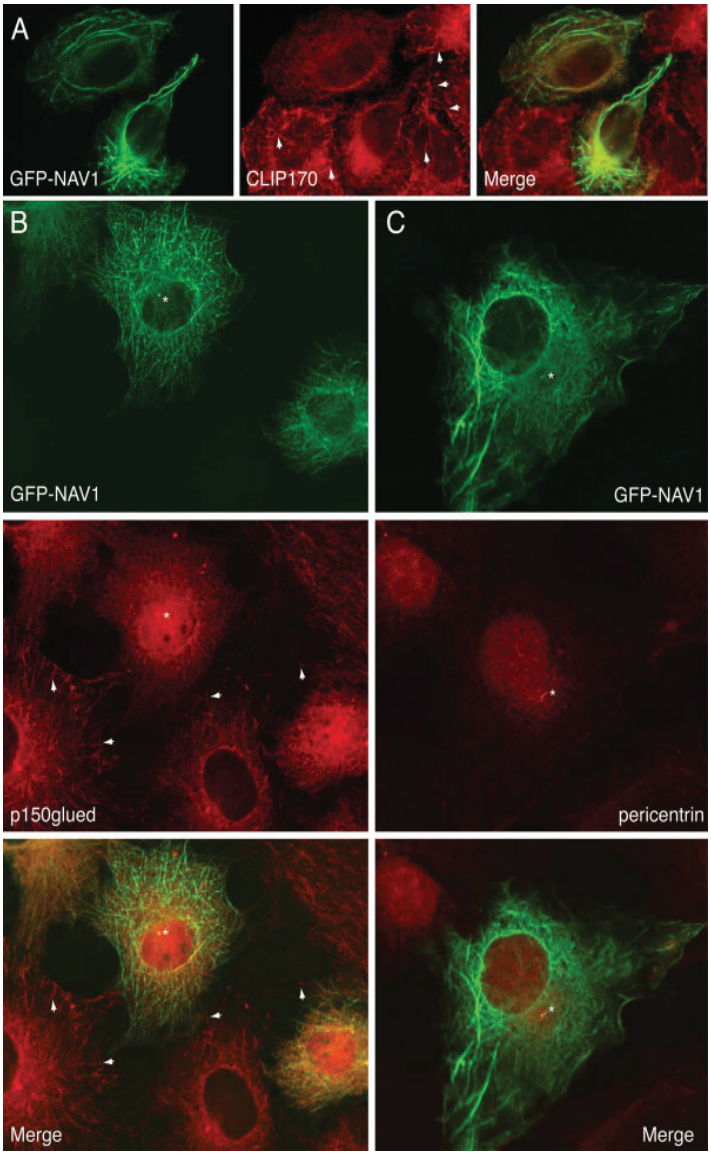

Fig. 3. Navigator binding sites at MT ends overlap with those of CAP_GLY-motif proteins. **A**: GFP-NAV1 expression affects CLIP-170 binding at MT ends. HeLa cells were transiently transfected with GFP-NAV1. After 1 day cells were fixed and stained for CLIP170 (red). In non-transfected cells CLIP-170 localizes to MT ends (arrows indicate clear examples of plus end staining). In GFP-NAV1-transfected cells CLIP-170 staining is much more diffuse. **B**: GFP-NAV1 expression specifically affects MT end accumulation of p150(glued). HeLa cells were transiently transfected with GFP-NAV1. After 1 day cells were fixed and stained for p150(glued) (red). Like CLIP-170, p150(glued) accumulates at MT ends in non-transfected cells (arrows indicate clear examples of plus end staining). In GFP-NAV1-transfected cells p150(glued) localization on MT ends is hardly observed. By contrast, centrosomal accumulation (indicated by the asterisk) is not significantly reduced. **C**: GFP-NAV1 localizes to centrosomes. HeLa cells were transiently transfected with GFP-NAV1. After 1 day cells were fixed and stained for pericentrin (red), a centrosomal marker. Notice the colocalization of GFP-NAV1 and pericentrin at centrosomes (indicated with the asterisk).

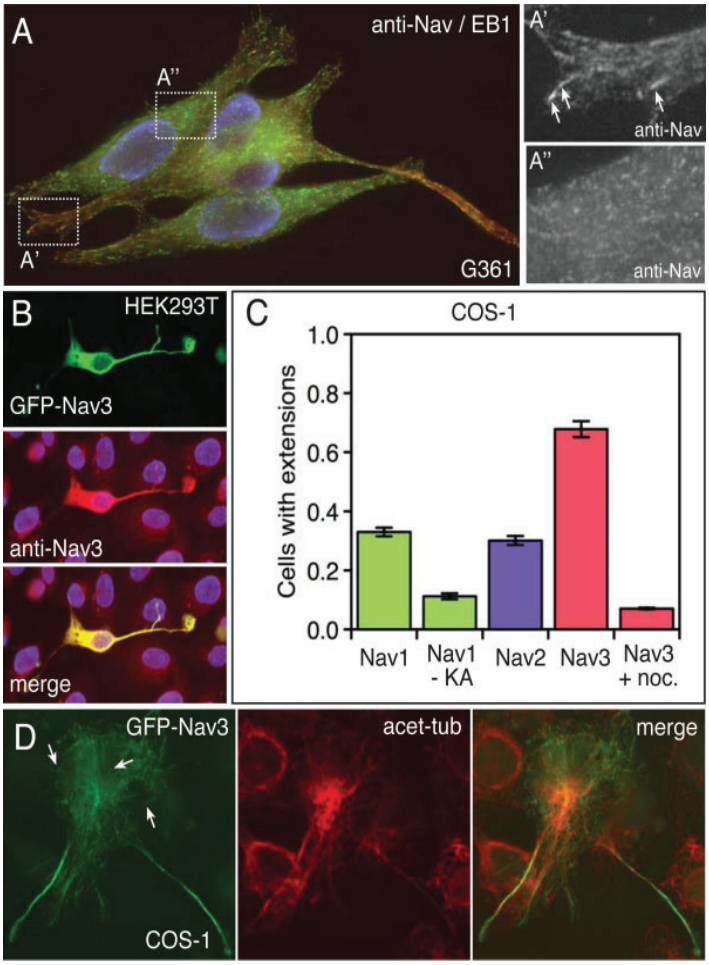

Fig. 4. Local regulation of Navigator MT localization. **A**: Asymmetric localization of endogenous Navigator. G361 cells seeded onto coverslips, become extended and occasionally grow extensions. Navigator proteins accumulate at the cell periphery and in the extensions, whereas EB1 distributes equally throughout the cells. Enlargement of the insets A′ and A″ reveals that Navigator plus end staining is more pronounced in the cellular periphery than in the cell interior (clear examples of MT end staining are indicated by the arrows). **B–D**: Expression of GFP-tagged Navigators induces formation of neurite-like extensions. In (B) HEK293T cells were transfected with GFP-NAV3 (green). After fixation cells were stained with anti-NAV3 antiserum (#1003-00). In (C) and (D) COS-7 cells were transfected with GFP-tagged wild type Navigators, as well as with ATPase-defective NAV1 (NAV1-KA). In (C) we quantified the fraction of COS-7 cells with extensions (+noc: nocodazole was added for 60 min to the transfected cells, error bars indicate SEM). In (D) an example staining is shown of a COS-7 cell transfected with GFP-NAV3 and stained with an antibody against acetylated tubulin. GFP-NAV3 localizes at MT ends in the cell body (clear examples are indicated by the arrows), and is enriched in the extensions.

(Fig. 1E, Supporting Information Movie S4). Thus, Navigators localize to centrosomes independent of an intact MT cytoskeleton. GFP-NAV1 is further detected in granular structures distributed throughout the cytoplasm (Supporting Information Movie S1, and data not shown), whereas GFP-NAV2 and NAV3 accumulate in membrane ruffles at the cell periphery (Fig. 1C). At higher expression levels Navigators appear to cause bundling of MTs (see Figs. 3–5 and Supporting Information Movies S7, S8). Interestingly, imaging in live cells demonstrates

that growing MTs are still abundantly present in cells containing MT bundles (see, e.g., Supporting Information Movie S8), suggesting that Navigators cause MT bundling without significantly depleting the pool of free tubulin dimers. Combined, the data show that Navigators are +TIPs that can influence the behavior of the MT network.

To examine the distribution of endogenous Navigator proteins we generated antibodies against the N- and C-terminus of NAV1 and NAV3 (Fig. 2A). Western blot analysis on extracts of HEK293T cells, transiently transfected with bio-GFP-NAV1, bio-GFP-NAV2, or bio-GFP-NAV3, indicate that the N-terminal antibodies are specific for NAV1 or NAV3 (Fig. 2B, Supporting Information Figure S1A). By contrast, the antisera against the C-terminus of NAV1 recognize all three Navigators, whereas antibodies against the C-terminus of NAV3 mainly recognize NAV2 and NAV3 (Fig. 2B, Supporting Information Figure S1A). In addition, all antibodies also recognize non-specific proteins (Supporting Information Figure S1A and data not shown). Immunofluorescence analysis in COS-7 cells, transfected with GFP-NAV1, -2, or -3 also suggests that anti-NAV1-N and anti-NAV3-N are specific for NAV1 and -3, respectively, while anti-NAV1-C is a pan-Navigator antiserum (Supporting Information Figure S1C and data not shown).

Northern blot analysis has revealed expression patterns of the Navigators in different cell lines [Peeters et al., 2004]. Based on this information we analyzed the localization of endogenous Navigator proteins in HeLa and G361 cells. Western blot analysis demonstrates expression of NAV1 in HeLa cells (Fig. 2C, left hand panel including inset, see also Supporting Information Figure S1B). In these cells NAV1 localizes at MT ends and on centrosomes (see long and short arrows, respectively, in left hand panel of Fig. 2C). In G361 cells anti-NAV1-N and anti-NAV3-N antibodies do not yield clear staining (data not shown), whereas incubation with the pan-Navigator antiserum (anti-NAV1-C) results in bright MT end labeling, as confirmed by co-localization experiments with anti-EB1 antibodies (right hand panels in Fig. 2C). These results indicate that G361 cells preferentially express NAV2, although we can not exclude the possibility that these cells express a short isoform of NAV1 or -3 that lacks the region recognized by the N-terminal antisera. In other cell lines we also documented MT end localization of the Navigators (data not shown). We therefore conclude that Navigator proteins are +TIPs.

Characterization of Navigator Binding Sites at MT Ends

We noted that in HeLa cells expressing GFP-tagged Navigator proteins the localization of endogenous CLIP-170 at MT ends is strongly diminished (Fig. 3A and Supporting Information Figure S2). These data suggest that Navigators compete with CLIP-170 for binding at MT ends. We next tested whether p150(glued), which is another CAP_GLY motif-containing protein, is also displaced by overexpression of Navigators. As shown previously [Vaughan et al., 2002] p150(glued) localizes both at MT ends and at the centrosome (Fig. 3B). Interestingly, overexpression of GFP-NAV1 abolishes MT end localization of p150(glued) but not its centrosome association. These data indicate that the binding sites on MT ends for Navigators and CAP_GLY-domain-containing proteins do overlap.

We next stained HeLa cells expressing GFP-NAV1 with antibodies against pericentrin, a valid centrosomal marker [Doxsey et al., 1994]. The labeling pattern of both proteins overlaps at the centrosome (Fig. 3C). Similar results were obtained with the other GFP-tagged fusion proteins and in co-staining experiments with Navigator and pericentrin antibodies (data not shown). Thus, Navigators localize to centrosomes. Remarkably, p150(glued) and NAV1 do not colocalize perfectly at the centrosome, i.e. p150(glued) staining is often seen around NAV1 (data not shown). Combined these results indicate that the manner by which p150(glued) and Navigators associate with centrosomes, is different from that by which the proteins recognize MT ends.

Navigators Alter the MT Cytoskeleton to Induce Neurite-Like Extensions

While in HeLa cells NAV1 localizes throughout the cytoplasm in a roughly homogenous manner we noted that in G361 cells Nav-staining is enriched within peripheral domains, including long extensions made by these cells (Fig. 4A). MT end accumulation of Navigator

Fig. 5. Dynamic behavior of GFP-NAV1. **A–H**: FRAP/FLIP analysis in transfected COS-7 cells. GFP-NAV1 was transiently transfected in COS-7 cells. After 1 day transfected cells were bleached. In (A-D) results of a single bleach experiment are shown, in (E-H) results of a repeated bleach experiment are shown. Bleaches were performed in the bleach zones (bz). In (A) and (E), the first images of the time-lapse experiments are shown, in (B) and (F) images are shown after the (first) bleach, and in (C) and (G) images at the end of the experiments are shown (Supporting Information Movies S7 and S8 show the complete time lapse experiments). In (D) and (H) average and normalized fluorescence recovery and loss are shown. Fluorescence intensities (FI) are plotted on the vertical axis with time (in seconds) on the horizontal axis.[Color figure can be viewed in the online issue, which is available at www.interscience.wiley.com.]

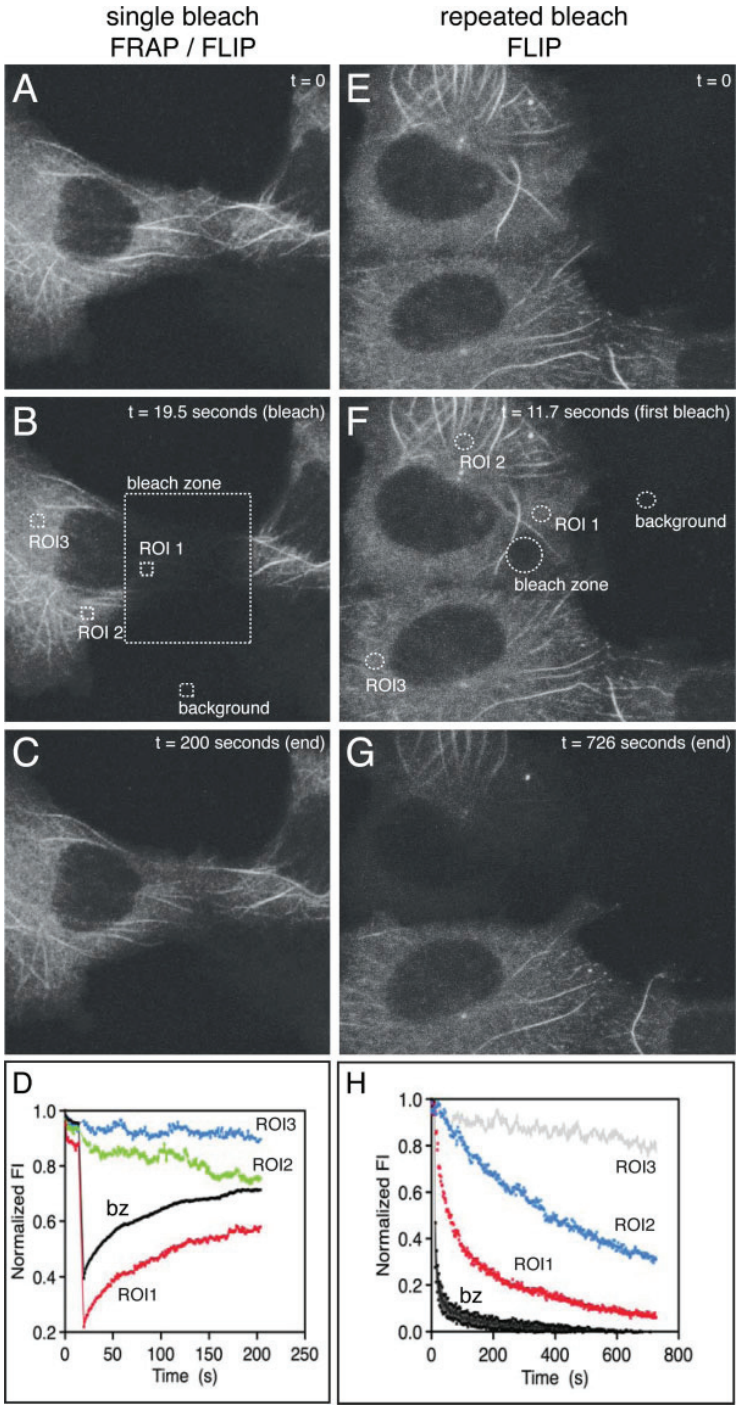
single bleach
FRAP / FLIP
repeated bleach
FLIP
A
t = 0
E
t = 0
B
t = 19.5 seconds (bleach)
bleach zone
ROI3
ROI 1
ROI 2
background
F
t = 11.7 seconds (first bleach)
ROI 2
ROI 1
background
bleach zone
ROI3
C
t = 200 seconds (end)
G
t = 726 seconds (end)
D
Normalized FI
1.0
0.8
0.6
0.4
0.2
ROI3
ROI2
bz
ROI1
0
50
100
150
200
250
Time (s)
H
Normalized FI
1.0
0.8
0.6
0.4
0.2
0.0
ROI3
ROI2
ROI1
bz
0
200
400
600
800
Time (s)

Figure 5.

protein is more pronounced in such peripheral regions, when compared to the centre of the cell (see insets in Fig. 4A; in fact, if not for the co-localization with EB1, the dot-like staining pattern in the centre of the G361 cell would not be recognized as a MT end). A similar pattern was noted in a number of other cell types (data not shown). The Nav-staining in G361 cells contrasts with the distribution of EB1, which, as shown previously [Akhmanova et al., 2001], localizes evenly on MT ends throughout polarized cells (Fig. 4A). Combined the results suggest that Navigator localization can be locally regulated, similar to the distribution of CLASPs [Akhmanova et al., 2001].

Overexpression of GFP-tagged Navigators in cells that are not normally polarized gives rise to long extensions (see, e.g., Figs. 4B–4D). This behavior was observed in all non-neuronal cell types tested. The ends of these extensions sometimes resemble pauzed growth cones (Fig. 4B), and inside the extensions we detected an enrichment of acetylated tubulin, a marker for stable MTs. In other experiments we detected dynamic movement of GFP-tagged Navigator inside the extension (Supporting Information Movie S5). We quantified the presence of these neurite-like extensions in COS-7 cells transfected with each of the three Navigators and found that GFP-NAV3 is most efficient in inducing extensions (Fig. 4C). This activity requires an intact MT network as the addition of nocodazole for 60 min abolishes neurite-like extensions. Addition of MT-depolymerizing agents also causes neurite retraction in primary neurons [Daniels, 1973]. COS-7 cells were next transfected with GFP-NAV1-KA, the ATPase-deficient form of NAV1. Despite the fact that this protein localizes to MT ends (Supporting Information Movie S6) hardly any extensions were observed in GFP-NAV1-KA expressing COS-7 cells (Fig. 4C). These results show that the ability of NAV1 to induce neurite-like extensions requires both an intact MT network as well as ATPase activity.

Navigators Move Slowly Through the Cytoplasm

While our work and that of others [Martinez-Lopez et al., 2005] emphasizes the tight link between Navigators and the MT network, work on NAV2 points to an association of Navigators with intermediate filaments [Muley et al., 2008]. Furthermore, the presence of a CH-motif in NAV2 and -3 indicates that Navigators interact with actin, as does the fact that GFP-NAV2 and -3 both accumulate in actin-rich ruffles at the cell periphery (Fig. 1C and data not shown). These data suggest that Navigators associate with other cellular structures than MTs and centrosomes. To address this issue we analyzed the dynamic behavior of GFP-tagged NAV1 in transiently transfected COS-7 cells. We photobleached a region of interest (ROI) within a cell and examined fluorescence recovery after photobleaching (FRAP) within the bleach zone, as well as fluorescence loss in photobleaching (FLIP) outside of the zone. We reasoned that fast recovery (or loss) of fluorescence indicates that NAV1 is likely to be freely diffusing through the cytoplasm, whereas if dynamics is slow the protein is likely to be bound to other intracellular structures.

Two types of bleaching experiment were performed: a single bleach in a rectangular ROI (Figs. 5A–5D), and an iterative bleach in a circular ROI (Figs. 5E–5H). In the first experiment it takes ~3 min for recovery of GFP-NAV1 signal inside the bleach zone (Fig. 5D). This recovery is slower than that of GFP-CLIP170, bleached in a similar manner [Drabek et al., 2006]. The data indicate that a significant fraction of GFP-NAV1 is not freely diffusing through the cytoplasm. Interestingly, fluorescence loss in a ROI nearby the bleach zone occurs more rapidly than in a ROI further away, supporting the idea of slow movement of Navigator protein through the cytoplasm. Also in experiments where cells are bleached in an iterative manner (Figs. 5E–5H) fluorescence loss is fastest inside the bleach zone and it occurs more rapidly in a ROI near the bleach zone than in a ROI further away (Fig. 5H). We therefore propose that GFP-NAV1 is bound to structures other than MTs. Alternatively, GFP-NAV1 is part of a high molecular weight complex that does not diffuse rapidly.

DISCUSSION

Since the first description of CLIP-170 [Perez et al., 1999], the number of +TIPs has increased dramatically [Akhmanova and Steinmetz, 2008]. One of the latest additions to this diverse group of proteins is NAV1 [Martinez-Lopez et al., 2005]. Because of a lack of appropriate antibodies, the localization of endogenous NAV1 could not be studied, and although GFP-tagged NAV1 was clearly shown to accumulate at MT ends, no live experiments were performed with this fusion protein. Studies on NAV2 actually did not reveal a preference of this protein for the MT end [Muley et al., 2008], and therefore the question remained whether Navigators are +TIPs or not. Using a live imaging approach we show here that all three Navigators are capable of tracking MT ends. Furthermore, localization studies with newly made antibodies against the Navigators reveal that the endogenous proteins also accumulate at MT ends. We therefore conclude that Navigators are valid +TIPs. We note that Navigators also localize to other intracellular structures. Recent data show that the actin-MT crosslinking factor ACF7, a +TIP that regulates cytoskeletal-focal adhesion dynamics and migration, has ATPase activity [Wu et al.,

2008]. Navigators are +TIPs with MT- and actin-binding domains, with an AAA-type ATPase activity, and with a role in migration. Given the parallels between ACF7 and Navigators, it will be interesting to examine the role of the latter in focal adhesion dynamics.

The CAP_GLY domains of CLIP-170 [Pierre et al., 1992; Perez et al., 1999] and CLIP-115 [Hoogenraad et al., 2000] play an essential role in the MT end binding of these +TIPs. Structural studies have shown that CAP_GLY motifs serve as recognition domains for C-terminally located EEY/F amino acids, which are present in EB1 and α-tubulin, and in CLIP-170 itself [Honnappa et al., 2006]. The C-terminal tyrosine (Y) of α-tubulin was shown to be essential for the in vivo MT end accumulation of CAP_GLY proteins [Peris et al., 2006]. Recent data have revealed that mammalian EB1 autonomously recognizes specific binding sites present at the ends of growing MTs, whereas CLIP-170 requires both EB1 and tyrosinated α-tubulin for its accumulation [Bieling et al., 2008]. Since Navigators compete with CAP_GLY domain proteins for MT end binding, we propose that Navigator binding sites overlap with those of CLIP-170. Thus, Navigators might also recognize the C-terminus of α-tubulin and/or EB1.

The mechanisms that lead to MT end specificity have been studied intensely, and several theories have been proposed. These can be divided into mechanisms that describe MT end specificity as dependent on the +TIP and tubulin/MTs alone, and those that involve a third factor. The first group of theories encompasses treadmilling, co-polymerization and one-dimensional diffusion; the second group encompasses motor-mediated delivery of +TIPs and "hitchhiking" on another +TIP [for review, see Akhmanova and Steinmetz, 2008]. We have recently proposed a novel "fast exchange" model to explain the mechanism of +TIP association [Dragestein et al., 2008]. Using fluorescence-based approaches, we could show that CLIP-170 and EB3, two central +TIPs, turn over rapidly on MT ends and that diffusion is rate limiting for their binding to MT plus ends. We also found that the ends of growing MTs contain a surplus of sites to which CLIP-170 binds with relatively low affinity [Dragestein et al., 2008]. Our results imply that the distribution of a +TIP on a MT end is linked to the structure of that MT end. This view was confirmed by in vitro studies [Bieling et al., 2007]. Despite their relatively slow cytoplasmic diffusion Navigators are able to accumulate at MT ends. Because the Navigator binding sites overlap with those of CLIP-170 we hypothesize that Navigators also exchange rapidly on MT ends. However, due to a low signal-to-noise ratio of MT-end-bound versus cytoplasmic GFP-Nav, we could not unequivocally establish whether this is the case.

Overexpression of classical MAPs often causes the bundling and stabilization of MTs [see, e.g., Kanai et al., 1992]. When CLIP-115 and -170 are overexpressed, MTs also bundle and become stable [Pierre et al., 1994; Hoogenraad et al., 2000]. A result of MT stabilization is that the pool of free tubulin is depleted and the growth rate of the remaining dynamic MTs is reduced. The fact that MT bundles were seen in fixed GFP-NAV1 expressing cells led to the conclusion that NAV1 causes MT stabilization [Martinez-Lopez et al., 2005]. However, our analysis in live cells shows that Navigators do not resemble classical MAPs: despite the presence of MT bundles many dynamic MTs are also seen. We hypothesize that Navigators can bring MTs together without stabilizing them like classical MAPs. This behavior, together with the striking asymmetric localization of Navigators, leads us to suggest that Navigators locally regulate the behavior of the MT network. In this sense the Navigator proteins are akin to CLASPs, ACF7 and APC [Galjart, 2005]. Furthermore, we observed highly dynamic GFP-NAV3-positive bundles in cell extensions. These bundles seem to buckle at the ends of cellular extensions, indicating that these might be MTs that push against the membrane or against another structure [Janson et al., 2003]. It was recently shown that in vitro the force generated by a bundle of MTs increases linearly with the number of MTs in the bundle [Laan et al., 2008]. Perhaps bundling of dynamic MTs, driven by Navigator proteins, contributes to the formation of long cellular extensions by extending the pushing force.

The ATPase domain of the Navigators is most similar to the one found in Katanin and Spastin [Frickey and Lupas, 2004]. Katanin was the first MT-severing enzyme discovered, whereas Spastin is a MT-severing protein, mutated in an autosomal dominant form of hereditary spastic paraplegia [McNally and Vale, 1993; Salinas et al., 2005]. Moreover, Spastin is important for neurite outgrowth [Wood et al., 2006]. The question is whether Navigators also sever MTs. To our opinion, the phenotype of Nav-expressing cells is not compatible with MT severing. In fact, only one in vitro study was thus far published on the ATPase activity of the Navigators and it actually attributed DNA helicase activity to NAV2 [Ishiguro et al., 2002]. We show that an intact MT network and a functional ATPase domain of NAV1 are both required for the induction of neurite-like extensions in non-neuronal cells. These results indicate that Navigators act on MTs using their ATPase domain. A role for Navigators in reorganization of the cytoskeleton to induce neurite outgrowth is consistent with recent data on mammalian NAV1 [Martinez-Lopez et al., 2005] and NAV2 [Muley et al., 2008]. Future studies should reveal how MT end binding contributes to this and to other functions of the Navigators.

CONCLUSIONS

Navigators are +TIPs that are locally regulate the cytoskeleton. Our data suggest that Navigators are not only adaptor proteins that relay signals downstream of specific signaling pathways, but that these proteins are also enzymes that can physically induce cell shape changes.

ACKNOWLEDGMENTS

The authors thank the Kazusa Research Institute (Japan) for sending the KIAA1419 (NAV2) cDNA clone and Drs. C. Hoogenraad and A. Akhmanova for providing the pbio-EGFP-C1 plasmid.

REFERENCES

Akhmanova A, Steinmetz MO. 2008. Tracking the ends: A dynamic protein network controls the fate of microtubule tips. Nat Rev Mol Cell Biol 9(4):309–322.

Akhmanova A, Hoogenraad CC, Drabek K, Stepanova T, Dortland B, Verkerk T, Vermeulen W, Burgering BM, De Zeeuw CI, Grosveld F, Galjart N. 2001. Clasps are CLIP-115 and -170 associating proteins involved in the regional regulation of microtubule dynamics in motile fibroblasts. Cell 104(6):923–935.

Bieling P, Laan L, Schek H, Munteanu EL, Sandblad L, Dogterom M, Brunner D, Surrey T. 2007. Reconstitution of a microtubule plus-end tracking system in vitro. Nature 450(7172):1100–1105.

Bieling P, Kandels-Lewis S, Telley IA, van Dijk J, Janke C, Surrey T. 2008. CLIP-170 tracks growing microtubule ends by dynamically recognizing composite EB1/tubulin-binding sites. J Cell Biol 183(7):1223–1233.

Cassimeris L, Pryer NK, Salmon ED. 1988. Real-time observations of microtubule dynamic instability in living cells. J Cell Biol 107(6 Pt 1):2223–2231.

Chen EB, Branda CS, Stern MJ. 1997. Genetic enhancers of sem-5 define components of the gonad-independent guidance mechanism controlling sex myoblast migration in *Caenorhabditis elegans* hermaphrodites. Dev Biol 182(1):88–100.

Coquelle FM, Caspi M, Cordelieres FP, Dompierre JP, Dujardin DL, Koifman C, Martin P, Hoogenraad CC, Akhmanova A, Galjart N, De Mey JR, Reiner O. 2002. LIS1, CLIP-170's key to the dynein/dynactin pathway. Mol Cell Biol 22(9):3089–3102.

Coy JF, Wiemann S, Bechmann I, Bachner D, Nitsch R, Kretz O, Christiansen H, Poustka A. 2002. Pore membrane and/or filament interacting like protein 1 (POMFIL1) is predominantly expressed in the nervous system and encodes different protein isoforms. Gene 290(1-2):73–94.

Daniels MP. 1973. Fine structural changes in neurons and nerve fibers associated with colchicine inhibition of nerve fiber formation in vitro. J Cell Biol 58(2):463–470.

de Boer E, Rodriguez P, Bonte E, Krijgsveld J, Katsantoni E, Heck A, Grosveld F, Strouboulis J. 2003. Efficient biotinylation and single-step purification of tagged transcription factors in mammalian cells and transgenic mice. Proc Natl Acad Sci USA 100(13): 7480–7485.

Dent EW, Gertler FB. 2003. Cytoskeletal dynamics and transport in growth cone motility and axon guidance. Neuron 40(2):209–227.

Doxsey SJ, Stein P, Evans L, Calarco PD, Kirschner M. 1994. Pericentrin, a highly conserved centrosome protein involved in microtubule organization. Cell 76(4):639–650.

Drabek K, van Ham M, Stepanova T, Draegestein K, van Horssen R, Sayas CL, Akhmanova A, Ten Hagen T, Smits R, Fodde R, Grosveld F, Galjart N. 2006. Role of CLASP2 in microtubule stabilization and the regulation of persistent motility. Curr Biol 16(22):2259–2264.

Dragestein KA, van Cappellen WA, van Haren J, Tsibidis GD, Akhmanova A, Knoch TA, Grosveld F, Galjart N. 2008. Dynamic behavior of GFP-CLIP-170 reveals fast protein turnover on microtubule plus ends. J Cell Biol 180(4):729–737.

Evans KJ, Gomes ER, Reisenweber SM, Gundersen GG, Lauring BP. 2005. Linking axonal degeneration to microtubule remodeling by Spastin-mediated microtubule severing. J Cell Biol 168(4): 599–606.

Folker ES, Baker BM, Goodson HV. 2005. Interactions between CLIP-170, tubulin, and microtubules: Implications for the mechanism of CLIP-170 plus-end tracking behavior. Mol Biol Cell 16(11):5373–5384.

Frickey T, Lupas AN. 2004. Phylogenetic analysis of AAA proteins. J Struct Biol 146(1-2):2–10.

Galjart N. 2005. CLIPs and CLASPs and cellular dynamics. Nat Rev Mol Cell Biol 6(6):487–498.

Hekimi S, Kershaw D. 1993. Axonal guidance defects in a *Caenorhabditis elegans* mutant reveal cell-extrinsic determinants of neuronal morphology. J Neurosci 13(10):4254–4271.

Honnappa S, Okhrimenko O, Jaussi R, Jawhari H, Jelesarov I, Winkler FK, Steinmetz MO. 2006. Key interaction modes of dynamic +TIP networks. Mol Cell 23(5):663–671.

Hoogenraad CC, Akhmanova A, Grosveld F, De Zeeuw CI, Galjart N. 2000. Functional analysis of CLIP-115 and its binding to microtubules. J Cell Sci 113:2285–2297.

Ishiguro H, Shimokawa T, Tsunoda T, Tanaka T, Fujii Y, Nakamura Y, Furukawa Y. 2002. Isolation of HELAD1, a novel human helicase gene up-regulated in colorectal carcinomas. Oncogene 21(41):6387–6394.

Janson ME, de Dood ME, Dogterom M. 2003. Dynamic instability of microtubules is regulated by force. J Cell Biol 161(6):1029–1034.

Kanai Y, Chen J, Hirokawa N. 1992. Microtubule bundling by tau proteins in vivo: Analysis of functional domains. Embo J 11(11): 3953–3961.

Karenko L, Hahtola S, Paivinen S, Karhu R, Syrja S, Kahkonen M, Nedoszytko B, Kytola S, Zhou Y, Blazevic V, Pesonen M, Nevala H, Nupponen N, Sihto H, Krebs I, Poustka A, Roszkiewicz J, Saksela K, Peterson P, Visakorpi T, Ranki A. 2005. Primary cutaneous T-cell lymphomas show a deletion or translocation affecting NAV3, the human UNC-53 homologue. Cancer Res 65(18):8101–8110.

Kikuno R, Nagase T, Nakayama M, Koga H, Okazaki N, Nakajima D, Ohara O. 2004. HUGE: A database for human KIAA proteins, a 2004 update integrating HUGEppi and ROUGE. Nucleic Acids Res 32(Database issue):D502–D504.

Laan L, Husson J, Munteanu EL, Kerssemakers JW, Dogterom M. 2008. Force-generation and dynamic instability of microtubule bundles. Proc Natl Acad Sci USA 105(26):8920–8925.

Lansbergen G, Grigoriev I, Mimori-Kiyosue Y, Ohtsuka T, Higa S, Kitajima I, Demmers J, Galjart N, Houtsmuller AB, Grosveld F, Akhmanova A. 2006. CLASPs attach microtubule plus ends to the cell cortex through a complex with LL5beta. Dev Cell 11(1):21–32.

Lee H, Engel U, Rusch J, Scherrer S, Sheard K, Van Vactor D. 2004. The microtubule plus end tracking protein orbit/MAST/CLASP acts downstream of the tyrosine kinase Abl in mediating axon guidance. Neuron 42(6):913–926.

Maes T, Barcelo A, Buesa C. 2002. Neuron navigator: A human gene family with homology to unc-53, a cell guidance gene from *Caenorhabditis elegans*. Genomics 80(1):21–30.

Martinez-Lopez MJ, Alcantara S, Mascaro C, Perez-Branguli F, Ruiz-Lozano P, Maes T, Soriano E, Buesa C. 2005. Mouse neuron navigator 1, a novel microtubule-associated protein involved in neuronal migration. Mol Cell Neurosci 28(4):599–612.

McNally FJ, Vale RD. 1993. Identification of katanin, an ATPase that severs and disassembles stable microtubules. Cell 75(3):419–429.

Merrill RA, Plum LA, Kaiser ME, Clagett-Dame M. 2002. A mammalian homolog of unc-53 is regulated by all-trans retinoic acid in neuroblastoma cells and embryos. Proc Natl Acad Sci USA 99(6):3422–3427.

Mishima M, Maesaki R, Kasa M, Watanabe T, Fukata M, Kaibuchi K, Hakoshima T. 2007. Structural basis for tubulin recognition by cytoplasmic linker protein 170 and its autoinhibition. Proc Natl Acad Sci USA 104(25):10346–10351.

Mitchison T, Kirschner M. 1984. Dynamic instability of microtubule growth. Nature 312(5991):237–242.

Moore SW, Tessier-Lavigne M, Kennedy TE. 2007. Netrins and their receptors. Adv Exp Med Biol 621:17–31.

Muley PD, McNeill EM, Marzinke MA, Knobel KM, Barr MM, Clagett-Dame M. 2008. The atRA-responsive gene neuron navigator 2 functions in neurite outgrowth and axonal elongation. Dev Neurobiol 68(13):1441–1453.

Ohara O, Nagase T, Ishikawa K, Nakajima D, Ohira M, Seki N, Nomura N. 1997. Construction and characterization of human brain cDNA libraries suitable for analysis of cDNA clones encoding relatively large proteins. DNA Res 4(1):53–59.

Peeters PJ, Baker A, Goris I, Daneels G, Verhasselt P, Luyten WH, Geysen JJ, Kass SU, Moechars DW. 2004. Sensory deficits in mice hypomorphic for a mammalian homologue of unc-53. Brain Res Dev Brain Res 150(2):89–101.

Perez F, Diamantopoulos GS, Stalder R, Kreis TE. 1999. CLIP-170 highlights growing microtubule ends in vivo. Cell 96(4):517–27.

Peris L, Thery M, Faure J, Saoudi Y, Lafanechere L, Chilton JK, Gordon-Weeks P, Galjart N, Bornens M, Wordeman L, Wehland J, Andrieux A, Job D. 2006. Tubulin tyrosination is a major factor affecting the recruitment of CAP-Gly proteins at microtubule plus ends. J Cell Biol 174(6):839–849.

Pierre P, Scheel J, Rickard JE, Kreis TE. 1992. CLIP-170 links endocytic vesicles to microtubules. Cell 70(6):887–900.

Pierre P, Pepperkok R, Kreis TE. 1994. Molecular characterization of two functional domains of CLIP-170 in vivo. J Cell Sci 107: 1909–1920.

Riehemann K, Sorg C. 1993. Sequence homologies between four cytoskeleton-associated proteins. Trends Biochem Sci 18(3):82–83.

Salinas S, Carazo-Salas RE, Proukakis C, Cooper JM, Weston AE, Schiavo G, Warner TT. 2005. Human spastin has multiple microtubule-related functions. J Neurochem 95(5):1411–1420.

Sambrook J, Fritsch EF, Maniatis T. 1989. Molecular Cloning: A Laboratory Manual, 2nd edition. New York: Cold Spring Harbor Laboratory Press.

Sammak PJ, Borisy GG. 1988. Direct observation of microtubule dynamics in living cells. Nature 332(6166):724–726.

Schulze E, Kirschner M. 1988. New features of microtubule behaviour observed in vivo. Nature 334(6180):356–359.

Schuyler SC, Pellman D. 2001. Microtubule "plus-end-tracking proteins": The end is just the beginning. Cell 105(4):421–424.

Stringham E, Pujol N, Vandekerckhove J, Bogaert T. 2002. unc-53 controls longitudinal migration in *C. elegans*. Development 129(14):3367–3379.

Vaughan PS, Miura P, Henderson M, Byrne B, Vaughan KT. 2002. A role for regulated binding of p150(Glued) to microtubule plus ends in organelle transport. J Cell Biol 158(2):305–319.

Weisbrich A, Honnappa S, Jaussi R, Okhrimenko O, Frey D, Jelesarov I, Akhmanova A, Steinmetz MO. 2007. Structure-function relationship of CAP-Gly domains. Nat Struct Mol Biol 14(10): 959–967.

Wood JD, Landers JA, Bingley M, McDermott CJ, Thomas-McArthur V, Gleadall LJ, Shaw PJ, Cunliffe VT. 2006. The microtubule-severing protein Spastin is essential for axon outgrowth in the zebrafish embryo. Hum Mol Genet 15(18): 2763–2771.

Wu X, Kodama A, Fuchs E. 2008. ACF7 regulates cytoskeletal-focal adhesion dynamics and migration and has ATPase activity. Cell 135(1):137–48.

Zhou FQ, Zhou J, Dedhar S, Wu YH, Snider WD. 2004. NGF-induced axon growth is mediated by localized inactivation of GSK-3beta and functions of the microtubule plus end binding protein apc. Neuron 42(6):897–912.

Supplemental data

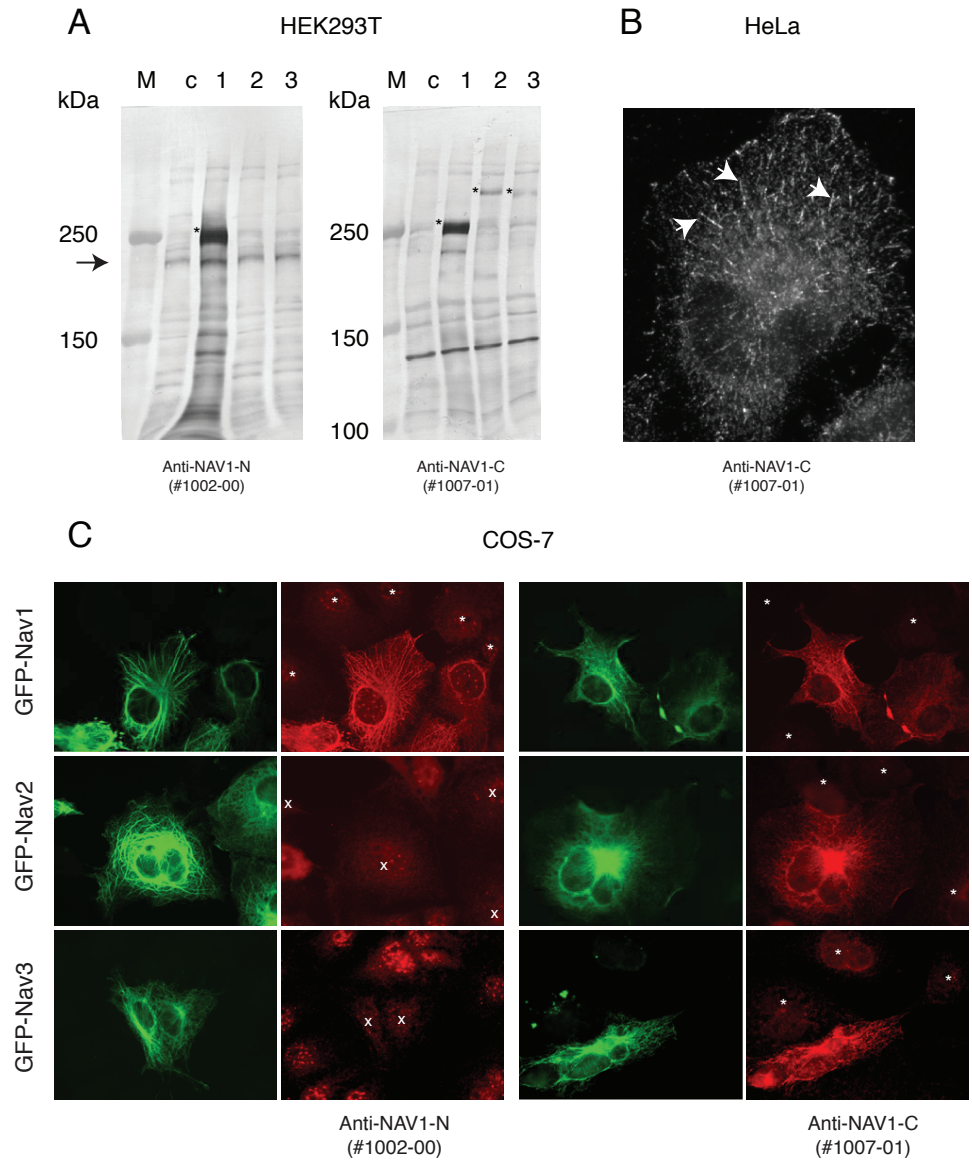

Figure S1. Characterization of antibodies against Navigator 1. See next page for the legend.

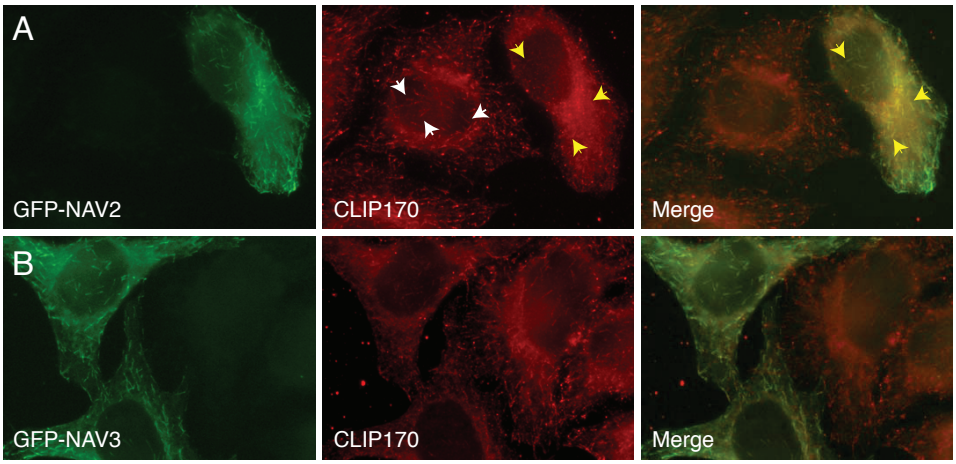

Figure S2. Navigator2 and -3 compete with CLIP-170 for binding at MT ends.
A, B) GFP-NAV2 (A) and GFP-NAV3 (B) expression affect CLIP-170 binding at MT ends. HeLa cells were transiently transfected with GFP-NAV2 or -3 (green signal). After one day cells were fixed and stained for CLIP170 (red signal). In nontransfected cells CLIP-170 localizes to MT ends (white arrows indicate clear examples of plus-end staining). In transfected cells CLIP-170 staining is much more diffuse, while both GFP-NAV2 and -3 clearly associate at MT ends (yellow arrowheads indicate examples of plus end staining).

Figure S1. Characterization of antibodies against Navigator 1.
A) Western blot analysis of #1002-00 and #1007-01 anti-Navigator antisera. GFPtagged Navigator1, -2, and -3 were expressed in HEK293T cells. As control (c) we used cells transfected with GFP only. Protein extracts of transiently transfected cells were incubated on western blot using #1002-00 and #1007-01 anti-Navigator antibodies. Molecular weight markers are indicated to the left (in kDa). The position of GFP-NAV1-3 is indicated by asterisks on the gels. The arrow points to a common protein found in all extracts, with the predicted size of NAV1. Note that both antibodies also crossreact with non-specific proteins.
B) Characterization of anti-NAV1-C (#1007-01) in cultured HeLa cells. An immunofluorescent analysis in fixed HeLa cells with antibody #1007-01 reveals staining of MT ends (clear examples are indicated by the arrows). Thus, a similar MTend staining pattern is obtained in HeLa cells using antibodies #1002-00 (see Figure 2C) and #1007-01.
C) Immunofluorescent characterization of of #1002-00 and #1007-01 anti-Navigator antisera. COS-7 cells were transfected with GFP-tagged NAV1, -2, or -3. Cells were fixed and stained with anti-NAV1-N (#1002-00) and anti-NAV1-C (#1007-01). GFP signal is in green, antibody signal is in red. In the red panels either transfected cells (x) or non-transfected cells (*) are indicated. Note that anti-NAV1-N (#1002-00) specifically recognizes GFP-NAV1 but not GFP-NAV2 or -3, despite their abundant overexpression (left panels). By contrast anti-NAV1-C (#1007-01) recognizes all three GFP-tagged fusion proteins (right hand panels).

Chapter 4

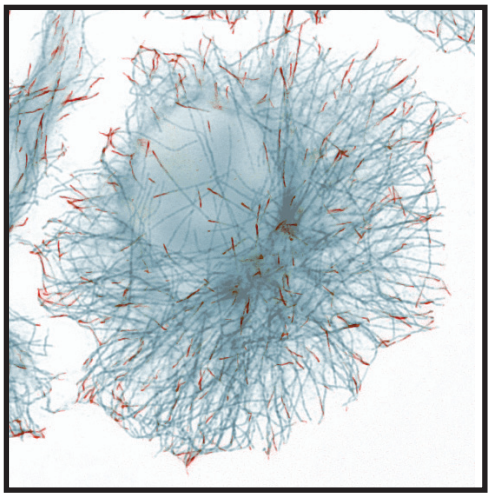

Navigators are EB-interacting proteins that link dynamic microtubules to the cortical actin network

Navigators are EB-interacting proteins that link dynamic microtubules to the cortical actin network

Jeffrey van Haren[1], Susana Montenegro Gouveia[1], Ilya Grigoriev[1], Anna Akhmanova[1], Frank Grosveld[1], Dieder Moechars[2], Pieter Peeters[2], Niels Galjart[1].

1) Department of Cell Biology and Genetics, Erasmus MC, P.O. Box 2040, 3000 CA Rotterdam, The Netherlands;
2) Johnson & Johnson Pharmaceutical Research and Development, Beerse, Belgium.

Running title: Navigators link the actin and microtubule networks.

Abstract

Mammalian Navigators (NAV1, -2, and -3) are homologues of the *C. elegans* UNC-53 protein, an ATPase involved in axon outgrowth and cell migration. Whereas UNC-53 has been implicated in the remodeling of the actin cytoskeleton, we have recently described that navigators are microtubule plus end tracking proteins (+TIPs) that influence the microtubule network. Here we show that navigators associate with the ends of growing microtubules via a direct interaction with EB-proteins. Navigators also localize to granular structures close to the ventral membrane of the cell. Dual-colour imaging studies demonstrate that Navigator-positive granules often align along actin tracks. They can capture EB3-positive microtubule ends and control microtubule dynamics. Treatment of cells with cytochalasin D, a well known actin depolymerizing agent, induces a complete redistribution of Navigators from microtubule ends to the actin cytoskeleton within 20 seconds. This relocalization is independent of actin depolymerization. The microtubule binding domain of NAV1 that is responsible for plus-end tracking also harbors the motif for association with actin filaments. Our data reveal a mechanism controlling Navigator localization and the link of dynamic microtubules to the cortical actin network.

Introduction

Three types of cytoskeletal elements exist in cells, i.e. actin, microtubules (MTs) and intermediate filaments (IFs). While IFs mainly provide strength, actin and MTs are used in widely different processes, including mitosis, cell migration, neuronal differentiation and transport of cargo. All three networks are built up of smaller subunits. The biochemical properties of the subunits and the filamentous networks are fairly well understood. The actin and MT cytoskeletal systems are polarized, allowing a cell to generate asymmetry, for example, by providing tracks for directed motor-mediated transport. By contrast, IFs are non-polar filaments. The dynamic behaviour and organization of actin, IFs and MTs are controlled by a large variety of proteins, most of which interact with only one, or at most two, of the networks. Plakins, cytoskeletal linker proteins interacting with IFs, actin and MT networks, form an intriguing exception to this rule (Karakesisoglou et al., 2000). One member of this family, ACF7, is an ATPase that uses its enzymatic activity to regulate dynamic interactions between networks, in order to sustain directional cell movement (Wu et al., 2008).

MTs are produced by the linear polymerization of α- and β-tubulin heterodimers into protofilaments. These assemble to form a hollow tube of 13 protofilaments. Tubulin subunits are preferentially incorporated at the MT plus end. MT assembly is intrinsically dynamic and MTs alternate between phases of growth, pause and shrinkage at their plus ends (Desai and Mitchison, 1997). Several MT-associated proteins (MAPs) link MTs to subcellular structures. A subclass of these proteins, the plus end-binding or -tracking proteins (+TIPs), associates specifically with the ends of growing MTs (Schuyler and Pellman, 2001). +TIPs have been shown to be important molecules in different organisms and cell systems (for review, see (Akhmanova and Steinmetz, 2008). *In vitro* experiments have revealed that the +TIPs EB1 and mal3p (the fission yeast homologue of EB1) autonomously recognize specific binding sites present at growing MT ends (Bieling et al., 2008; Bieling et al., 2007). CLIP-170, the prototype +TIP (Diamantopoulos et al., 1999; Perez et al., 1999), does not track by itself, but requires composite binding sites of end-accumulated EB1 and tyrosinated alpha-tubulin for tip-tracking (Bieling et al., 2007). Using fluorescence-based approaches in living cells, we have shown that both CLIP-170 and EB3 turn over rapidly on MT ends and that diffusion is rate limiting for their binding to MT plus ends (Dragestein et al., 2008). We also found that the ends of growing MTs contain a surplus of sites to which CLIP-170 binds with relatively low affinity. These cellular data correlate well with *in vitro* results. The current view is that the EB-proteins (EB1,

-2, and -3) are the conserved core components of MT ends, with which all other +TIPs interact, and that all +TIPs turn over rapidly at MT ends. Recent data suggest that EB-proteins themselves promote persistent MT growth (Komarova et al., 2009).

A subgroup of +TIPs, including the CLASPs (Akhmanova et al., 2001), APC (Etienne-Manneville and Hall, 2003), and ACF7 (Kodama et al., 2003), is able to selectively stabilize MTs, for example at the leading edge of motile cells, by associating with the MT lattice on segments near MT ends. These proteins act as linkers between MT ends and specific subcellular structures, such as focal adhesions. This selective capture of MTs often occurs after the activation of an upstream signaling molecule, for example, after activation of members of the Rho-family of small GTPases (Gundersen et al., 2004). It has been hypothesized that the MT-stabilizing activity of APC (Wen et al., 2004) and CLASPs (Mimori-Kiyosue et al., 2005) requires *in situ* binding of these +TIPs to EB1.

The protein product of the *C. elegans unc-53* gene has been linked to the migration and outgrowth of muscles, axons and excretory canals (Stringham et al., 2002). In mammals three UNC-53 homologues have been described, called Neuron Navigator1, -2, and -3 (Maes et al., 2002). Navigator proteins belong to the family of AAA+ ATPases (ATPases associated with diverse cellular activities) (Frickey and Lupas, 2004). In addition, NAV1 was shown to bind MTs and to accumulate at MT ends (Martinez-Lopez et al., 2005), while NAV2 was shown to bind MTs and localize to IFs (Muley et al., 2008). A recent report has linked UNC-53 to the actin network via the Arp2/3 complex (Schmidt et al., 2009). We have recently demonstrated that all three navigators are +TIPs involved in reorganization of the MT cytoskeleton (van Haren et al., 2009). Here, we show that navigators depend on EB-proteins for plus end tracking *in vivo* and *in vitro*. In living cells navigators localize to granular structures that often align along actin tracks and that can capture EB3-coated dynamic MTs. Our data further reveal an actin binding motif in all three Navigators, which can be rapidly activated by the addition of the fungal toxin cytochalasin D. Our data indicate that Navigators interact with both the actin and MT network. Thus, similar to ACF7 (Wu et al., 2008), Navigators couple ATPase activity to a localization to all three cytoskeletal networks.

Results

MT plus-end localization of the navigators depends on EB-proteins.

We have recently shown that all three mammalian Navigator proteins are +TIPs (van Haren et al., 2009). To examine whether this distribution depends on EB-proteins, we stained HeLa cells transfected with GFP-tagged NAV1, -2, or -3 with anti-EB1 antiserum. For all three Navigators we detected strong colocalization with EB1 at MT ends (Figure 1A, B, and data not shown). Quantification of fluorescent signals shows that EB1 and Nav1 colocalize at MT ends, but EB1 is relatively brighter at the outer most end, when compared to Nav1 (Figure 1C). Similar staining patterns have previously been described for other +TIPs (Komarova et al., 2005; Wittmann and Waterman-Storer, 2005). Knockdown of EB1 using a siRNA-mediated approach significantly diminished GFP-NAV1 localization at MT ends in cells that also displayed reduced EB1 staining (Figure 1D, E). Similar results were found for all GFP-tagged Navigators (data not shown). By contrast, knockdown of NAV1 in HeLa cells did not abrogate the MT end localization of EB1 (data not shown) or p150glued (Figure 1F), a protein that depends on EB1 and CLIP-170 for its MT end localization (Lansbergen et al., 2004). We conclude that the accumulation of NAV1 at MT ends depends on EB1 but not vice versa.

In Navigator-overexpressing cells CLIP-170 and p150glued are displaced from MT ends and instead a diffuse cytoplasmic signal is observed for these proteins (van Haren et al., 2009) (see also Figure S1). These results suggest that CLIPs and Navigators have overlapping binding sites on MTs. By contrast, in NAV1 overexpressing cells, EB1 is attracted to Navigator-positive structures (Figure 1G). These results indicate that Navigators can bind to EB1 and MTs simultaneously. When Navigators are present in excess they are able to dominantly alter EB1 distribution.

All +TIPs described to date have been shown to interact with EB-proteins. There is no a priori reason to suspect why Navigators would not show such an interaction. Indeed, a mass spectrometry analysis of HeLa proteins copurifying with GST-tagged EB1 revealed NAV1 as one of the top scoring EB1-interacting candidates (S.M.G. and A.A., unpublished results). Pull down assays using lysates of cells transfected with GFP-NAV1, -2, or -3, revealed that all three proteins interact with GST-EB1 and not with a control GST-tagged protein (Figure S2B). We therefore set out to examine which domain of the Navigators is responsible for EB1 binding and plus-end tracking. A MT binding (MTB) domain has been previously identified in NAV1 (Martinez-Lopez et al., 2005). We fused this MTB domain to a GFP-tag and

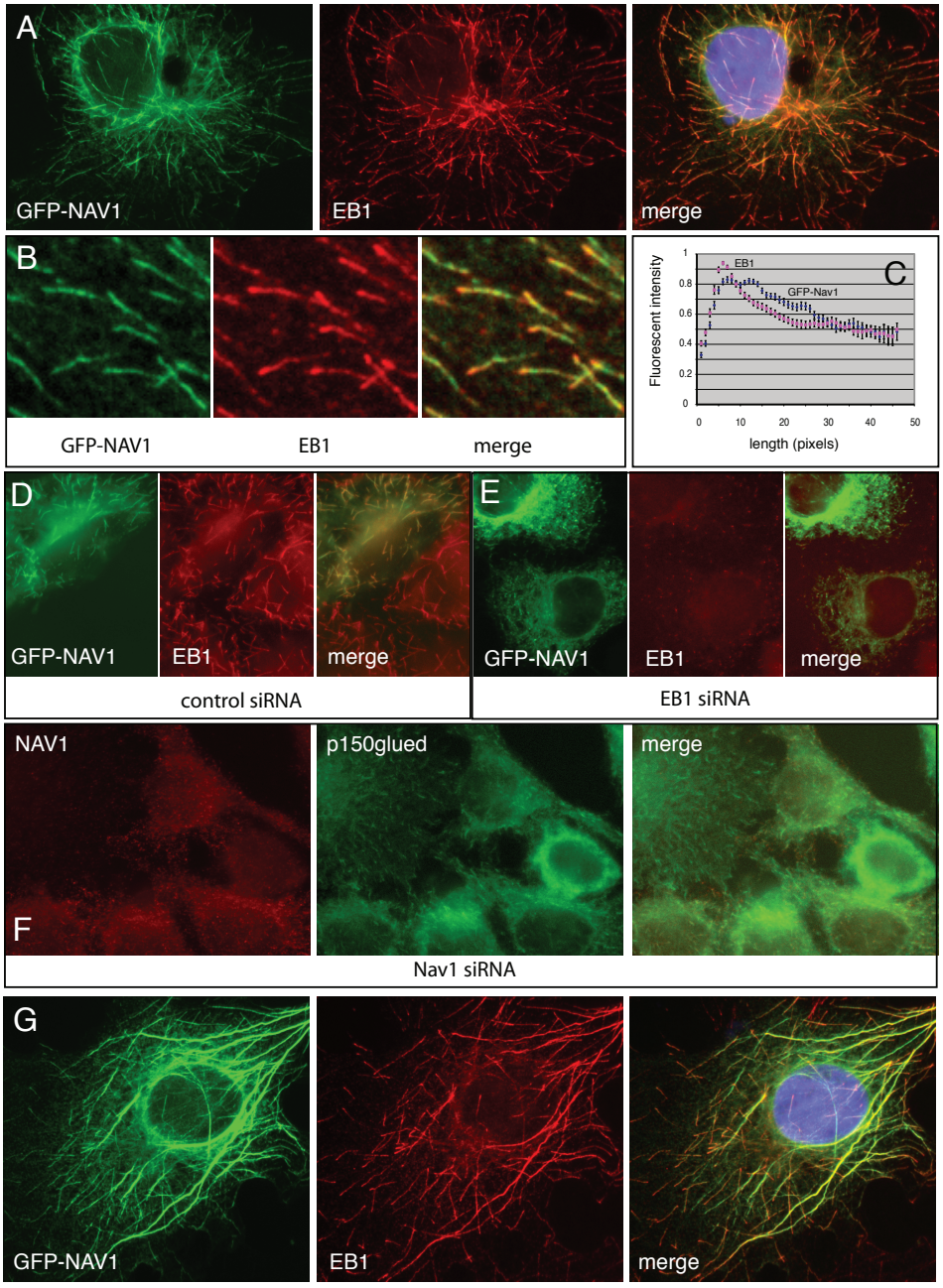

Figure 1. Navigator localization at microtubule ends depends on EB1. Legend on the next page.

Figure 1. Navigator localization at microtubule ends depends on EB1

A-C) GFP-Nav1 colocalization with EB1. HeLa cells stably expressing GFP-NAV1 (green) were fixed and stained with an antiserum against EB1 (red). Colocalization between the two +TIPs is observed and is quantified in panel C.

D, E) EB1 knockdown influences NAV1 localization. HeLa cells stably expressing GFP-NAV1 (green) were transfected with siRNAs against EB1, or a control oligo. After 3 days cells were fixed and stained with a mouse monoclonal antibody against EB1 (red).

F) NAV1 knockdown does not influence the localization of other +TIPs at MT ends. HeLa cells were transfected with a siRNA against NAV1. After 3 days cells were fixed and stained with a rabbit antiserum against NAV1 (red) and a mouse monoclonal antibody against p150glued (green).

G) GFP-NAV1 bundles colocalize with EB1. HeLa cells were transfected with GFP-NAV1 (green). Cells were fixed after 24 hours and stained with an antiserum against EB1 (red). When GFP-NAV1 is overexpressed it causes bundling of MTs. EB1 is attracted to the bundles, whereas CLIPs are not.

expressed it in HeLa cells. This fragment showed weak plus-end tracking in vivo at low expression levels, and MT bundling at high levels (data not shown). Using lysates of HEK293T cells transiently expressing the MTB domain or the C-terminal half of NAV1, we were able to show an interaction between this domain and all three EB-proteins fused to GST in an in vitro binding assay (Figure S2C). We then generated His-tagged fusions of this MTB domain (called F1) and smaller fragments of this domain, F2 and F3 (Figure 2A). These fragments were purified and used for several in vitro binding assays. Both the complete MTB domain and His-tagged MTB-F2 bound efficiently to GST-EB1 but his-MTB-F3 did not (Figure 2A, B).

We subsequently tagged MTB-F2 with a 6xhis-GFP tag, after which we purified this His-GFP-MTB-F2 fragment to near homogeneity using Ni-NTA beads (Figure 2C). In an *in vitro* MT plus-end tracking assay (Bieling et al., 2007) using purified tubulin, EB1 and His-GFP-MTB-F2, this domain of NAV1 was able to track MT ends, but only in the presence of unlabelled EB1 (Figure 2D) and not autonomously (data not shown). Our data show that the MTB-F2 domain of NAV1 interacts directly with EB1 and that it is able to track MT ends *in vitro*.

Navigator-positive granules at the ventral cortex.

We noted that the localization of GFP-tagged Navigators in HeLa cells differs significantly depending on which part of the cell is imaged (Figure 3 and data not shown). In the middle and top of the cell a prominent association with the ends of growing MTs is observed (Figure 3A), whereas at the bottom of the same cell labeling is granular (Figure 3B) and quite static as compared to MT end labeled GFP-NAV1 (Movie 1). The lifetime of Navigator granules is in the order of minutes (data

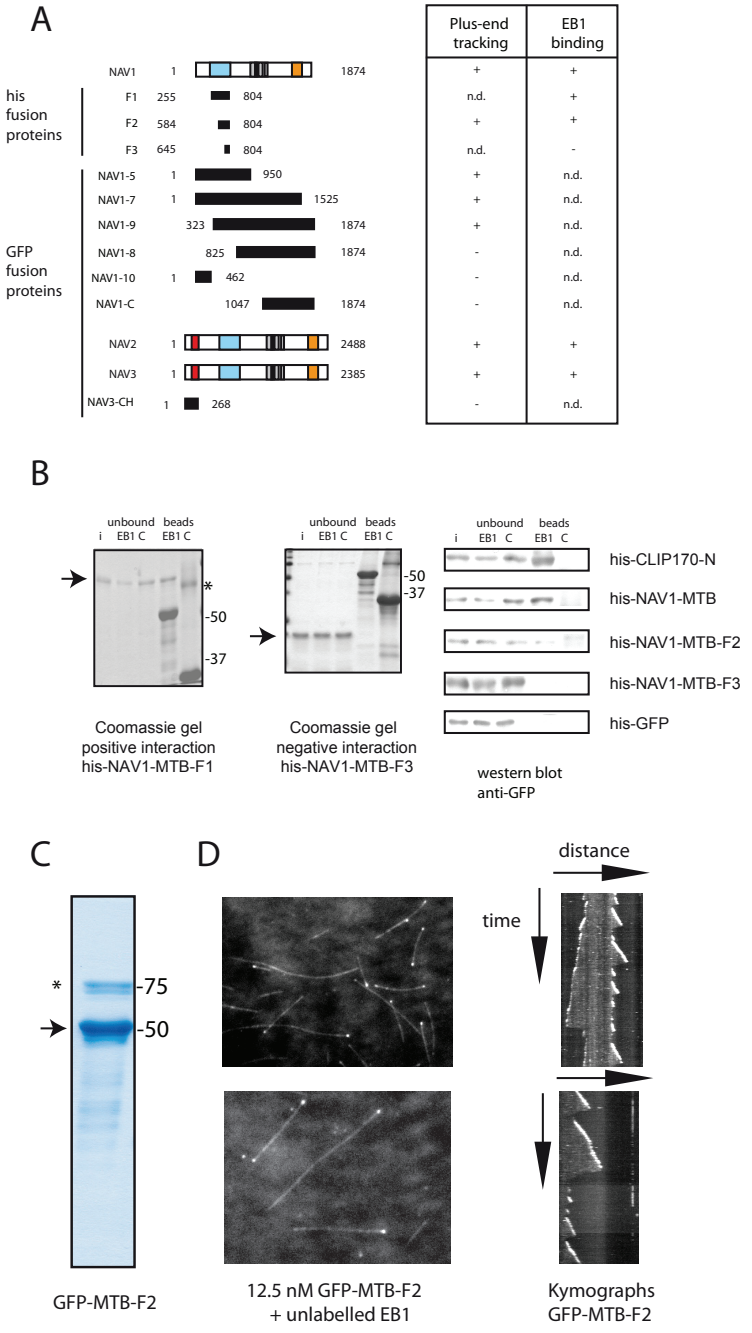

Figure 2. Analysis of MT plus-end tracking behaviour of navigator proteins

A) Structure and properties of Navigator proteins and mutants. The domain architecture of full length NAV1, -2, and -3 is depicted in the left hand panel. Amino acid numbers are indicated. MT-binding domain

(blue), ATPase domain (orange), calponin homology domain (red), and potential coiled-coil domains (grey) are indicated. His-tagged and GFP-tagged fusion proteins are indicated below the corresponding navigator proteins. The ability of the different mutants to track MT plus ends *in vitro* or *in vivo*, and their ability to bind to EB1, is indicated to the right. N.D stands for "not determined".

B) In vitro binding assays. His-tagged fusion proteins depicted in panel A were incubated with GST-EB1 and a GST-tagged control protein (GST D2.1) coupled to glutathione beads. After incubation, the supernatant (the unbound fraction) was removed. Beads were washed and bound proteins were eluted from the beads by boiling. Proteins were resolved by SDS-PAGE, and His-tagged proteins were directly visualized by Coomassie Brilliant Blue (the two panels on the left show a positive interaction, his-NAV1-MTB-F1 and a negative interaction, his-NAV1-MTB-F3, see arrows) as well as by western blot using anti-his antiserum. Loading from left to right: I: input (loaded 1/60th), unbound fractions of his-fusions after incubation with GST-EB1 or control beads (loaded 1/60th), and the bound fractions (loaded 1/20th). The asterisk (*) marks a background protein copurifying with GST-D2.1.

C) Purification of his-GFP-MTB2-F2. The MTB-F2 domain of NAV1 was expressed as a his-GFP fusion protein in Rosetta (DE3) pLysS E.coli and purified using Ni-NTA beads (Qiagen). The asterisk (*) marks two background proteins of around 75 kDa.

D) In vitro MT plus-end tracking assay. TIRF microscopy of 12.5 nM his-GFP-MTB-F2 (green) on dynamic MTs in the presence of 50nM unlabelled EB1. Images of MTs labeled with his-GFP-MTB-F2 are shown to the left, and examples of corresponding kymographs (space-time plots) are shown to the right.

not shown). Other cell types also show these Navigator-positive granules (data not shown) although in HeLa cells the phenomenon is most pronounced. GFP-tagged NAV2 also localizes to similar granules, while GFP-NAV3 can not be detected (data not shown). It should be noted that the granules are more difficult to show with antibodies, perhaps because of the fixation conditions (data not shown). In many instances the granular GFP-NAV1 signal is aligned in tracks (Figure 3C, arrows). Kymograph analysis indicates that "dynamic" MT-end-associated GFP-NAV1 can convert into granular GFP-NAV1 (Figure 3D).

To examine the localization and behaviour of NAV1-positive granules in more detail, as well as the influence of MTs and EB-proteins, we performed dual-colour TIRF microscopy in HeLa cells transfected with GFP-NAV1 and EB3-mCherry. The results show that NAV1-granules are indeed located at the bottom of the cell, close to the ventral membrane (Figure 3E, see also Movie 2). Kymograph analysis (Figure 3F) reveals 4 types of GFP-NAV1 granules: single-positive granules formed by growing EB3 positive MT ends (1), GFP-NAV1- and EB3-mCherry-double-positive granules formed by growing MTs (2), pre-existing granules (not formed by a passing MT end) with a dynamically changing EB3 and NAV1 signal (3), and highly static GFP-NAV1-positive granules with no apparent relationship to EB3-mCherry (4). Strikingly, NAV1-positive granules can capture EB3-mCherry MT ends, giving rise to oscillatory EB3-mCherry movements. These results indicate that upon contact

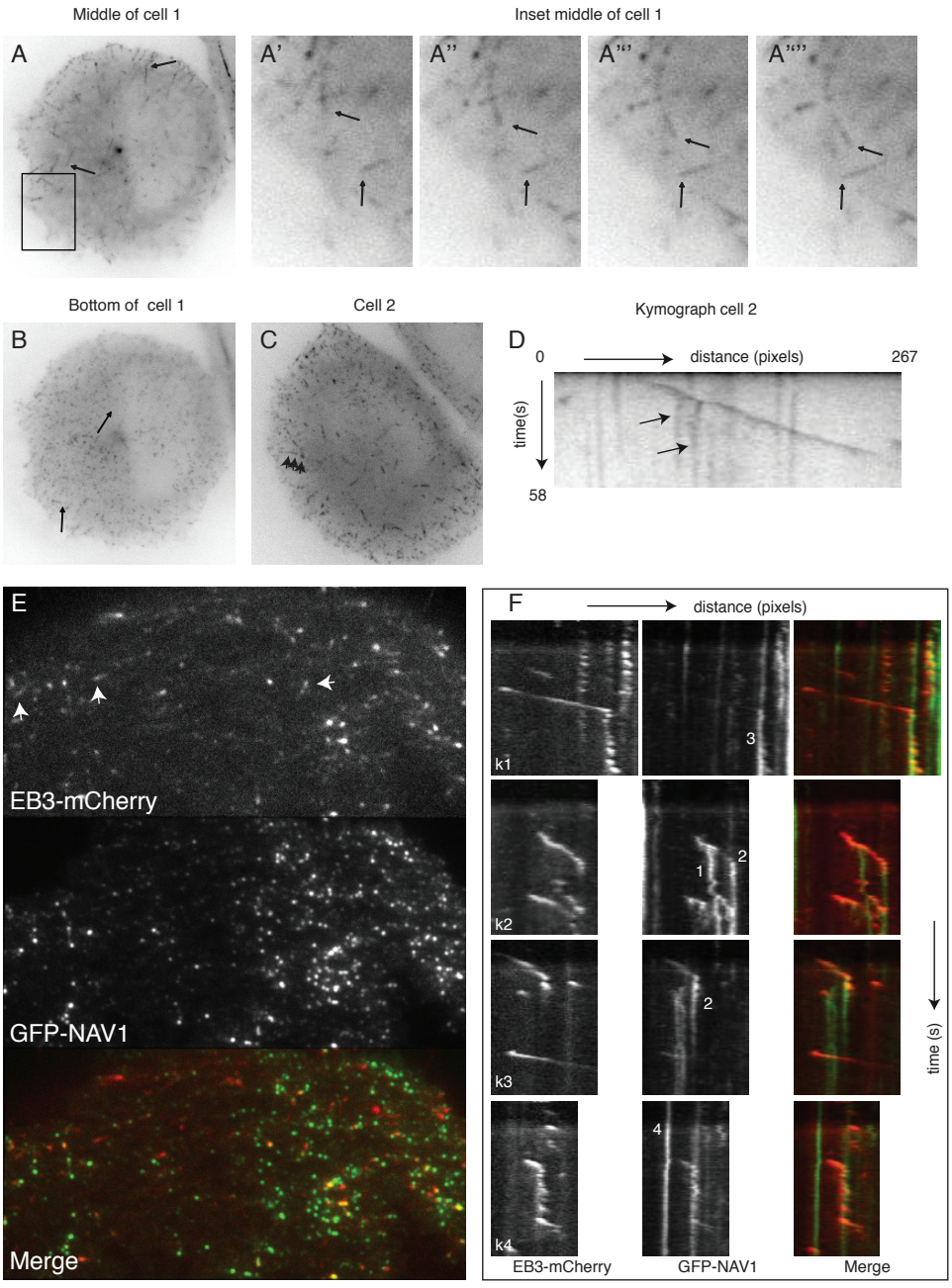

Figure 3. NAV1 localizes to MT ends and to foci near the membrane. Legend on the next page.

Figure 3. NAV1 localizes to MT ends and to foci near the membrane
A-D) Time-lapse recording of GFP-NAV1 in HeLa cells. Imaging was performed on a wide-field microscope (1 fps, see Movie 1). In panel A an image of the middle part of a cell is shown, whereas in panel B the bottom of the same cell is shown. In panel C the bottom of another cell is shown. Panels A'-A''' show enlarged subsequent still images of the inset in A. MT ends decorated with GFP-NAV1 are seen in A (clear examples are indicated with arrows). GFP-NAV1 also localizes to the centrosome. In B, C granular staining is more prominent. In panel D a kymograph is depicted with diagonal signal representing GFP-NAV1 on the ends of growing MTs and the vertical signal representing static granules. Arrows indicate examples of granules that appeared as the MT passed by.
E, F) TIRF microscopy of GFP-NAV1 and EB3-mCherry in transfected cells. HeLa cells were co-transfected with GFP-NAV1 (green) and EB3-mCherry (red). After 24 hours cells were imaged with a TIRF microscope equipped with a dual view system. The merge (or overlay) of the two signals is shown in the bottom panel in E. In F several kymographs are shown, depicting common behaviour of GFP-NAV1 and EB3-mCherry. Numbers correspond to the different types of granules observed (for details see main text).

of the end of a dynamic EB3-mCherry-coated MT with a NAV1-positive granule the MT may become temporarily stabilized near the end, perhaps by mediating rescue. Thus, NAV1 can temporarily capture MTs near the ventral cortex of cells.

Navigator-positive granules are linked to the cortical actin network
High resolution time-lapse imaging of NAV1-positive granules in HeLa cells shows that granules can appear and disappear but that the majority of these structures remain stationary (Movies 1, 2). Some granules undergo fast displacements, suggesting motor-mediated movement. Imaging with longer time intervals reveals that the majority of granules move when cells stretch (data not shown). Even after nocodazole treatment (10 μM) (which causes depolymerization of the MT network) for 1 hr, the granules remain stationary, and move when cells stretch (Movie 3). These results suggest that NAV1-positive granules are somehow linked to the ventral plasma membrane. Interestingly, when cells were treated for 1 hr with 10 μM cytochalasin D, which depolymerizes the actin network, we observed clustering of NAV1 granules, suggesting that these structures are linked to the cortical actin network. To examine whether NAV1-positive granules in untreated cells colocalize with filamentous actin we performed dual-colour TIRF imaging using GFP-NAV1 and Lifeact-mCherry, which labels the entire F-actin network. We observed partial alignment of granules on the cortical actin network (Figure 4A, see also Movie 4). Combined the data indicate that NAV1-positive granules are directly or indirectly linked to the cortical actin network.

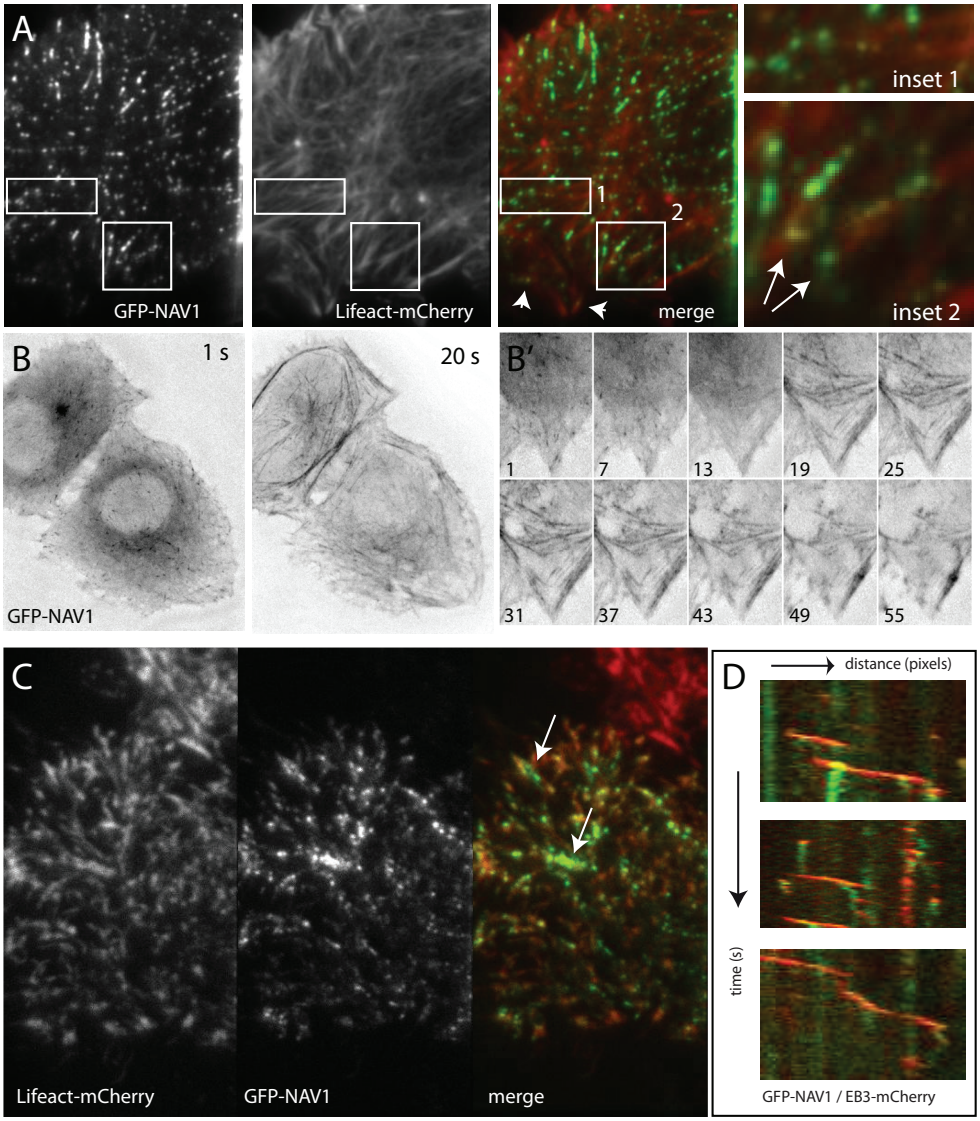

Figure 4. Reversible localization of NAV1 to MT ends and the actin network

A, C) TIRF microscopy of GFP-NAV1 and Lifeact-mCherry. HeLa cells were co-transfected with GFP-NAV1 (green) and Lifeact-mCherry (red), a marker for filamentous actin. After 24 hours cells were imaged with a TIRF microscope equipped with a dual view system. Merged images of the two signals are shown on the right. GFP-NAV1 can colocalize with the actin network, forming granules that align with actin filaments (arrows in inset 2).

B, B') Fast relocalization of GFP-NAV1. HeLa cells expressing GFP-NAV1 were imaged with a wide field microscope and then treated with cytochalasin D. A fast relocalization (within 20 seconds) from MT ends (left panel) to actin stress fibers (right panel) is observed. In B' still images of a time lapse analysis of

GFP-NAV1 is shown. Numbers indicate frames (1 frame per 3 seconds). Cytochalasin D was added at frame 10 (30 s) to a final concentration of 10 μM (localization of GFP-NAV1 at the actin network is clearly visible at frame 19 (57 s).
D) TIRF microscopy of GFP-NAV1 and EB3-mCherry. HeLa cells were co-transfected with GFP-NAV1 (green) and EB3-mCherry (red) and cells were treated with 10 μM cytochalasin D for approximately one hour. At this time point GFP-NAV1 is found on MT ends again because the actin network is almost completely gone.

Navigators contain actin binding modules that can be specifically activated

To investigate further the link between Navigators and the actin network we decided to perturbe actin dynamics during time lapse imaging of GFP-NAV1 using cytochalasin D (which binds actin filaments and prevents elongation at the fast growing (or barbed) end) and latrunculin A (which binds actin monomers thereby preventing polymerization). It should be noted that after incubating cells with 10 μM cytochalasin D or 0.5 μM latrunculin A for 5 minutes, many actin filaments can still be found in most cells (see Figure S3C, D, E).

Strikingly, addition of cytochalasin D (10 μM) induced an almost immediate relocalization of GFP-NAV1, from MT ends to the actin network (Figure 4B, B', Figure S3A). NAV2 and -3 also relocalize after cytochalasin D treatment (data not shown), but not their interaction partner EB1 (Figure S1C). Interestingly, latrunculin A does not induce such a redistribution of Navigator proteins (Figure S3B). However, latrunculin A treatment followed by cytochalasin D does induce the relocalization of Navigators to the remaining actin stress fibers (Figure S3D-E') showing that it is not the depolymerization of the actin network itself that causes redistribution of Navigators after cytochalasin D treatment. It should be noted that it has been reported that cytochalasin D induces several side effects besides actin depolymerization, such as Rho activation and tyrosine phosphorylation of proteins.

After 5 minutes of incubation with cytochalasin D, NAV1-positive granules are not significantly affected in number and still colocalize with the remaining actin network (Figure 4C, Movies 5, 6). Interestingly, as the actin network continues to depolymerize, Navigator localization to MT plus-ends is restored, and we frequently observed the formation of NAV1 granules at these plus-ends (Figure 4D).

Combined, the data indicate that cytochalasin D treatment activates an actin binding motif in Navigator proteins, which causes their redistribution from MT ends to the actin network. Concomitantly, the EB-Navigator interaction is disrupted, because EB proteins continue to accumulate on MT plus-ends. Strikingly, upon redistribution of the Navigators to actin filaments, p150glued associates with microtubule ends

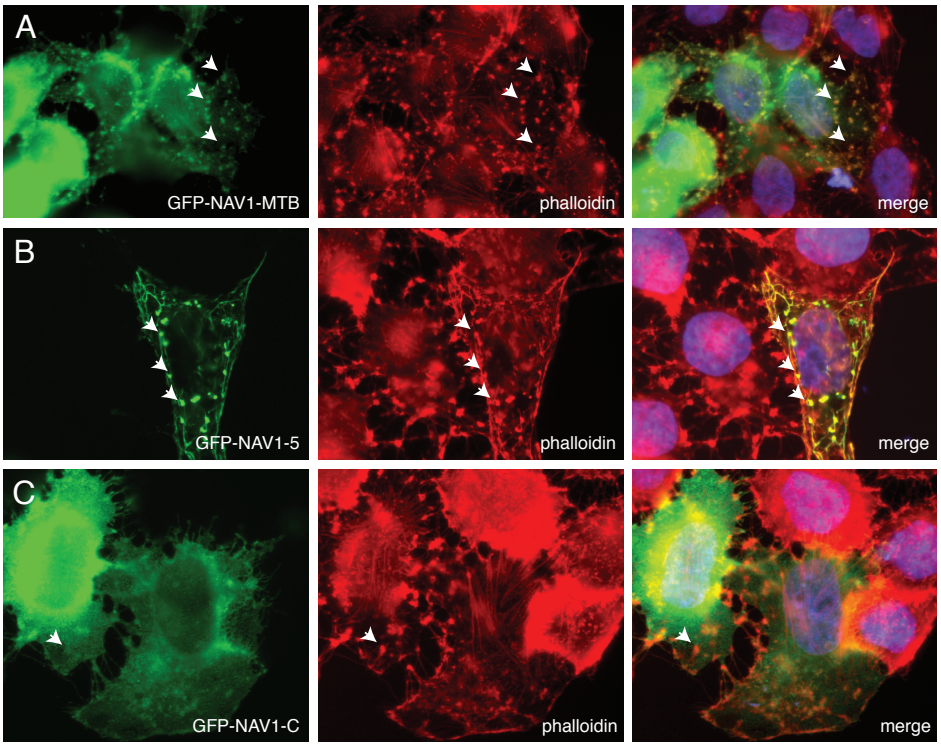

Figure 5. MTB domain harbors an actin relocalization motif
A-C) Immunofluorescent analysis of cytochalasin D-treated cells. HeLa cells were transfected with different GFP-tagged NAV1 mutants (green). Cells were treated with cytochalasin D and subsequently fixed and stained with phalloidin (red). Examples of mutants that do (GFP-NAV1-MTB and GFP-NAV1-5) and mutants that do not (GFP-NAV1-C) relocalize significantly to the actin network are shown.

again (Figure S1B), supporting the hypothesis that p150glued and Navigators have overlapping binding sites at microtubule ends.

To determine which domain of NAV1 is responsible for the cytochalasin D-mediated localization to the actin network we transfected HeLa cells with the deletion mutants depicted in Figure 2A, treated these cells with cytochalasin D, and stained with phalloidin. Interestingly, the MTB domain of NAV1 strongly colocalizes with phalloidin positive structures (Figure 5B), whereas other domains do not (Figure 5C and data not shown). Thus, NAV1 harbors a domain that can localize to two cytoskeletal networks.

Discussion

It has been clearly established that UNC-53 is involved in axon outgrowth and the migration of specific cell types (Stringham et al., 2002). However, the mode of action of this protein and its mammalian homologues remains unclear. Recent data link UNC-53 to the actin network through binding of Abi-1 (Schmidt et al., 2009). Others, including us (Martinez-Lopez et al., 2005; van Haren et al., 2009), have described a link between Navigators and the MT network. Here we show that Navigator proteins actually localize to both the actin and MT network and that these proteins can quickly relocalize between actin and MT ends. These data indicate that Navigators organize both cytoskeletal networks. The precise function of Navigators can only be uncovered once substrates of the ATPase activities are known. Nevertheless, Navigators share an interesting number of properties with spektraplakins such as ACF7, such as actin binding, MT plus-end tracking and ATPase activity (Wu et al., 2008).

The MTB domain of NAV1 was delineated earlier (Martinez-Lopez et al., 2005). We have found that this domain also harbors the module that interacts directly with EB1. The same domain (MTB-F2) tracks MT ends *in vitro* in the presence of EB1. It has been shown that an IP-di-peptide in APC is critical for its interaction with EB1 (Honnappa et al., 2005). The domain of CLASPs that interacts with EB1 (Mimori-Kiyosue et al., 2005) also contains such IP-residues (Galjart, 2005). Other EB-interacting proteins also harbor an IP-di-peptide (Akhmanova and Steinmetz, 2008). Interestingly, the MTB domain of NAV1 also contains an IP-di-peptide, which is conserved in NAV2 and -3. It is likely that this forms the core EB1-interaction motif.

The NAV1 MTB domain also harbours the motif that is responsible for an interaction with the actin network. Future research will be aimed at dissecting the exact residues important for the latter interaction. Relocalization to the actin network depends on treatment of cells with cytochalasin D. It is not dependent on depolymerization of the actin network because treatment with latrunculin does not elicit a switch. Our data suggest that binding of the Navigators to f-actin and EB1 is mutually exclusive. This is logical: if Navigators would bind actin and EB1 simultaneously, they would attract EB1 to the actin network and thereby cause significant effects on the MT network. It is worthwhile noting that the formin mDia2 binds EB1 and MTs with its F1H2 domain, a core actin binding region (Bartolini et al., 2008). The F1H2 domain also contains an IP-di-peptide.

Based on overexpression studies, we have suggested that Navigator binding sites on MT ends overlap with those of the CLIPs (van Haren et al., 2009). Our present results with cytochalasin D are consistent with this hypothesis, as the

relocalization of overexpressed NAV1 and -2 to the actin network allows (re-)binding of CLIPs to MT ends.

We show in HeLa cells that NAV1 localizes to MT plus ends and to granular structures that are evenly distributed over the ventral membrane of the cell. This asymmetric localization differs from that of +TIPs such as CLASPs that accumulate at the edge of the cell (Mimori-Kiyosue et al., 2005). Such a polarized distribution may play an important role in cellular migration or outgrowth, both processes to which Navigators have been linked in mammals and in *C. elegans*. We are currently investigating Navigator mediated actin- microtubule crosstalk in such cellular processes.

In conclusion, Navigators can associate with MT-ends and with the F-actin network. Furthermore they influence MT dynamics via granules that are linked to the cortical actin network.

Materials and Methods

Constructs and antibodies

NAV1-derived mutants were made by using appropriate restriction enzyme sites or by using PCR. Amino acids present in the different mutants (and the mutant proteins themselves) are depicted in Figure 2. cDNAs were cloned into the pGEX (GE Healthcare), pET28a (EMD biosciences), pEGFP-C1,2,3 (Invitrogen), or pbio-EGFP-C3 vectors. In the Lifeact construct (Riedl et al., 2008) the EGFP was exchanged for mCherry (kind gift of Dr. G. Montagnac and P. Chavrier).

NAV1-MTB (F1): Have used the following primers for amplifying the MTB domain: Forward primer Nav-1: TCTTAGATCTCATATGGAGTCCCAGAGAAAGAGG, Reverse primer Nav-1: TCTTGTCGACCTACTTGTCAAGA TTGGCTAG. The resulting fragment was ligated into the NdeI/SalI sites of pET28a, and the BglII/SalI sites for ligation into pbioEGFP-C1.

His-NAV1-MTB-F2, the following primers were used to amplify the F2 fragment, which was subsequently ligated into pET28a: Forward primer (NdeI): TCTTAG ATCTCATATGGACCGCCTGAGTGATGCTAAG, Reverse primer (SalI): TCTTG TCGACCTACTTGTCAAGATTGGCTAG. His-NAV1-MTB-F3, the following primers were used to amplify the F3 fragment, which was subsequently ligated into pET28a: Forward primer (NdeI site): CTTAGATCTCATATGCGCAAGACTAG CTTAGATGT, Reverse primer (SalI site): TCTTGTCGACCTACTTGTCAAGATT GGCTAG. His-GFP-NAV1-F2 was generated by ligating GFP into the NdeI site of His-NAV1-MTB-F2. All bioGFP NAV1,2,3 fragments were cloned into pbioEGFP plasmids, NAV1-5: KpnI and ApaLI sites were used, NAV1-7: AseI and SalI were used, NAV1-9: SacII/MluI fragment ligated into SacII/MluI sites of pbioEGFP-C3, NAV1-8: BglII/MluI fragment ligated into BglII/MluI sites of pbioEGFP-C3, NAV1-10: pbioGFP-NAV1 was digested with Eco47III and SpeI (blunted) fragment including the vector backbone was gel-extracted and re-ligated, NAV1-C: pbioGFP-Nav1 was cut with BamHI and BglII and the large fragment resulting from this was re-ligated, this results in a bioGFP fusion with the C-terminal part, NAV3-CH: AseI-SwaI fragment of bioNAV3 was cloned into AseI-SmaI sites of pbio-EGFP.

In vitro plus-end tracking assay.

The plus-end tracking assay was carried out as described before (Komarova et al., 2009). The concentration of purified His-GFP-NAV1-F2 used was 12.5 nM, and unlabelled purified EB1 was used at a concentration of 50 nM.

Pull downs.

Pull down experiments using cell extracts, were carried out as described before (van Haren et al., 2009). In vitro binding assays were carried out as described previously (Lansbergen et al., 2004), using purified GST-EB1, 2, and 3 and GST only or GST-D2.1 as a control (GST fused to the zinc-finger domains of Zfp-37). Various his-fusions were used, which were expressed in Rosetta (DE3) pLysS E.coli (EMDbiosciences), and purified using Ni-NTA beads (Qiagen). Protein concentrations were determined using the BCA Protein Assay (Pierce). Purified GST fusions coupled to Glutathione beads 4b (GE Healthcare) were incubated with purified his-fusions of NAV1 (or CLIP170 or GFP as positive and negative controls).

Expression in mammalian cells

HeLa and HEK293T cells were grown as described (Drabek et al., 2006). For immunofluorescence experiments cells were transfected using Fugene 6 (Roche), or Metafectene Pro (Biontex), at a confluency of approximately 30%. In some experiments nocodazole (10 µM) was added for 30-60 minutes prior to analysis. In other experiments cytochalasin D (Sigma Aldrich) at a concentration of 10 µM, was added prior to or during imaging. In other experiments latrunculin A (Sigma Aldrich) (100 µg/ml stock) was used at a concentration of 0.5 µM.

References

Akhmanova, A., C.C. Hoogenraad, K. Drabek, T. Stepanova, B. Dortland, T. Verkerk, W. Vermeulen, B.M. Burgering, C.I. De Zeeuw, F. Grosveld, and N. Galjart. 2001. Clasps are CLIP-115 and -170 associating proteins involved in the regional regulation of microtubule dynamics in motile fibroblasts. *Cell*. 104:923-35.

Akhmanova, A., and M.O. Steinmetz. 2008. Tracking the ends: a dynamic protein network controls the fate of microtubule tips. *Nat Rev Mol Cell Biol*. 9:309-22.

Bartolini, F., J.B. Moseley, J. Schmoranzer, L. Cassimeris, B.L. Goode, and G.G. Gundersen. 2008. The formin mDia2 stabilizes microtubules independently of its actin nucleation activity. *J Cell Biol*. 181:523-36.

Bieling, P., S. Kandels-Lewis, I.A. Telley, J. van Dijk, C. Janke, and T. Surrey. 2008. CLIP-170 tracks growing microtubule ends by dynamically recognizing composite EB1/tubulin-binding sites. *J Cell Biol*. 183:1223-33.

Bieling, P., L. Laan, H. Schek, E.L. Munteanu, L. Sandblad, M. Dogterom, D. Brunner, and T. Surrey. 2007. Reconstitution of a microtubule plus-end tracking system in vitro. *Nature*. 450:1100-5.

Desai, A., and T.J. Mitchison. 1997. Microtubule polymerization dynamics. *Annu Rev Cell Dev Biol*. 13:83-117.

Diamantopoulos, G.S., F. Perez, H.V. Goodson, G. Batelier, R. Melki, T.E. Kreis, and J.E. Rickard. 1999. Dynamic localization of CLIP-170 to microtubule plus ends is coupled to microtubule assembly. *J Cell Biol*. 144:99-112.

Drabek, K., M. van Ham, T. Stepanova, K. Draegestein, R. van Horssen, C.L. Sayas, A. Akhmanova, T. Ten Hagen, R. Smits, R. Fodde, F. Grosveld, and N. Galjart. 2006. Role of CLASP2 in Microtubule Stabilization and the Regulation of Persistent Motility. *Curr Biol*. 16:2259-64.

Dragestein, K.A., W.A. van Cappellen, J. van Haren, G.D. Tsibidis, A. Akhmanova, T.A. Knoch, F. Grosveld, and N. Galjart. 2008. Dynamic behavior of GFP-CLIP-170 reveals fast protein turnover on microtubule plus ends. *J Cell Biol*. 180:729-37.

Etienne-Manneville, S., and A. Hall. 2003. Cdc42 regulates GSK-3beta and adenomatous polyposis coli to control cell polarity. *Nature*. 421:753-6.

Frickey, T., and A.N. Lupas. 2004. Phylogenetic analysis of AAA proteins. *J Struct Biol*. 146:2-10.

Galjart, N. 2005. CLIPs and CLASPs and cellular dynamics. *Nat Rev Mol Cell Biol*. 6:487-98.

Gundersen, G.G., E.R. Gomes, and Y. Wen. 2004. Cortical control of microtubule stability and polarization. *Curr Opin Cell Biol*. 16:106-12.

Honnappa, S., C.M. John, D. Kostrewa, F.K. Winkler, and M.O. Steinmetz. 2005. Structural insights into the EB1-APC interaction. *Embo J*. 24:261-9.

Karakesisoglou, I., Y. Yang, and E. Fuchs. 2000. An epidermal plakin that integrates actin and microtubule networks at cellular junctions. *J Cell Biol*. 149:195-208.

Kodama, A., I. Karakesisoglou, E. Wong, A. Vaezi, and E. Fuchs. 2003. ACF7: an essential integrator of microtubule dynamics. *Cell*. 115:343-54.

Komarova, Y., C.O. De Groot, I. Grigoriev, S.M. Gouveia, E.L. Munteanu, J.M. Schober, S. Honnappa, R.M. Buey, C.C. Hoogenraad, M. Dogterom, G.G. Borisy, M.O. Steinmetz, and A. Akhmanova. 2009. Mammalian end binding proteins control persistent microtubule growth. *J Cell Biol*. 184:691-706.

Komarova, Y., G. Lansbergen, N. Galjart, F. Grosveld, G.G. Borisy, and A. Akhmanova. 2005. EB1 and EB3 Control CLIP Dissociation from the Ends of Growing Microtubules. *Mol Biol Cell*. 16:5334-45.

Lansbergen, G., Y. Komarova, M. Modesti, C. Wyman, C.C. Hoogenraad, H.V. Goodson, R.P. Lemaitre, D.N. Drechsel, E. van Munster, T.W. Gadella, Jr., F. Grosveld, N. Galjart, G.G. Borisy, and A. Akhmanova. 2004. Conformational changes in CLIP-170 regulate its binding to microtubules and dynactin localization. *J Cell Biol*. 166:1003-14.

Maes, T., A. Barcelo, and C. Buesa. 2002. Neuron navigator: a human gene family with homology to unc-53, a cell guidance gene from Caenorhabditis elegans. *Genomics*. 80:21-30.

Martinez-Lopez, M.J., S. Alcantara, C. Mascaro, F. Perez-Branguli, P. Ruiz-Lozano, T. Maes, E. Soriano, and C. Buesa. 2005. Mouse Neuron navigator 1, a novel microtubule-associated protein involved in neuronal migration. *Mol Cell Neurosci*. 28:599-612.

Mimori-Kiyosue, Y., I. Grigoriev, G. Lansbergen, H. Sasaki, C. Matsui, F. Severin, N. Galjart, F. Grosveld, I. Vorobjev, S. Tsukita, and A. Akhmanova. 2005. CLASP1 and CLASP2 bind to EB1 and regulate microtubule plus-end dynamics at the cell cortex. *J Cell Biol*. 168:141-53.

Muley, P.D., E.M. McNeill, M.A. Marzinke, K.M. Knobel, M.M. Barr, and M. Clagett-Dame. 2008. The atRA-responsive gene neuron navigator 2 functions in neurite outgrowth and axonal elongation. *Dev Neurobiol*. 68:1441-53.

Perez, F., G.S. Diamantopoulos, R. Stalder, and T.E. Kreis. 1999. CLIP-170 highlights growing microtubule ends in vivo. *Cell*. 96:517-27.

Riedl, J., A.H. Crevenna, K. Kessenbrock, J.H. Yu, D. Neukirchen, M. Bista, F. Bradke, D. Jenne, T.A. Holak, Z. Werb, M. Sixt, and R. Wedlich-Soldner. 2008. Lifeact: a versatile marker to visualize F-actin. *Nat Methods*. 5:605-7.

Schmidt, K.L., N. Marcus-Gueret, A. Adeleye, J. Webber, D. Baillie, and E.G. Stringham. 2009. The cell migration molecule UNC-53/NAV2 is linked to the ARP2/3 complex by ABI-1. *Development*. 136:563-74.

Schuyler, S.C., and D. Pellman. 2001. Microtubule “plus-end-tracking proteins”: The end is just the beginning. *Cell*. 105:421-4.

Stringham, E., N. Pujol, J. Vandekerckhove, and T. Bogaert. 2002. unc-53 controls longitudinal migration in C. elegans. *Development*. 129:3367-79.

van Haren, J., K. Draegestein, N. Keijzer, J.P. Abrahams, F. Grosveld, P.J. Peeters, D. Moechars, and N. Galjart. 2009. Mammalian Navigators are microtubule plus-end tracking proteins that can reorganize the cytoskeleton to induce neurite-like extensions. *Cell Motil Cytoskeleton*.

Wen, Y., C.H. Eng, J. Schmoranzer, N. Cabrera-Poch, E.J. Morris, M. Chen, B.J. Wallar, A.S. Alberts, and G.G. Gundersen. 2004. EB1 and APC bind to mDia to stabilize microtubules downstream of Rho and promote cell migration. *Nat Cell Biol*. 6:820-30.

Wittmann, T., and C.M. Waterman-Storer. 2005. Spatial regulation of CLASP affinity for microtubules by

Rac1 and GSK3{beta} in migrating epithelial cells. *J Cell Biol*. 169:929-39.
Wu, X., A. Kodama, and E. Fuchs. 2008. ACF7 regulates cytoskeletal-focal adhesion dynamics and migration and has ATPase activity. *Cell*. 135:137-48.

Supplemental Data

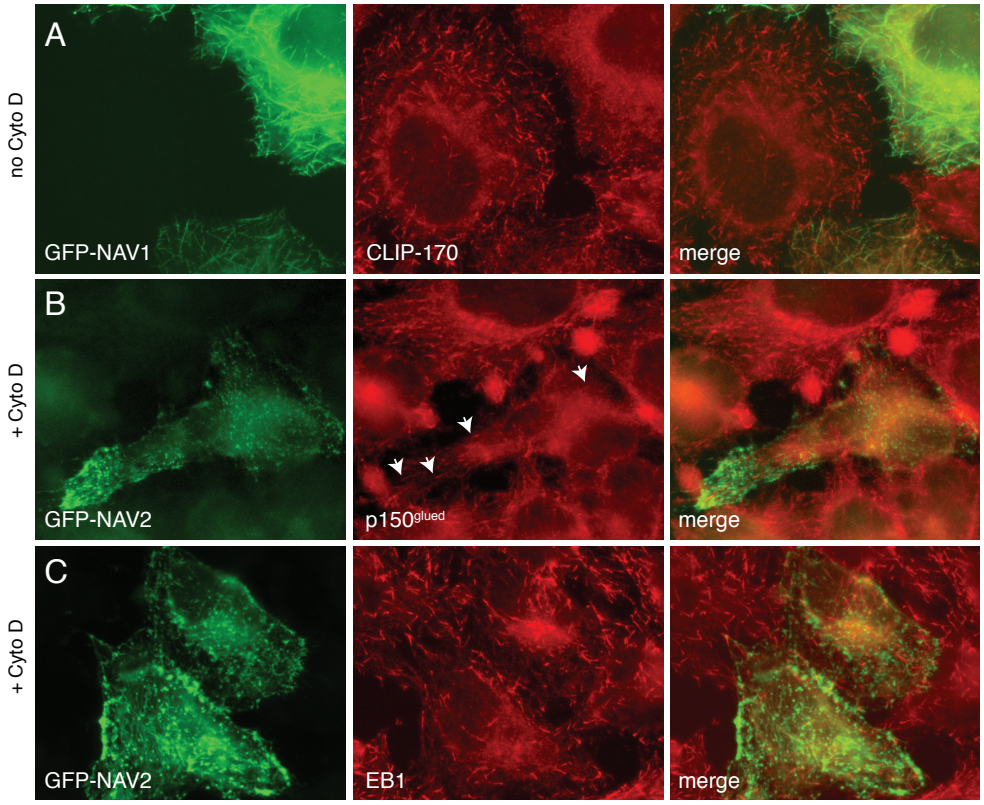

Figure S1. Competition between Navigators and CLIPs at MT ends.

A) NAV1 overexpression displaces CLIP-170. HeLa cells overexpresisng GFP-NAV1 (green) were fixed and stained for endogenous CLIP-170 (red). In cells where GFP-NAV1 is abundantly present at MT ends CLIP-170 signal is diffuse.

B) p150glued signal at MT ends is restored after cytochalasin D treatment. HeLa cells expressing GFP-NAV2 (green) were treated with cytochalasin D, fixed and stained for endogenous p150glued (red). This protein is found at MT ends in cells expressing GFP-NAV2. In non-treated GFP-NAV2-expressing cells, the p150glued signal is diffuse (van Haren et al., 2009) .

C) EB1 remains bound to MT ends after cytochalasin D treatment. HeLa cells expressing GFP-NAV2 (green) were treated with cytochalasin D, fixed and stained for endogenous EB1 (red). This protein is found at MT ends irrespective of GFP-NAV2 or treatment.

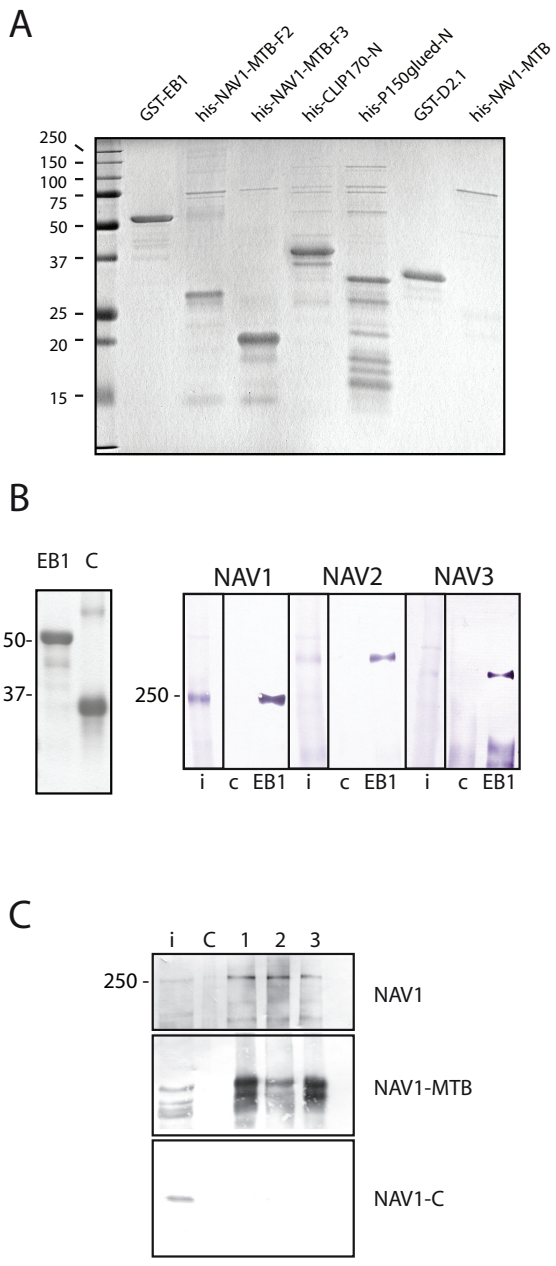

Supplemental Figure S2. Navigator-EB interaction.

A) SDS-PAGE of his-tagged Navigators, his-CLIP170-N, his-P150glued-N and GST-tagged EB1 and D2.1(used as a control).

B) Interaction of full length, GFP-tagged Navigators with GST-EB1. C: control (GST-D2.1, see Materials and Methods).

C) NAV1 interacts with all EB-proteins. GFP-tagged full length NAV1, its MTB domain, or its C-terminal domain, were incubated with GST-tagged EB1, -2, or -3 (C: GST only; i: input). Material bound to beads was washed, eluted by boiling and analyzed by western blot.

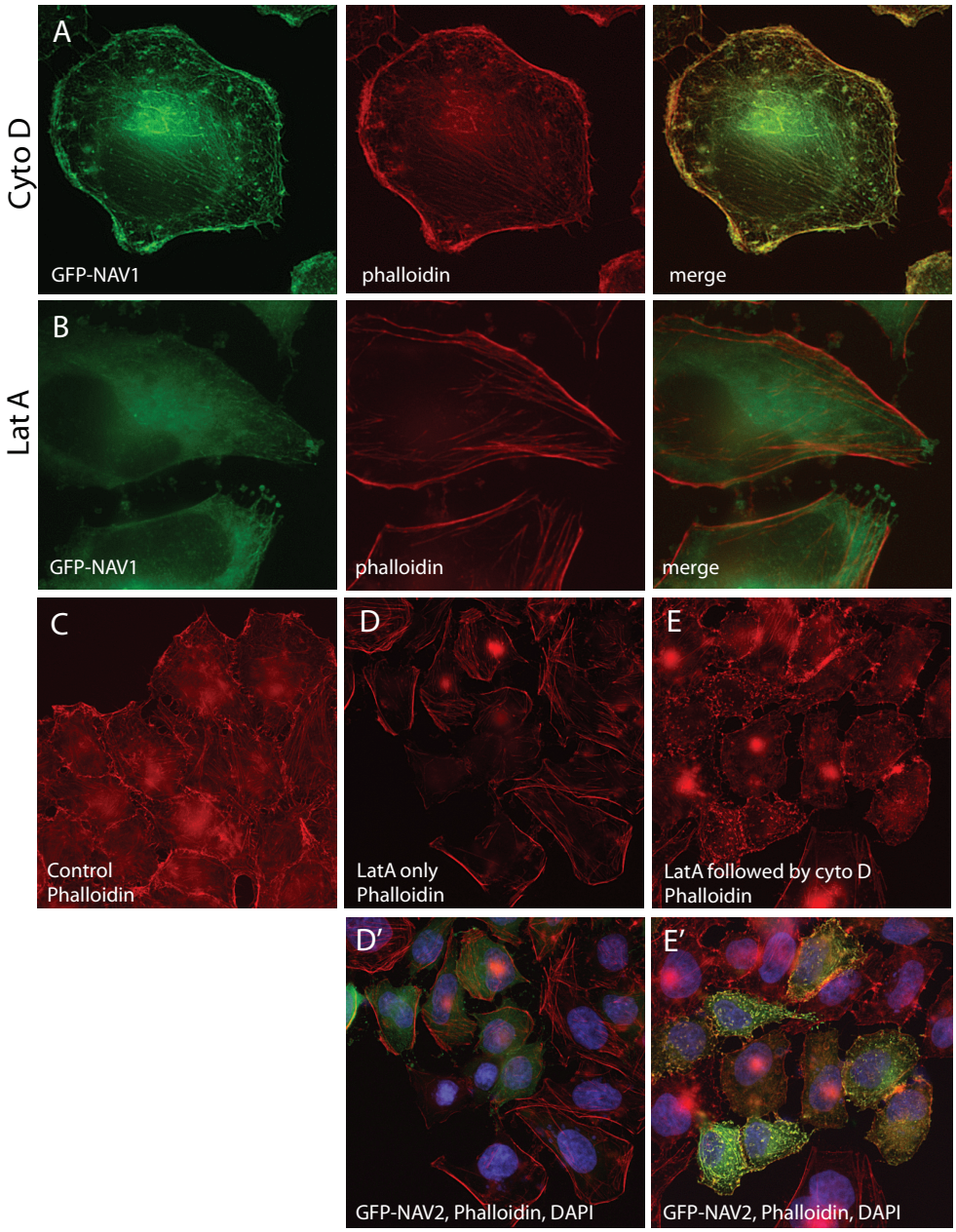

Figure S3. Relocalization of Navigators is not due to actin depolymerization. Legend on the next page.

Figure S3. Relocalization of Navigators is not due to actin depolymerization.
All cells were fixed with PFA and stained with phalloidin A594 (red).
A) HeLa cells, transfected with GFP-NAV1 (green) were treated with cytochalasin D (Cyto D) for 15 minutes. B) HeLa cells, transfected with GFP-NAV1 (green) were treated with latrunculin A (LatA) for 5 minutes. C) Phalloidin staining in untreated cells. D, D') cells treated with LatA (5 min). E, E') cells treated with LatA (5 min) followed by Cyto D (2 min). D', E') Show merged images of GFP-NAV2 (green), Phalloidin A594 (red) and DAPI (blue) (to visualize the nuclei). Colocalization of GFP-NAV2 and phalloidin gives a yellow signal, which is clearly visible in E' but not in D'.

Supplemental Movies

Movie 1
This movie shows the asymmetric distribution of GFP-NAV1 in a HeLa cell.
In the center of the cell, MT plus-end labeling can be observed, near the ventral cortex of cells, GFP-NAV1 shows a granular pattern.

Movie 2
TIRF microscopy of a HeLa cell expressing GFP-NAV1 and EB3-mCherry

Movie 3
Effect of nocodazole on NAV1 granules. 1hr before imaging 10 μM nocodazole was added to the culture medium. time (s) is indicated in the upperleft corner

Movie 4
TIRF microscopy of GFP-NAV1 and Cherry-Lifeact

Movies 5, 6
TIRF microscopy of GFP-NAV1 and Cherry-Lifeact after cytochalasin D treatment.

Chapter 5

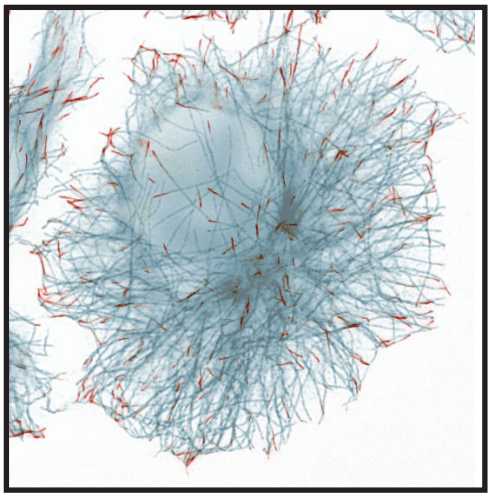

Proteomic analysis of Navigator-interacting proteins

Proteomic analysis of Navigator-interacting proteins

Jeffrey van Haren, Jeroen Demmers, Karel Bezstarosti, Katharina Draegestein, Frank Grosveld, Niels Galjart.

Department of Cell Biology and Genetics, Erasmus MC, P.O. Box 2040, 3000 CA Rotterdam, The Netherlands.

Work in progress

Running title: Navigator-interacting proteins

Abstract

Mammalian Navigators are the homologues of the *C. elegans* UNC-53 protein, an ATPase that is involved in axon outgrowth and cell migration. A tight link between Navigator function and the cytoskeleton has thus far been established. Here we describe results of a proteomic analysis aimed at identifying Navigator-interacting proteins. Surprisingly, we find that B23 (nucleophosmin) and fibrillarin interact with Navigator proteins, implying a function for Navigators in ribosome biogenesis, centrosome dynamics, and cellular stress sensing. The same domain that is responsible for targeting Navigators to MT plus ends and the actin network interacts with these nucleolar constituents. Fluorescence-based imaging studies in living cells reveal that Navigator1 (NAV1) is a nucleo-cytoplasmic shuttling protein. RNAi-mediated knock down of NAV1 affects nucleolar morphology and centrosome numbers. Our data reveal a promiscuous protein-protein interaction module that allows Navigators to associate with many different proteins inside cells. We propose that this domain serves to couple Navigators to their target proteins. Our data also indicate that NAV1 and nucleophosmin share a number of cellular targets suggesting that these proteins function in common pathways.

Introduction

In the nematode *C. elegans* the *unc-53* locus encodes a protein required for anterior-posterior guidance of migrating cells and axons, and for egg-laying, correct backward locomotion, normal body size, and male mating (Chen et al., 1997; Stringham et al., 2002). The UNC-53 protein is orthologous to human NAV1, -2, and -3 (Maes et al., 2002). Both for UNC-53 and the NAVs several isoforms have been described, most of which contain C-terminal sequences with an AAA-ATPase domain (Frickey and Lupas, 2004). A number of studies have linked UNC-53/NAV function to regulation of the cytoskeleton (Martinez-Lopez et al., 2005; Muley et al., 2008; Schmidt et al., 2009; van Haren et al., 2009a). For example, all three Navigator proteins are microtubule (MT) plus-end tracking proteins (+TIPs), associating specifically with the ends of growing MTs (van Haren et al., 2009a). These results indicate that navigators are ATPases with a role in cytoskeleton remodeling.

Interestingly, the MT binding (MTB) domain that is responsible for targeting NAV1 to MT ends also contains the motif required for actin relocalization (van Haren et al., 2009b). On the other hand, reports have appeared that suggest a role for NAV2 and/or -3 in the formation of nuclear pores (Coy et al., 2002) and that even assigned DNA helicase activity to NAV2 (Ishiguro et al., 2002). These data suggest that Navigator function might not be restricted to the cytoskeleton.

Recently, a biotin-streptavidin pull down approach followed by mass spectrometry-based analysis has been developed that allows quick identification of proteins interacting with the biotinylated bait (Grosveld et al., 2005). In this approach the protein of interest is tagged at its N- or C-terminus with a small peptide sequence that is recognized by the *E. coli* biotin-ligase BirA. After biotinylation the protein is affinity-purified in a single step using streptavidin-coated superparamagnetic beads. If purification is performed using low stringency conditions, interaction partners are co-purified. The latter can subsequently be identified using mass spectrometry. Here we describe novel proteins interacting with biotinylated Navigators. Our data suggest a completely new function for NAV1.

Materials and Methods

Biotin pulldowns from HEK293T cell extracts.

One day before transfection, HEK293T cells were seeded into DMEM/F10 medium, supplemented with 10%FCS and antibiotics. Using 7-10 µg of the plasmid encoding the bio-tagged protein, and 4 µg of plasmid encoding BirA per 10 cm dish, cells were transfected at 80-90 % confluency with either Lipofectamine 2000 (Invitrogen) or PEI (Sigma Aldrich). One day after transfection, the medium was replaced with 5 ml PBS after which the cells were flushed out of the dishes with a 10 ml pipette and centrifuged for 5 minutes at 200g. Cells were lysed in lysis buffer (500 µl per 10cm dish, 20 mM HEPES pH7.5, 150mM KCl, 1% Triton X-100, 10% glycerol, Complete Protease Inhibitor cocktail (Boehringer)). Cell lysates were incubated on ice for 1 hr (extracts were gently mixed a few times during this period) and centrifuged for 10 minutes at 13000 rpm. Supernatants were incubated for 1 hour at 4 ^{0}C with Dynal M280 beads, which were blocked in buffer (20 mM HEPES pH7.5, 150mM KCl, 0.1% Triton X-100, 10% glycerol) for 30-60 minutes prior to use and put in a magnetic particle separator with excess blocking buffer removed. Approximately 50 µl beads were used per 10 cm dish. Beads were washed six times in 20mM HEPES pH7.5, 150mM KCl, 0.1% Triton X-100, 10% glycerol. Bound material was eluted from the the beads by adding SDS-PAGE sample buffer (2x sample buffer: 125 mM Tris HCl pH6.8, 4% SDS, 20% Glycerol, 0.004% Bromophenol Blue, see also (Sambrook et al., 1989)) and boiling for 5 minutes. Eluates were loaded on a SDS-PAGE gel and analysed by mass spec.

Mass spectrometry.

For mass spectrometry samples were treated and analyzed as described (Wilm et al., 1996). Data analysis and protein identification was done as reported (Lansbergen et al., 2006). The Mascot search algorithm (version 2.0, MatrixScience) was used for searching against the NCBI database (taxonomy: *H. sapiens*). The Mascot score cut-off value for a positive protein hit was set to 40. Mass spectrometry results of all three navigator proteins are available upon request.

Antibodies.

Anti-fibrillarin antibodies have been described (Heath et al., 2008).
Anti-B23 (sc-32256, Santa Cruz) was used 1:1000 for western blot and 1:100 for IF.

RNAi-mediated knockdown.

For western blot analysis of NAV1 knockdown HeLa cells were grown in 6 cm dishes and scraped 3 days after transfection. Cells were lysed in 150 ul of lysis buffer, and sonicated. About 10 % (i.e. 15 ul) of the total extracts were loaded on gel.

Immunofluorescence and live imaging.

For immunofluorescence analysis cells were transfected with GFP-NAV1-C, grown on coverslips, and fixed and stained as described (van Haren et al., 2009a). Live imaging studies and FRAP experiments were also carried out in transfected cells, as published (van Haren et al., 2009a). In the iterated bleaching experiment 9 images were acquired (frame rate set at one image per second) prior to bleaching. We subsequently repeatedly bleached a circular ROI with a diameter of 45 pixels (0.15 micron/pixel). Each bleach period lasted 2.7 seconds and was followed by a pauze of 1 second (for the acquisition of two images one second apart). A total of 400 images was acquired in this experiment (total time of experiment 726 seconds). Fluorescence loss in photobleaching (FLIP) in small ROIs outside of the bleach zone were calculated. The average background value was deducted from the fluorescence intensity in each ROI. Subsequently curves were normalized, and values from small nearby ROIs were averaged to obtain FLIP measurements nearby and further away from the bleach zone.

Results

Novel Navigator-interacting proteins.

We recently used the biotinylation-tagging approach to purify full length Navigator proteins (van Haren et al., 2009a). Under low stringency conditions a number of proteins are co-purified, some of which appear to be specific for the Navigators (Figure 1). Unknown proteins co-purifying with bio-GFP-Navigators were identified by mass spectrometry, classified by BLAST searches and compared to control pull downs. This analysis revealed that several nucleolar proteins, including B23/nucleophosmin and fibrillarin, interact with Navigators and not with the control proteins (e.g. CLIP-170). B23 is a nucleo-cytoplasmic shuttling protein involved in ribosome synthesis, and the gene encoding B23 is frequently mutated in cancer (Grisendi et al., 2005). Fibrillarin is a box C/D-snoRNAs-associating protein implicated in the processing of ribosomal RNA (Kiss et al., 2006).

To confirm interactions and to delineate the domain(s) responsible, we performed co-precipitations with full length bio-GFP-NAV1 as well as with selected mutant NAV1 proteins (Figure 2A, described in (van Haren et al., 2009b)). Strikingly, we found that the MTB domain of NAV1 is able to pull down both B23 and fibrillarin, whereas the C-terminus of NAV1 does not interact (Figure 2B). Consistent with these results a mutation in the ATPase domain of NAV1 (van Haren et al., 2009a) does not affect binding to the nucleolar proteins (Figure 2B). These results suggest that the MTB domain of NAV1 is a promiscuous protein-protein interaction module, targeting navigators to the cytoskeleton as well as to nucleolar components.

The MTB domain of Navigator proteins is quite basic with an isoelectric point of 10.2. In contrast, the isoelectric point of B23 is 4.38. Such differences in charge are likely to play a role in the interaction between NAVs and B23.

A role for NAV1 in nucleolar function and mitosis.

In interphase cells B23 is mainly nucleolar whereas Navigators are mainly cytoplasmic. To examine a possible colocalization between NAV1 and B23 we therefore investigated the distribution of the two proteins in fixed cells in mitosis using antibodies against B23 and NAV1. The data show that endogenous NAV1 is localized to the mitotic spindle (Figure 3A), as well as the centrosome (Figure 3A, B). In addition GFP-NAV1 localizes to the mitotic spindle as well (and shows a cortical localization from anaphase onwards) (Figure 3C). Thus, a centrosomal localization is a constant feature of NAV1 during the cell cycle (van Haren et al., 2009a). B23 and NAV1 co-localize at centrosomes during mitosis (Figure 3B), suggesting a shared

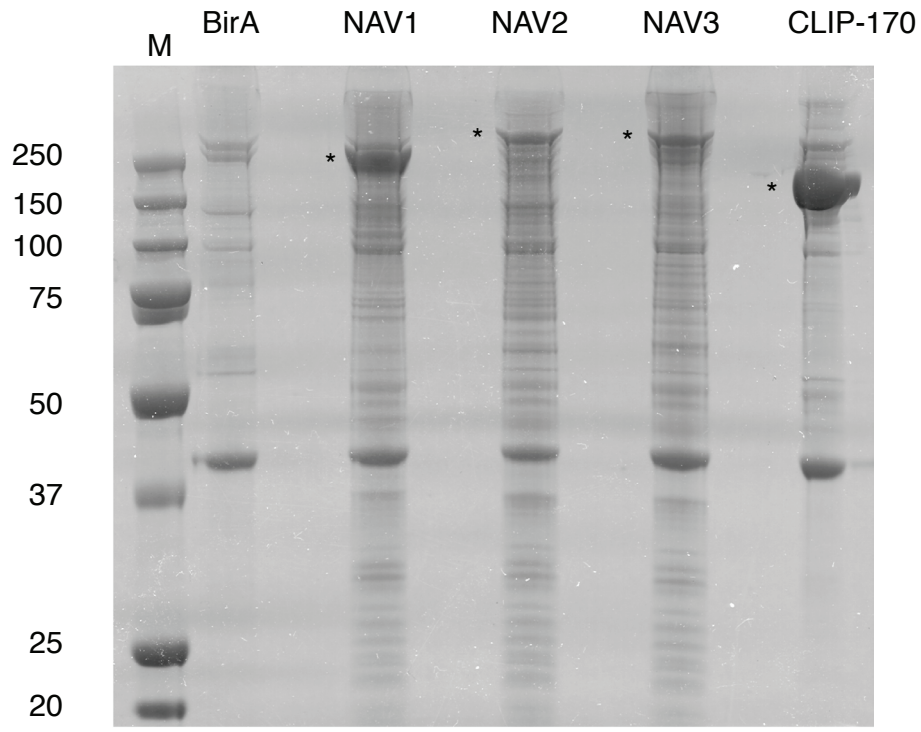

Figure 1. Purification of navigators and their interacting proteins.
A) Purification of bio-GFP-tagged navigators. Biotinylated, GFP-tagged navigators (lanes 2-4) and CLIP-170 (lane 5) were overexpressed in HEK293T cells together with the BirA enzyme. Lane 1 shows an extract of cells expressing BirA only. The bio-GFP-fusion proteins (asterisks indicate the positions of the respective full length proteins) were purified under mild conditions. Gels were stained with Coomassie brilliant blue. Potential navigator-interacting proteins were identified by mass spectrometry.

role in centrosome dynamics for these proteins.

To examine the role of NAV1 we used an RNAi-mediated knock down approach using different siRNAs against NAV1. Western blot analysis suggests that NAV1 levels can be efficiently reduced after 3 days (Figure 4A). Strikingly, in interphase cells nucleolar morphology is different from control cells upon depletion of NAV1, as detected with antibodies against fibrillarin and B23 (Figure 4B). The shape of the nucleoli appears less uniform than in control cells, in which most nucleoli are round. Overexpression of GFP-NAV1 did however not displace B23 from the nucleolus, nor did NAV1 itself accumulate in the nucleolus (data not shown). Furthermore, the number of cells with multipolar spindles is highly increased in NAV1-depleted cells, whereas the number of cells with monopolar spindles is decreased (Figure 4C).

These multipolar spindles contained multiple centrosomes, as visualized by pericentrin and γ-tubulin staining (Figure 4C). Combined our results indicate that NAV1 has a role in nucleolar morphology as well as in mitosis.

NAV1 is a nucleo-cytoplasmic shuttling protein.

Because NAV1 interacts with B23 and is involved in nucleolar morphology in interphase cells we investigated whether, similar to B23, the protein can shuttle between cytoplasm and nucleus. Nuclear import of Navigator 1,2 and 3 could well be mediated via a putative nuclear localization signal (NLS) located near the C-terminus of these proteins (see Figure 6C). Cells were transfected with GFP-NAV1 and a region of interest (ROI) inside the nucleus was bleached in an iterative manner. This causes loss of fluorescence inside the bleach zone, as well as elsewhere in the nucleus (Figure 5A, C), indicating that GFP-NAV1 does accumulate to some extent in the nucleus. Interestingly, we also observed fluorescence loss in the cytoplasm (Figure 5A, C). Conversely, bleaching of GFP-NAV1 in the cytoplasm causes loss in fluorescence in the nucleus (Figure 5B, D). These results indicate that GFP-NAV1 shuttles between nucleus and cytoplasm. To investigate further the mechanisms by which Navigators shuttle in and out of the nucleus we treated cells with Leptomycin B (LMB). LMB, a *Streptomyces* metabolite, inhibits nuclear export mediated by the protein CRM1. CRM1 is a member of the importin β family and a receptor for the nuclear export signal (NES) of proteins. LMB binds directly to CRM1 thereby disrupting its interaction with NES sequences (Yashiroda and Yoshida, 2003). We transfected cells with the NLS containing GFP-NAV1-C (C-terminal 827 amino acids), which is a protein that does not interact with B23 or fibrillarin (Figure 2B) and that is mainly localized to the cytoplasm in non-treated cells (Figure 6A). By contrast treatment of cells with LMB caused the retention of GFP-NAV1-C in the nucleus of cells, which was already clearly visible within 1 hr after LMB addition (Figure 6B), suggesting that NAV1-C makes use of the CRM1 system to exit the nucleus and confirming the notion that NAV1 is a nucleo-cytoplasmic shuttling protein.

Interestingly, we did not observe this strong nuclear accumulation with the full length proteins after LMB treatment, suggesting that alternative nuclear export pathways mediate nuclear export of Navigators as well.

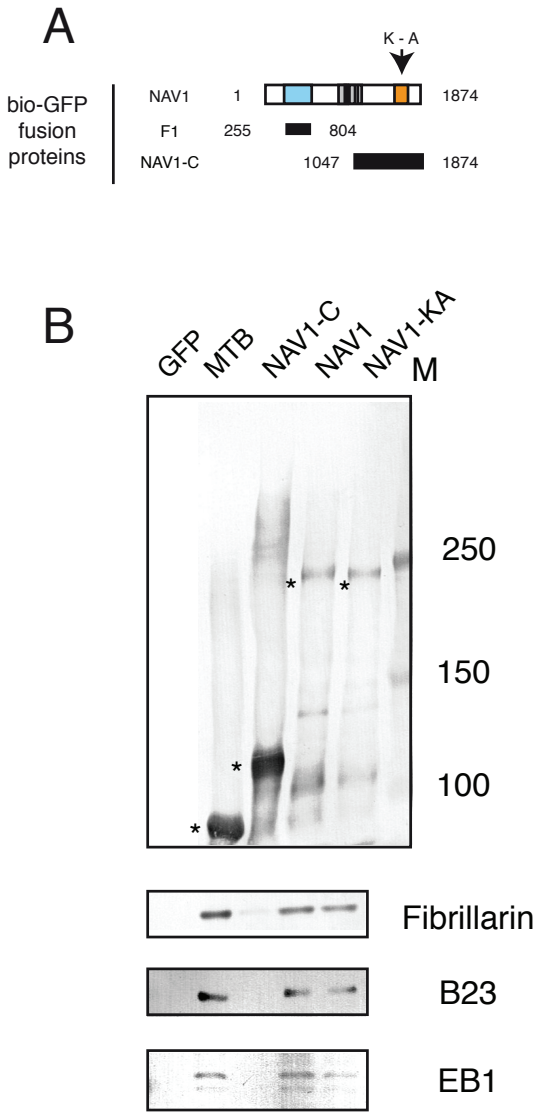

Figure 2. NAV1 interacts with nucleolar components.

A) Domain architecture of NAV1 and mutant proteins. Amino acid numbers are indicated. MT-binding domain (blue), ATPase domain (orange), calponin homology domain (red), and potential coiled-coil domains (grey) are indicated. GFP-tagged fusion proteins are indicated underneath NAV1. The arrow points to the approximate position a highly conserved lysine (K) residue that was mutated to alanine (A) in order to generate a mutant NAV1 protein defective in ATPase activity.

B) Biotinylated proteins and interaction partners were purified as described in Figure 1. Proteins were separated by SDS-PAGE and blotted. Western blots were incubated with antibodies against GFP (upper large panel), B23, fibrillarin, or EB1 (lower panels).

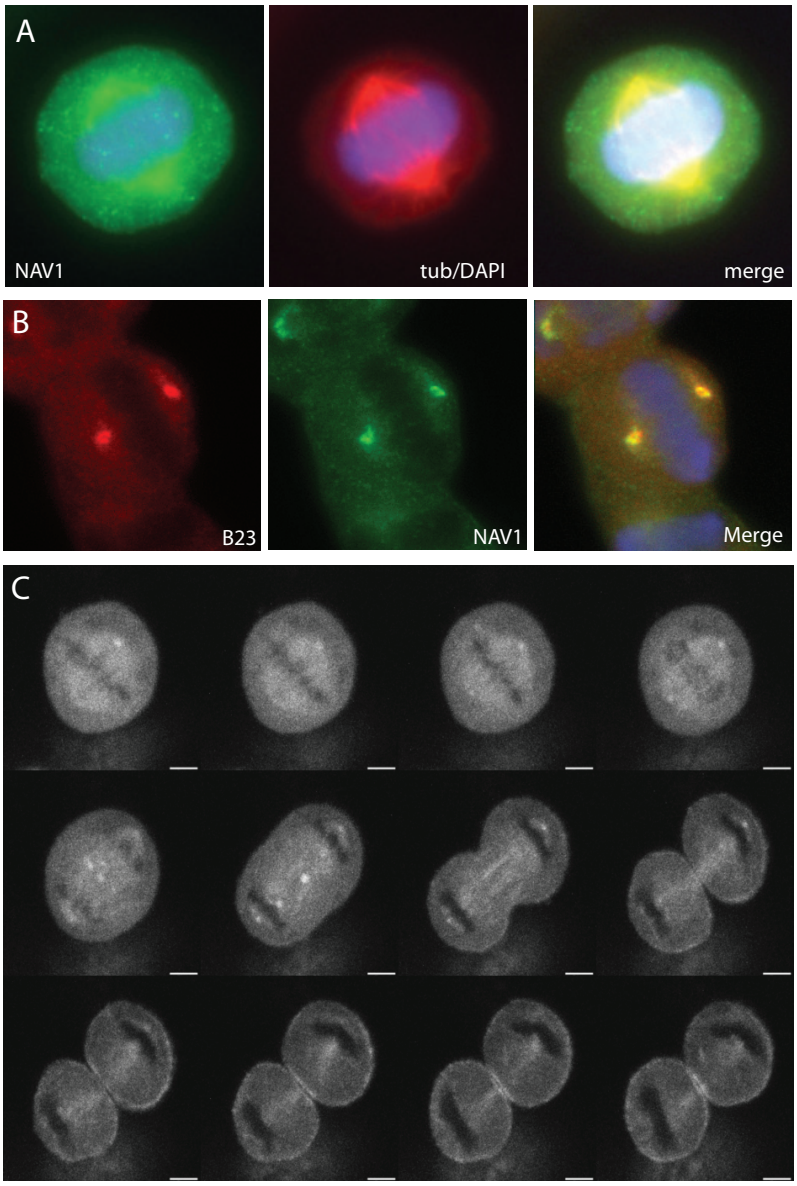

Figure 3. NAV1 localizes to the mitotic spindle and colocalizes with B23.
A) NAV1 localizes to the mitotic spindle. HeLa cells were stained with antibodies against NAV1 (green) and tubulin (red). DAPI (blue) stains the DNA.
B) Colocalization of NAV1 with B23. HeLa cells were stained with antibodies against NAV1 (red) and B23 (green). DAPI (blue) stains the DNA. Notice colocalization of B23 and NAV1 on the centrosome.
C) Montage of a movie of GFP-NAV1 in a mitotic HeLa cell. Note the spindle localization and the cortical localization of NAV1 from anaphase onwards.

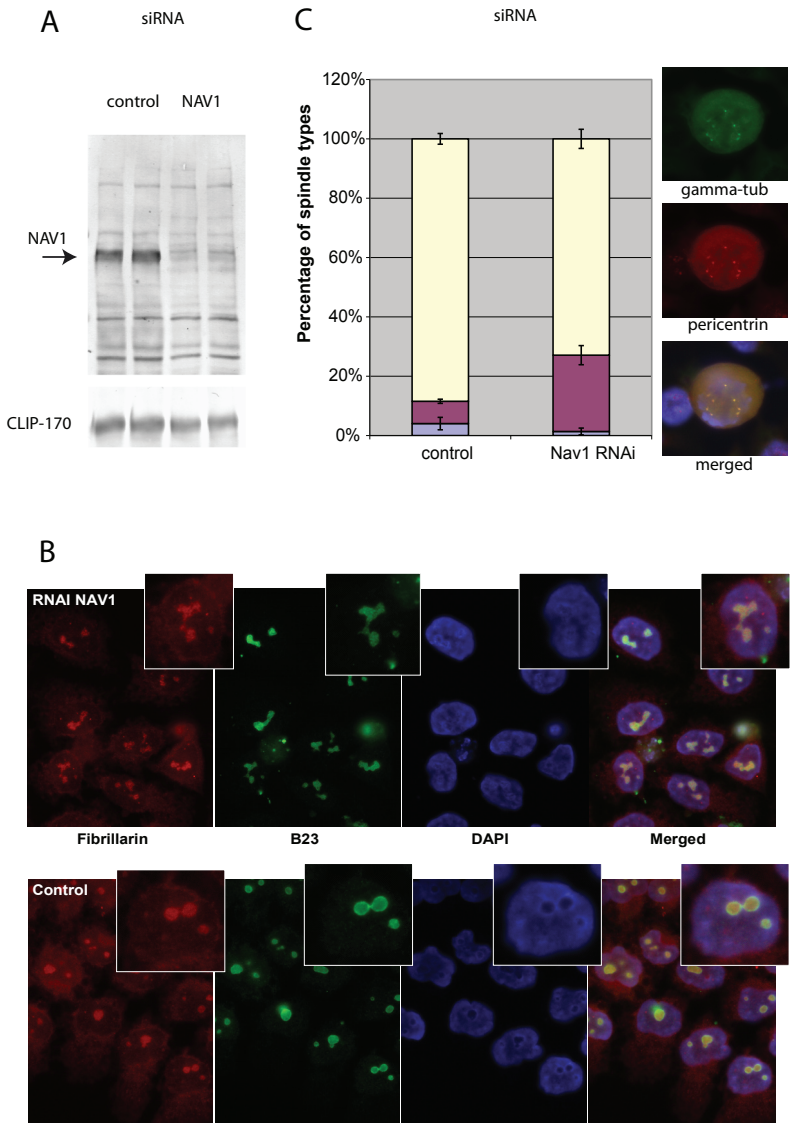

Figure 4. RNAi-mediated knockdown of NAV1.

A) Western blot analysis. HeLa cells were transfected with siRNAs against NAV1. Cells were harvested 3 days after transfection and the depletion of NAV1 tested by western blot.

B) Nucleolar morphology in HeLa cells after depletion of NAV1. HeLa cells were transfected with a siRNA against NAV1 or a negative control siRNA. Three days after transfection cells were fixed and stained with antibodies against fibrillarin (red), B23 (green) and DAPI (blue).

C) Spindle morphology was quantified (monopolar (blue), normal spindle (yellow) and multipolar (purple)). Multipolar spindles contained multiple centrosomes as visualized by pericentrin (red) and γ-tubulin staining (green).

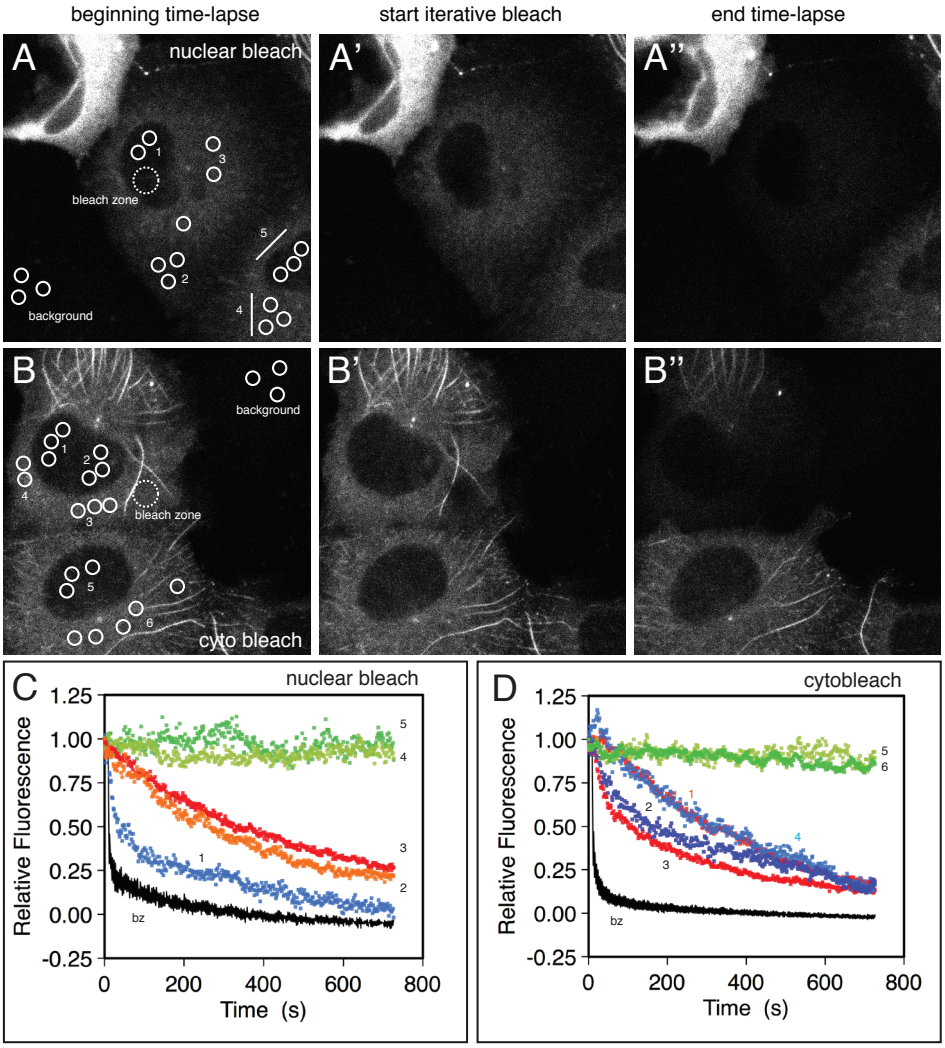

Figure 5. Dynamic behaviour of GFP-NAV1.

A-D) FRAP analysis in transfected COS-7 cells. GFP-Nav1 was transiently transfected in COS-7 cells. After one day transfected cells were subjected to FRAP analysis. In (A, C) results of an iterative photobleaching in the nucleus are shown, in (B, D) results of a published (van Haren et al., 2009a) iterative bleach experiment in the cytoplasm are shown, with additional ROIs. Bleaches were performed in the bleach zones (bz). In A and B, the first images of the time-lapse experiments are shown, images after the first bleach are shown in A' and B', and images at the end of the experiments are shown in A'' and B''. In C and D normalized fluorescence loss curves are shown. Fluorescence intensities are plotted on the vertical axis with time (in seconds) on the horizontal axis.

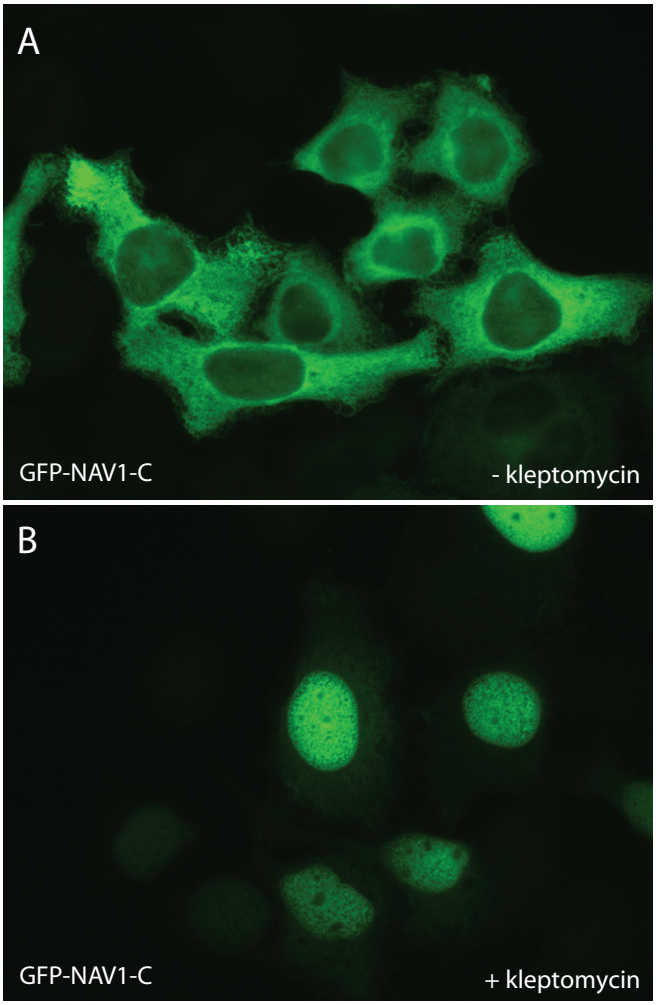

C

NAV1	**KKKKS WLRSSFNKAFS IKKGPK**
NAV2	**KKKKRKNWVNELRSSFKQAFGKKKSPK**
NAV3	**KKKKKNWVNSRGSELRSSFKQAFGKKK**

Figure 6. NAV1-C shuttles between cytoplasm and nucleus in interphase
A, B) Cells transfected with GFP-NAV1-C (green) were either treated with (+) leptomycin B for 24 hours, or not treated (-). Afterwards cells were fixed with cold Methanol/EGTA.
C) Putative nuclear localization signals in NAV1, 2 and 3.

Discussion

Using a mass spectrometry-based analysis we have identified novel navigator-interacting proteins. Somewhat surprisingly, two nucleolar components came up as interacting partners, i.e. B23 and fibrillarin. Although ribosomal proteins are often typified as contaminants in these types of proteomic approaches, we found that in the case of the Navigators at least the interactions with B23 and fibrillarin are specific. Interestingly, these protein-protein interactions are mediated by a domain of ~550 amino acids inside the Navigators that was previously shown to bind tubulin and MT ends (Martinez-Lopez et al., 2005), as well as EB1 and F-actin (van Haren et al., 2009b). The domain lacks a typical protein-protein interaction motif, such as a coiled-coil region. It will be interesting to determine the number of proteins able to bind this Navigator domain and how interactions are mediated. We propose that the domain serves to target the ATPase activity of the Navigators to specific subcellular sites and/or substrates.

Previous FRAP results have shown that NAV1 is a relatively immobile cytoplasmic protein (van Haren et al., 2009a). Here we show that NAV1 shuttles between cytoplasm and nucleus and that nuclear NAV1 is also rather immobile, suggesting it is either bound to nucleic acid, or part of a large complex. The documentation of helicase activity in NAV2 (Ishiguro et al., 2002) is interesting in this context. The iterative bleaching experiment furthermore indicates that cytoplasmic NAV1 is more immobile than nuclear NAV1, as cytoplasmic NAV1 is bleached more rapidly. Furthermore, our data shows that NAV1 contains a functional nuclear localization signal and functional nuclear export signals.

Depletion of B23 in HeLa cells causes distortion of nucleolar structure and of the cytoskeleton, due to defects in centrosomal MT nucleation (Amin et al., 2008). We show here that there is a striking similarity in the phenotype of B23- and NAV1-depleted cells. Moreover, like NAV1, B23 shuttles from the nucleolus/nucleus to the cytoplasm, its shuttling requiring a conserved LMB-sensitive CRM1-binding site. As these two proteins interact we propose that they are involved in common pathways. B23, or nucleophosmin (NPM), is a nucleolar phospho-protein that is abundantly expressed in proliferating cells (Feuerstein et al., 1988). B23 plays a role in several different processes including: ribosome biogenesis (Maggi et al., 2008), histone protein chaperoning (Murano et al., 2008), and transcriptional control (Colombo et al., 2002).

B23 has also been shown to play an important role in centrosome replication (Okuda et al., 2000), and in addition, B23 knockout MEFs showed increased

numbers of centrosomes per cell and an increased number of multipolar spindles (Grisendi et al., 2005). Interestingly we found an increased number of centrosomes in the multipolar spindles in NAV1 RNAi treated HeLa cells as well. Perhaps centriole replication is affected in these cells. However, we cannot exclude that this increased number of centrosomes results from other mitotic defects. Defective cytokinesis can also result in cells with aberrant centrosome numbers.

In conclusion, Navigators shuttle between the cytoplasm and the nucleus and they have a function in both cytoskeletal organization during mitosis and the maintenance of nucleolar structure. It is likely that this involves a protein complex with B23. Perhaps NAV1 provides the ATPase activity for some of the functions to which B23 has been coupled, for example its chaperone activity.

References

Amin, M.A., S. Matsunaga, S. Uchiyama, and K. Fukui. 2008. Depletion of nucleophosmin leads to distortion of nucleolar and nuclear structures in HeLa cells. *Biochem J*. 415:345-51.

Chen, E.B., C.S. Branda, and M.J. Stern. 1997. Genetic enhancers of sem-5 define components of the gonad-independent guidance mechanism controlling sex myoblast migration in Caenorhabditis elegans hermaphrodites. *Dev Biol*. 182:88-100.

Colombo, E., J.C. Marine, D. Danovi, B. Falini, and P.G. Pelicci. 2002. Nucleophosmin regulates the stability and transcriptional activity of p53. *Nat Cell Biol*. 4:529-33.

Coy, J.F., S. Wiemann, I. Bechmann, D. Bachner, R. Nitsch, O. Kretz, H. Christiansen, and A. Poustka. 2002. Pore membrane and/or filament interacting like protein 1 (POMFIL1) is predominantly expressed in the nervous system and encodes different protein isoforms. *Gene*. 290:73-94.

Feuerstein, N., S. Spiegel, and J.J. Mond. 1988. The nuclear matrix protein, numatrin (B23), is associated with growth factor-induced mitogenesis in Swiss 3T3 fibroblasts and with T lymphocyte proliferation stimulated by lectins and anti-T cell antigen receptor antibody. *J Cell Biol*. 107:1629-42.

Frickey, T., and A.N. Lupas. 2004. Phylogenetic analysis of AAA proteins. *J Struct Biol*. 146:2-10.

Grisendi, S., R. Bernardi, M. Rossi, K. Cheng, L. Khandker, K. Manova, and P.P. Pandolfi. 2005. Role of nucleophosmin in embryonic development and tumorigenesis. *Nature*. 437:147-53.

Grosveld, F., P. Rodriguez, N. Meier, S. Krpic, F. Pourfarzad, P. Papadopoulos, K. Kolodziej, G.P. Patrinos, A. Hostert, and J. Strouboulis. 2005. Isolation and characterization of hematopoietic transcription factor complexes by in vivo biotinylation tagging and mass spectrometry. *Ann N Y Acad Sci*. 1054:55-67.

Heath, H., C.R. de Almeida, F. Sleutels, G. Dingjan, S. van de Nobelen, I. Jonkers, K.W. Ling, J. Gribnau, R. Renkawitz, F. Grosveld, R.W. Hendriks, and N. Galjart. 2008. CTCF regulates cell cycle progression of alphabeta T cells in the thymus. *Embo J*. 27:2839-50.

Ishiguro, H., T. Shimokawa, T. Tsunoda, T. Tanaka, Y. Fujii, Y. Nakamura, and Y. Furukawa. 2002. Isolation of HELAD1, a novel human helicase gene up-regulated in colorectal carcinomas. *Oncogene*. 21:6387-94.

Kiss, T., E. Fayet, B.E. Jady, P. Richard, and M. Weber. 2006. Biogenesis and intranuclear trafficking of human box C/D and H/ACA RNPs. *Cold Spring Harb Symp Quant Biol*. 71:407-17.

Lansbergen, G., I. Grigoriev, Y. Mimori-Kiyosue, T. Ohtsuka, S. Higa, I. Kitajima, J. Demmers, N. Galjart, A.B. Houtsmuller, F. Grosveld, and A. Akhmanova. 2006. CLASPs attach microtubule plus ends to the cell cortex through a complex with LL5beta. *Dev Cell*. 11:21-32.

Maes, T., A. Barcelo, and C. Buesa. 2002. Neuron navigator: a human gene family with homology to unc-53, a cell guidance gene from Caenorhabditis elegans. *Genomics*. 80:21-30.

Maggi, L.B., Jr., M. Kuchenruether, D.Y. Dadey, R.M. Schwope, S. Grisendi, R.R. Townsend, P.P. Pandolfi, and J.D. Weber. 2008. Nucleophosmin serves as a rate-limiting nuclear export chaperone for the Mammalian ribosome. *Mol Cell Biol*. 28:7050-65.

Martinez-Lopez, M.J., S. Alcantara, C. Mascaro, F. Perez-Branguli, P. Ruiz-Lozano, T. Maes, E. Soriano, and C. Buesa. 2005. Mouse Neuron navigator 1, a novel microtubule-associated protein involved in neuronal migration. *Mol Cell Neurosci*. 28:599-612.

Muley, P.D., E.M. McNeill, M.A. Marzinke, K.M. Knobel, M.M. Barr, and M. Clagett-Dame. 2008. The atRA-responsive gene neuron navigator 2 functions in neurite outgrowth and axonal elongation. *Dev Neurobiol*. 68:1441-53.

Murano, K., M. Okuwaki, M. Hisaoka, and K. Nagata. 2008. Transcription regulation of the rRNA gene by a multifunctional nucleolar protein, B23/nucleophosmin, through its histone chaperone activity. *Mol Cell Biol*. 28:3114-26.

Okuda, M., H.F. Horn, P. Tarapore, Y. Tokuyama, A.G. Smulian, P.K. Chan, E.S. Knudsen, I.A. Hofmann, J.D. Snyder, K.E. Bove, and K. Fukasawa. 2000. Nucleophosmin/B23 is a target of CDK2/cyclin E in centrosome duplication. *Cell*. 103:127-40.

Sambrook, J., E.F. Fritsch, and T. Maniatis. 1989. Molecular cloning: a laboratory manual, 2 Edition. Cold Spring Harbor Laboratory Press, New York.

Schmidt, K.L., N. Marcus-Gueret, A. Adeleye, J. Webber, D. Baillie, and E.G. Stringham. 2009. The cell migration molecule UNC-53/NAV2 is linked to the ARP2/3 complex by ABI-1. *Development*. 136:563-74.

Stringham, E., N. Pujol, J. Vandekerckhove, and T. Bogaert. 2002. unc-53 controls longitudinal migration in C. elegans. *Development*. 129:3367-79.

van Haren, J., K. Draegestein, N. Keijzer, F. Grosveld, P. Peeters, D. Moechars, and N. Galjart. 2009a. Mammalian navigators are microtubule plus-end tracking proteins that can reorganize the cytoskeleton to induce neurite-like extensions. *Cell Motil Cytoskeleton*. in press.

van Haren, J., S. Montenegro Gouveia, I. Grigoriev, A. Akhmanova, F. Grosveld, D. Moechars, P. Peeters, and N. Galjart. 2009b. Navigators are EB-interacting proteins that link dynamic microtubules to the cortical actin network. *manuscript in preparation*.

Wilm, M., A. Shevchenko, T. Houthaeve, S. Breit, L. Schweigerer, T. Fotsis, and M. Mann. 1996. Femtomole sequencing of proteins from polyacrylamide gels by nano-electrospray mass spectrometry. *Nature*. 379:466-9.

Yashiroda, Y., and M. Yoshida. 2003. Nucleo-cytoplasmic transport of proteins as a target for therapeutic drugs. *Curr Med Chem*. 10:741-8.

Chapter 6

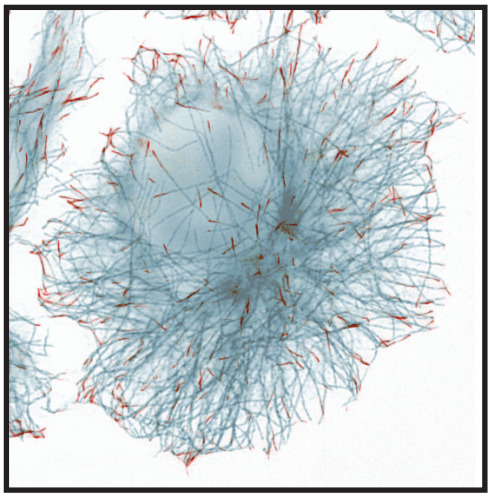

Discussion

Chapter 6 Discussion

6.1 The expression of Navigators during development and disease

+TIPs are important regulators of the cytoskeleton. Some +TIPs control MT dynamics, others, like ACF7, serve a role in regulating actin-MT crosstalk. Again other +TIPs, like the *Drosophila* RhoGEF2, function in signal transduction. Navigators are +TIPs that function in the outgrowth and migration of cells. Both in *C. elegans* and in mammals, Navigators play a role during development. In addition, several groups have reported misregulation of these proteins in different types of cancer, including colorectal cancers, neuroblastomas and cutaneous T cell lymphomas (Coy et al., 2002; Ishiguro et al., 2002; Karenko et al., 2005).

Mammalian Navigators are highly expressed in the developing nervous system and in adult tissues such as skeletal muscle, heart, liver and kidney. Transcription of NAV2 is upregulated by all-trans retinoic acid. NAV2 (also named HELAD1) transcription was also found to be upregulated by nuclear β-catenin (Coy et al., 2002; Ishiguro et al., 2002; Merrill et al., 2002). HELAD1 was found in a screen for genes that were affected in their activity in SW480 cells by the expression of adAPC, which encodes the 20 amino acid repeat domain of APC. Previously, it was found that expression of this fragment resulted in decreased levels of β-catenin, and decreased expression of Tcf/LEF target genes. HELAD 1 was found to be downregulated by this APC fragment. The AAA domain of HELAD1 has helicase activity *in vitro*, hence the name HELAD1 (Helicase, Apc Down-regulated). Furthermore, the HELAD1 gene was upregulated in 80 % of the colon-cancer tissues examined. Combined, the data suggest that HELAD1/ NAV2 is under the control of the β-catenin/ Tcf transcription complex (Ishiguro et al., 2002). Interestingly, this places NAV2 downstream of the Wnt signaling pathway, which plays an important role during development. Additionally, this pathway is frequently disrupted in different types of cancer (Klaus and Birchmeier, 2008). This may explain why Navigators are misregulated in many types of cancer.

6.2 Navigators, cellular outgrowth and cell extrinsic cues

Several groups have shown a link between Navigators and cellular outgrowth. For example, *unc-53* mutations give rise to cellular outgrowth defects of different cell types including neurons, muscle cells, and excretory cells (Hekimi and Kershaw, 1993; Stringham et al., 2002). Nav1 was shown to be required for directional outgrowth of

pontine neurons (Martinez-Lopez et al., 2005). Furthermore it was shown that NAV2 is indispensable for the retinoic acid induced outgrowth of neurites of SH-SY5Y cells (Muley et al., 2008). The sensory deficits in Nav2 hypomorphic mice also favor the idea that Navigators play a role in the development of the nervous system (Peeters et al., 2004).

Data from mammalian Navigators and their *C. elegans* homolog UNC-53 suggest that these proteins function downstream of guidance molecules. In the case of Nav1, a link to the netrin pathway has been established, i.e. when Nav1 expression is knocked down in rat pontine neuronal explants, neurons become insensitive to a netrin-1 gradient (Martinez-Lopez et al., 2005). Netrins bind to both the UNC-5 receptor and to the Deleted in Colorectal Carcinoma (DCC) receptor. The DCC receptor mainly mediates attraction whereas the UNC-5 receptor mainly activates repulsion. Interestingly, migrating pontine neurons require the DCC receptor for netrin-mediated attraction (Yee et al., 1999). This suggests that Navigators function downstream of activated DCC receptors. DCC activation by netrin-1 has been shown to activate Rac-1 and Cdc42, both positive regulators of growth cone progression (Shekarabi et al., 2005). Activation of Rac-1 by DCC is mediated by a Rho GEF named Trio. This protein is homologous to a *C. elegans* Rho GEF named UNC-73 (Briancon-Marjollet et al., 2008), which activates the Rac homologs MIG-2 and CED-10 (Kishore and Sundaram, 2002).

Interestingly, in *C. elegans* a genetic link between the *unc-73* and *unc-53* genes exists that controls the anterior-posterior (AP) migration of the sex myoblasts. The migration of sex myoblasts along the AP axis requires multiple cell extrinsic guidance cues but not the netrin orthologue UNC-6 (Branda and Stern, 2000).

In these examples, there appears to be a difference in the cell extrinsic cues to which *C. elegans* UNC-53 and mammalian Nav1 respond, however the pathway downstream of these cues is partially conserved as both involve Trio/UNC-73.
In conclusion, it is likely that Navigators function downstream of cell extrinsic signals. Unraveling the pathways upstream of Navigators is important, as it is probable that these are essential for the regulation of Navigator activity.
In the next paragraph I will discuss the phenotype of *unc-53* mutants, and what is known about the genetic pathways in which this gene functions.

6.3 The *C. elegans unc-53* phenotype

In *unc-53* mutants, cell migration along the AP axis is mainly affected (see figure 1). By contrast, dorsal-ventral (DV) migration is largely unaffected (Stringham et al.,

2002). Cells that are affected in their outgrowth include the touch receptor neurons, the excretory cell and the sex myoblasts. UNC-53 is also expressed in body wall muscle cells and overexpression of UNC-53 leads to overextension of these cells. In *C. elegans* there are distinct pathways that mediate AP and DV migration of cells. Guidance along the dorsoventral axis is quite well understood and involves two guidance molecules, i.e. UNC-6 and SLT-1 (a homolog of slit). UNC-6 is secreted by ventral cord axons. It attracts axons that express UNC-40 (homologous to DCC and neogenin receptors) and repels axons that express both UNC-5 and UNC-40 towards the dorsal side (Wadsworth, 2002). At the same time, dorsal muscle cells secrete SLT-1, which repels axons that express the SAX-3 receptor (homologous to robo) towards the ventral side of the worm (Hao et al., 2001) (See Figure 1).

Guidance along the anteroposterior axis is much less understood, but has been shown to involve the Wnt pathway. In mutants of *egl-20* (one of the five *C. elegans* Wnt genes), the polarity of two mechanosensory neurons (ALM and PLM) is often reversed (Silhankova and Korswagen, 2007; Zou, 2006).

In *unc-53* mutants, these cells are also affected in their outgrowth, although no polarity reversals have been reported in these mutants. The ALM and PLM cells represent four of the six touch receptor neurons which include 2 posterior lateral microtubule (MT) cells (PLM), 2 anterior lateral MT cells (ALM), one anterior (AVM) and one posterior ventral MT cell (PVM) (see figure 1). In *unc-53* mutants these cells do not extend in the anterior direction as far as they do in the wild type worms and they are often misguided. In addition, the PLM cells show aberrant branching and aberrant branch morphology. It was shown by Hekimi and Kershaw that the ALM and PLM cells have differential requirements for *unc-53* during their outgrowth and guidance along the AP axis. The PLM cells need *unc-53* along the whole trajectory of outgrowth. The ALM cells only require the gene in the last third of their outgrowth. It was suggested that there is a spatially restricted requirement for UNC-53 activity (Hekimi and Kershaw, 1993).

Because these cells do not only fail in their outgrowth but also frequently meander, it is probable that a cell extrinsic cue is misinterpreted or not sensed by these cells. Even though the mammalian Nav1 is thought to function downstream of the guidance molecule netrin in the directed outgrowth of neurons, netrins are likely not to be important for UNC-53 dependent AP migration. This is because in *C. elegans*, the UNC-6 (netrin) pathway mainly controls DV migration and not migration along the AP axis. In addition, it was shown that ectopic expression of UNC-5 (a netrin receptor) in these cells induces UNC-6 dependent dorsal outgrowth of the

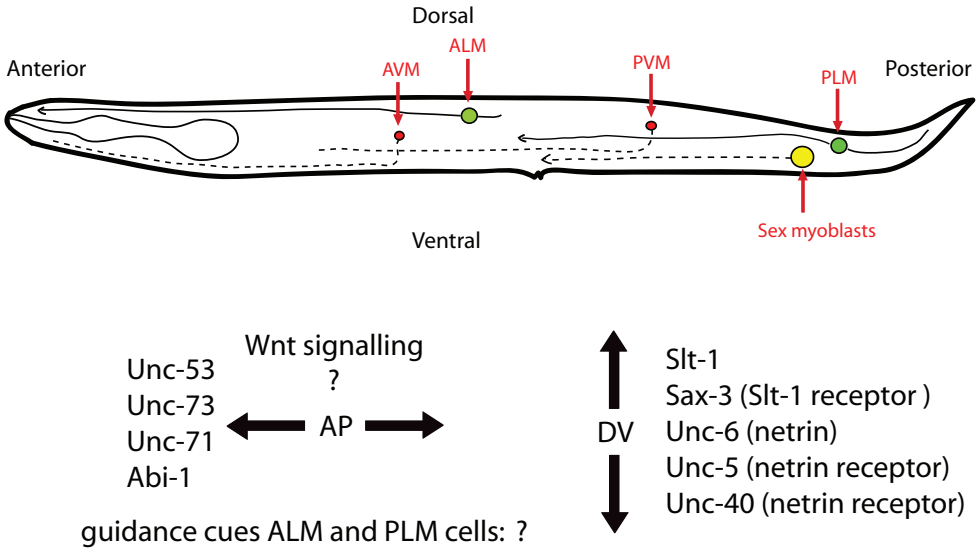

Figure 1. Schematic overview of *C. elegans*

This picture shows the trajectories of the mechanosensory neurons AVM, ALM, PVM and PLM and the migration trajectory of the sex myoblasts. The overview shows some of the molecules that are important for directional migration. The pathways that control DV migration are quite well understood, but AP migration is much less understood. Sax-3 is homologous to the mammalian Robo receptors, Unc-40 is homologous to the mammalian "Deleted in Colorectal Carcinoma" (DCC) receptor.

ALM and PLM cells (Hamelin et al., 1993).

UNC-53 may act downstream of these netrin and slit homologs in some cells, but it is likely that the ALM and PLM cells require other cell extrinsic cues for outgrowth along the AP axis. Interestingly, it was shown that human NAV2 can rescue the outgrowth phenotype of the PLM cells. This suggests that NAV2 and UNC-53 have at least partially conserved functions (Muley et al., 2008), and that NAV2 can also function independently of netrin.

Other cells that show defective migration along the AP axis in *unc-53* mutants are the sex myoblasts. These cells develop into the sex muscles which are required for egg laying. During development the sex myoblasts migrate from the posterior end of the animal anteriorly until they reach the area where the vulva will form (Sulston and Horvitz, 1977). This migration involves two mechanism, namely a gonad dependent attraction (GDA) mechanism and a gonad independent attraction mechanism (GIM) (Chen and Stern, 1998). Gonad dependent migration depends on the attraction molecule EGL-15 (an FGF like molecule), which is secreted by

the gonads (Lo et al., 2008). When the gonads are ablated by laser microsurgery, sex myoblasts still migrate along the anteroposterior axis. The attraction molecule that mediates this directional migration is unknown, but it has been shown that the GIM requires a pathway involving *unc-53*, *unc-71* and *unc-73* (Huang et al., 2003; Stringham et al., 2002). As mentioned in paragraph 6.2, the UNC-73 protein is homologous to the mammalian Rho GEF Trio.

unc-71 is one of the four ADAM ("a disintegrin and metalloprotease") genes in *C. elegans*. ADAMs are involved in cell adhesion and proteolysis. Some ADAMs can cleave the extracellular domains of transmembrane proteins (Huang et al., 2003). ADAMs can interact with integrins, and these interactions can regulate integrin-mediated cell migration (Huang et al., 2005). Interestingly UNC-71 appears not to be expressed in the sex myoblasts. In addition, it was shown that expression of full length UNC-71 in the sex myoblasts exclusively does not rescue their migration defects in *unc-71* mutants. But expression of UNC-71 driven by a promoter (Psur-5) which is active in almost all cells does rescue the phenotype. This means that UNC-71 functions in a cell non-autonomous manner in the GIM. This role for UNC-71 in sex myoblast migration provides a link to the extracellular cues involved in the GIM and to the receptors that function upstream of UNC-53 in these cells (Huang et al., 2003).

In conclusion, several proteins have been identified that function together with UNC-53 to control cellular outgrowth and migration of sex myoblasts, one of which (UNC-71) works externally from the sex myoblasts, again showing that UNC-53 activity is regulated by cell extrinsic cues.

6.4 Why are NAVs +TIPs?

Navigators are the first +TIPs identified that induce the formation of long cellular extensions in cell types that do not normally make these structures. Navigator activity in the outgrowth of cells might be linked to MT bundle formation. MT bundles generated by the Navigators are dynamic, and this dynamic behavior may be important for the ability of MTs to generate long cellular extensions. It was recently shown that the pushing force of a MT increases linearly with the number of MTs in a bundle (Laan et al., 2008). Navigator-induced outgrowth of cells requires MTs, because when the MT network is depolymerized with nocodazole, the extensions disappear immediately. Thus, Navigators might allow a bundled MT network to push against membranes. Another possibility is that the Navigator ATPase domain works from the MT end to regulate the cytoskeleton. Perhaps Navigators can reorganize

the cortical actin network such that it enables MTs to push out the plasma membrane. Interestingly, the neuronal protein MAP2, which bundles MTs also induces the formation of long cellular extensions when expressed in non neuronal cells, but only after these cells are treated with cytochalasin D, which disrupts the actin network (Edson et al., 1993).

A link between Navigators and actin has been proposed before (Stringham et al., 2002). Navigators contain putative LKK domains and a calponin homology domain, both of which are found in actin binding proteins. Furthermore, Stringham et al. reported that UNC-53 bound to F-actin in vitro (Stringham et al., 2002), although no data was shown to prove this. We have observed Navigator containing foci that partially colocalized with actin filaments (Chapter 4). Interestingly these NAV foci are preferentially localized at the ventral side of the cell, which is the side where the cell adheres to the substratum. These NAV foci can influence MT dynamics. It appears as if these structures capture MTs. In addition we found that Navigators show a striking relocalization from MT ends to actin filaments (independently of the foci). We observed relocalization when we added cytochalasin D, a fungal toxin that depolymerizes the actin network by capping barbed ends, but not when we added another actin depolymerizing toxin latrunculin A, which binds soluble actin. It has been shown that cytochalasin D induces other effects besides depolymerizing the actin network, for example, it can induce tyrosine phosphorylation of certain proteins, and it has been shown to activate Rho. Our data suggest that the effect of cytochalasin D on Navigator localization is independent of actin-depolymerization itself. Preliminary data suggest that this relocalization can be blocked by the addition of sodium orthovanadate, an inhibitor of tyrosine phosphatases, alkaline phosphatases and some ATPases, implicating phosphorylation in the relocalization event. Even though, sodium orthovanadate is not very specific, the effect of it on Navigator translocation argues against a model whereby cytochalasin D changes the structure of the actin filament in such away that allows Navigators to bind.

We have determined that the domain responsible for actin relocalization lies within the MTB of NAV1. Our data suggest that Navigators have an actin binding domain which is normally only activated in the ventral part of the cell. Perhaps Navigators work downstream of specific activated receptors to capture MTs via a locally controlled mechanism. Such local control of MT dynamics has also been shown for a protein complex containing IQGAP and CLIP170 (Fukata et al., 2002).

Navigators are interaction partners of EB proteins. EBs are essential for MT end tracking of Navigators. Navigators, on the other hand, can attract EBs to MT

bundles and to Navigator aggregates when overexpressed. Interestingly we have also found that Navigators can make a switch between binding to EBs and the actin network. Binding of Navigator to one of these structures is mutually exclusive for the other. Perhaps the NAV1-actin interaction inhibits the NAV1-EB1 interaction via sterical hindrance, caused by overlapping binding sites. This makes sense, because both the EB and the actin binding region are located in the same stretch of around 400 amino acids. We are currently trying to map these interaction domains with greater precision. Mutual exclusion might be a common mechanism to keep the level of free unbound EB proteins in the cell at a constant level. There are so many EB binding proteins in the cytoplasm that if the interactions with these binding partners are not strictly controlled, this could easily attract all EBs away from MT ends.

In conclusion, Navigators are microtubule and actin associated proteins. Although it remains to be seen what the exact function of these proteins is, it is very likely that they are direct modulators of the cytoskeleton, thereby facilitating cellular outgrowth and migration.

References

Branda, C.S., and M.J. Stern. 2000. Mechanisms controlling sex myoblast migration in Caenorhabditis elegans hermaphrodites. *Dev Biol*. 226:137-51.

Briancon-Marjollet, A., A. Ghogha, H. Nawabi, I. Triki, C. Auziol, S. Fromont, C. Piche, H. Enslen, K. Chebli, J.F. Cloutier, V. Castellani, A. Debant, and N. Lamarche-Vane. 2008. Trio mediates netrin-1-induced Rac1 activation in axon outgrowth and guidance. *Mol Cell Biol*. 28:2314-23.

Chen, E.B., and M.J. Stern. 1998. Understanding cell migration guidance: lessons from sex myoblast migration in C. elegans. *Trends Genet*. 14:322-7.

Coy, J.F., S. Wiemann, I. Bechmann, D. Bachner, R. Nitsch, O. Kretz, H. Christiansen, and A. Poustka. 2002. Pore membrane and/or filament interacting like protein 1 (POMFIL1) is predominantly expressed in the nervous system and encodes different protein isoforms. *Gene*. 290:73-94.

Edson, K., B. Weisshaar, and A. Matus. 1993. Actin depolymerisation induces process formation on MAP2-transfected non-neuronal cells. *Development*. 117:689-700.

Fukata, M., T. Watanabe, J. Noritake, M. Nakagawa, M. Yamaga, S. Kuroda, Y. Matsuura, A. Iwamatsu, F. Perez, and K. Kaibuchi. 2002. Rac1 and Cdc42 capture microtubules through IQGAP1 and CLIP-170. *Cell*. 109:873-85.

Hamelin, M., Y. Zhou, M.W. Su, I.M. Scott, and J.G. Culotti. 1993. Expression of the UNC-5 guidance receptor in the touch neurons of C. elegans steers their axons dorsally. *Nature*. 364:327-30.

Hao, J.C., T.W. Yu, K. Fujisawa, J.G. Culotti, K. Gengyo-Ando, S. Mitani, G. Moulder, R. Barstead, M. Tessier-Lavigne, and C.I. Bargmann. 2001. C. elegans slit acts in midline, dorsal-ventral, and anterior-posterior guidance via the SAX-3/Robo receptor. *Neuron*. 32:25-38.

Hekimi, S., and D. Kershaw. 1993. Axonal guidance defects in a Caenorhabditis elegans mutant reveal cell-extrinsic determinants of neuronal morphology. *J Neurosci*. 13:4254-71.

Huang, J., L.C. Bridges, and J.M. White. 2005. Selective modulation of integrin-mediated cell migration by distinct ADAM family members. *Mol Biol Cell*. 16:4982-91.

Huang, X., P. Huang, M.K. Robinson, M.J. Stern, and Y. Jin. 2003. UNC-71, a disintegrin and metalloprotease (ADAM) protein, regulates motor axon guidance and sex myoblast migration in C. elegans. *Development*. 130:3147-61.

Ishiguro, H., T. Shimokawa, T. Tsunoda, T. Tanaka, Y. Fujii, Y. Nakamura, and Y. Furukawa. 2002. Isolation of HELAD1, a novel human helicase gene up-regulated in colorectal carcinomas. *Oncogene*. 21:6387-94.

Karenko, L., S. Hahtola, S. Paivinen, R. Karhu, S. Syrja, M. Kahkonen, B. Nedoszytko, S. Kytola, Y. Zhou, V. Blazevic, M. Pesonen, H. Nevala, N. Nupponen, H. Sihto, I. Krebs, A. Poustka, J. Roszkiewicz, K. Saksela, P. Peterson, T. Visakorpi, and A. Ranki. 2005. Primary cutaneous T-cell lymphomas show a deletion or translocation affecting NAV3, the human UNC-53 homologue. *Cancer Res*. 65:8101-10.

Kishore, R.S., and M.V. Sundaram. 2002. ced-10 Rac and mig-2 function redundantly and act with unc-73 trio to control the orientation of vulval cell divisions and migrations in Caenorhabditis elegans. *Dev Biol*. 241:339-48.

Klaus, A., and W. Birchmeier. 2008. Wnt signalling and its impact on development and cancer. *Nat Rev Cancer*. 8:387-98.

Laan, L., J. Husson, E.L. Munteanu, J.W. Kerssemakers, and M. Dogterom. 2008. Force-generation and dynamic instability of microtubule bundles. *Proc Natl Acad Sci U S A*. 105:8920-5.

Lo, T.W., C.S. Branda, P. Huang, I.E. Sasson, S.J. Goodman, and M.J. Stern. 2008. Different isoforms of the C. elegans FGF receptor are required for attraction and repulsion of the migrating sex myoblasts. *Dev Biol*. 318:268-75.

Martinez-Lopez, M.J., S. Alcantara, C. Mascaro, F. Perez-Branguli, P. Ruiz-Lozano, T. Maes, E. Soriano, and C. Buesa. 2005. Mouse Neuron navigator 1, a novel microtubule-associated protein involved in neuronal migration. *Mol Cell Neurosci*. 28:599-612.

Merrill, R.A., L.A. Plum, M.E. Kaiser, and M. Clagett-Dame. 2002. A mammalian homolog of unc-53 is regulated by all-trans retinoic acid in neuroblastoma cells and embryos. *Proc Natl Acad Sci U S A*. 99:3422-7.

Muley, P.D., E.M. McNeill, M.A. Marzinke, K.M. Knobel, M.M. Barr, and M. Clagett-Dame. 2008. The atRA-responsive gene neuron navigator 2 functions in neurite outgrowth and axonal elongation. *Dev*

Neurobiol. 68:1441-53.
Peeters, P.J., A. Baker, I. Goris, G. Daneels, P. Verhasselt, W.H. Luyten, J.J. Geysen, S.U. Kass, and D.W. Moechars. 2004. Sensory deficits in mice hypomorphic for a mammalian homologue of unc-53. *Brain Res Dev Brain Res*. 150:89-101.
Shekarabi, M., S.W. Moore, N.X. Tritsch, S.J. Morris, J.F. Bouchard, and T.E. Kennedy. 2005. Deleted in colorectal cancer binding netrin-1 mediates cell substrate adhesion and recruits Cdc42, Rac1, Pak1, and N-WASP into an intracellular signaling complex that promotes growth cone expansion. *J Neurosci*. 25:3132-41.
Silhankova, M., and H.C. Korswagen. 2007. Migration of neuronal cells along the anterior-posterior body axis of C. elegans: Wnts are in control. *Curr Opin Genet Dev*. 17:320-5.
Stringham, E., N. Pujol, J. Vandekerckhove, and T. Bogaert. 2002. unc-53 controls longitudinal migration in C. elegans. *Development*. 129:3367-79.
Sulston, J.E., and H.R. Horvitz. 1977. Post-embryonic cell lineages of the nematode, Caenorhabditis elegans. *Dev Biol*. 56:110-56.
Wadsworth, W.G. 2002. Moving around in a worm: netrin UNC-6 and circumferential axon guidance in C. elegans. *Trends Neurosci*. 25:423-9.
Yee, K.T., H.H. Simon, M. Tessier-Lavigne, and D.M. O'Leary. 1999. Extension of long leading processes and neuronal migration in the mammalian brain directed by the chemoattractant netrin-1. *Neuron*. 24:607-22.
Zou, Y. 2006. Navigating the anterior-posterior axis with Wnts. *Neuron*. 49:787-9.

Summary

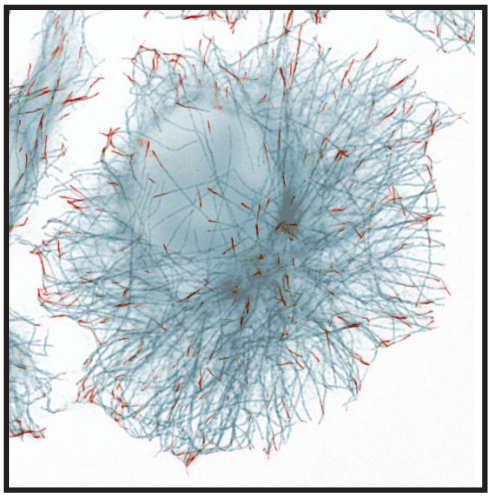

Samenvatting

Summary

The human body is composed of trillions of cells. These astoundingly complex biological machines are the basic units of life and are at the base of everything we do. The human body contains hundreds of different cell types organized into specialized organs and tissues, each having specific functions. The cells lining our intestines are, for example, responsible for digesting food and taking up nutrients, whereas muscle cells enable us to move our limbs. Cells in the brain are responsible for our memory and even for our consciousness.

Even though the size of the nucleus of a mammalian cell has a diameter of around 10 microns it contains almost 2 meters of DNA, encoding around 25000 genes. These genes are the recipes for the production of proteins. Some genes are active in every cell (and some proteins are therefore produced in every cell); others are only active in specific cell types. Differences in the protein composition between cell types likely relate to the different functions of these cell types. Proteins have many different functions, including roles in cell metabolism, DNA replication, nutrient uptake, and cell structure. Even though a great deal of information about the function of thousands of proteins exists, the function of many proteins is still unknown, let alone how they collaborate to make a cell a functional and organized unit. To understand how the machinery of life functions, it is essential to understand all of its components. Such information also broadens our understanding of various human diseases, and ultimately enables the development of targeted therapeutics against these diseases.

Cell function is intimately connected to cell shape, an important determinant of which is the cytoskeleton. The cytoskeleton is a tightly organized network of protein filaments that provides cells with structural stability and mediates intracellular organization and transport. One component of the cytoskeleton is the microtubule (MT) network. MTs are tubes with a diameter of around 25 nm, and they are composed of the proteins α- and β-tubulin. One α-tubulin molecule pairs with a β-tubulin molecule to form a heterodimer. These tubulin dimers assemble into long strands (protofilaments) that interact laterally with each other to form a tube structure. In general, MTs are composed of 13 protofilaments. MTs are highly dynamic, and as such, cells can quickly reorganize their MT network whenever and wherever this is necessary. For example, in less than half an hour, cells completely reorganize their interphase MT network to build up the mitotic spindle, which in turn segregates the genetic material during cell division. Also during cell migration and outgrowth a dynamic MT network is of great advantage.

Important mediators of MT dynamics are the MT associated proteins (MAPs). These proteins have a variety of functions. Some of them stabilize and bundle MTs, others affect the polymerization speed of MTs, and some can even sever MTs. A special family of MAPs are the MT plus-end tracking proteins or +TIPs. These proteins can associate with the growing ends of MTs and can modulate the dynamic behavior of MTs. To understand how +TIPs exert their effects on the MT end, it is important to understand how these proteins accumulate at MT ends. In chapter 2, we show that the +TIPs CLIP170 and EB1 both exchange rapidly on MT ends. Furthermore we show that CLIP170 binds with low affinity to a structural feature at the MT end (that decays in a temperature sensitive and exponential fashion). In chapters 3 and 4 we describe the Navigator proteins, a novel small family of +TIPs that are homologous to UNC-53, a protein found in the small nematode *C.elegans*. UNC-53 contains an AAA-type ATPase domain and plays an important role in the outgrowth of different cells along the anterio-posterior axis. These cells include the mechanosensory neurons, the sex muscle precursor cells and the excretory cells. When the *unc-53* gene is mutated, these cells fail to migrate to their normal position. The three mammalian Navigators (NAV1, 2, 3) are also ATPases and some studies have linked NAVs to cellular migration and outgrowth. We show that all Navigators are +TIPs and that overexpression of these proteins induces the formation of long cellular extensions, which, in the case of NAV1, depends on an intact ATPase domain.

How might NAVs bind MT ends and what could be the function of this association? We show that Navigators require EBs to bind to MT ends and that the MT binding (MTB) domain of NAV1 mediates its binding to EB1, -2, and -3. We also show that Navigators form granule-like structures near the basal membrane of the cell. These structures partially colocalize with F-actin (another component of the cytoskeleton) and are capable of altering MT dynamics. We often observe pausing MTs at these “granules”. Furthermore we show that the NAV1 MTB domain harbors an actin binding motif that can be activated by the addition of a fungal toxin named cytochalasin D. Addition of this compound induces a rapid translocation of cytoplasmic Navigators to the F-actin network. Based on the results described in Chapter 4 we propose that Navigators are actin-MT crosslinking factors, and that one function of an EB-Navigator interaction might be to capture MTs.

In chapter 5, we report on the identification of other binding partners of Navigator proteins and show a potential function for NAV1 in nucleolar organization and in mitosis. Based on the results described in this thesis we can conclude that Navigators are ATPases that are truly associated with various cellular activities. In

chapter 6, I describe what is known about the pathways in which *C.elegans* Navigator functions and I try to draw parallels with mammalian Navigators. This provides us with leads for further investigation of the functions of this intriguing protein family.

Samenvatting

Het menselijk lichaam bestaat uit triljarden cellen. Deze ongelofelijk complexe biologische machientjes zijn de basis-eenheden van het leven, en zij liggen aan de basis van alles dat we doen. Het menselijk lichaam bevat honderden verschillende cel types die georganiseerd zijn in gespecialiseerde organen en weefsels met ieder hun eigen specifieke functies. De cellen die de wand van onze ingewanden bekleden zijn van groot belang voor de digestie van voedsel, en ook voor het opnemen van voedingstoffen. Spiercellen zorgen ervoor dat we onze ledematen kunnen bewegen. En een enorm complex netwerk van honderden miljarden onderling verbonden cellen in ons brein vormt ons geheugen en ook ons bewustzijn.

De meeste cellen in ons lichaam bevatten een celkern, een organel met een diameter van ongeveer 10 micron. Dit organel bevat bijna twee meter DNA, welke rond de 25000 genen bevat. Deze genen zijn de recepten voor de productie van eiwitten. Sommige genen zijn actief in iedere cel (en sommige eiwitten worden daarom geproduceerd in iedere cel); andere genen zijn alleen actief in specifieke cel types. Verschillen in de eiwit samenstelling van verschillende cel typen correleert hoogst waarschijnlijk met de verschillende functies van deze cellen. Eiwitten hebben een grote verscheidenheid aan functies, inclusief functies in cel metabolisme, DNA replicatie, opname van voedingsstoffen, en cel structuur.

Hoewel er al heel wat bekend is over de functie van duizenden eiwitten, is de functie van heel veel andere eiwitten nog niet bekend, laat staan ons begrip van hoe al deze eiwitten samenwerken om een cel goed te laten functioneren. Om te kunnen begrijpen hoe de cellulaire machinerie functioneert, is het essentieel om te begrijpen uit welke componenten zij is opgebouwd en hoe al die componenten samenwerken. Deze informatie geeft ons ook meer inzicht in hoe bepaalde ziektes tot stand komen, en maakt het uiteindelijk mogelijk om gerichte therapieën te ontwikkelen tegen deze ziektes.

Cel functie is sterk gekoppeld aan celvorm, welke voor een belangrijk deel gereguleerd wordt door het celskelet. Het celskelet is een strak gereguleerd netwerk van eiwit filamenten die de cel voorzien van structurele stabiliteit en die de interne organisatie van de cel en intracellulair transport verzorgen. Een belangrijke component is het microtubuli (MT) netwerk. Dit netwerk speelt een belangrijke rol in celdeling, celmigratie en intracellulair transport. Microtubuli zijn buisjes met een diameter van ongeveer 25 nanometer, en deze zijn opgebouwd uit de eiwitten α- en β-tubuline. Een α-tubuline molecuul vormt een paar met een β-tubuline molecuul en vormt zo een heterodimeer. Een dergelijk dimeer kan een kop-staart interactie

aangaan met een andere dimeer en op deze manier een keten vormen (een protofilament). Deze protofilamenten hebben polariteit, met aan het ene uiteinde een α-tubuline en aan het andere een β-tubuline molecuul. Protofilamenten kunnen laterale interacties vormen met andere protofilamenten en op die manier een buisje vormen. De meeste microtubuli in een cel bestaan uit 13 protofilamenten. Als een dergelijk buisje eenmaal gevormd is kan deze aan beide uiteinden groeien door het inbouwen van nieuwe tubuline dimeren. Er is echter een verschil in de efficiëntie waarmee dimeren ingebouwd kunnen worden aan beide uiteindes. Het uiteinde van microtubuli waar het β-tubuline eiwit beschikbaar is, ofwel het plus-einde, groeit veel sneller dan het andere einde dat ook wel min-einde genoemd wordt. Microtubuli zijn erg dynamische structuren, en dat maakt het voor de cel mogelijk om dit netwerk heel snel te reorganiseren, waar en wanneer dit noodzakelijk is. Bijvoorbeeld, in minder dan een half uur, kunnen cellen hun MT netwerk compleet reorganiseren om de mitotische spoelfiguur te vormen, die het genetische materiaal verdeeld over twee dochtercellen tijdens de celdeling. Ook tijdens cel migratie en uitgroei is een dynamisch MT netwerk van groot belang.

Belangrijke regulatoren van het dynamische gedrag van microtubuli zijn de Microtubule Associated Proteins, ofwel MAPs. Deze eiwitten hebben een verscheidenheid aan functies. Sommigen stabiliseren en bundelen het MT netwerk. Anderen beïnvloeden de groeisnelheid van microtubuli en sommigen zijn zelfs in staat om microtubuli in tweeën te klieven. Een speciale familie van MAPs zijn de “Microtubule plus-end tracking proteins”, ofwel +TIPs. Deze eiwitten kunnen heel specifiek aan de groeiende uiteindes van microtubuli binden en kunnen het dynamische gedrag van microtubuli sterk beïnvloeden. Om te kunnen begrijpen hoe deze eiwitten hun functie kunnen uitoefenen, is het belangrijk om te begrijpen hoe deze eiwitten accumuleren op de uiteindes van microtubuli. In hoofdstuk 2 van dit proefschrift beschrijven we hoe de +TIPs CLIP-170 en EB1 beide snel uitwisselen op de uiteindes van microtubuli. Verder laten we zien dat CLIP-170 een structurele eigenschap van het MT einde kan herkennen, en dat deze CLIP-170 bindingsplaatsen op exponentiele en temperatuur afhankelijke wijze verdwijnen.

In hoofdstuk 3 en 4 beschrijven we de Navigator eiwitten, een nieuwe familie van +TIPs die homoloog zijn aan UNC-53, een eiwit dat gemaakt wordt door de kleine nematode, *C. elegans*. UNC-53 bevat een ATPase domein van het AAA-type, en dit eiwit speelt een belangrijke rol tijdens de migratie en uitgroei van verschillende cellen langs de antero-posterieure as (de AP-as) van deze rondworm. Deze cellen zijn onder andere; de mechanosensory neuronen, de sex-muscle precursor cellen

en de excretory cellen. Als het *unc-53* gen gemuteerd is, slagen deze cellen er niet in om naar de juiste positie te migreren of uit te groeien.
De drie zoogdier Navigators zijn ook ATPases en sommige studies hebben ook deze eiwitten gekoppeld aan celmigratie en uitgroei. Wij laten zien dat alle Navigators +TIPs zijn, en dat overexpressie van deze eiwitten resulteert in de formatie van lange cel extensies, die in het geval van NAV1, een intact ATPase domein vereisen. Hoe kunnen Navigators aan MT eindjes binden en wat is de functie van deze interactie? We laten zien dat Navigators EBs nodig hebben om aan MT eindjes te kunnen binden en dat het MT bindings (MTB) domein van NAV1 aan EB1, 2 en 3 kan binden. Verder laten we zien dat Navigators asymmetrisch gelokaliseerd zijn in de cel, ze binden namelijk niet alleen aan MT plus eindjes, maar ze lokaliseren ook in granule-achtige structuren vlakbij het basale membraan van de cel. Deze structuren colokaliseren gedeeltelijk met F-actine (een andere component van het celskelet), en zijn in staat om het dynamische gedrag van microtubuli te beïnvloeden. We hebben vaak pauzerende microtubuli waargenomen bij deze granules. Verder laten we zien dat het MTB domein van NAV1 een actine bindings motief bevat dat geactiveerd kan worden door cytochalasin D (een schimmel toxine). Het toevoegen van dit toxine veroorzaakt een snelle relokalisatie van Navigator eiwitten naar het actine netwerk. Gebaseerd op de resultaten in hoofdstuk 4 stellen we voor dat Navigators actin-MT crosslinking factoren zijn, en dat de EB-Navigator interactie een koppeling tussen dynamische microtubuli en actine filamenten kan bewerkstelligen.
In hoofdstuk 5 rapporteren we over de identificatie van andere bindingspartners van de Navigators en laten zien dat deze eiwitten mogelijk een functie hebben in de organisatie van nucleoli en in mitose. Gebaseerd op de resultaten beschreven in dit proefschrift, concluderen we dat Navigators AAA-ATPases zijn die echt geassocieerd worden met verscheidene cellulaire activiteiten. In hoofdstuk 6 beschrijf ik wat er bekend is over de signaal transductie wegen waarin de *C. elegans* Navigator functioneert, en probeer ik deze te vergelijken met de situatie in zoogdieren. Dit geeft ons aanknopingspunten die we kunnen gebruiken om meer te weten te komen over de regulatie en de functie van deze intrigerende eiwitten.

Curriculum Vitae

Name: Jeffrey Antonius Johannes van Haren
Born: 27-06-1981, Tiel, The Netherlands

Education:

2008-present
Post-doctoral scientist
Department of Cell Biology, Erasmus MC, Rotterdam

2003-2008
PhD student
Department of Cell Biology, Erasmus MC, Rotterdam
“Navigating Cells and Cytoskeletal Networks with a novel family of AAA-ATPases”
Promotor: Prof.dr. Frank Grosveld, Copromoter: Dr.ir. Niels Galjart

2002-2003
Internship at the University of California Santa Barbara, Santa Barbara
“Mutants of the global regulator Lrp that specifically inhibit pap phase variation from the OFF to the ON state”
Supervisors: Prof. David Low, Dr. Aaron Hernday, Dr. Bruce Braaten

1999-2003
Bachelor of Applied Science
Molecular Biology, Hogeschool van Utrecht, Utrecht

1993-1999
HAVO
GSG Lingecollege, Tiel

Publications

Dragestein, K.A., W.A. van Cappellen, **J. van Haren**, G.D. Tsibidis, A. Akhmanova, T.A. Knoch, F. Grosveld, and N. Galjart. 2008. Dynamic behavior of GFP-CLIP-170 reveals fast protein turnover on microtubule plus ends. *J Cell Biol*. 180:729-37.

van Haren, J., K. Draegestein, N. Keijzer, J.P. Abrahams, F. Grosveld, P.J. Peeters, D. Moechars, and N. Galjart. 2009. Mammalian Navigators are microtubule plus-end tracking proteins that can reorganize the cytoskeleton to induce neurite-like extensions. *Cell Motil Cytoskeleton*. in press

van Haren, J., S.M. Gouveia, I. Grigoriev, A. Akhmanova, F. Grosveld, P.J. Peeters, D. Moechars, and N. Galjart. Navigators are EB-interacting proteins that link dynamic microtubules to the cortical actin network. Manuscript in preparation

PhD Portfolio Summary

Name PhD student: Jeffrey van Haren Erasmus MC Department: Cell Biology Research School: Medisch-Genetisch Centrum Zuid-West Nederland	PhD period: November 2003 – November 2008 Promotor(s): Prof.dr. F.G. Grosveld Supervisor: Dr.ir. N.J. Galjart

1. PhD training

	Year
General academic skills	
- Safe Laboratory techniques	2004
- Radiation Safety Course (Level 5b). Rotterdam	2004
In-depth courses (e.g. Research school, Medical Training)	
- Experimental Approach to Molecular and Cell Biology, Rotterdam	2005
Presentations	
- 17th MGC symposium, Rotterdam (presentation)	2007
- Annual Dutch Meeting on Molecular and Cellular Biophysics, Lunteren (poster)	2004
- Annual Dutch Meeting on Molecular and Cellular Biophysics, Lunteren (poster)	2005
- Annual Dutch Meeting on Molecular and Cellular Biophysics, Veldhoven (poster)	2006
- 6th MGC- Cancer Research UK Graduate Student Conference, Luik (poster)	2005
- Microtubules and Motors symposium, Utrecht (presentation)	2009
International conferences	
- ELSO 2008; Frontiers of cellular, developmental and molecular biology, Nice, France (poster)	2008
- MCRI Microtubule dynamics workshop, Oxted, United Kingdom (poster)	2008
Other	
- Member of the organising committee of the 7th Joint MGC - Cancer Research UK Graduate Student Conference 2006, Oxford, United Kingdom	2006

Dankwoord

Eindelijk is ie er, mijn proefschrift! Promoveren is een tijdrovende bezigheid, heb ik gemerkt! Vijf en een half jaar zijn voorbijgevlogen alsof het niets is. Maar ik heb er een hoop van geleerd. Ik wil een heleboel mensen bedanken voor hun bijdrage aan dit proefschrift, maar ook voor hun gezelligheid en vriendschap.

Allereerst wil ik jou bedanken, Frank!
De werkbesprekingen op vrijdag zijn altijd interessant en leuk!
De informele sfeer bij deze werkbespreking is geweldig. Ik heb er een hoop van geleerd en vaak erg gelachen. Je stelt altijd precies de juiste vragen. Bedankt voor alle waardevolle adviezen.

Niels, good day mate! Bedankt voor een heleboel zaken. Bedankt voor je hulp en advies, voor je optimisme en oneindige enthousiasme, maar ook voor de ruimte en vrijheid die je aan jouw promovendi geeft. Juist die ruimte om nieuwe proeven te bedenken en te proberen is waar ik het meeste van geleerd heb. Het heeft een tijdje geduurd, maar mijn onderzoek heeft steeds meer richting gekregen en ik heb meer slagkracht gekregen om dingen goed uit te kunnen zoeken. Ik ben blij dat ik hier nog twee en een half jaar kan blijven om onderzoek te doen aan celmigratie. Ik ben ook gedetermineerd om te achterhalen wat die ATPase activiteit van Navigators nu precies doet.

Pieter Peeters en Dieder Moechars: eigenlijk zijn jullie de initiators van het hele Navigator project. Bedankt daarvoor! Pieter, ik vind het leuk dat je in mijn promotiecommissie zit.

Natuurlijk wil ik ook de andere leden van de kleine en grote commissie bedanken:
Gert, Dies en Anna. Bedankt voor het lezen van mijn proefschrift. Jullie commentaar was erg waardevol, en heeft zeker meegeholpen om het proefschrift te verbeteren. Anna, ik wil jou ook bedanken voor al je advies en hulp in de laatste jaren. Gert, literatuurbespreking is altijd leuk, maar waar blijven die appelkanjers toch de laatste tijd? Joost Gribnau en Casper Hoogenraad, bedankt dat jullie in mijn promotiecommissie zitten.

Verder wil ik mijn collega's uit Leiden van het "van molecuul to cel" project bedanken. Mieke Mommaas en Jan Pieter Abrahams, leuk dat jullie in mijn promotiecommissie zitten. Ik wil ook mijn fellow AIOs Daniel de Geus en Sandra Zovko bedanken. Verder wil ik bedanken: Roman Koning, Mathieu Noteborn, Henk Koerten en Bram Koster. Onze maandelijkse meeting was altijd leuk en interessant. Daniel, tubuline zuiveren uit varkenshersenen, was erg leuk.

Katha, bedankt voor alle gezelligheid, "mellow mornings" in de middag, en je grappige verhalen over konijnen! Ook bedankt voor al je hulp. Het was altijd leuk om resultaten met je te bespreken. Je hebt een enorme talen- en wiskunde knobbel, en erg veel inzicht. Ik vond het leuk om je paranimf te zijn. En ik ben blij dat jij nu mijn paranimf bent. (Ik herinner me trouwens een legendarisch optreden van ene Niels Galhaas en ene C.eleGert op het promotie feest van jou en Martijn)

Daniel, ouwe gabber! Je was mijn "partner in crime" op het gebied van allerlei experimentele probeersels. Sommige van die probeersels zijn niet echt gelukt, andere werken prima. We hebben heel wat gelachen, tussen de experimenten door, en op AIO retreats en feestjes. Ik vond het leuk om je paardenimf te zijn. Ook bedankt voor je hulp met indesign en andere proefschrifterige zaken. Ik wens je heel veel succes in Breda, ik weet zeker dat je het daar goed gaat doen!
Susana, you rock! Thanks for your help with the EB work. This has really helped me! It's amazing to see the rate at which you are publishing papers! You will have a fantastic thesis. Also thanks for many nice parties!
Jeroen, bedankt voor het identificeren van honderden potentiele Navigator interactie partners. Ik heb nog genoeg te doen!
Athina, I'm glad that we're defending on the same day. Thanks for your help! I wish you good luck on the 10th of June!

Frank: WWWAAAAAAAAAAAAAAZZZZZZZZZZZZZUUUUUPPPPP!!!!
Bedankt voor al de gezelligheid, voor alle goede gesprekken en voor de vele biertjes die we gedronken hebben! Ook bedankt voor al jouw creatieve inslagen!!! Het was een goeie binnenkomer om na 2 weken in het lab al mee te doen aan het lab1030 pantomime filmpje; elektroporeren in mijn onderbroek!! Om over de jaren daarna maar te zwijgen. De brainstorm sessies en het maken van al die filmpjes was echt lachen. Unfashion day gaf me de mogelijkheid om een hele dag in mijn aussie (met bijpassende mexicaanse snor) rond te lopen in het lab (toch iets dat ik altijd al een

keer wilde doen!). Als echte wereldreiziger is de welbekende KPN “vrijdagmiddag-CD” erg van toepassing op jou: “Want thuis blijven dat is toch zonde” (met Surinaams accent). En je verhalen over die reizen zijn altijd erg leuk en zorgen ervoor dat ik ook een beetje last begin te krijgen van de reiskriebels. Rome en Berlijn waren trouwens erg tof.

Michael, de sterkste man van lab1030. En ook nog eens Nederlands kampioen behangtrekken (zoals Marja verstond toen je op een maandagochtend het lab in kwam en vertelde dat je Nederlands kampioen bankdrukken was geworden!). Bedankt voor de gezelligheid, voor alle gesprekken en ook voor het maken van allerlei filmpjes. Het is altijd lachen om naar de nieuwste surf-filmpjes te kijken, of naar filmpjes waarin je aan het zwemmen bent met witte haaien! Jij bent trouwens ook een behoorlijke wereldreiziger!

Suzanne, bedankt voor al je gezelligheid, het is altijd leuk om met je te kletsen! Leuk dat je nu in Duitsland zit. Volgens mij gaat het hartstikke goed daar. Trouwens, bedankt voor je fiets!!!! Zijn de Duitse M und Ms net zo lekker?

Marco, ouwe U makker! Als laboudste was je een soort mentor, maar wel de gekste mentor ooit! We hebben behoorlijk door het lab lopen springen en Frans Bauer teksten geschreeuwd. Het was leuk om je op te zoeken in Braunschweig met zo ongeveer de halve afdeling! En ook Berlijn was erg tof! Het lab was ineens een stuk stiller toen jij weg ging.

Mijn andere ouwe U maatjes, Marja en Nanda: bedankt voor alle gezelligheid, tijdens de lunch en aan de bench! Stiekem heb ik al jullie bench-ruimte in het lab ingepikt toen jullie weg gingen, maar die ruimte begin ik langzaam weer kwijt te raken.....

Laura, thanks for all the fun and for a lot of nice conversations. Thanks for teaching me a lot of Spanish words. I kind of miss the Dutch Wednesdays, on which we always taught you one Dutch word (Usually a dirty or a very uncommon word….). Btw, thanks for telling me that I have an account at a very strange bank (the **Rabo**bank).

Gideon, bedankt voor de gezelligheid en voor de foute muziek. Laatst hebben we nog even naar de altijd foute Huub Hangop CD geluisterd!

Of course, I want to thank all the other people that work or have worked in lab 710/1030: Ksenija, Helen, Filipe, Jurriaan, Michiel, Anna, Ana, Soraya, Ralph, Lisa, Widia, Kerstin, Liu and Linda: Thanks for creating a great atmosphere in the lab!

Rick en Phebe, het is altijd gezellig wanneer jullie in de buurt zijn!

Rick, ook nog bedankt voor het “schilderen” van een van de muren van mijn oude appartement! (met een fles wijn ☺). Verder wil ik de hele lunchgroep bedanken (vooral Björn) voor alle grappige, rare en soms ietwat ranzige verhalen!

Cristina, it is always fun to chat with you. Btw, I don't think I will ever forget how to buy a rabbit in Spain.
Maureen, het is altijd leuk om koffie met je te drinken en te kletsen in de celkweek, en af en toe een balletje te gooien in het park!
Wat betreft kletsen in de celkweek zijn er nog veel meer mensen die ik wil bedanken. Iris (heel veel succes in de States!), Annegien, Petra, Eskew, Erik, Evelien, Gerben, Alwin en nog vele anderen. Jullie maken het leven achter de flow-kast een stuk gecelliger (grapje van mijn broer) en grappiger!
I would also like to thank all those colleagues who had diner with me in the faculty restaurant over the last years, because I had diner there "quite" often. Miyata and Kumiko, probably you are my best diner buddies. Thanks for all the conversations!

I would like to thank the people from Anna's lab: Ilya, Babet and Carol. Rick, ouwe master-fotograaf! Het was leuk om met jou, Dolf en Dies naar de Kwade Hoek te gaan. Ik denk dat we dat soort tochten vaker moeten organiseren!
Verder wil ik bedanken: Robert, Anne, Marjon, Lalini, Ilona, Bob, Luna en Pascal (succes met jouw promotie!). Martijn en Karin, het was altijd erg leuk om met jullie te kletsen over wetenschap en over van alles en nog wat.
Jan Jos, bedankt voor het organiseren van al die Terschelling weekenden, dat was iedere keer erg gezellig! Verder wil ik natuurlijk bedanken: Marike, Jasperina, Melle, Arthur en de computer guys.

Thanks to all the people from cluster 15 for help with experiments or just for nice conversations, dinners and awesome parties! To name a few: Sanja, Patrick, Tau, Rik, Dubi, Martine, Noorie, Ekim, Siska, Gina, Daan, Suzanne, Joost, Toroti, Debbie, Tiago, Umut, Robert Jan, Ernie, Erik, Raymond, Sjaak, Petra, Petros, Laura, Farzin, Alireza, Akiko, Magda, Karl, Kay, Oscar, Justine, Michael, Marieke and Audrey. This list is far from complete, so also thanks to everyone who I forgot to mention.

Ik wil ook al mijn vrienden en familie bedanken, waarvan een aantal in het bijzonder: Mijn "Utrecht " vrienden: Haciali, Robin, Jochum en Jelle. Vrijdagavond om 21:00 bij "het Neutje" was altijd een goed moment om de week door te nemen, en biertjes te drinken. Ik heb jullie behoorlijk verwaarloosd de laatste tijd. Hopelijk kunnen we snel weer een paar dagen op stap met zijn allen!
Michiel, Jasper, Paul en Saskia. Mijn vrienden uit Tiel. Ik vind het leuk dat we elkaar regelmatig zien. Ook wil ik mijn ouwe makkers uit Santa Barbara; Peter, Erik en

Christiaan nog even noemen. Dat was toch echt een geweldige tijd. Leuk dat we zo af en toe afspreken.
Oma, het is altijd leuk om met u te praten over wetenschap en over voeding. U weet daar erg veel vanaf.
Ma, bedankt voor je nooit aflatende steun en voor alles dat je voor ons doet. Jouw kracht en doorzettingsvermogen zijn een groot voorbeeld voor mij. De laatste jaren waren niet makkelijk. Vanaf het moment dat pa plotseling ziek werd veranderde alles. Ik heb erg veel bewondering en waardering voor hoe je alles aangepakt hebt.
Pa, bedankt voor alles. Ik mis je.
Dennis, mijn grote broer. Je bent goed bezig! Ik ben er erg trots op dat je met deze snelheid een goed lopend bedrijf vanaf de grond hebt opgebouwd! En ik wil je bedanken voor al je aanmoedigingen en steun. Leuk dat je mijn paranimf bent. Ook wil ik mijn schoonzus Marlous bedanken.

Cheers Mates!!!!!!!!!!

Jeffrey (Ief, Gel-free, Jeffrito and even “Flipje”)